Import mechanisms of pyocins G and AP41

By Iva Atanaskovic

St. Edmund Hall

Infection Immunology and Translational Medicine

A thesis presented for the degree of Doctor of Philosophy at the University of Oxford

Trinity Term 2021

Supervised by Professor Colin Kleanthous and Professor Martin Maiden

Declaration

I confirm that the work presented in this thesis, submitted for the degree of Doctor of Philosophy, is my own original work. Work that is not my own is referenced. This thesis has not been previously submitted at this or any other university.

Iva Atanaskovic

April 2021

Word count including tables, figure legends, appendices and references: 39273

Acknowledgements

I am deeply thankful to many people who supported me in this work. I would like to thank Professor Colin Kleanthous for the opportunity to do research in his group, for his supervision and support, and for keeping me enthusiastic and excited about my work. I would like to thank the entire Kleanthous Lab for an amazing time that I had during my stay in Oxford. I would especially like to thank: Nick Housden for his ideas, supervision, comments on manuscripts and help with experimental design; Renata Kaminska for her help with cloning and protein purification; Connor Sharp for his help with bioinformatics and programming; Nathalie Reichmann for help with microscopy data collection, data analysis, and help with manuscript preparation; Patrick Inns and Sandip Kumar for their help with microscopy data analysis; Melissa Webby for her help with mass spectrometry and manuscript preparation; Cara Press for her help with circular dichroism spectroscopy; Hannah Behrens, Paul White, Jonathan Goult and Vivian Yeung for many discussions about pyocins; and Joanna Szczepaniak for many useful discussions and comments on manuscripts. At the Department of Biochemistry, I would like to thank: Edward Lowe for help with homology modelling of Hur and the setting up of crystallization screens; David Staunton for help with mass spectrometry and differential scanning calorimetry. I would also like to thank Professor Martin Maiden for being my co-supervisor. During this work I have collaborated with the Walker lab at the University of Glasgow, and I would like to thank: Dan Walker for useful discussions; and Khedidja Mosbahi for testing PyoG against a clinical isolate strain collection and in a *Galleria* infection model.

I would like to thank the Wellcome Trust and the Infection, Immunity and the Translational Medicine Programme for funding this research and providing me with necessary training. I would also like to thank the people involved in this Programme, especially Professor Chris Tang and Dawn Gibbons, for all the help and guidance during my DPhil.

Outside of work, I would like to thank my friends and family for their support. I would especially like to thank my parents, Aleksandra and Milan, for always being present and supportive. I would also like to thank my sisters, Ana and Mia, for their love, friendship and support.

Abstract

Pseudomonas aeruginosa is a priority pathogen for antibiotic development. Multi-drug-resistant strains of this bacterium cause serious nosocomial infections and are the leading cause of death in cystic fibrosis patients. Pyocins, bacteriocins of *P. aeruginosa*, are protein antibiotics deployed during intraspecies bacterial competition. Pyocins are produced by more than 90 % of *P. aeruginosa* strains. Due to their diversity and potency, pyocins may have utility as last resort antibiotics against *P. aeruginosa*. In this thesis, the import mechanism of two poorly-understood nuclease pyocins, G and AP41, was explored using microbiological, biochemical, biophysical and cell-based approaches. Pyocin G (PyoG) was previously identified by the Kleanthous lab through bioinformatics analysis of *P. aeruginosa* genomes. I demonstrate that PyoG binds Hur (Hemin uptake receptor), an outer membrane TonB1 dependent transporter. Hur binds hemin *in vitro*, and this interaction is blocked by PyoG. Both PyoG and Hur interact with TonB1, which links proton motive force generation across the inner membrane with energy-dependent pyocin translocation across the outer membrane, most likely through Hur. Inner membrane translocation of PyoG requires the conserved inner-membrane AAA^{+}ATPase/protease, FtsH, similar to the situation for *E. coli*-specific colicins. Surprisingly, however, this translocation step also requires TonB1 as well as the unstructured N-terminus of PyoG that binds TonB1. Moreover, inner membrane translocation is dependent on the so-called Pyocin S domain, which is conserved amongst nuclease bacteriocins. Pyocin AP41, like PyoG, requires TonB1 and FtsH to kill *P. aeruginosa* and the unstructured N-terminus of AP41 is similarly involved in binding TonB1. The outer membrane receptor of AP41 remains unknown, but there are indications that FhaC, a putative hemagglutinin transporter, may be the outer membrane receptor and/or translocator.

List of abbreviations

AF488 - Alexa Fluor 488

CD - Circular dichroism

CF - cystic fibrosis

CFTR - cystic fibrosis transmembrane conductance regulator

CFU - colony forming unit

Col - colicin

CPA - common polysaccharide antigen

DMSO - dimethyl sulfoxide

DNA - deoxyribonucleic acid

DSC - Differential scanning calorimetry

DTT - Dithiothreitol

EDTA - Ethylenediaminetetraacetic acid

ESI - Electrospray ionization

h - hours

HEPES - 4-(2-hydroxyethyl)-1-piperazineethanesulfonic acid

Im - immunity protein

IM - inner membrane

IPTG - isopropyl β- d-1-thiogalactopyranoside

ITC - Isothermal titration calorimetry

kDa - kilo Dalton

LPS - lipopolysaccharide

min - Minutes

MMBL - Monocot mannose-binding lectin

MS - Mass spectrometry

NTA - nitrilotriacetic acid

OM - outer membrane

OMP - Outer membrane protein

OSA - O-specific antigen

PBS - phosphate-buffered saline

PCR - Polymerase chain reaction

PMF - Proton motive force

PMSF - phenylmethylsulfonyl fluoride

Pyo - pyocin

SDS - Sodium dodecyl sulphate

SDS-PAGE - Sodium dodecyl sulphate polyacrylamide gel electrophoresis

TBDT - TonB dependent transporter

TEV - Tobacco etch virus-protease

Tm - Melting temperature

Tris - trisaminomethane

v/v - Volume by volume

w/v - Weight by volume

β-OG - n-octyl-β-d-glucoside

Table of Contents

List of Figures

List of Tables

1. General introduction

1.1. Pathogenicity and antibiotic resistance of *Pseudomonas aeruginosa*

P. aeruginosa is a Gram-negative bacterium. The composition of its multi-layered cell envelope enables it to thrive in diverse environments: from water and soil to plant and animal tissues (Moradali *et al.* 2017). In humans, *P. aeruginosa* is an opportunistic pathogen and is particularly problematic in immunocompromised patients. The organism is a common cause of burn and surgical wound infections, eye, skin, bone, joint, urinary tract and lung infections. Such infections can be fatal, especially in the case of chronic pneumonia in patients suffering from cystic fibrosis (CF). CF is a multisystem disease caused by a mutation in the CF transmembrane conductance regulator (CFTR) gene. A resulting defect in chloride ion channels leads to mucus building up in the lungs. This enables *P. aeruginosa* to form robust biofilms in CF lungs, where it adapts to the lung environment and remains unaffected by the host inflammatory response. Chronic pneumonia in CF patients can lead to respiratory failure and death (Azam & Khan 2019). Therefore, there is a need for understanding the pathogenic lifestyle of *P. aeruginosa* and for the development of an efficient antibiotic treatment against this bacterium.

The need for developing antibiotics against *P. aeruginosa* is highlighted by the occurrence of multidrug resistant strains, commonly isolated from hospital equipment and patients with hospital-acquired infections, such as ventilator-associated pneumonia and pneumonia associated with CF (Lister *et al.* 2009). The Antimicrobial Resistance Surveillance in Europe 2015 Report has indicated that *P. aeruginosa* resistance is common (>10% of outbreaks): 13.7% of *P. aeruginosa* isolates were resistant to at least three antimicrobial

groups, and 5.5% of *P. aeruginosa* isolates were resistant to five antimicrobial groups (ECDC, 2015). The molecular mechanisms of *P. aeruginosa* antimicrobial resistance are diverse: alteration of cell envelope permeability, efflux of antibiotics through pumps, degradation or inactivation of antibiotics, and formation of biofilms (Moradali *et al.* 2017). Due to these mechanisms *P. aeruginosa* strains can be resistant to most of the available antimicrobial agents, from carbapenem to the third-generation cephalosporins, which are the preferred options for treating multidrug-resistant bacteria (Azam & Khan 2019). Carbapenem-resistant *P. aeruginosa* strains have been listed as a pathogen of critical priority for research and discovery of new antibiotics (WHO, 2017). Researchers have therefore focused on the development of new therapeutic strategies against multi-drug resistant *P. aeruginosa*: quorum-sensing inhibition, biofilm inhibition and degradation, virulence attenuation, vaccine development, phage therapy, and the development of antimicrobial peptides and proteins (Pang *et al.* 2019).

1.2. The cell envelope of *P. aeruginosa*

As with other Gram-negative bacteria, the *P. aeruginosa* cell envelope is composed of an asymmetric outer membrane with a phospholipid inner leaflet and a lipopolysaccharide (LPS) outer leaflet, a periplasm, and a cytoplasmic membrane with a symmetric phospholipid bilayer (Chevalier *et al.* 2017). The outer membrane of *P. aeruginosa* functions as a selective permeability barrier, since it contains numerous transporters for exchange of signals and nutrients with the environment. The composition of these transporters varies with environmental changes. Different transporters are present in the membranes of planktonic

and biofilm cells, or in free living or pathogenic *P. aeruginosa* (Hill *et al.* 2017; Mordali *et al.* 2017).

1.2.1. Outer membrane transporters of *P. aeruginosa*

The *P. aeruginosa* outer membrane contains numerous channels and transporters (Figure 1-1), such as porins. Porins are β-barrel proteins with water-filled diffusion channels that enable nutrient import. Porin barrels are made of antiparallel β-sheets with hydrophilic residues facing the inside of the barrel. Unlike the porins of *Enterobacteriaceae*, all porins of *P. aeruginosa* are substrate-specific. In other words, *P. aeruginosa* lacks large general porins, like OmpF and OmpC (Chevalier *et al.* 2017). Therefore, the outer membrane of *P. aeruginosa* is characterised by very low permeability, 12.5-fold less permeable than *Escherichia coli*, which partly contributes to the high antibiotic resistance of this bacterium (Hancock & Brinkman 2002). Even though the functions of *P. aeruginosa* porins are not fully understood, they can be split into the following functional groups: control of cell envelope stability (OprF, OprH), sugar uptake (OprB, OprB2, OpdF, OpdO), phosphate uptake (OprP, OprO), amino acid uptake (OprD, OpdC, OpdP, OpdT, OpdI, OprQ, OpdB, OpdJ) and uptake of benzoic acid derivatives (OpdK, OpdL). In summary, porins of *P. aeruginosa* are involved in nutrient import and in the maintenance of outer membrane organisation and integrity (Chevalier *et al.* 2017). The major porin of *P. aeruginosa* is OprF, an 18 sheet β-barrel homologous to OmpA of *E. coli*. It has a peptidoglycan binding domain which anchors the outer membrane to the peptidoglycan layer and is important for maintaining cell shape in varying osmotic conditions. OprF has also been associated with adhesion to lung epithelia, biofilm and outer membrane vesicle formation (Cassin & Tseng 2019). The smallest *P. aeruginosa* porin is an 8 sheet β-

barrel, OprH. It is induced under Mg^{2+} starvation and has been associated with resistance to the polycationic antibiotic, polymyxin B (Young *et al.* 1992). The link between OprH upregulation and polymyxin B resistance is not fully understood, but its LPS binding properties suggest that this porin also has a role in maintaining outer membrane stability (Edrington *et al.* 2011).

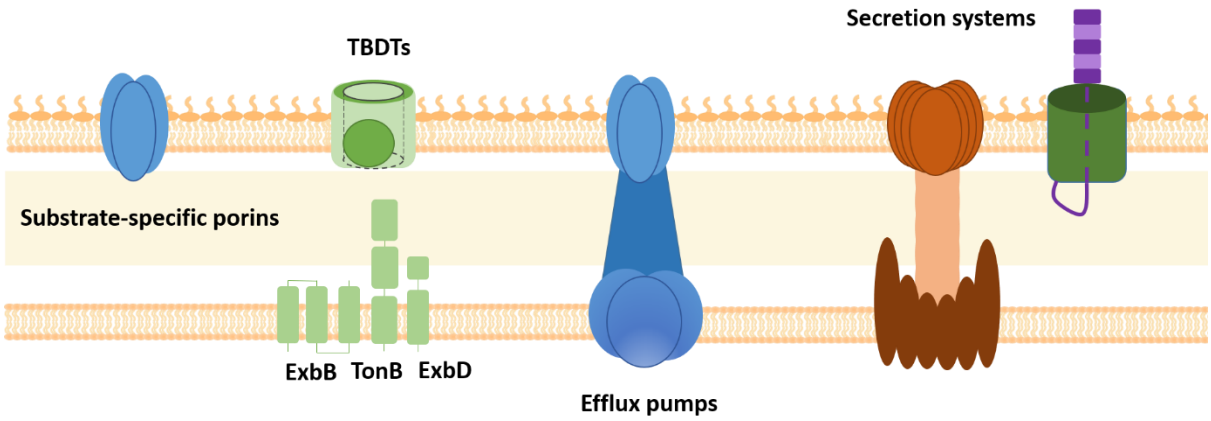

Figure 1-1. A summary of outer membrane protein (OMP) transporters in the *P. aeruginosa* cell envelope. The envelope of *P. aeruginosa* contains substrate specific porins, TonB dependent transporters (TBDTs) coupled to the TonB system in the inner membrane, efflux pumps, and numerous systems for protein secretion.

Another group of outer membrane proteins are the TonB dependent transporters (TBDTs). All TBDTs are energised by the TonB protein system, which links the proton motive force (PMF) generated across the inner membrane with nutrient translocation across the outer membrane. These transporters are larger than porins and consist of a 22-stranded transmembrane β-barrel that encloses a globular plug domain. Ligand binding sites are

formed from residues on the walls and extracellular loops of the β-barrel, and residues on the extracellular side of the plug (Noinaj *et al.* 2010). A conserved TonB binding box is localised in the N-terminus of the plug. After binding of the ligand to the receptor, the transporter undergoes a conformational change. Current models of import, which remain controversial, suggest that the plug domain unfolds and gets pulled by TonB from the periplasmic side of the outer membrane. This dislocates the plug and creates a pore for ligand import (White *et al.* 2017; Hickman *et al.* 2017). Many questions about TBDT driven import remain unresolved: what is the extent of the plug movement and unfolding, does the plug fully exit the barrel of the transporter and are these characteristics of transport conserved for different TBDTs and different ligands across species?

P. aeruginosa TBDTs (Table 1-1) are involved in the uptake of vitamins and chelated metal complexes, typically iron and zinc in the form of siderophores. Siderophores vary in complexity from small molecules such as citrate, to iron-containing proteins, such as hemoglobin and transferrin (Smith & Wilks 2015; Marshall *et al.* 2009; Llamas *et al.* 2006). TBDTs are also involved in the import of zinc (Lhospice *et al.* 2017) and copper (Quintana *et al.* 2017). In addition to their nutrient import function, TBDTs can also serve as surface sensors in signalling cascades, some of which are linked to virulence. Some TBDTs have a signalling domain at the N-terminus. After ligand binding, this sequence interacts with periplasmic proteins and modulates activation of σ factors that regulate virulence factor gene expression. For instance, the ferri-pyoverdine siderophore receptor FpvA activates the PvdS σ factor in the cytoplasm, as a result of ferri-pyoverdine binding to FpvA. PvdS then causes the expression of virulence factors, such as siderophores, exotoxins and endopeptidases (Beare *et al.* 2003). Similarly, VreA is a TBDT with an unknown ligand, which regulates the PUMA3

regulon responsible for the regulation of various *P. aeruginosa* virulence factors (Quesada *et al.* 2016).

Table 1-1. Functions of TonB dependent transporters in the *P. aeruginosa* PAO1.

Protein product	Locus tag	Function	Reference
ChtA	PA4675	Aerobactin receptor	Ciuv *et al.* (2006).
BtuB	PA1271	Cobalamin transporter	Luscher *et al.* (2018).
OprC	PA3790	Copper transport	Quintana *et al.* (2017).
FecA	PA3901	Fe(III) dicitrate transport	Marshall *et al.* (2009).
FptA	PA4221	Fe(III)-pyochelin receptor	Ankenbauer & Quan (1994).
PirA	PA0931	Ferric enterobactin receptor	Ghysels *et al.* (2005).
PfeA	PA2688	Ferric enterobactin receptor	Moynie *et al.* (2019).
FiuA	PA0470	Ferrichrome receptor	Hannauer *et al.* (2010).
FemA	PA1910	Ferric-mycobactin receptor	Llamas *et al.* (2008).
FoxA	PA2466	Ferrioxamine and ferrichrome receptor	Llamas *et al.* (2006).
FpvAI	PA2398	Ferripyoverdine receptor	Shen *et al.* (2005).
FpvAII	PA4168	Ferripyoverdine receptor	Ghysels *et al.* (2004).
HasR	PA3408	Heme uptake	Smith & Wilks (2015).
PhuR	PA4710	Heme/Hemoglobin receptor	Smith & Wilks (2015).
Hur	*PA1302*	Hemin transporter	Otero-Asman *et al.* (2019).
VreA	PA0674	PUMA3 signal transduction pathway, expression of virulence factors	Quesada *et al.* (2016).
FvbA	PA4156	Vibriobactin uptake	Elias *et al.* (2011).
Sppr	PA2057	Xenosiderophore transporter	Pletzer *et al.* (2016).
CntO	PA4837	Zink uptake receptor	Lhospice *et al.* (2017).
	PA0151	Probable TonB-dependent receptors	
	PA0192		
	PA0434		
	PA0781		
	PA1322		
	PA1365		
	PA1613		
	PA1922		
	PA2070		
	PA2089		
	PA2289		
	PA2335		

	PA2590		
	PA2911		
	PA3268		
	PA4514		
	PA4897		
	PA5505		

The *P. aeruginosa* outer membrane also contains transporters involved in ligand export rather than import. Such proteins are implicated in efflux machineries, outer membrane biogenesis, or protein secretion. Efflux pumps are proteinacious active transporters with broad substrate specificity. In *P. aeruginosa*, they are involved in the export of toxins, such as antibiotics and other secondary metabolites. Efflux pumps span the cell envelope and can pump out various antibiotics, which makes them associated with multidrug resistance. There are several families of such pumps, but most of them belong to the resistance nodulation division (RND) family (Venter *et al.* 2015). RND pumps are tripartite and composed of cytoplasmic membrane transporters, periplasmic linker proteins and an outer membrane porin. Some examples are the MexAB-OprM pump, linked to β-lactam resistance (Dreier & Ruggerone 2015), and MexXY-OprM pump, linked to tetracycline, erythromycin, and gentamicin resistance (Azam & Khan 2019). Overexpression of multiple efflux pumps has been found in numerous multidrug-resistant clinical isolates of *P. aeruginosa* (Shigemura *et al.* 2015).

Functions of outer membrane exporters can also be linked to outer membrane biogenesis. Transporters involved in biogenesis are highly conserved between *P. aeruginosa* and other Gram-negative bacteria. One such transporter is BamA, an essential β-barrel outer

membrane protein insertase (Ghequire *et al.* 2018), or LptD, the LPS-assembly protein (Andolina *et al.* 2018).

Finally, *P. aeruginosa* produces a broad panel of secretion systems (TSS), all of which have an outer membrane protein exporter (Bleves *et al.* 2010). *P. aeruginosa* outer membrane transporters can be part of two-step secretion systems (T2SS, T5SS), coupled with the Sec or the Tat machinery in the inner membrane, or build translocons with a one-step mechanism for direct injection of exoproteins from the cytoplasm into the environment (T1SS, T3SS, T6SS). Outer membrane proteins of T1SS form trimers with an extended periplasmic region for direct export of exoproteins. One example is the HasF homo-trimer, which forms a complex with an inner membrane ABC transporter for the export of the HasAp hemophore (Ma *et al.* 2003). Secretins are another type of outer membrane protein involved in protein secretion. They are a part of T2SS or T3SS. Secretins oligomerise and form large channels in the outer membrane which are coupled to other components of the secretion system. One example is XcpQ, an outer membrane T2SS secretin, which is a general secretion system for the export of folded proteins in *P. aeruginosa*. XcpQ assembles a 12 subunit multimer, forming a ring-shaped structure with a 90 Å central cavity, a channel large enough for the passage of folded exoproteins (Douzi *et al.* 2017). T3SS secretins, such as PscC, also oligomerise and form large pores in the outer membrane, allowing the passage of the needle-like structure deployed for one-step secretion (Galle *et al.* 2012). T5SS exporters are β-barrels in the outer membrane, involved in autotransport or two-partner secretion. Autotransporters form a barrel in the outer membrane and then expose a catalytic passenger domain on the cell surface. On the other hand, β-barrels of two-partner secretion systems are separate from the exported passenger protein. One example is the LepA transporter, required for the secretion of the LepA protease involved in the activation of the host inflammatory response

(Bleves *et al.* 2010); or the filamentous hemaggluitinin (FHA) system, in which the FHA transporter secretes FHA, a molecule linked to cell adhesion and virulence (Sun *et al.* 2016). The system has also been linked to a bacterial competition mechanism called contact dependent inhibition (Mercy *et al.* 2016).

1.2.2. The TonB system

The TonB system enables energy coupled transport across the outer membrane and the transduction of extracellular signals. It has been linked to nutrient import in Gram-negative bacteria (Braun 1995), but also to protein secretion in *Myxococcus xanthus* (Gomez-Santos *et al.* 2019). By a mechanism that has yet to be fully elucidated, the TonB system couples the PMF across the inner membrane with events at the outer membrane. The system is composed of three inner membrane proteins: ExbB, ExbD, and TonB.

The transmembrane topology and organisation of the TonB-ExbB-ExbD complex is conserved between *E. coli* and *P. aeruginosa* (Zhao & Poole, 2009). TonB and ExbD have a similar topology: a short N-terminal domain, a transmembrane domain, a flexible linker, and a C-terminal periplasmic domain. The periplasmic domain of TonB is larger than that of ExbD. It extends through the periplasm to interact with outer membrane proteins. ExbB has three transmembrane segments and a cytoplasmic domain (Postle & Kadner 2003). The three proteins act as part of a complex. Five copies of ExbB are arranged as a pentamer around a ExbD dimer, forming a channel for proton passage (Figure 1-2). The inner membrane helix of TonB directly interacts with the ExbBD oligomer. This organisation of the complex enables proton channelling through ExbBD to link the PMF and conformational changes of TonB, which in turn can change conformation of outer membrane proteins (Celia *et al.* 2019). ExbBD

is homologous to MotAB, a membrane-embedded motor complex of the bacterial flagellum. Like ExbBD, MotAB is composed of a central rotor MotB dimer surrounded by 5 MotA stator units (Deme *et al.* 2020). This structural homology between ExbBD and MotAB implicates that the TonB system undergoes rotational motion in the cell envelope.

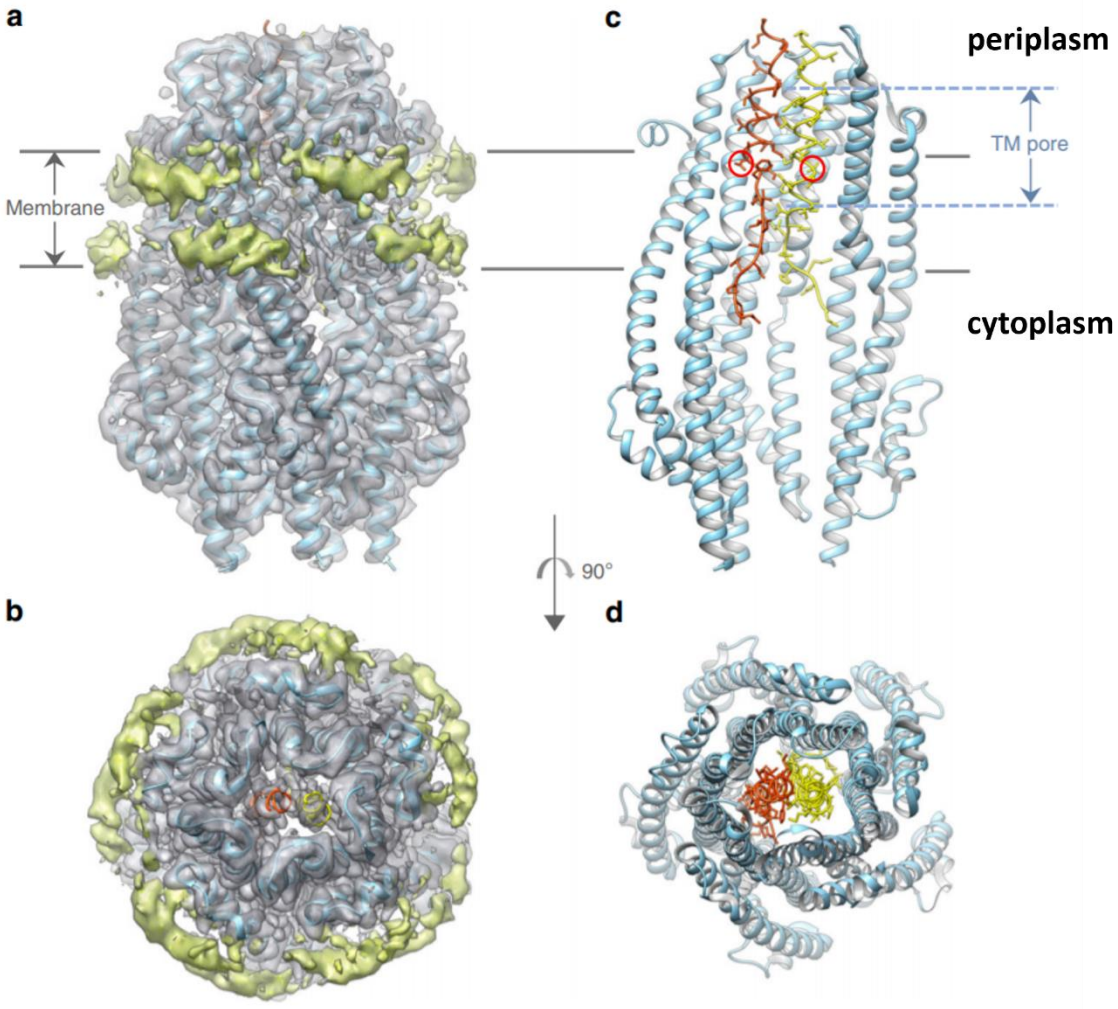

Figure 1-2. Cryo-EM Structure of the ExbB-ExbD complex in lipid nanodiscs. a – Perpendicular view. The proteins are shown in gray, while the nanodisc is shown in green. The boundary of the nanodisc allows one to estimate the position of the lipid membrane. B - View from the

periplasm. c - Ribbon representation of the reconstructed atomic model. The ExbB pentamer is shown in cyan. For clarity, only three ExbB subunits are represented. The two TM domains of the two ExbD subunits are shown in red and yellow. D - Ribbon representation of the reconstructed atomic model, viewed from the periplasm. Image taken from Celia *et al.* (2019).

Several models have been proposed to explain how TonB transduces the PMF to the outer membrane: the propeller model, the shuttle model, the rotational surveillance and energy transfer (ROSET) model and the pulling model (Celia *et al.* 20). In the propeller model, a TonB dimer undergoes a rotary motion in a PMF dependent manner. TonB binds the TonB box of a TBDT and rotates to pull the TBDT plug, enabling ligand import. In this way, the energy of the rotary motion gets transduced to the outer membrane (Postle & Kadner 2003). The model is challenged by crystal structures of several TBDTs demonstrating that only one copy of TonB binds to the TBDT (Postle *et al.* 2010). In the shuttle model it is proposed that energised TonB shuttles between the two membranes to deliver its energy to the TBDT, but this model has been abandoned (Postle & Kadner 2003). The ROSET model, like the propeller model, suggests that TonB rotation is required for energy transduction. Rotational motion is supported by *in vivo* experiments with GFP-TonB, demonstrating that TonB motion depends on ExbB, ExbD and the PMF. The ROSET model also includes a role for the dimer of TonB: one copy could bind to peptidoglycan and position the other copy in proximity of the TBDT (Klebba 2016). In the pulling model, the periplasmic domain of TonB binds to the ligand-bound TBDT. The Ton complex then exerts a pulling force that partially unfolds the TBDT plug, allowing the ligand to pass into the periplasm. This model is supported by molecular dynamics simulations, which demonstrate that the interaction between TonB and the TBDT is strong enough for

TonB to remain attached to the TonB box while the applied force gradually unfolds the plug domain (Chimento *et al.* 2005). In addition, atomic force microscopy experiments demonstrate that the TonB-TBDT interaction is strong enough to sustain extension and partial unfolding of the plug (Hickman *et al.* 2017). Recent spin labelling experiments suggest that an allosteric change of the plug, rather than its pulling/unfolding, is sufficient for the opening of the TBDT and ligand import (Nilaweera *et al.* 2021).

In *P. aeruginosa* there are 3 isoforms of the TonB protein (TonB1, TonB2, TonB3), each associated with a different cellular function. TonB1 is linked to iron acquisition and cell signalling. Its periplasmic domain interacts with TBDTs in the outer membrane, providing energy for ligand import. Apart from mediating ligand import, interaction of TonB1 and a TBDT can trigger signalling cascades, as mentioned in section 1.2.1. For instance, TonB1 is necessary for the import of the siderophore pyoverdine through the FpvA receptor. The interaction of TonB1 and the FpvA plug is also necessary for the activation of σ factors involved in the regulation of FpvA and pyoverdine synthesis, in response to extracellular iron (Shirley & Lamont 2009). TonB2 is also coupled with ExbB-ExbD, but its role has yet to be discovered. Unlike TonB1, TonB2 is not essential for growth under iron starvation, but is nevertheless upregulated during iron limitation. Therefore, the involvement of TonB2 in iron acquisition is not clear (Zhao & Poole 2000). It is not known if the third isoform, TonB3, is coupled with ExbB-ExbD, but there is evidence of its involvement in twitching motility and extracellular assembly of Type IV pili (Huang *et al.* 2004).

1.2.3. The cell envelope and iron acquisition

Iron is essential for the growth and virulence of *P. aeruginosa* (Minadri *et al.* 2016). Therefore, this bacterium has several iron acquisition systems and can scavenge both ferrous (Fe^{2+}) and ferric (Fe^{3+}) iron. Transport of Fe^{2+} depends on outer membrane porins and the Feo system. Fe^{3+} can be taken up in several forms: ferri-siderophores, heme and heme–protein complexes, ferric–transferrin/lactoferrin complexes, and ferric–citrate. Transport of ferric complexes depends on specific TBDTs and the TonB1-ExbB-ExbD complex.

Fe^{2+} is the predominant form of iron in anaerobic conditions, or in microaerobic conditions and low pH. *P. aeruginosa* can generate Fe^{2+} via the extracellular reduction of Fe^{3+} involving phenazine compounds (Cornelis & Dingemans 2013). Fe^{2+} is more soluble then Fe^{3+}, and can diffuse freely through outer membrane porins (Minandri *et al.* 2016). Fe^{2+} is further transported across the inner membrane by the Feo system. The system is composed of 3 proteins: FeoB, a GTPase that forms a channel in the inner membrane for Fe^{2+} import (Seyedmohammad *et al.* 2016), and two probable transcription regulators, FeoA and FeoC (Lau *et al.* 2016).

Fe^{3+} is the predominant form of iron in aerobic conditions. It is highly insoluble and usually sequestered in the form of ferric salts, oxides, or bound to host iron-binding proteins. To obtain this form of iron *P. aeruginosa* produces siderophores, iron chelating molecules, that can take up ferric iron from the environment. Two major siderophores of *P. aeruginosa* are pyochelin and pyoverdin. Both chelate iron in the extracellular medium and transport it into the cell *via* a specific TBDT: FptA transports pyochelin (Ankenbauer & Quan, 1994) and FpvA transports pyoverdin (de Chial *et al.* 2003). *P. aeruginosa* can also uptake xenosideophores, siderophores produced by other microorganisms. For instance, FiuA and

FoxA are two *P. aeruginosa* TBDTs that can transport ferrichrome, a siderophore of fungal origin (Hannauer *et al.* 2010; Ciuv *et al.* 2007). Siderophore uptake systems also involve inner membrane and cytoplasmic sigma and anti-sigma factors. Therefore, siderophores trigger signalling cascades and feedback loops that regulate the production of the siderophore and its uptake system components (Beare *et al.* 2003). In this way, *P. aeruginosa* can tune siderophore production with the availability of iron in the medium. Siderophore-dependent signalling cascades are also linked to regulation of virulence factor expression and *P. aeruginosa* pathogenesis (Minandri *et al.* 2016; Beare *et al.* 2003).

For successful host colonisation, *P. aeruginosa* has to acquire iron from host tissues. In mammalian hosts, iron is mostly bound to iron binding proteins, such as transferrin and lactoferrin, or present in the form of heme and bound to hemoproteins. Siderophores of *P. aeruginosa* can compete with iron-binding proteins of the host (Xiao & Kisaalita 1997), or *P. aeruginosa* can acquire iron from heme, heme derivatives, and hemoglobin via two import systems: Phu and Has (Figure 1-3). In the Phu system, heme, or hemin, a chlorinated form of heme, is directly extracted from hemoglobin by a TBDT called Phu. Phu can also bind free heme. In the Has system, heme is first extracted by a secreted protein, the HasA hemophore. The hemophore-heme complex is then recognised by a TBDT called HasR. Once in the periplasm, heme binds to a periplasmic binding protein (PhuT) and gets transported into the cell by an ABC transporter (PhuUVW). In the cytoplasm, heme binds to a heme chaperone and is then delivered to the heme oxygenase HemO to be degraded to biliverdin and free Fe^{2+} (Cornelis & Dingemans 2013).

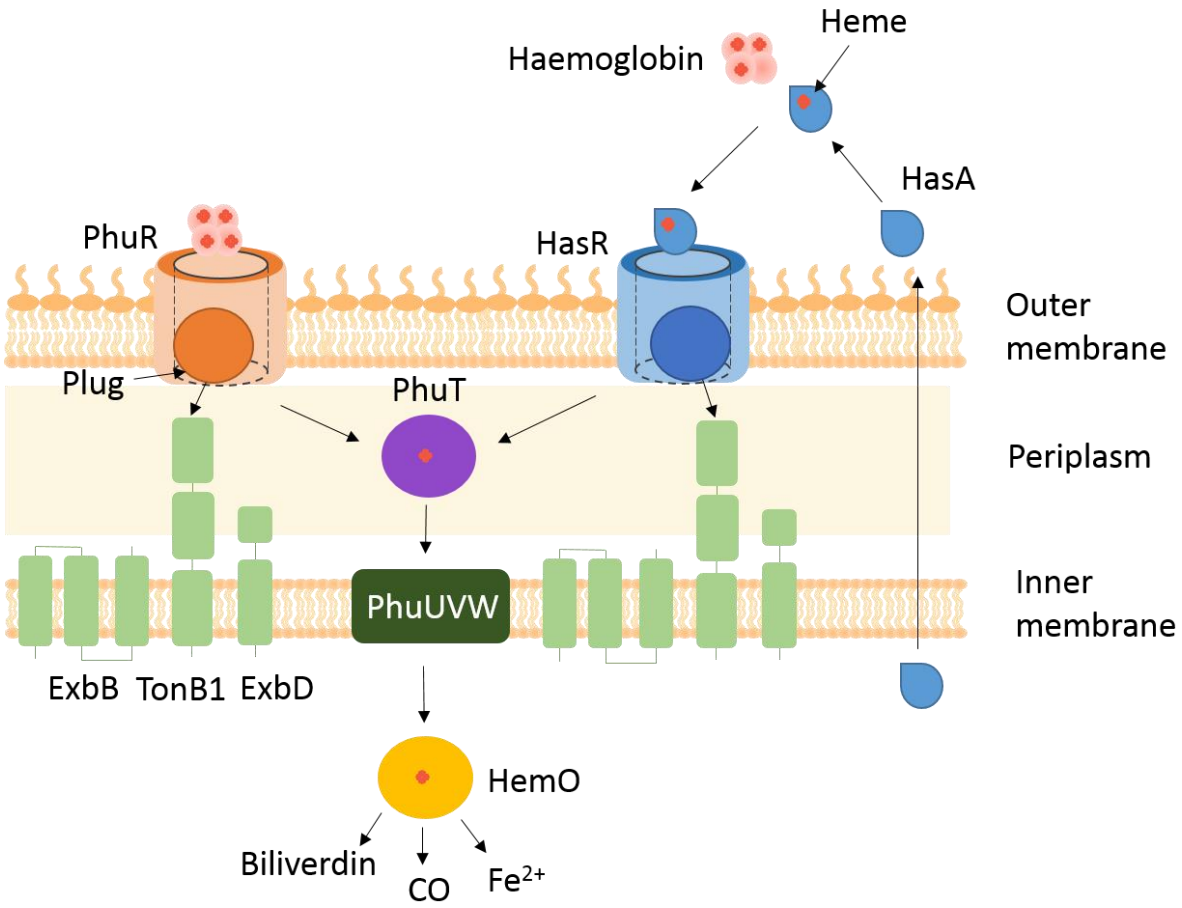

Figure 1-3. Heme import systems of *P. aeruginosa*. Two heme import systems of *P. aeruginosa* are Phu and Has. The Phu system is composed of PhuR, an outer membrane TonB dependent transporter. PhuR binds heme through interaction with hemoglobin. Upon heme binding, PhuR interacts with TonB1 in the periplasm via a plug domain and undergoes a conformational change that opens a channel for heme passage. HasR does not take up heme from hemoglobin directly, but via the HasA hemophore released by the cell. HasR is also coupled to TonB1. Once heme enters the periplasm, it binds to a periplasmic binding protein (PhuT) and is transported to the cytoplasm via ABC transporters (PhuUVW). In the cytoplasm, heme binds to HemO, a heme oxygenase, that oxidises heme to biliverdine and releases soluble Fe^{2+} into the cell.

1.2.4. The cell envelope and antibiotic development

The *P. aeruginosa* cell envelope serves as a permeability barrier that enables selective exchange of molecules between the cell and its environment. This function of the envelope is essential in *P. aeruginosa* pathogeneses for several reasons. The highly selective permeability of the *P. aeruginosa* envelope, caused primarily by selectivity of its porins, protects this bacterium from host molecules that can be toxic to the bacterium. This is also the *P. aeruginosa* mechanism of resistance to many antibiotics (Chevalier *et al.* 2017). Additionally, the composition of the *P. aeruginosa* envelope varies greatly with changes in the environment during the course of an infection (Moradali *et al.* 2017). An important aspect of this is the upregulation of nutrient uptake systems that enable *P. aeruginosa* to scavenge nutrients from host tissues, such as iron uptake systems (Cornelis & Dingemans 2013). Therefore, the cell envelope is a valuable source of new targets for the design of antibiotics and antivirulence factors directed against *P. aeruginosa*.

Most antibiotics used to treat *P. aeruginosa* infections must penetrate the cell envelope to reach intracellular targets. *P. aeruginosa* responds to the presence of antibiotics by decreasing the number of non-specific porins and replacing them by more selective channels for nutrient uptake. Changes in porin content and expression levels have been associated with resistance to broad-spectrum drugs such as carbapenems and cephalosporins. For example, down-regulation of the OprD porin has been associated with carbapenem resistance in clinical *P. aeruginosa* isolates (Pang *et al.* 2019). Therefore, more promising antibiotics for *P. aeruginosa* would be those that target outer membrane transporters which are essential for virulence and get upregulated during host infection. Some currently investigated antimicrobials that exploit virulence associated cell envelope

components in *P. aeruginosa* are: protein epitope mimetic molecules, lectin inhibitors, HasA-antimicrobial complexes, and pyocins.

The LPS biosynthesis pathway is a potential antibiotic target since it is essential in *P. aeruginosa* and other Gram-negative bacteria. During outer membrane biogenesis, new LPS is transported to the cell surface by the LPS transport machinery (LptA-G). The final transport step, from the periplasm to the cell surface, is enabled by the outer membrane transporter LptD and the periplasmic lipoprotein LptE. The normal functioning of the LptD-E complex has also been linked to antibiotic resistance and virulence of *P. aeruginosa* (Lo Sciuto *et al.* 2018). The LptD-E complex and LPS transport can be inhibited by a newly discovered family of macrocyclic protein epitope mimetic molecules, such as murepavadin. Murepavadin is currently in clinical trials for the treatment of multidrug resistant *P. aeruginosa* infections. It binds to the periplasmic domain of LptD to block LPS transport (Andolina *et al.* 2018).

Lectins are bacterial outer membrane proteins that mediate adherence to host tissues. In *P. aeruginosa*, they mediate adherence to lung epithelia and are important for biofilm formation. Therefore, lectin inhibitors are being considered as agents for the prevention of *P. aeruginosa* infections, or for the disruption of the initial attachment of *P. aeruginosa* to human lung epithelia (Pang *et al.* 2019). For example, GalAG2, a glycopeptide dendrimer, binds a *P. aeruginosa* lectin LecA and inhibits biofilm formation *in vitro* (Kadam *et al.*, 2011).

HasA, a hemophore of the *P. aeruginosa* HasAP system, is important for iron acquisition and virulence (Figure 1-3). It enables *P. aeruginosa* to pirate extracellular heme in host tissues. HasA binds heme and other porphyrins and delivers them to the cell through the HasR receptor. HasA is rather promiscuous and can capture a plethora of hydrophobic metal

complexes (Shirataki *et al.* 2014). Therefore, the HasRA route can be exploited for the delivery of antimicrobials which HasA can bind. One such antimicrobial is gallium phthalocyanine (GaPc). HasA enabled the water insoluble GaPc to be mistakenly acquired by *P. aeruginosa* through HasR. GaPc can then be activated by near infrared radiation, and used for photosterilization of *P. aeruginosa* (Shisaka *et al.* 2019).

1.3. Pyocins of *P. aeruginosa*

Another group of antimicrobials against *P. aeruginosa* are pyocins. Pyocins are protein antibiotics of *P. aeruginosa* that have a narrow-spectrum of activity against this bacterium. These proteins could be developed into new antimicrobials for treating *P. aeruginosa* infections, as demonstrated in various *in vivo* models (Behrens *et al.* 2017). Pyocins are effective in a murine lung infection model (McCaughey *et al.* 2016b) and can kill *P. aeruginosa* in biofilms (Smith *et al.* 2012). An advantage of developing the clinical use of pyocins is their potency and narrow spectrum activity against *P. aeruginosa*. Their modular organisation means they can be readily engineered to alter strain specificity (Kageyama *et al.* 1996). They seem not to be toxic for the host (Behrens *et al.* 2017), but little is known about the antigenicity of pyocins and their effect on the host immune system.

Pyocins belong to a larger group of proteinaceous antibiotics, called bacteriocins. Like all bacteriocins, pyocins are used by *P. aeruginosa* to compete for resources by killing competitors, usually of the same bacterial species. Pyocin expression is regulated through the PrtN activator, that binds to P-box elements in pyocin promoters upon DNA damage. PtrN binding to DNA requires RecA dependent cleavage of the PtrR repressor (Ghequire & De Mot 2014). Pyocin producers express the toxin together with an immunity protein that inhibits

pyocin toxicity. In this way, a producer is protected from its own pyocin. In the case of nuclease pyocin-immunity pairs, the complex is released from the cell by an unknown mechanism. Pyocins can then bind to the sensitive strain, which doesn't produce the immunity protein (Figure 1-4). To reach their cellular target pyocins interact with proteins in the cell envelope that assemble energised import machineries called translocons (Atanaskovic & Kleanthous 2019). Understanding how pyocins target and kill bacterial cells will help explain their narrow-spectrum killing activity and aid in the clinical development of this class of *P. aeruginosa* specific antibiotics.

1.3.1. Pyocin diversity

Pyocins, their translocon components, and their cellular targets, vary extensively, which is an advantage of their potential clinical application. All pyocins can be categorised into three groups based on their structure: modular pyocins, lectin-like pyocins, and tailocins (Figure 1-5).

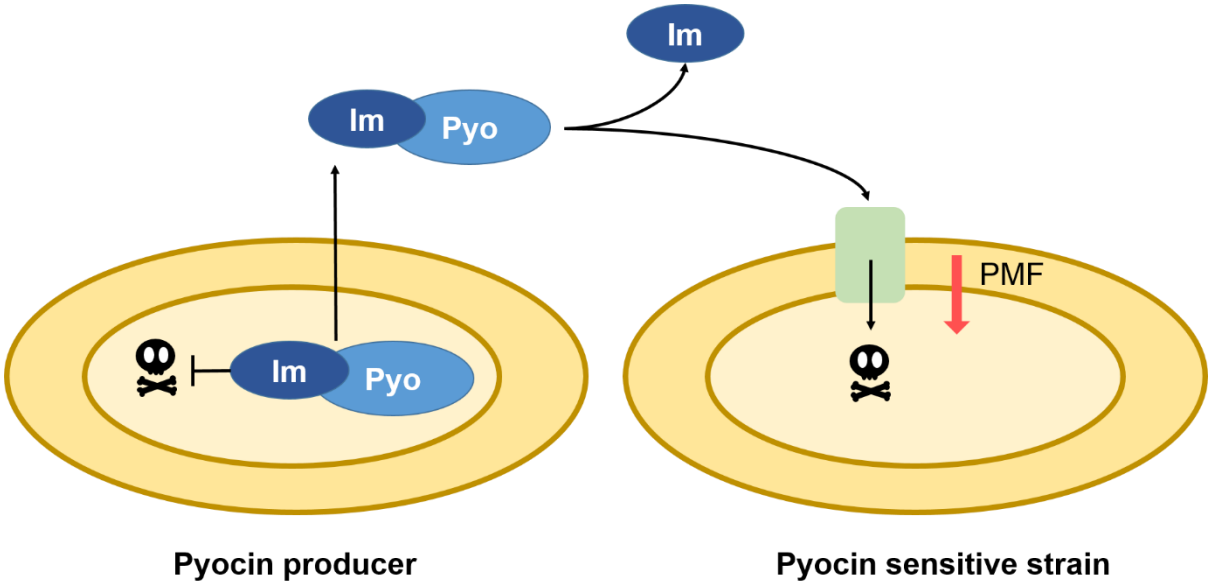

Figure 1-4. Pyocins are used for intraspecies competition by *P. aeruginosa*. A pyocin producing strain is protected from its own pyocin (Pyo) by an immunity protein (Im), which binds to the pyocin and inhibits its toxic activity. The Pyo-Im complex is released from the producing cell by an unknown mechanism. The pyocin is then transported though the envelope of the sensitive strain in a PMF-dependent manner, to reach its cellular target and cause cell death. Cell envelope components involved in pyocin translocation compose the pyocin translocon and are here labelled with a green box (figure modified from Atanaskovic *et al.* 2020).

Modular pyocins have a similar modular structure to colicins, bacteriocins of *E. coli* (Cascales *et al.* 2007). Their size varies significantly, ranging from 289 amino acids for pyocin PaeM to 777 amino acids for pyocin AP41 (Ghequire & De Mot 2014). Modular pyocins are elongated, helical, multidomain proteins, with domains linked to translocation at the N-terminus, and a cytotoxic domain at the C-terminus (Figure 1-5A). The immunity protein forms an ultra-high-affinity complex with the cytotoxic domain and inhibits its activity (Behrens *et*

al. 2020; Joshi *et al.* 2015). Modular pyocins display a range of killing mechanisms: nucleases that kill cells by DNA or RNA degradation; pore formers that kill cells by forming pores in the inner membrane; pyocins that inhibit peptidoglycan biosynthesis through lipid II degradation (Ghequire & De Mot 2014).

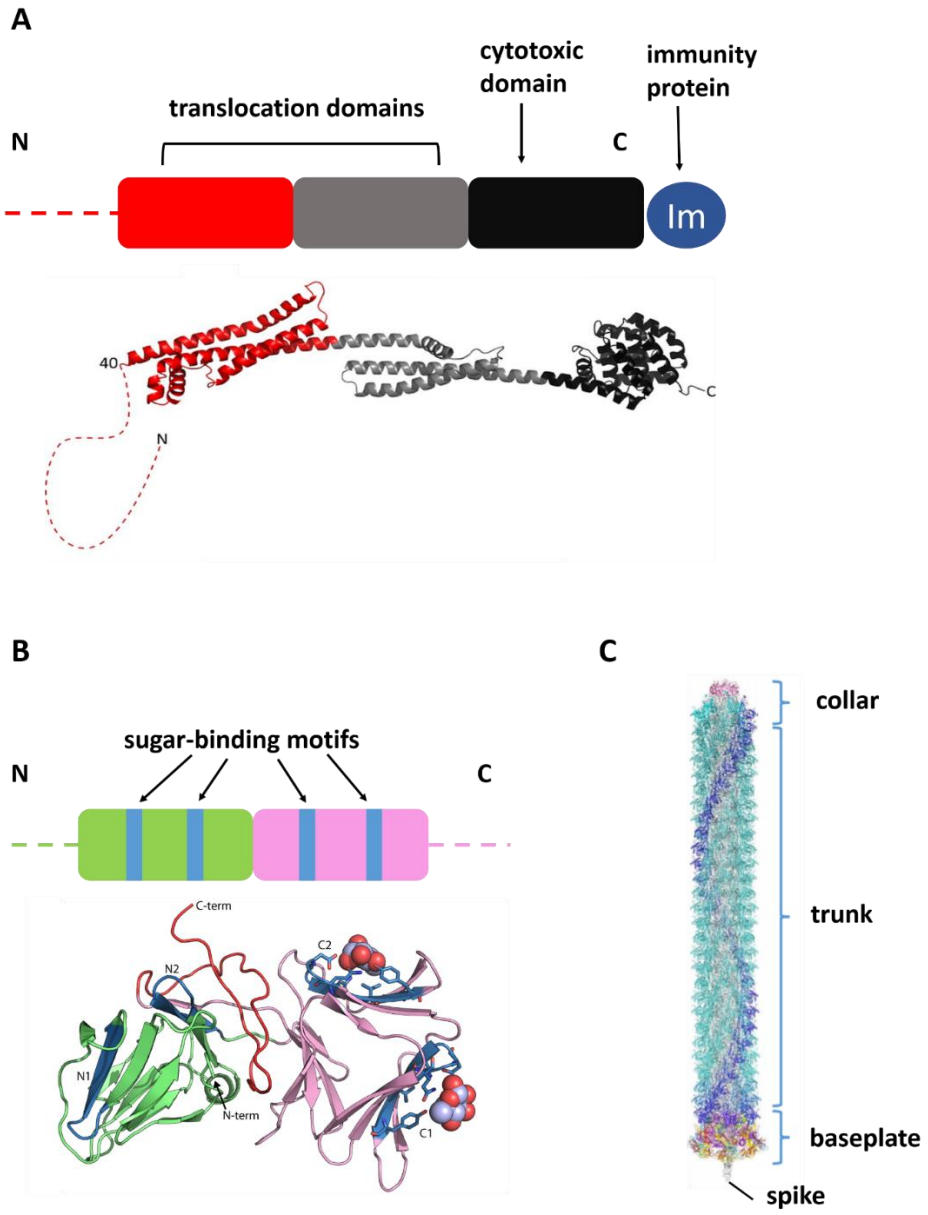

Figure 1-5. Diversity of pyocins. Based on their structure, complexity and organisation, pyocins of *P. aeruginosa* group into modular pyocins (A), lectin-like pyocins (B) and tailocins (C). A – a modular pyocin is composed of several domains. There is always one cytotoxic

domain at the C-terminus, and at least two domains involved in the translocation process. The cytotoxic domain interacts with the immunity protein (Im), which inhibits its enzymatic or pore-forming activity. The translocation domains interact with cell envelope proteins that translocate the pyocin to its cellular target. The N-terminus is generally unstructured - shown as a dashed line. For illustrative purposes, the crystal structure of pyocin S5 (PyoS5; residues 40 to 505) is shown. The two translocation domains are shown in red and grey, and the pore-forming cytotoxic domain is in black. The first 39 residues are not resolved and are represented (to scale) by a red dashed line (structure representation taken from Behrens *et al.* (2020)). B – lectin like pyocins are also multi domain proteins, but lack a definitive cytotoxic domain. They have several monocot mannose-binding lectin motifs that bind to D-rhamnose in the *P. aeruginosa* LPS. The crystal structure of pyocin L1 (residues 2-256) in complex with α-D-rhamnose is shown. The N-terminal domain is shown in green and the C-terminal domain in pink. α-D-rhamnose is represented as spheres, and sugar binding motifs are highlighted in blue (structure representation taken from McCaughey *et al.* (2014)). C – tailocins are multi-protein pyocins of *P. aeruginosa*. Their structure resembles bacteriophage tails. Tailocins are composed of a multimeric trunk connected to a baseplate. Tail fiber proteins extend from the baseplate and attach to proteins on the bacterial cell surface. Contraction of the trunk inserts the core of the trunk in the envelope, which then perforates the inner membrane and kills the cell via the spike proteins. Cryo-EM structure of tailocin R2 is shown (Ge *et al.* 2020). Tail fiber proteins and the inner trunk are not visible in the structure.

Nuclease pyocins are translocated to the cytoplasm where they degrade nucleic acids causing cell death. Most nuclease pyocins share a conserved HNH motif in their cytotoxic

domain. It consists of two antiparallel β-strands connected with a loop and flanked by an α-helix with a divalent cation binding site between the two (Walker *et al.* 2002). Another conserved domain in nuclease pyocins is the Pyocin S domain. Since this domain is specific to pyocins that translocate across the inner membrane to kill bacterial cells, it has been suggested that it is associated with inner membrane translocation (Sharp *et al.* 2017). Pyocins that are very similar in their N-terminal translocation domains, but differ in their cytotoxic domain, belong to the same pyocin group and share the same translocation pathway (Sharp *et al.* 2017). Seven such groups of nuclease pyocins have been found in *P. aeruginosa* genomes (Figure 1-6): S1 (pyocins S1, S6, SD1 and G), S2 (pyocin S2, SD2, S7), S3 (pyocin S3, SD3, S3C), S4 (pyocin S4), S9 (pyocin S9), Sn (pyocin Sn) and the AP41 group (pyocin AP41 and S8). Both pyocin G (PyoG) and pyocin Sn have been detected only *in silico* by a bioinformatic pipeline that searches for genes containing the Pyocin S domain in *P. aeruginosa* (Sharp *et al.* 2017). Both G and Sn are predicted to be non-HNH nucleases. Together with pyocin S3 (Ghequire & De Mot 2014), these are the only 3 non-HNH nucleases in *P. aeruginosa*.

A

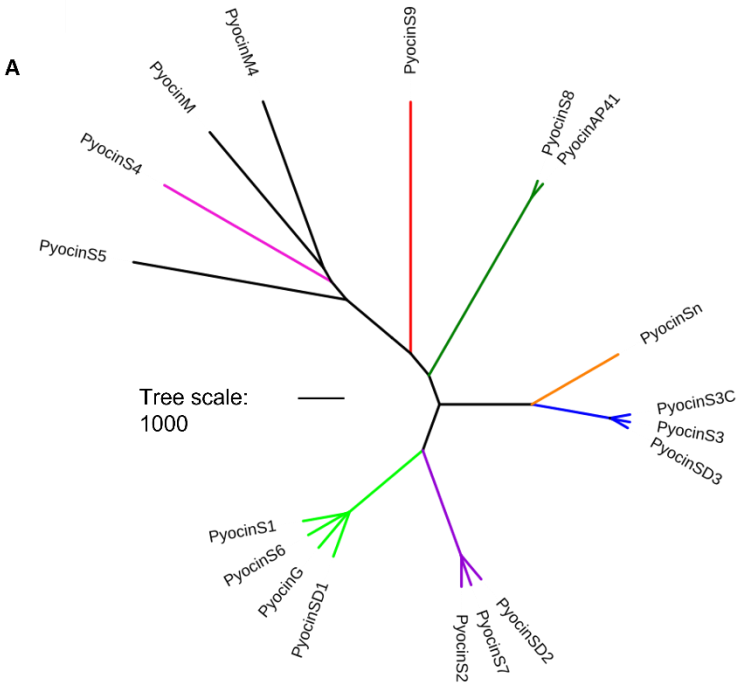

B

C

Group	Pyocin	Mode of action	Receptor/translocator
AP41	AP41	DNase (HNH)	??
	S8	DNase (HNH)	
S1	S1	DNase (HNH)	??
	SD1	tRNase	
	S6	rRNase	
	G	Nuclease	
S2	S2	DNase (HNH)	CPA/FpvAI
	SD2	tRNase	
	S7	rRNase	
S3	S3	DNase	CPA/FpvAII
	SD3	tRNase	
	S3C	DNase (HNH)	
S4	S4	tRNase	FpvAI
S9	S9	DNase (HNH)	??
Sn	Sn	Nuclease	??
S5	S5	Pore forming	CPA/FptA
M	PaeM	Lipid II degradation	FiuA
M4	PaeM4	Lipid II degradation	Hur

Figure 1-6. The diversity of modular pyocins from *P. aeruginosa*. A - The phylogenetic tree was calculated in Jalview (Waterhouse *et al.* 2009) using the Neighbour-joining method based on the alignment of pyocin translocation domains. Nuclease pyocin groups are labelled with different colours. Pyocins of the same group cluster based on the similarity of their

translocation domains. Therefore, they likely share the same or similar translocation machinery in the cell envelope, but may kill the cell by different mechanisms. B – structure of the conserved Pyocin S domain (ColE9$^{170-300}$, PDB 5EW5), which was used for the search of nuclease pyocins in *P. aeruginosa* genomes (Sharp *et al.* 2017). C - In the table, the names of pyocin groups are listed, together with the killing mechanism and known components of the translocation machinery. The work in this thesis focuses largely on the uptake pathway of PyoG from the S1 group, as well as work on pyocin AP41.

Less is known about the diversity of pore forming and lipid II degrading pyocins. Pore forming pyocins act by translocating to the periplasm and depolarising the inner membrane. Unlike immunity proteins of nuclease pyocins, which are cytoplasmic, immunity proteins of pore forming pyocins insert in the inner membrane to block pore formation by a poorly understood mechanism. The only pore former described in *P. aeruginosa* is pyocin S5 (PyoS5; Figure 1-5A). This pyocin is effective *in vivo* – it can rescue mice from a lethal *P. aeruginosa* lung infection if a single 75 µg dose is applied intranasally 1 h post-infection (McCaughey *et al.* 2016b). The PyoS5 structure harbours valuable information for understanding the killing mechanism for this group of pyocins. It is composed of a pore forming domain and two tandemly repeated helical domains, which are also present in other pyocins. These two domains have distinct functions in the import process: one recognises a component of the *P. aeruginosa* LPS, the common polysaccharide antigen (CPA), to concentrate the pyocin on the cell surface, while the other domain interacts with the S5 translocator, FptA, in the outer membrane (Behrens et al 2020). The two lipid II degrading pyocins of *P. aeruginosa* are PaeM (Barreteau*et al.* 2012) and PaeM4 (Ghequire & Ozturk 2018). They share a cytotoxic domain

similar to colicin M, but the N-terminal domains are different (Figure 1-6), indicating that these two pyocins have a distinct import mechanism.

Lectin-like pyocins, contrary to colicin-like pyocins, do not contain a known cytotoxic domain and an immunity protein (Ghequire *et al.* 2018a). Their killing is genus rather than species-specific. The key feature of lectin-like pyocins is the presence of tandem monocot mannose-binding lectin motifs (Figure 1-5B). Pyocin L1 is the best characterised lectin-like pyocin in *P. aeruginosa*. It binds to D-rhamnose with high affinity (McCaughey *et al.* 2014). D-rhamnose is a sugar specific for the CPA of *P. aeruginosa*. Therefore, the interaction with D-rhamnose enables L1 to target *P. aeruginosa* and accumulate on its surface. The amino-terminal domain of lectin-like pyocins interacts with a polymorphic external loop of the outer membrane protein insertase BamA (Ghequire *et al.* 2018b). This inhibits outer membrane biogenesis and leads to cell death, but the exact mechanism by which lectin-like pyocins inhibit the BamA function is still unknown.

Tailocins are phage tail-like bacteriocins of *P. aeruginosa*. Based on structural differences, this group splits into R and F-type tailocins (Ghequire & De Mot 2014). R-type tailocins (Figure 1-5C) are built from a double hollow cylinder that consists of a rigid inner core and a contractile outer trunk. The tip of the inner core contains spike proteins. A baseplate is attached to the trunk, serving as a docking point for the six tail fibres. As with bacteriophages, the fibres have a role in anchoring the tailocin to target cells, usually through the binding of LPS. Proteins that define strain-specificity are located at the distal portion of the fibres (Williams *et al.* 2008). F-type tailocins, similar to R-type pyocins, are rods with a baseplate and fibres for target cell binding, but they lack the outer trunk. Both types kill cells in the same way: after binding to target cells, the tailocin contracts, the core inserts in the

envelope, and the spike proteins perforate the inner membrane causing depolarisation and cell death (Ghequire & De Mot 2014).

1.3.2. Discovery of pyocin receptors and translocators

To kill competitors, pyocins first have to be imported into target cells. Import begins with binding of the pyocin to a receptor and subsequently a translocator, which could be the same protein, on the surface of sensitive cells. The specificity of a pyocin-receptor interaction narrows down the target range of these toxins. Therefore, pairing up bacteriocins and their receptors can aid their clinical application. If pyocin-receptor pairs are known, it can also be established which strains of *P. aeruginosa* are sensitive to a specific pyocin, or which combinations of pyocins can be used for the killing of a specific strain (Atanaskovic & Kleanthous 2019).

To date, several pyocins have been paired-up with their receptors, which are either LPS or specific TBDTs in the *P. aeruginosa* cell envelope (Figure 1-6). Out of 7 groups of nuclease pyocins, receptors are known for 3 (Ghequire & De Mot 2014). All 3 of these are different isoforms of FpvA, the ferric-pyoverdine receptor. It is still unknown if nuclease pyocins can parasitise nutrient import routes other than that of pyoverdine. Therefore, discovery of new pyocin receptors will be important for broadening our understanding of the import mechanisms these modular toxins employ. Here, the approaches which have been used previously for the discovery of new receptors and translocators of modular bacteriocins are summarised.

Bacteriocin neutralization experiments can be used to determine if a bacteriocin receptor is within the protein or LPS fraction of the outer membrane (Weltzien & Jesaitis 1971). If a bacteriocin is mixed with a cell fraction that contains the receptor, this fraction will inhibit its toxic activity. Neutralization experiments have also been used to test if a specific nutrient import pathway is hijacked by a bacteriocin. Competitive ligand binding can block either bacteriocin activity or nutrient uptake. For example, such experiments suggested that pyocin S3 and pyoverdine both bind to the FpvAII receptor in *P. aeruginosa* (Baysse *et al.* 1999). An alternative approach in receptor discovery is one that combines neutralization assays with cell wall fractionation and protein purification. The first step is to single out an outer membrane sub-fraction which contains receptor neutralization activity. Further analysis by mass spectrometry can aid receptor discovery. Fractionation is usually performed simultaneously for membranes of bacteriocin resistant and sensitive strains, in order to find fractions which have neutralizing activity only in the bacteriocin sensitive strain (Sabet & Schnaitman 1973). A limitation to neutralization experiments is that they require high receptor yields in membrane fractions.

Bacteriocin receptors can also be identified by pull-downs, using a bacteriocin of interest as bait. Bacteriocin-receptor complexes can be co-eluted from affinity columns and tryptic peptides analysed by mass spectrometry for receptor identification. For example, hexahistidine-tagged immunity protein complexed to colicin E9 (ColE9) and immobilised on a nickel affinity column was used to purify components of the ColE9 translocon from *E. coli* cell envelope extracts (Housden *et al.* 2005). Again, low expression levels of the receptor, or low binding affinity between the receptor and the bacteriocin, can be a challenge in this approach. This can be overcome by defining growth conditions which induce an increase in bacteriocin sensitivity due to receptor overexpression. For instance, pyocins S2, S3, S4 and S5 are more

effective if *P. aeruginosa* is cultivated in iron-deprived media due to the upregulation of siderophore receptors that are hijacked by the pyocin (Baysse *et al.* 1999; Denayer *et al.* 2007; Elfarash *et al.* 2012, 2014).

Bacteriocin receptors can also be identified by the isolation and characterisation of bacteriocin-resistant mutants (Cotter 2014; McCaughey *et al.* 2014). Picking up genetic differences between resistant and sensitive strains can pinpoint the receptor gene. A major challenge in this approach is to distinguish between resistant and tolerant strains and to rule out possible indirect effects of detected mutations. Therefore, it is always necessary to rule out tolerance by testing growth kinetics of isolated mutants in the presence of varying bacteriocin concentrations. Neutralization assay, or use of a fluorescently labelled bacteriocin, have also been used to characterise resistant mutants and to test if the mutation disrupts cell surface association of a bacteriocin (Behrens *et al.* 2020; White *et al.* 2017; Rassam *et al.* 2015). Screening of genomic or mutant libraries is another approach. For example, genomic fragments from a bacteriocin-sensitive strain can be transformed into a bacteriocin-resistant background in order to identify a fragment that causes bacteriocin sensitivity and potentially carries a receptor gene (Pilsl *et al.* 1999; Smajs & Weinstock 2001). Another approach is to construct a transposon mutant library in a bacteriocin-sensitive background and look for insertion sites that aid resistance (Baysse *et al.* 1999; de Chial *et al.* 2003; Elfarash *et al.* 2014; Ghequire *et al.* 2017). However, if a receptor is an essential gene a library search might fail to show the receptor.

1.3.3. Import of nuclease pyocins

Despite their sequence and receptor diversity, some features of pyocin import appear to be conserved. The similarity of nuclease pyocins and colicins is not just reflected in their modular organisation, but also in their import mechanisms. Like colicins, pyocins parasitise nutrient import machineries to translocate across the cell envelope and reach their periplasmic or cytoplasmic targets. This process requires interactions between pyocins and cell envelope components, and the PMF as an energy source (Atanaskovic & Kleanthous 2019).

Pyocins bind to outer membrane receptors (Figure 1-7), which adhere the pyocin to the cell surface. After receptor binding, pyocins recruit outer membrane translocators to cross into the periplasm. In pyocins characterised thus far, the receptor and translocator are two separate outer membrane components (Figure 1-7A). Nuclease pyocins S2, SD2, SD3, and the S5 pore former, all bind CPA as the outer membrane receptor, and then translocate through a specific TBDT (Behrens *et al.* 2020; White *et al.* 2017; McCaughey *et al.* 2016a). Some pyocins do not bind CPA, such as pyocin S1 and AP41 (McCaughey *et al.* 2016a). These pyocins may exploit one or several outer membrane proteins as a receptor/translocator (Figure 1-7B). All pyocin translocators which have been identified so far are TBDTs and are coupled to the TonB1-ExbB-ExbD system (Atanaskovic & Kleanthous 2019). Therefore, pyocin killing activity also depends on this system. As seen in pyocins S2, SD2 and S5, the TonB1 binding box is not only present on the TBDT, but also on the pyocin (Behrens *et al.* 2020; White *et al.* 2017; McCaughey *et al.* 2016a). It appears that this box is always localised in the unstructured N-terminus, preceding the N-terminal receptor binding domain. A similar arrangement is found in group B colicins that target *E. coli* cells (Cascales *et al.* 2007).

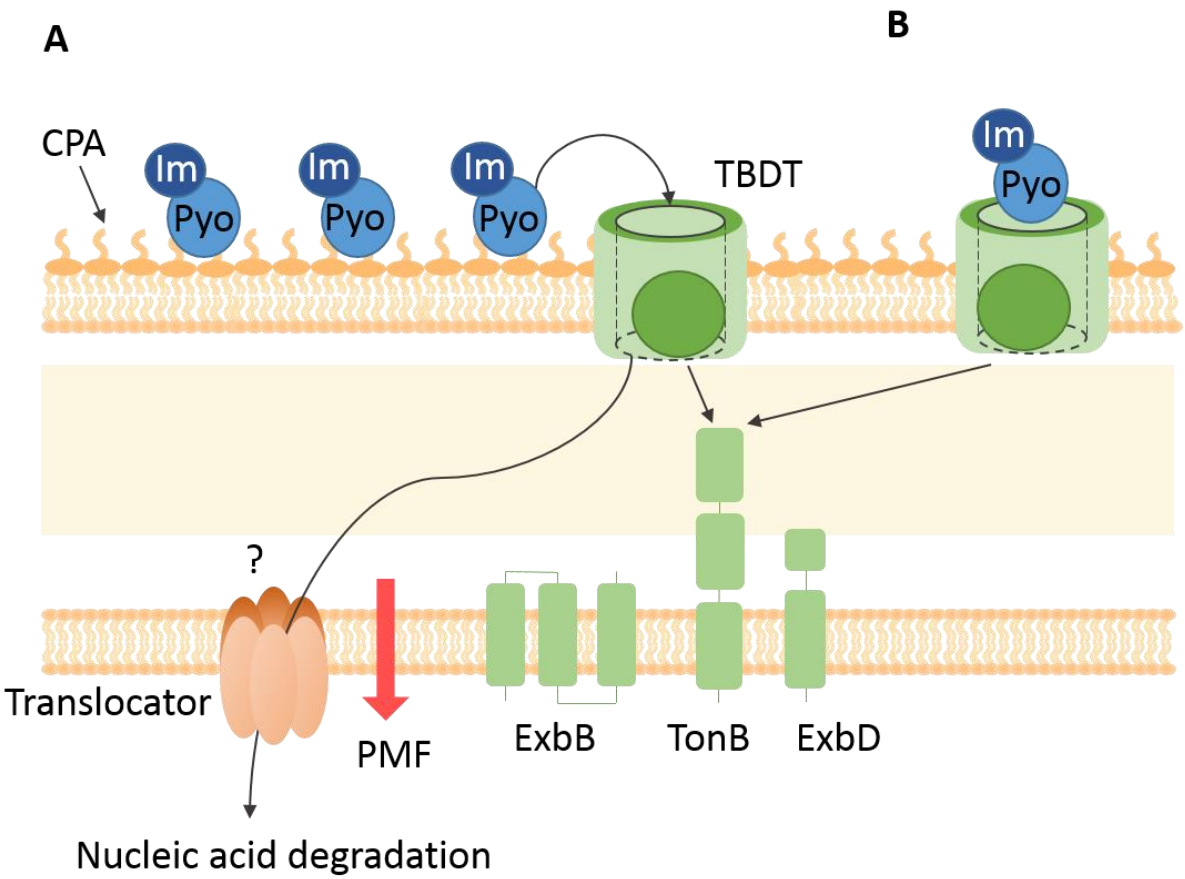

Figure 1-7. Summary of known import mechanisms for modular pyocins. Pyocins bind to cell envelope components to concentrate on the cell surface. Some pyocins bind CPA as their cell surface receptor (A). Alternatively, the receptor and the translocator may be the same cell envelope component (B). After receptor binding, pyocins can interact with an outer membrane TonB dependent transporter (TBDT), which they use as an outer membrane translocator. TBDTs interact with TonB in the periplasm upon binding pyocin. This interaction causes a conformational change in the TBDT, which involves the dislocation of the plug domain and opening of the TBDT channel for pyocin passage. This translocation step depends on the PMF. In addition, for nuclease pyocins, an inner membrane translocation step is required. It is not known which inner membrane proteins are required for this step, nor if a specific translocator is involved.

Translocator binding typically involves some form of molecular mimicry where the pyocin mimics the cognate ligand of the TBDT and occupies the same binding site (White *et al.* 2017). During the next stage, pyocin binding to the translocator induces similar conformational changes in the TBDT as its cognate ligand. Subsequently, the plug of the TBDT is displaced by PMF-linked TonB, which opens a channel in the TBDT. The molecular details of these events are still unclear. The pyocin now passes its N-terminal TonB box through the TBDT channel where it is thought to bind either the same or another copy of TonB. TonB now pulls the pyocin through the channel and into the periplasm in the form of an unfolded or partially unfolded polypeptide chain (White *et al.* 2017). Translocation of pore forming pyocins stops in the periplasm. They insert in the inner membrane and do not require an inner membrane translocation step for their activity (Behrens *et al.* 2020). Nuclease pyocins, however, translocate across the inner membrane. It is not known how this occurs. The identity of the inner membrane translocator in *P. aeruginosa* has not been determined. In *E. coli*, the essential AAA+ ATPase/protease FtsH in the inner membrane has been associated with the import of nuclease colicins (Walker *et al.* 2007).

FtsH is conserved amongst Gram-negative bacteria. It recognises misfolded or misincorporated membrane proteins and has a role in membrane protein quality control. It can also degrade cytosolic proteins that harbour specific signal sequences, called degrons. In *E. coli*, FtsH-dependent degradation of cytoplasmic proteins has been linked to regulation of heat-shock gene expression, regulation of the superoxide stress response, control of LPS and phospholipid biosynthesis, removal of non-functional proteins in the cytoplasm, and lysis/lysogeny decision of phage λ (Westphal *et al.* 2012). FtsH has two transmembrane helices in the N-terminus, which flank a periplasmic domain. The C-terminal cytoplasmic region consists of an AAA+ ATPase and a zinc metalloprotease domain (Figure 1-8). Subunit

interactions are via the N-terminal region, enabling six FtsH monomers to form a ring in the inner membrane. Misfolded proteins are directed from the inner membrane into the FtsH ring, and are first bound by the AAA+ ATPase domain, which unfolds and translocates substrates into the proteolytic chamber of the FtsH hexamer (Langklotz *et al.* 2012). In *E. coli*, *ftsH* is an essential gene. It is necessary for the regulation of the LPS:phospholipid ratio in the outer membrane. This is due to FtsH mediated cleavage of LpxC, a key enzyme in LPS biosynthesis. Therefore, in *E. coli* deletion of FtsH requires a suppressor mutation which leads to upregulation of the FabZ enzyme required for fatty acid biosynthesis. This suppressor mutation restores the LPS:phospholipid ratio (Schakermann *et al.* 2013). *ftsH* deletion mutants of *E. coli* with upregulated FabZ are resistant to nuclease colicins. Point mutations affecting just the protease or just the ATPase activity of FtsH also render cells colicin resistant, meaning that FtsH functions have to be preserved for nuclease colicin import (Walker *et al.* 2007). The exact role of FtsH in colicin import is unknown. Firstly, it is not clear if the observed colicin resistance phenotype is a direct consequence of *ftsH* deletion, or a secondary effect, due to changes in cell envelope composition and stability. If FtsH is directly involved in colicin import, this would mean that colicins pass through the pore of the FtsH hexamer to enter the cytoplasm. Before this, colicins might have to insert into the inner membrane, since no periplasmic substrates of FtsH have been described. Membrane insertion and nonvoltage-gated channel forming activity in planar lipid bilayers has been detected for ColE9 and E2 (Mosbahi *et al.* 2009; Vankemmelbeke *et al.* 2012), so membrane insertion might be an inner membrane translocation step preceding entry to the pore of FtsH. After entering the FtsH ring, colicins would then be exposed to the protease domain of FtsH, and probably undergo a cleavage step prior to entering the cytoplasm. Proteolytic processing during import has indeed been demonstrated for some colicins (Chauleau *et al.* 2011; Mora & Zamaroczy 2014).

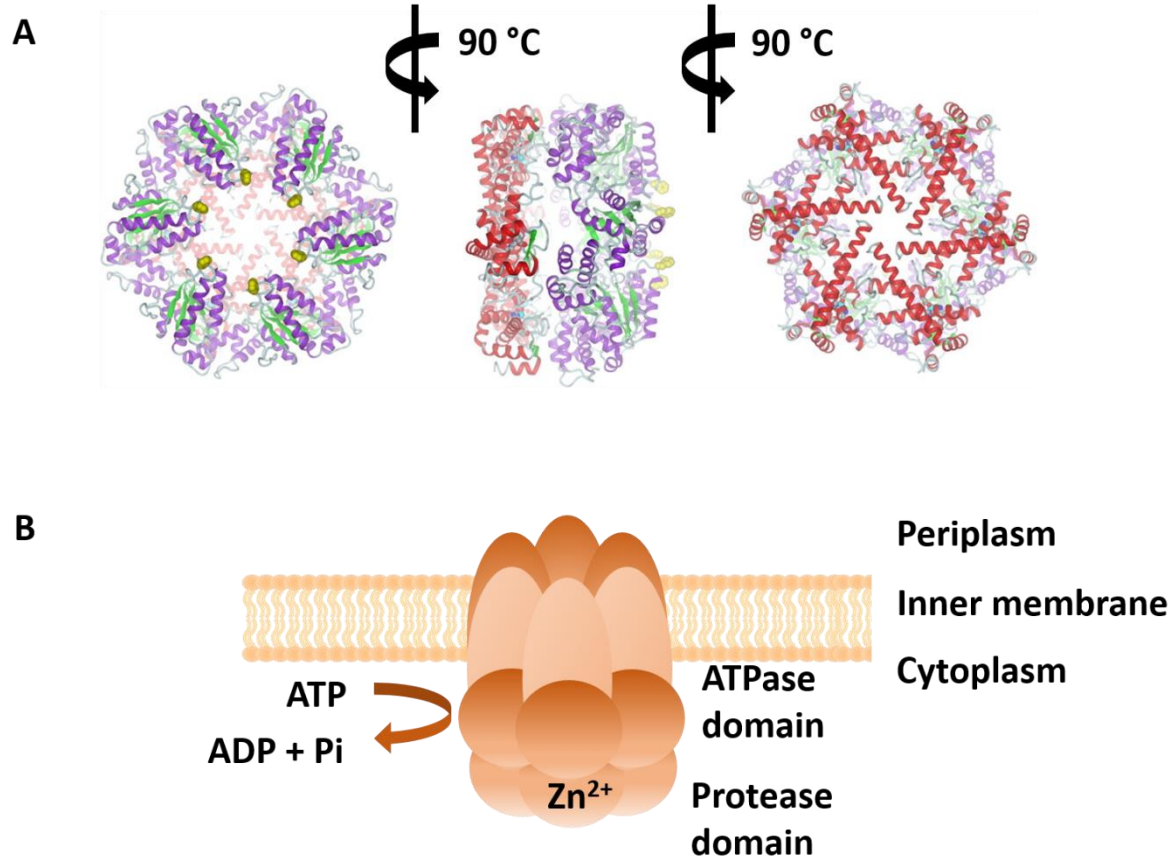

Figure 1-8. Organization of the FtsH hexamer. A – Structure of the FtsH hexamer from *Thermotoga maritima* (structure representation taken from Bieniossek *et al.* (2009)). Views onto AAA ring (left), side (middle) and protease (right) are shown. The protease ring is shown in red and the AAA ring in magenta and green. B – schematic representation of the FtsH ring in the inner membrane. Each subunit is inserted into the inner membrane, with the ATPase and the protease domain in the cytoplasm.

FtsH could also be involved in the translocation of nuclease pyocins. FtsH is conserved between *P. aeruginosa* and *E. coli* (68 % protein sequence identity). Still, there are differences in FtsH substrate specificity between these two organisms. FtsH in *P. aeruginosa* is not involved in LpxC processing (Langklotz *et al.* 2011). Therefore, FtsH is only conditionally

essential in *P. aeruginosa*: a *ΔftsH* mutant of PAO1, the laboratory strain of *P. aeruginosa*, is viable in buffered or salt free media (Hinz *et al.* 2011). Very little is known about the substrate specificity of *P. aeruginosa* FtsH. RpoH, the heat shock sigma factor, appears to be the major substrate of *P. aeruginosa* FtsH (Basta *et al.* 2020). The protease has also been shown to be required for secretion of secondary metabolites, motility, biofilm formation, autolysis and aminoglycoside resistance in this organism (Kamal *et al.* 2019). Still, its involvement in nuclease pyocin import has yet to be demonstrated.

1.4 Aims of this work

Nuclease pyocins are potent, diverse and narrow spectrum protein antibiotics that can be used to treat *P. aeruginosa* infections. However, a limitation in the future biomedical use of pyocins is the occurrence of pyocin resistance. A specific strain of *P. aeruginosa* is intrinsically resistant to all pyocins it produces, due to the presence of immunity protein genes in pyocin operons. Additionally, resistance can occur due to spontaneous mutations affecting pyocin translocon components. This can be overcome through the use of cocktails comprising pyocins that have different cell envelope targets and different immunity proteins. Therefore, mining *P. aeruginosa* genomes for novel pyocin genes is an important step in developing this class of antibiotics as therapeutics. Pairing up pyocins and their outer membrane receptors is also required, since it can help in determining the strain coverage of a specific pyocin and aid in cocktail design. In this study, it was sought to broaden our understanding of nuclease pyocin import by focusing on two proteins: pyocins G and AP41.

A bioinformatics pipeline that searches genomes of different bacteria for nuclease bacteriocins led to the discovery of a new nuclease pyocin, named pyocin G (PyoG). The aim

of the presented work was to test the activity of this pyocin and find out more about its import mechanism. PyoG belongs to the S1 group. None of the translocon components of the S1 group are known. It was therefore investigated which cell envelope proteins are required for PyoG import into *P. aeruginosa* cells. More specifically, it was aimed to find the outer membrane receptor and translocator of PyoG and discover its function in *P. aeruginosa*. Furthermore, PyoG was used as a model pyocin to study the inner membrane translocation step of protein antibiotics. The aim was to elucidate which inner membrane proteins are involved in pyocin import, and which pyocin domains are essential for this translocation step.

Pyocin AP41 is a nuclease pyocin for which there are no known translocon components. This pyocin was effective at killing *P. aeruginosa* in a murine lung infection model (McCaughey *et al.* 2016). Due to potency of AP41 in this model, the aim of this work was to investigate its import mechanism: what is the outer membrane receptor and/or translocator of AP41, is the import Ton or Tol dependent, and which proteins are required for the inner membrane translocation step.

2. Materials and Methods

All chemicals were purchased from Sigma Aldrich, with the exception of n-octyl-β-D-glucopyranoside (β-OG) (Enzo Life Sciences). DNA restriction enzymes were purchased from (New England Biolabs (NEB)). All chromatography columns were purchased from GE Healthcare.

2.1 Sequence analysis and genome searches

All bacteriocin sequences used in this study are deposited in the National Centre for Biotechnology (NCBI) database under the following accession numbers: pyocin AP41 (GenBank accession no. BAA02196.1), PyoG (GenBank accession no. ETV05907.1), S1 (UniProtKB/Swiss-Prot accession no. Q06583.2), S6 (GenBank accession no. KYO98147.1), pyocin S13 (NCBI Reference Sequence accession no. WP_023116694.1), carocin D (GenBank accession no. ADH95192.1).

Sequence alignments were made by Clustal Omega (Madeira *et al.* 2019) and visualised by ESPript 3.0 (Robert and Goet 2014). PFAM domains were searched for by SMART (Letunic and Bork 2018). TonB dependent transporters in the *P. aeruginosa* PAO1 genome were identified by HMMER 3.3 (Eddy 2011) using the TonB plug domain (PFAM domain PF07715).

2.2 Bacterial strains, media and growth conditions

All strains (Table 2-1) were cultured in LB (10 g/L tryptone, 10 g/L NaCl, 5 g/L yeast extract, pH 7.2) or M9 medium (8.6 mM NaCl, 18.7 mM NH_4Cl, 42.3 mM Na_2HPO_4, 22.0 mM

KH_2PO_4, 0.4% w/v glucose, 2 mM $MgSO_4$, 0.1 mM $CaCl_2$) at 37 °C with shaking (140 rpm). *E. coli* BL21ΔABCF was cultured in LB Lennox (10 g/L tryptone, 5 g/L NaCl, 5 g/L yeast extract, pH 7.2) at 30 °C with shaking (140 rpm). BL21ΔABCF was a gift from Jack Leo (Addgene strain number #102270). *P. aeruginosa ΔftsH* was grown on salt free LB medium. TonB mutants of *P. aeruginosa*, and the parent strain PAO6609, were grown in LB medium supplemented with 100 µM $FeCl_3$. All *P. aeruginosa* transposon mutants were grown in the presence of 10 µg/mL tetracycline. 100 µg/mL of carbenicilin and 25 µg/mL of irgasan was used for selecting plasmid transformants of *P. aeruginosa* or *E. coli*.

Table 2-1. List of strains used in this study.

Species	Strain	Characteristics	Source
Escherichia coli	BL21(DE3)	Expression of His-tagged bacteriocins and TonB1	New England Biolabs
	BL21ΔABCF	Expression of His-tagged Hur; *ompA*, *lamB*, *ompC*, *ompF* quadruple knockout strain	Meuskens *et al.* (2017).
	NEB5α	Plasmid propagation	New England Biolabs
	S17-1	Conjugation with *P. aeruginosa*; contains chromosomally integrated *tra* genes	American Type Culture Collection
Pseudomonas aeruginosa	PAO1	wild type	Washington Library Jacobs *et al.* (2003).
	PA14	Clinical isolate, burn wound	Lee *et al.* (2006).
	PAO1 *Δrmd*	LPS biosynthesis mutants.	Murphy *et al.* (2014).
	PAO1 *ΔwbpM*		
	PAO1 *ΔwbpL*		
	TEP1	Clinical isolate, sepsis	University of Glasgow, UK
	TEP2	Clinical isolate, sepsis	
	TEP3	Clinical isolate, sepsis	
	TEP4	Clinical isolate, sepsis	
	TEP5	Clinical isolate, sepsis	
	TEP6	Clinical isolate, sepsis	

	TEP7	Clinical isolate, sepsis	
	TEP8	Clinical isolate, sepsis	
	TEP9	Clinical isolate, sepsis	
	TEP10	Clinical isolate, sepsis	
	P1	Clinical mucoid isolate, young CF patient	Royal Hospital for Sick Children, Glasgow, UK
	P2	Clinical mucoid isolate, young CF patient	
	P3	Clinical mucoid isolate, young CF patient	
	P4	Clinical mucoid isolate, young CF patient	
	P5	Clinical isolate, young CF patient	
	P7	Clinical isolate, young CF patient	
	P8	Clinical isolate, young CF patient	
	P9	Clinical isolate, young CF patient	
	P10	Clinical isolate, young CF patient	
	P11	Clinical isolate, young CF patient	
	P12	Clinical isolate, young CF patient	
	P13	Clinical isolate, young CF patient	
	P14	Clinical isolate, young CF patient	
	P15	Clinical isolate, young CF patient	
	P17	Clinical isolate, young CF patient	
	P18	Clinical isolate, young CF patient	
	P19	Clinical isolate, young CF patient	
	PA7	Clinical isolate, non-respiratory	Roy *et al.* (2010).
	C763	Clinical isolate, CF patient	Stewart *et al.* (2014).
	J1385	Clinical isolate, CF patient	
	J1532	Clinical mucoid isolate, CF patient	
	PA62	Environmental isolate, soil	
	PAO1 *ΔftsH*	*ftsH* deletion mutant	Lee *et al.* (2015).

	PAO6609	*met-9011 amiE200 strA pvd-9*	Shirley & Lamont (2009).
	PAO6609 *ΔtonB1*	*tonB1* transposon mutant	
	PAO6609 *ΔtonB2*	*tonB2* transposon mutant	
	PAO6609 *ΔtonB3*	*tonB3* transposon mutant	
	PW1052	PAO1 transposon insertion in PA0040 (*fhaC1*)	Washington Library Jacobs *et al.* (2003).
	PW2063	PAO1 transposon insertion in PA0041 (*fhaB1*)	
	PW5140	PAO1 transposon insertion in PA2463 (*fhaC2*)	
	PW5138	PAO1 transposon insertion in PA2462 (*fhaB2*)	
P. aeruginosa complemented strains	*Δhur* p*hur*	*PA1302* transposon insertion mutant of PAO1 (PW3356) complemented with p*hur* (please see table 2-2 for the list of plasmids)	This study
	ΔftsH p*ftsH*	*ΔftsH* mutant of PAO1 complemented with p*ftsH*	
	pFtsH	*ΔftsH* mutant of PAO1 complemented with pREN144	
	pFtsH H416Y	*ΔftsH* mutant of PAO1 complemented with pREN145	
	pTonB1	*ΔtonB1* mutant of PAO6609 complemented with p*tonB1*	
	pTetTonB1	*ΔtonB1* mutant of PAO6609 complemented with pTetTonB1	
Transposon mutants of *P. aeruginosa* PAO1 TonB dependent transporters (TBDTs)		Locus with transposon insertion	
	PW1255	*PA0151*	Washington Library Jacobs *et al.* (2003).
	PW1334	*PA0192*	
	PW1793	*PA0434*	
	PW1861	*PA0470 (fiuA)*	
	PW2217	*PA0674 (vreA)*	
	PW2418	*PA0781*	
	PW2689	*PA0931 (pirA)*	
	PW3296	*PA1271 (btuB)*	
	PW3356	*PA1302 (hur)*	
	PW3399	*PA1322*	

	PW3483	*PA1365*	
	PW3881	*PA1613*	
	PW4347	*PA1910 (femA)*	
	PW4367	*PA1922*	
	PW9719	*PA2057 (sppR)*	
	PW10435	*PA2070*	
	PW4597	*PA2089*	
	PW4870	*PA2289*	
	PW4938	*PA2335*	
	PW5144	*PA2466 (foxA)*	
	PW5348	*PA2590*	
	PW5503	*PA2688 (pfeA)*	
	PW5892	*PA2911*	
	PW6483	*PA3268*	
	PW6749	*PA3408 (hasR)*	
	PW7415	*PA3790 (oprC)*	
	PW7590	*PA3901 (fecA)*	
	PW8043	*PA4156 (fvbA)*	
	PW7180	*PA4221 (fptA)*	
	PW8599	*PA4514*	
	PW8871	*PA4675 (chtA)*	
	PW8934	*PA4710 (phuR)*	
	PW9134	*PA4837 (cntO)*	
	PW9241	*PA4897*	
	PW10317	*PA5505*	
	PW5036	*PA2398 (fpvA)*	
	PW4649	*PA4168 (fpvB)*	
Transposon mutants of *P. aeruginosa* PAO1 porins		Locus with transposon insertion	
	PW1783	*PA0427 (oprM)*	
	PW4135	*PA1777 (oprF)*	
	PW2742	*PA0958 (oprD)*	
	PW7877	*PA4067 (oprG)*	
	PW3127	*PA1178 (oprH)*	
	PW5186	*PA2495 (oprN)*	
	PW6333	*PA3186 (oprB)*	
	PW6503	*PA3279 (oprP)*	
	PW6505	*PA3280 (oprO)*	
	PW8747	*PA4597 (oprJ)*	

2.3 Plasmids

pET21a(+) was used as a backbone for the expression of genes in *E. coli*. pMMB190 was used for gene expression in *P. aeruginosa*. All plasmids are listed in Table 2-2, and primers used for their construction in Table 2-3.

pNGH174 was constructed by Dr Nicholas Housden, and contains the pyocin AP41-Im gene sequences (Genewiz), codon optimized for expression in *E. coli* and cloned into pET21a(+). Derivatives of this plasmid are pAP41-30-C and pAP41-C, that contain the first 30 residues of AP41 fused to its cytotoxic domain, or just the cytotoxic domain, respectively. pAP41-30-C was constructed by inserting *Sac*I sites after codon 30 (primers 174-640Sac-F/R) and 639 (174-30Sac-F/R) in pNGH174, and by cutting out the region in-between the two sites. pAP41-C was constructed by inserting an *NdeI* site before codon 640 (174-640Nde-F/R), and by cutting out the region in-between the two *Nde*I sites.

pNGH262 was constructed by Dr Nicholas Housden, and contains the PyoG-Im gene sequences (Genewiz), codon optimized for expression in *E. coli* and cloned into pET21a(+). The derivatives of this plasmid are pG1-255, pG1-485-Cys and pG485-640. pG1-255 was constructed by inserting an *Xho*I site after codon 255 (262-255Xho-F/R) in pNGH262 and by cutting out the region in-between the two *Xho*I sites. pG1-485-Cys was constructed by PCR, amplifying the first 485 residues of PyoG and by adding a cysteine at the C-terminus of the construct by PCR mutagenesis (G485-Cys-F/R). pG485-640 was constructed by adding an *Nde*I site before codon 485 (262-485Nde-F/R) in pNGH262 and by cutting out the region in between the two *Nde*I sites. pG1-255-Cys was constructed by introducing a cysteine and *Xho*I site after codon A255 in pNGH262, and cutting out the region between the two *Xho*I sites. pGΔ1-30 was constructed by introducing *Nde*I site after codon T30 in pNGH262 and cutting

out the fragment between the two *Nde*I sites. pG31-485-Cys was constructed by by introducing *Nde*I site after codon T30 in pG1-485-Cys and deleting the fragment between the two *Nde*I sites. pS2-G was constructed by introducing a *Sac*I site after codon V215 in pPW06. The fragment encoding the S2 receptor binding domain was cut out with *Nde*I and *Sac*I, and cloned into pNGH262 with a *Sac*I site after reside A255. pS2-AP41 was constructed by introducing a *Sac*I site after codon P558. DNA encoding the AP41 cytotoxic domain and immunity protein were cloned between *Sac*I and *Xho*I sites.

P. aeruginosa genes were either cloned from *P. aeruginosa* PAO1 genomic DNA or synthesised by Genewiz. p*oprH* was constructed by cloning *oprH* from PAO1 (OprH-F/R) into pMMB190. pOmpF(ss)OprH was constructed by cloning synthetic *oprH* with the OmpF signal sequence, codon optimized for expression in *E. coli*, into pET21a(+). p*ftsH* was constructed by cloning *ftsH* from PAO1 (FtsH-F/R) into pMMB190. p*hur* was constructed by cloning synthetic *hur*, codon optimized for the expression in both *P. aeruginosa* and *E. coli*, into pMMB190. pHur was constructed by swapping the first 29 residues of *hur* with the OmpF signal sequence (OmpF(ss)-Hur-F/R) and inserting a His_{10}-TEV (His10TEV-Hur-F/R) by PCR.

Table 2-2. List of plasmids used in this study.

Plasmid	Code	Protein	Backbone	Description	Source
pET21a(+)				pBR322 origin, His-tag, Amp^r	NEB
pMMB190				Broad-host-range cloning vector, Amp^r, pMMB66EH, *tac* promoter, LacZα	Morales *et al.* (1991).
pNGH174		AP41, ImAP41-His_6	pET21a(+)	DNA encoding His_6-Im-AP41 cloned at *Nde*I and *Hind*III sites	Joshi *et al.* (2015).

pAP41-30-C	IA25	AP41$^{\Delta 31-639}$, ImAP41-His$_6$	pET21a(+)	DNA encoding His$_6$-Im-AP41Δ31-639 cloned at *Nde*I and *Hind*III sites	This study
pAP41-C	IA22	AP41$^{640-777}$, ImAP41-His$_6$	pET21a(+)	DNA encoding His$_6$-Im- AP41$^{640-777}$ cloned at *Nde*I and *Hind*III sites	This study
pNGH262		PyoG, ImG-His$_6$	pET21a(+)	DNA encoding His$_6$-Im-PyoG cloned at *Nde*I and *Hind*III sites	This study, Nicholas Housden
pNGH263		ImG-His$_6$	pACYCDuet1	DNA encoding PyoG immunity protein cloned at *Nde*I and *Xho*I	This study, Nicholas Housden
pG1-255	IA35	PyoG$^{1-255}$-His$_6$	pET21a(+)	DNA encoding PyoG$^{1-255}$-His$_6$ cloned at *Nde*I and *Hind*III sites	This study
pG1-485-Cys	IA38	PyoG$^{1-485}$Cys-His$_6$	pET21a(+)	DNA encoding PyoG$^{1-485}$-Cys-His$_6$ cloned at *Nde*I and *Hind*III sites	This study
pG1-255-Cys	IA51	PyoG$^{1-255}$Cys-His$_6$	pET21a(+)	DNA encoding PyoG$^{1-255}$-Cys-His$_6$ cloned at *Nde*I and *Hind*III sites	This study
pGΔ1-30	IA54	PyoG$^{\Delta 1-30}$, ImG-His$_6$	pET21a(+)	DNA encoding His$_6$-Im-PyoG, lacking the first 30 residues of PyoG, cloned at *Nde*I and *Hind*III sites	This study
pG31-485-Cys	IA53	PyoG$^{31-485}$Cys-His$_6$	pET21a(+)	DNA encoding PyoG$^{31-485}$-Cys-His$_6$ cloned at *Nde*I and *Hind*III sites	This study
pS2-G	IA73	PyoS2$^{1-209}$-PyoG$^{256-640}$, ImG-His$_6$	pET21a(+)	N-terminal domain of PyoS2 fused to PyoG	This study

pS2-AP41	IA45	PyoS2$^{1-558}$-AP41$^{640-777}$, ImAP41-His$_6$	pET21a(+)	PyoS2 with a cytotoxic domain of AP41	This study
pG-S2-G	IA72	PyoG$^{1-255}$-S2$^{328-556}$-G$^{486-640}$, ImG-His$_6$	pET21a(+)	PyoG with the translocation domain of PyoS2	This study
pS21-30-G	IA71	PyoS2$^{1-30}$-G$^{31-640}$, ImG-His$_6$	pET21a(+)	First 30 residues of PyoG swapped for first 30 residues of PyoS2	This study
pPW06		PyoS2, ImS2-His$_6$	pET21a(+)	DNA encoding PyoS2, ImS2-His$_6$ cloned at *Nde*I/*Xho*I sites	White *et al.* (2017).
pPW17		His$_6$-TEV-TonB1$^{109-342}$	pETM11	DNA encoding His$_6$-TEV-TonB1$^{109-342}$ from PAO1 cloned at *Nco*I and *Sac*I sites	White *et al.* (2017).
pTonBB1		TonB$^{1-102}$ - TonB1$^{201-342}$	pACYCDuet-1	DNA encoding *E. coli* TonB$^{1-102}$, translationally fused to *P. aeruginosa* TonB1$^{201-342}$, cloned at *Nde*I and *Xho*I sites	Behrens *et al.* (2020).
p*ftsH*	IA31	FtsH	pMMB190	*ftsH* from PAO1 cloned into at *Bam*HI and *Hind*III sites	This study
p*oprH*	IA17	OprH	pMMB190	*oprH* from PAO1 cloned into at *Bam*HI and *Hind*III sites	This study
pOmpF(ss)OprH	REN130	OprH	pET24a(+)	*oprH* from PAO1 with the OmpF signal sequence cloned at *Nde*I and *Hind*III sites	This study
p*hur*	IA28	Hur	pMMB190	*hur* (*PA1302*) from PAO1 cloned at *Bam*HI and *Hind*III sites	This study

pHur	IA32	His_{10}-TEV-Hur	pET21a(+)	DNA encoding His_{10}-TEV-Hur from PAO1 with the OmpF signal sequence cloned at *Nde*I and *Hind*III sites	This study
pREN144	REN144	His_6-TEV-FtsH	pMMB190	*ftsH* from PAO1 with an N-terminal His6 and TEV site	This study
pREN145	REN145	His_6-TEV-FtsH, point mutation H416Y	pMMB190	*ftsH* H416Y from PAO1 with an N-terminal His_6 and TEV site	This study
p*tonB1*	IA61	TonB1	pMMB190	*tonB1* from PAO1	This study
pTetTonB1	IA65	Tet-TonB1	pMMB190	T7-$TetA^{2-32}$-$TonB1^{112-342}$, TonB1 and TetA genes are from PAO1	This study

Table 2-3. List of primers used in this study.

Primer	Sequence (5' → 3')	Use
174-30Sac-F	CAGGTACGGGATGAGCTCTGGTGTCG GCGGTGGC	Introduction of *Sac*I site after codon P30 in pNGH174
174-30Sac-R	GCCACCGCCGACACCAGAGCTCATCC CGTACCTG	
174-640Sac-F	ACGCGGGTCACGGAGCTCGTACACGA TGTACAGAGG	Introduction of *Sac*I site before codon P640 in pNHG174
174-640Sac-R	ACATCGTGTACGAGCTCCGTGACCCG CGTGACG	
174-640Nde-F	GTTCGTCACGCGGCATATGGTCACGG TACACGATGTACAG	Introduction of *Nde*I site before codon P640 in pNGH174
174-640Nde-R	CTGTACATCGTGTACCGTGACCATATG CCGCGTGACGAAC	
262-255Xho-F	ACCGAGCCGTTCTCGAGAGCTGGCAT GGCG	Introduction of *Xho*I site after codon A255 in pNGH262
262-255Xho-R	CGCCATGCCAGCTCTCGAGAACGGCT CGGT	
G485-Cys-F	AAAAAACTCGAGTGTGTTAAACATGA CGTACACAGGTTTG	Cloning of $PyoG^{1-485}$-Cys from pNGH262
G485-Cys-R	AAAAAACATATGGCACGTCCGATTG	

G255-Cys-Xho-F	CACCGAGCCGTTCTCGAGACAAGCTG GCATGGC	Introduction of Cys and *Xho*I site after codon A255 of PyoG, for the construction of $PyoG^{1-255}$-Cys
G255-Cys-Xho-F	CCATGCCAGCTTGTCTCGAGAACGGCT CGGTGG	
G30-Nde-F	GGTGGTGGCACGCATATGGGTATTGG TCCGATC	Introduction of *Nde*I site after codon T30 of PyoG, for the construction of $PyoG^{\Delta 1-30}$ and $PyoG^{31-485}$Cys-His_6
G30-Nde-R	CGGACCAATACCCATATGCGTGCCACC ACC	
G255-Sac-F	GAAGAACAGGCGCGTGAGCTCCAGCA AGCTGCTATTCGC	Introduction of *Sac*I site after codon A255 of PyoG, for the construction of the PyoS2-G chimera
G255-Sac-R	GAATAGCAGCTTGCTGGAGCTCACGC GCCTGTTCTTCGG	
S2-215-Sac-F	GGAAGGCAAATGTCGAGCTCGAGAA AAAAGTGCAGTCC	Introduction of *Sac*I site after codon V215 of PyoS2, for the construction of the PyoS2-G chimera
S2-215-Sac-R	GACTGCACTTTTTTCTCGAGCTCGACA TTTGCCTTCC	
S2-558-Sac-F	GTTCAGGGATCCGGAGCTCCGGGATG TACCTGGTGC	Introduction of *Sac*I site after codon P558 of PyoS2, for the construction of the PyoS2-AP41 chimera
S2-558-Sac-R	CAGGTACATCCCGGAGCTCCGGATCC CTGAACATCAC	
FtsH-F	AAAAAAGGATCCACGGGCGAGGGTTC ATAAAG	Cloning of *ftsH* from PAO1 genomic DNA into pMMB190
FtsH-R	AAAAAAGCTTAATCGGGGGTGACATT GAGG	
OprH-F	AAAAAAGGATCCATGAAAGCACTCAA GACTCTC	Cloning of OprH from PAO1 genomic DNA into pMMB190
OprH-R	AAAAAAAAGCTTTTAGAACTTGTAGTT GGCGCCC	
OmpF(ss)-Hur-F	ATGAAGCGCAACATTTTAGCGGTCATC GTGCCGGCTCTGCTGGTCGCGGGCAC CGCGAATGCCGCGGAACGTCGCTTTG ATCTGC	Replacing the PAO1 Hur signal sequence with the *E. coli* OmpF signal sequence
OmpF(ss)-Hur-R	GGCATTCGCGGTGCCCGCGACCAGCA GAGCCGGCACGATGACCGCTAAAATG TTGCGCTTCATGCTGGGATCCCCGGG AATTCG	
His10TEV-Hur-F	CATCATCATCATCATCATCATCATC ATGAAAACCTGTATTTTCAGGGCGCG GAACGTCGCTTTGATCTGC	Introduction of His_{10}-TEV in pHur
His10TEV-Hur-R	GCCCTGAAAATACAGGTTTTCATGATG ATGATGATGATGATGATGATGGG CATTCGCGGTGCCCGC	

2.4 Molecular biology techniques

2.4.1 Extraction of genomic DNA

Genomic DNA was extracted from an overnight culture of *P. aeruginosa* PAO1, grown at 37 °C in LB. 2 mL of culture was pelleted at 5000 ×g for 10 minutes. Genomic DNA was purified using the DNeasy Blood & Tissue Kit (Qiagen) following the instructions (including instructions for pre-treatment of Gram-negative bacteria).

2.4.2 Polymerase chain reaction (PCR)

PCR was used to: amplify DNA fragments from either genomic or plasmid DNA; introduce mutations in plasmid DNA. Phusion HF polymerase (NEB) was used for all PCR reactions. The polymerase was used at 0.02 units/µL, in 1X GC buffer (NEB), 12 % DMSO and 200 µM deoxynucleotides mix. Primers (Table 2-3) were used at 0.5 µM. Genomic DNA was used as a template at 20 ng/µL and plasmid DNA was used at 1 ng/µL. All PCR reactions were performed in Mastercycler X50 (Eppendorf) in a 50 µL reaction volume. Initial denaturation was done at 98 °C for 3 min. Denaturation was then done at 98 °C for 2 min, annealing at 50 °C for 30 s, and extension at 72 °C for 1 min per 1 kb of amplicon. This was repeated for a total of 30 cycles, with a final extension step at 72 °C for 10 min. Whole plasmid mutagenesis was performed using the same cycle, but the extension temperature was dropped to 68 °C. All reactions were purified using the Monarch PCR Purification Kit (NEB). PCR products were analysed by agarose gel electrophoresis (section 2.4.3). Amplicons of correct size were digested by restriction enzymes and gel purified for cloning. Whole plasmid mutagenesis

products were digested with 0.8 units/µL of *DpnI* in 1X CutSmart Buffer (NEB), for 2 h at 37 °C. In this way, methylated parental DNA was removed prior to transformation.

2.4.3 DNA gel electrophoresis

DNA gel electrophoresis was used for the analysis of PCR products and for the extraction of amplicons after digestion with restriction enzymes. 1 % (w/v) agarose gels were prepared by melting agarose in 0.5X Tris/Borate/EDTA buffer (TBE) (44.5 mM Tris-HCl pH 8.3, 44.5 mM boric acid, 1 mM ethylenediaminetetraacetic acid (EDTA)) and mixed with 1x SybrSafe dye. 1 µL sample loading dye (30 % (w/v) glycerol, 6 mM EDTA, 0.4 % (w/v) bromophenol blue) was added to 5 µL sample and loaded onto the gel. Electrophoresis was run at 80 V constant voltage in 0.5X TBE. GeneRuler 1 kb DNA ladder was used for the analysis of amplicon size.

2.4.4 Restriction enzyme digests

All enzymes were used at 10 units/µL, in 1X CutSmart buffer (NEB), at 37 °C for 2 hours. Digested DNA was separated using agarose gel electrophoresis and extracted using the Monarch Gel Extraction Kit.

2.4.5 DNA ligation

T4 DNA ligase at 100 units/µL and in 1X Ligation Buffer (NEB) was used for the ligation of restriction digested PCR products and plasmid backbones. Ligations were performed at

room temperature for 15 min. 5 µL of ligation reaction was then directly used for the transformation of 50 µL of competent cells.

2.4.6 Bacterial chemical transformation

Chemically competent *E. coli* NEB5α cells were purchased from NEB. *E. coli* BL21ΔABCF or Sm 17-1 competent cells were prepared by $CaCl_2$ treatment. 50 mL of over-night culture, grown at 37 °C in LB, was pelleted on 5000 *x g* for 10 min. Cells were resuspended in 50 mL ice cold 0.1 M $CaCl_2$ and kept on ice for 30 min. Cells were then pelleted again and resuspended in 1 mL 0.1 M $CaCl_2$ and incubated on ice for 5 more min before transformation.

Competent cells were transformed by heat shock. 50 µL of competent cells were mixed with 5 µL of DNA. Cells were incubated on ice for 30 min, shocked for 30 s at 42 °C, and then incubated on ice for another 10 min. Cells were then plated on LB agar with antibiotics.

2.4.7 Bacterial conjugation

P. aeruginosa PAO1 was transformed via conjugation with *E. coli* S17-1 carrying a plasmid of interest. PAO1 was grown overnight at 43 °C, and S17-1 at 37 °C, with shaking, in LB medium. 2 mL of each culture was pelleted on 5000 *x g,* 10 min. Each strain was then resuspended in 100 µL of LB medium and the two strains mixed together. The entire mix was then spotted on top of an antibiotic free LB agar plate. The plate was incubated on 37 °C for 8 h. The lawn was then scraped from the plate and resuspended in 1X phosphate buffer saline (PBS) pH 7. The suspension was serially diluted in PBS. 100 µL of each dilution was plated on

LB agar with 25 μg/mL irgasan, for selecting against S17-1, and 100 μg/mL carbenicillin, for selecting against untransformed PAO1.

2.4.8 Purification and sequencing of plasmid DNA

Plasmid DNA was isolated from NEB5α cultures grown at 37 °C in LB with the appropriate antibiotic, using Monarch Plasmid Miniprep kit (NEB). Sequencing was through the company Genewiz.

2.5 Protein expression and purification

2.5.1 Expression and purification of pyocins and pyocin derivatives

Pyocins containing the cytotoxic domain were expressed in complex with the His-tagged immunity protein. For PyoG expression, cells were co-transformed with pNGH263, which encodes the PyoG immunity protein, to increase pyocin yield. Pyocins lacking the cytotoxic domain were expressed with an N-terminal His-tag. *E. coli* BL21 was used for heterologous protein expression. Cells were grown at 37 °C with shaking, in LB medium supplemented with the appropriate antibiotic and induced with 1 mM IPTG (isopropyl β- d-1-thiogalactopyranoside) after reaching an OD_{600} of 0.7. Cells were grown for a further 3 hours after induction and then pelleted at 4500 *x g* for 20 min. Cells were resuspended in Lysis buffer (50 mM Tris-HCl pH 7.8, 500 mM NaCl, 10 mM imidazole) with the addition of 1 mM phenylmethylsulfonyl fluoride (PMSF). Sonication was done on ice at 70% maximum amplitude intervals of 3 s on, 7s off (total duration 3 min) using a Misonix S-4000 ultrasonic

liquid processor fitted with a 3/8-inch stud probe. Cell debris was pelleted at 10 000 *x g* for 20 min and the supernatant filtered with a 0.45 µm syringe filter. The cell lysate was then loaded on a 5 mL HisTrap HP column, equilibrated in Lysis buffer. After washing off unbound proteins, pyocins were eluted using an imidazole gradient reaching 250 mM imidazole. Fractions containing the protein of interest were pooled and dialysed overnight against 4 L of Gel Filtration buffer (50 mM Tris-HCl pH 7.8, 250 mM NaCl) using a 12-14 kilo Dalton (kDa) molecular weight cut-off membrane (Spectra/Por, Spectrum). Pyocins were further purified by gel-filtration, on a HiLoad 26/60 Superdex 200 pg column equilibrated in the Gel Filtration buffer and eluted fractions pooled, snap frozen and stored at -20 °C.

2.5.2 Expression and purification of TonB1 soluble fragments

His-tagged TonB1$^{109\text{-}342}$ was purified as described previously (White *et al.*, 2017). Briefly, TonB1 was expressed in *E. coli* BL21. Cells were harvested and sonicated, and the protein was purified by a HisTrap HP column using the same protocol as for pyocins. TonB1 was then dialysed against 50 mM Tris-HCl pH 7.8, 250 mM NaCl overnight, and then incubated with 0.1 mg/mL His6-Tobacco etch virus-protease (TEV) for 5 h, at room temperature. Tag free TonB1 was purified on a HisTrap HP column, followed by gel filtration using a HiLoad 26/60 Superdex 200 pg column equilibrated in 50 mM Tris-HCl pH 7.8, 250 mM NaCl. TonB1 was stored at -20 °C.

2.5.3 Expression and purification of outer membrane proteins

Outer membrane proteins of *P. aeruginosa* were heterologously expressed in *E. coli* BL21ΔABCF. Cells were grown in LB Lennox medium supplemented with antibiotic, at 30 °C with shaking. After reaching an OD_{600} of 0.7, cells were induced with 0.1 mM IPTG and grown for a further 3 h. Cells were pelleted at 4500 *x g* for 20 min, resuspended in 50 mM Tris-HCl pH 7.8 and sonicated as described above. Cell debris was removed by centrifugation at 5000 *x g* for 10 min. Total membranes were pelleted at 200 000 *x g* for 45 min. Inner membrane proteins were extracted in 50 mM Tris-HCl pH 7.8, 2 % (v/v) Triton X-100. Outer membranes were pelleted at 200 000 *x g* for 45 min and outer membrane proteins were extracted in 50 mM Tris-HCl pH 7.8, 2 % (w/v) β-OG, 5 mM EDTA. Insoluble proteins were removed by another ultracentrifugation step at 200 000 *x g* for 45 min.

OprH was expressed without a purification tag. The outer membrane extract was first loaded on a HiLoad 26/60 Superdex 75 pg column equilibrated in 50 mM Tris-HCl pH 7.8, 1 % (w/v) β-OG, 5 mM EDTA. OprH was further purified on SP Sepharose Fast Flow column equilibrated in 50 mM Tris-HCl pH 7.8, 1 % (w/v) β-OG, 5 mM EDTA, and eluted using a LiCl gradient reaching 500 mM. LiCl was next removed using a HiPrep 26/10 Desalting column and pooled protein fractions stored at -20 °C.

Hur was expressed with an N-terminal His_{10}-tag, followed by a TEV cleavage site. EDTA was removed from outer membrane extracts on a HiPrep 26/10 Desalting column, equilibrated in 50 mM Tris-HCl pH 7.8, 1 % (w/v) β-OG. The extract was then loaded on a HisTrap HP column and eluted using an imidazole gradient (20-500 mM imidazole). Hur was further purified using a HiLoad 26/60 Superdex 200 pg column equilibrated in 50 mM Tris-HCl pH 7.8, 1 % (w/v) β-OG, and stored at -80 °C. The purification tag was removed by 0.1 mg/mL

His_6-TEV protease treatment in the same buffer, at room temperature for 5 h. Tag free Hur was re-purified on a HisTrap HP column, and stored at -80 °C.

2.5.4 Sodium dodecyl sulphate polyacrylamide gel electrophoresis (SDS-PAGE)

SDS-PAGE was performed using Hoefer Mighty Small SE250 tanks, or Mini Gel Tanks (ThermoFisher Scientific) in case of gradient gels. 12% bisacrylamide gels were used for proteins larger than 20 kDa, or 4-20 % gradient precast Tris-glycine gels (ThermoFisher Scientific) for proteins smaller than 20 kDa or cross-linked protein complexes. Samples were mixed with 4X loading buffer (200 mM Tris-HCl pH 6.8, 8% w/v sodium dodecyl sulphate (SDS), 0.4% w/v bromophenol blue, 40% glycerol, 400 mM β-mercaptoethanol) to yield 1X loading buffer. Subsequently, they were heated to 98 °C for 5 min and loaded onto the gel, usually in a volume of 10 µL. Samples containing proteins cross-linked with formaldehyde were not heated. Pierce Unstained Protein MW Marker was used for estimating the molecular weight of proteins. Gels were run at 30 mA constant current in running buffer (25 mM Tris, 192 mM glycine, 3.5 mM SDS), or at a constant voltage of 225 V in case of gradient gels. Gels were stained in 50% ethanol, 10 % acetic acid and 2.5 g/L Coomassie Brilliant Blue R250.

2.5.5 Western Blot detection of Tet-TonB1

P. aeruginosa ΔtonB1 was transformed with Tet-TonB1 and expressed without induction from pMMB190. 1 L culture of this strain was grown overnight on 37˚C. Cells were pelleted, resuspended in 50 mM Tris-HCl pH 8, and lysed by sonication. Cell debris was removed by centrifugation (5000 *x g,* 5 min). The supernatant was centrifuged at 200 000 *x g*

for 45 min. The membrane pellet was resuspended in 1 % n-dodecyl-β-D-maltoside (DDM), 50 mM Tris-HCl pH 8 and incubated on 4 °C overnight. The extract was centrifuged again at 200 000 *x g* for 45 min, and Tet-TonB1 was detected in the supernatant by western blot. The extract was run on a 15% SDS-PAGE gel (30 mA, 30 min), blotted on Sequi-Blot PVDF membrane (Bio-Rad #1620182) and blocked with 8% Marvel dried skimmed milk in Tris-buffered saline buffer with Tween 20 (TBST buffer) for 1 h at room temperature. Blots were probed with primary rabbit anti-T7 (1:1000, Merck AB3790) antibodies in 4% milk in TBST buffer overnight at room temperature. The membrane was washed with TBST buffer (5 × 1 min) and probed with secondary anti-rabbit antibody conjugated with peroxidase (1:1000, Merck #A6154). Blots were washed as described above and detection was carried out using Amersham ECL Western Blotting Select Detection Reagent (GE Lifesciences #RPN2235), according to the manufacturer's instructions in GBOX-CHEMI-XRQ. Images were recorded using GeneSys software.

2.5.6 Differential scanning calorimetry (DSC)

The melting temperature of proteins, as an indication of their integrity, was determined by DSC performed on Malvern VP Capillary DSC by Dr. David Staunton, Molecular Biophysics Suite, Department of Biochemistry, University of Oxford. A 10 µM sample of OprH was used in 50 mM Tris pH 8, 1 % β-OG. Pyocin constructs were tested at 20 µM in 10 mM potassium phosphate pH 8, 20 mM NaF.

2.5.7 Circular dichroism (CD) spectroscopy

Proteins were dialysed into 10 mM potassium phosphate pH 8, 20 mM NaF, and were diluted to 0.1 mg/ml. CD spectra were obtained using a Jasco J-815 Spectropolarimeter over a wavelength range of 260-190 nm, a digital integration time of 1 second and a 1 nm bandwidth. CD data in millidegrees were converted to mean residue ellipticity by dividing by molar concentration and number of peptide bonds.

2.5.8 Protein quantification and assessment of purity

Protein concentration was measured using absorbance at 280 nm (Eppendorf Biophotometer), which was converted to concentration using the sequence based predicted molar extinction coefficient (ExPASy ProtParam, Table 2-4). The presence of scattering impurities, like protein aggregates, was checked by measuring the absorbance at 320 nm.

Protein purity was assessed by SDS-PAGE. Protein identity was confirmed by peptide mass fingerprinting, performed by Dr. Sabrina Liberatori (Proteomics Facility, Department of Biochemistry, University of Oxford) or Dr. Melissa Webby (Kleanthous laboratory). Protein mass was confirmed by denaturing electrospray ionisation mass spectrometry (ESI-MS), performed by Dr. David Staunton, Molecluar Biophysics Suite, Department of Biochemistry, University of Oxford.

Table 2-4. Calculated protein molecular weights and molar extinction coefficients, used for determination of protein concentration. All protein molecular weights were confirmed by mass spectrometry (* Signal sequence cleaved).

Protein	Molecular weight (Da)	Molar extinction coefficient [$M^{-1}cm^{-1}$]
PyoG	69008.20	61770
Immunity G-His_6	10978.52	12950
PyoG-G_4S-Cys	69426.62	61895
$PyoG^{1-255}$-His_6	28549.21	15930
$PyoG^{1-485}$-Cys-His_6	52117.21	37485
$PyoG^{1-255}$-Cys-His_6	28894.62	15930
$PyoG^{\Delta 1-30}$	66088.01	58790
$PyoG^{31-485}$Cys-His_6	49197.02	34505
$PyoS2^{1-209}$-$PyoG^{256-640}$	64706.23	62230
$PyoS2^{1-558}$-$AP41^{640-777}$	75626.74	67270
$PyoG^{1-255}$-$S2^{328-556}$-$G^{486-640}$	69842.15	61770
$PyoS2^{1-30}$-G^{31-640}	69340.71	61770
$TonB1^{109-342}$	25570.5	6990
His_{10}-TEV-Hur*	94430.27	151735
Pyocin AP41	83880.73	67270
Immunity AP41-His_6	11344.84	6990
$AP41^{\Delta 31-639}$	20546.88	23950
$AP41^{640-777}$	15384.34	20970
OprH*	19842.86	24410

2.6 Pyocin cytotoxicity assays

2.6.1 Plate killing assays

P. aeruginosa was grown in LB at 37 °C to an OD_{600} of 0.6. Bacterial lawns were prepared by addition of 250 µl of culture to 5 ml of molten soft LB-agar (0.75% (w/v) agar in LB), and were poured over LB-agar plates. Once set and dry, 3 µl of 3-fold serially diluted

pyocins, ranging from 10 µM to ~57 pM, was spotted on top of the lawn. Lawns were grown overnight at 37 °C and cytotoxicity was determined by observation of clearance zones.

2.6.2 Liquid killing assays

Liquid killing assays were performed in 96 well flat bottom plates containing 200 µL of LB. Media was supplemented with 100 µM $FeCl_3$ in case of *tonB* mutants, or without NaCl in case of the *ftsH* mutant. Overnight cultures of tested strains were adjusted to an OD_{600} of 1 and diluted 100 times in fresh growth medium with or without 10 µM PyoG. OD_{600} was monitored on a CLARIOstar Plus microplate reader (BMG Labtech) at 37 °C for 20 h. All measurements were performed in triplicate.

2.6.3 *Galleria mellonella* larvae infection model

G. mellonella larvae were obtained from Livefood UK and used for *in vivo* testing of PyoG activity. *P. aeruginosa* PAO1 was grown in LB at 37 °C to an OD_{600} of 0.6. Cells were then washed twice and diluted in sterile PBS. Inocula were serially diluted and plated on LB agar plates for CFU counting. Groups of 10 larvae were injected with 10 µL of bacterial suspension in the hemocoel via the last right pro-limb, with PBS used as a negative control. Following challenge, larvae were placed in an incubator at 37°C and treated 3 h post-infection by injection of 10 µL of 10 µM PyoG in the hemocoel via the last left pro-limb. Survival was followed for 48 h. Larvae were considered dead when unresponsive to touch. Experiments were conducted in triplicate by Dr. Khedidja Mosbahi, Institute of Infection, Immunity, and Inflammation, University of Glasgow.

2.7 Binding assays

2.7.1 Formaldehyde cross-lining

Binding of pyocin AP41 to the components of the Ton or the Tol system were assessed by formaldehyde cross-linking. Proteins were mixed to a final concentration of 10 µM in 20 mM HEPES pH 7.8, 100 mM NaCl and incubated in the presence of 1 % formaldehyde for 1 h, at room temperature. Complex formation was then assessed on a 10 % SDS-PAGE gel.

2.7.2 Analytical gel filtration

Proteins were mixed to a final concentration of 10 µM in 50 mM Tris-HCl pH 7.8, 100 mM NaCl, and loaded on a Superdex 200 10/300 GL column equilibrated in the same buffer. 1% (w/v) β-OG was added to the buffer when OprH was used. For proteins smaller than 25 kDa, Superdex 75 10/300 GL was used. Elution profiles were compared for the complex and for individual proteins.

2.7.3 Isothermal titration calorimetry (ITC)

The binding affinity of pyocin AP41, or AP41 derivatives, and TonB1 was measured by ITC. ITC was performed in a MicroCal iTC200 at 25 °C in 50 mM Tris-HCl pH 7.8, 100 mM NaCl. AP41 was at 200 µM in the syringe, and TonB1 was at 26 µM in the cell of the instrument. The data were fit to a single binding site model in Microcal LLC Origin software. The experiment was performed in triplicate.

2.7.4 *In vivo* protein pull-downs

The pyocin AP41-Im complex was used as bait to pull-down outer membrane proteins involved in its import. A 1 L culture of *P. aeruginosa* PAO1 was grown over-night in LB at 37 °C, 140 rpm. Cells were pelleted (4500 *x g,* 20 min) and resuspended to 10 mL of LB, to which 1 mg of pyocin and 1 % of formaldehyde were added. This was incubated for 30 min at room temperature. Cells were then washed 3 times in LB to remove unbound pyocin. Outer membrane proteins were extracted as described in section 2.5.3. The extract was then loaded onto a HisTrap HP column equilibrated in 50 mM Tris-HCl, 250 mM NaCl, 1 % (w/v) β-OG, and proteins eluted using an imidazole gradient reaching 250 mM. Fractions were analysed on a 10 % SDS-PAGE gel and compared to a negative control that did not contain any pyocin.

2.7.5 *In vitro* protein pull-downs

In vitro pull-downs were performed either using the PyoG-ImG-His_6 complex or His_{10}-TEV-Hur as bait. Proteins were mixed to a final concentration of 10 µM in binding buffer (50 mM Tris-HCl pH 7.8, 250 mM NaCl, with the addition of 1 % (w/v) β-OG if Hur was used). 300 µL of Ni-NTA resin (QIAGEN) was washed in the same buffer and added to 100 µL of protein mix. The resin was then transferred to a Spin Column (Pierce) and washed until no absorbance at 280 nm could be detected in the wash. Proteins were eluted in 100 µL of the binding buffer with the addition of 500 mM imidazole and analysed on a 12 % SDS-PAGE gel.

2.7.6 Pull-downs of hemin with Hur

Pull-downs with His_{10}-TEV-Hur as prey were used to detect bound hemin. 10 µM Hur was mixed with 1 mM hemin (Sigma) in a 250 µL reaction volume, in the presence or absence of 10 µM PyoG. 750 µL of Ni-NTA resin in 50 mM Tris-HCl pH 8, 1 % β-OG was added to the mix. The beads were washed in the same buffer with the addition of 250 mM NaCl on a Spin Column until no absorbance could be detected at 280 and 410 nm. 410 nm was determined as the absorbance maximum for hemin in binding buffer with β-OG. Proteins were then eluted in 250 µL of binding buffer with 500 mM imidazole. Absorbance spectra of eluted proteins and hemin were measured (Jasco V-550 UV-Visible Spectrophotometer) in the 250-700 nm range. The relative amount of hemin-to-protein was determined by dividing the 410 nm hemin peak by the 280 nm protein peak. Experiments were performed in triplicate.

2.8 Fluorescence microscopy

2.8.1 Conjugation of maleimide fluorophores to proteins

Pyocins were fluorescently labelled using Alexa Fluor 488 C5 maleimide (AF488) fluorophore that was linked to proteins via an engineered C-terminal cysteine. The protein was first reduced in 10 mM DTT for 2 h at room temperature. DTT was removed on a 5 mL HiTrap desalting column equilibrated into 50 mM Tris-HCl pH 7, 100 mM NaCl. Pyocins were then incubated for 1 h at room temperature with a 3-fold molar excess of AF488. The reaction was quenched with 5 mM DTT. The solution was centrifuged at 16 000 *x g* for 30 min to remove protein aggregates and desalted as before. Unbound AF488 was removed by running

the labelled protein on a Superdex 200 10/300 GL column equilibrated in 50 mM Tris-HCl pH 7, 100 mM NaCl. The absorbance was measured at 280 nm and 494 nm using a V-550 UV-Visible Spectrophotometer (Jasco), and labelling efficiency determined as described in the manufacturer's protocol (Molecular Probes Inc, 2006). All fluorescently labelled proteins used for microscopy were labelled with greater than 95% efficiency.

2.8.2 Labelling of live *P. aeruginosa* cells with fluorescent pyocins

Fluorescent pyocins were used to label *P. aeruginosa* PAO1. Bacteria were grown overnight in M9 medium at 37 °C with shaking. 1 mL of this overnight culture was pelleted and resuspended in 10 mL M9 medium and grown until an OD_{600} of 0.5. All pelleting steps were performed at 7000 *x g* for 3 min. 1 mL of cells was washed in PBS pH 7, and labelled with 2 µM pyocin for 30 min at room temperature. The unbound pyocin was removed by three washes in PBS. For the trypsin protection assay, after labelling, cells were exposed to 0.5 mg/mL trypsin for 1 h at 30 °C, in PBS with 35 µg/mL chloramphenicol. After a final washing step, bacteria were resuspended in 30 µL of PBS. 3 µL of cells were then loaded onto agarose pads, prepared using Geneframes (Thermo Scientific). 80 µL of 1% (w/v) agarose in PBS was pipetted into the Geneframe (17×28 mm). The surface was flattened with a cover slip and excess agar removed. Once the agar solidified the cover slip was removed, the bacterial suspension added and a new coverslip attached to the adhesive side of the Geneframe.

2.8.3 Labelling of *P. aeruginosa* sphaeroplasts with fluorescent pyocins

Bacteria were grown overnight in M9 medium at 37 °C with shaking. 1 mL of this overnight culture was pelleted and resuspended in 10 mL M9 medium and grown until an OD600 of 0.5. All pelleting steps were performed at 3000 *x g* for 10 min. 1 mL of cells was pelleted and resuspended in PBS pH 7, with the addition of 0.5 M sucrose, 20 mM EDTA and 1.5 mg/mL lysozyme, and incubated for 45 min at room temperature. Cells were then washed with PBS, 0.5 M sucrose, and mixed with 2 µM fluorescent pyocin. After 30 min incubation at room temperature, unbound pyocin was removed by three washes in PBS, 0.5 M sucrose. For the trypsin protection assay, after labelling, cells were exposed to 0.5 mg/mL trypsin for 1 h at 30 °C, in PBS, 0.5 M sucrose. After a final washing step, bacteria were resuspended in 30 µL of PBS, 0.5 M sucrose and loaded onto agar pads as described above. Agar was supplemented with 0.5 M sucrose to prevent the bursting of the sphaeroplasts.

2.8.4 Image collection and data analysis

All images were collected on an Oxford Nanoimager S microscope. Images were collected at 100 ms exposure and 20 % 488 nm laser power. For every image, 20 frames were collected and merged using the command “Zproject” in Image J. Average fluorescence was measured for a total of 50 cells per condition per repeat, and was corrected by subtracting the average background fluorescence. All experiments were conducted in triplicate. The fluorescence intensity of experimental groups (groups exposed to fluorescent pyocin) was compared to the unlabelled control by the Kruskal-Wallis test, using Dunn’s test as the post hoc procedure (confidence level 0.001). The analysis was performed by GraphPad Prism version 6.04 for Windows, GraphPad Software, La Jolla California USA, www.graphpad.com.

3. Identification of PyoG translocon components

3.1 Introduction

Mining *P. aeruginosa* genomes for novel pyocin genes is an important step in developing this class of protein antibiotics as therapeutics. Therefore, a bioinformatics pipeline developed by our laboratory represents a valuable tool for detecting and exploring the diversity of pyocins (Sharp *et al.* 2017). Using this pipeline to search for the conserved Pyocin S domain (PF06958) in genomes of different Gram-negative bacteria, several new putative nuclease pyocin genes were discovered, including *pyoG*.

pyoG encodes a 640 amino acid protein toxin in which the first 485 residues are similar to pyocins S1, S6 and SD1 (Appendix F-1). Due to these similarities PyoG, was classed as an S1 group pyocin. Based on sequence homology to pyocin S1 and carocin D, three functional domains of PyoG were annotated (Figure 3-1). All S1 group pyocins have two conserved N-terminal domains required for translocation (Domain l and domain ll, Figure 3-1) (Sano *et al.* 1993). Both are essential for pyocin-induced killing. Domain II corresponds to the conserved Pyocin S domain (Appendix F-2), used in the original search for novel bacteriocins (Sharp *et al.* 2017). Based on this conservation within the group, the domain boundaries of PyoG domain I and domain II could be assigned from alignment to PyoS1. The cytotoxic domain (Domain III) and the immunity protein of PyoG are highly similar to carocin D, an endonuclease bacteriocin from *Pectobacterium carotovorum* (Roh *et al.* 2010), allowing for logical annotation of these domains (Figure 3-1). This domain does not have an HNH motif, commonly found in nuclease bacteriocins. However, due to the lack of structural data on pyocins of the S1 group, exact domain boundaries of PyoG are unknown.

Due to conservation of the receptor binding and translocation domains amongst all S1 group pyocins, they must all recognise and bind the same cell envelope receptors during import into cells. However, none of the proteins involved in the import process for S1 group pyocins are currently known. Therefore, identifying the proteins required for PyoG translocation is important for the potential clinical application of all S1 group pyocins.

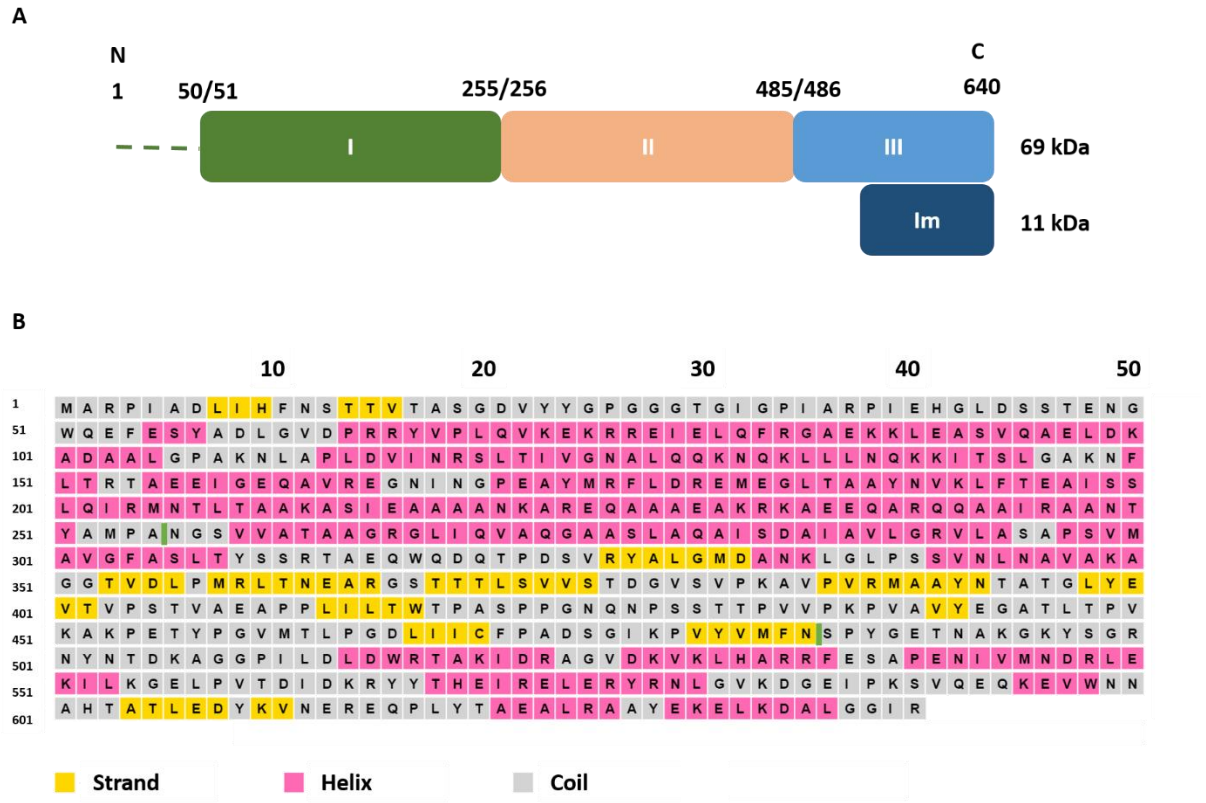

Figure 3-1. Probable domain organization of PyoG (A). Residue numbers are shown above domain boundaries. The first 50 residues are predicted to be disordered by DisEMBL 1.5 (Linding *et al.* 2003). Domains I-II were annotated based on probable domain organization of PyoS1 (Sano *et al.* 1993), and the secondary structure prediction of PyoG (B). The secondary structure prediction was generated by PSIPRED (McGuffin *et al.* 2000). Domain I is involved in receptor binding and Domain II in pyocin translocation, both being essential for killing (Sano

et al. 1993). Domain II corresponds to the Pyocin S domain (Figure 1-1; PF06958), conserved amongst modular nuclease bacteriocins (Sharp *et al.* 2017). Doman III is the cytotoxic nuclease domain. The immunity protein and Domain III are homologous to carocin D, an endonuclease bacteriocin from *Pectobacterium carotovorum* (Roh *et al.* 2010).

3.1.1 Aims

The aim of this chapter was to express and purify PyoG and test its cytotoxic activity against clinical isolates of *P. aeruginosa*, including its efficacy in a *Galleria mallonella* infection model. The aim was also to investigate the cell envelope components required for translocation of the pyocin and propose a model of its import. The latter goal was addressed via a transposon mutant screen, followed by *in vitro* pull-down assays to validate proposed interactions between PyoG and cell-envelope proteins.

3.2 Results

3.2.1 Expression and purification of PyoG

PyoG was heterologously expressed in *E. coli* BL21(DE3) in complex with its immunity protein (ImG- His_6). In order to successfully express PyoG, it was necessary to have an extra copy of *imG* expressed from a separate plasmid. It is likely that excess ImG was required for PyoG expression due to the inherent toxicity of PyoG to host cells. An excess of ImG could inhibit this PyoG toxicity during over expression in cells, which in turn increased PyoG yield. The PyoG-ImG-His_6 complex was purified using affinity chromatography with a HisTrap HP column. After binding the protein to the column through the C-terminal hexhistidine tag on ImG, the complex was eluted using an imidazole gradient (15-160 mM) (Figure 3-2). To buffer exchange and remove residual contaminants, the PyoG-ImG-His_6 complex was subject to gel filtration using a HiLoad 26/60 Superdex 200 pg column (Figure 3-3). Three peaks were observed in the resulting SEC chromatogram (Figure 3-3), however SDS-PAGE confirmed that only fractions corresponding with the main elution peak II contained the PyoG-ImG-His_6 complex. Other peaks were located at the column void volume (Peak I) and total column volume, thus are consistent with aggregate and small contaminants, respectively. PyoG-ImG-His_6 containing fractions were pooled, concentrated, and the protein identity was confirmed by peptide mass fingerprinting. The final protein (Figure 3-4 A) concentration determined by UV absorbance at 280 nm, assuming a sequence-based extinction coefficient of 61770 $M^{-1}cm^{-1}$. The yield of PyoG-ImG-His_6 complex was ~10 mg of protein per L of bacterial culture.

To test if the purified pyocin complex was folded and active a killing assay was carried out (Figure 3-4 B). PyoG-ImG was applied to *P. aeruginosa* PAO1 at concentrations from 4.5

nM to 10 µM. Areas of clearance are consistent with PyoG-mediated killing, observed to ~40 nM (Figure 3-4 B). These results confirmed that the isolated PyoG-ImG complex was folded and active against *P. aeruginosa* PAO1 strain.

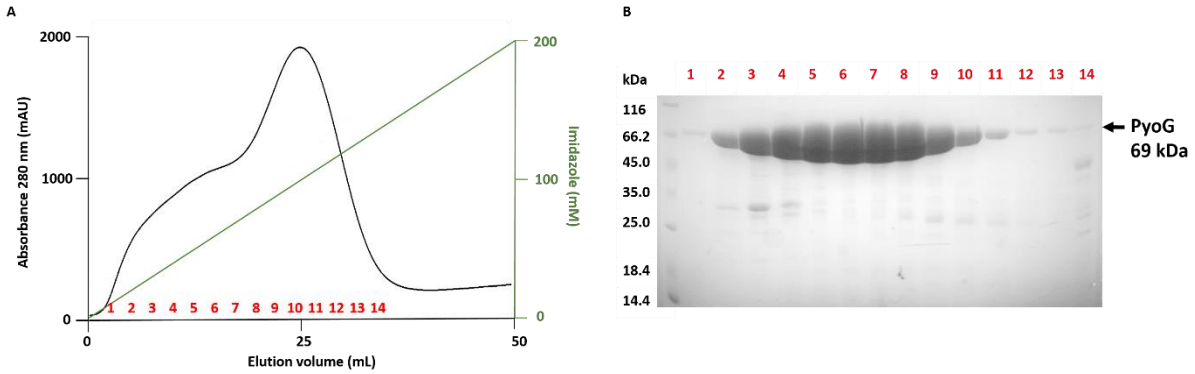

Figure 3-2. Affinity chromatography of PyoG (69 kDa) in complex with ImG-His_6 (11 kDa). A – Chromatogram following UV absorbance at 280 nm during imidazole gradient elution of the PyoG-ImG-His_6 complex from a HisTrap HP column. The complex was purified in 50 mM Tris-HCl pH 7.8, 500 mM NaCl and eluted over a gradient reaching 200 mM imidazole at a 3 mL/min flow rate. B – a 12 % SDS-PAGE gel showing fractions from the elution. Fractions are labelled with red numbers and their positions are shown on the elution profile in A. Position of PyoG is labelled on the right side of the gel. ImG cannot be seen on this gel.

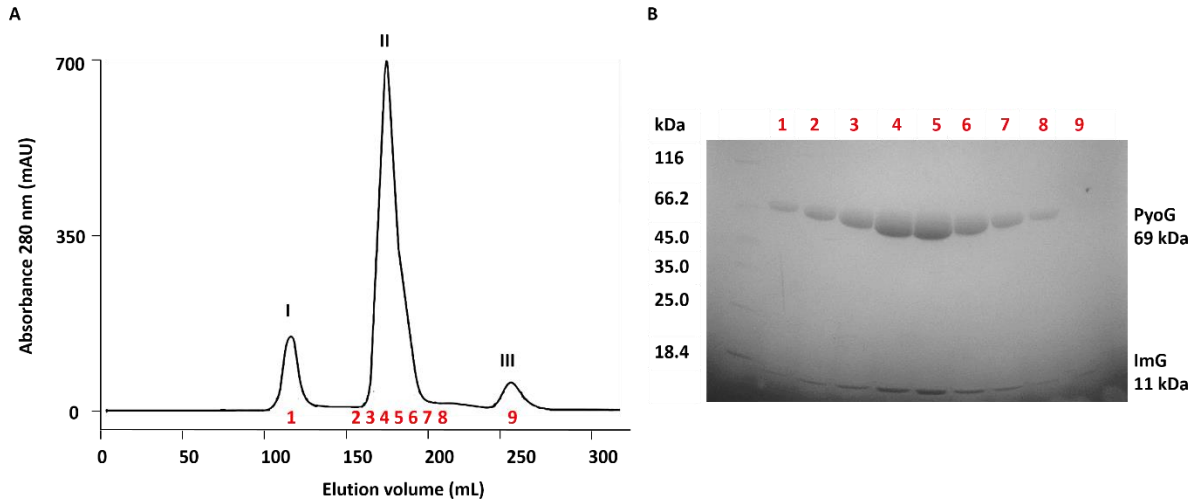

Figure 3-3. Gel filtration of the PyoG-ImG-His_6 complex. A – Chromatogram tracing UV absorbance at 280 nm showing the elution profile of the PyoG-ImG-His_6 complex on a 26/60 Superdex S200 pg column. The complex was purified in 50 mM Tris-HCl pH 7.8, 250 mM NaCl. B – fractions from the profile are labelled with red numbers and are shown on a 4-20 % SDS-PAGE gel. Peak II fractions containing PyoG (69 kDa) and ImG (11 kDa) were pooled for further studies. Average protein yield was 10 mg of protein per L of cell culture.

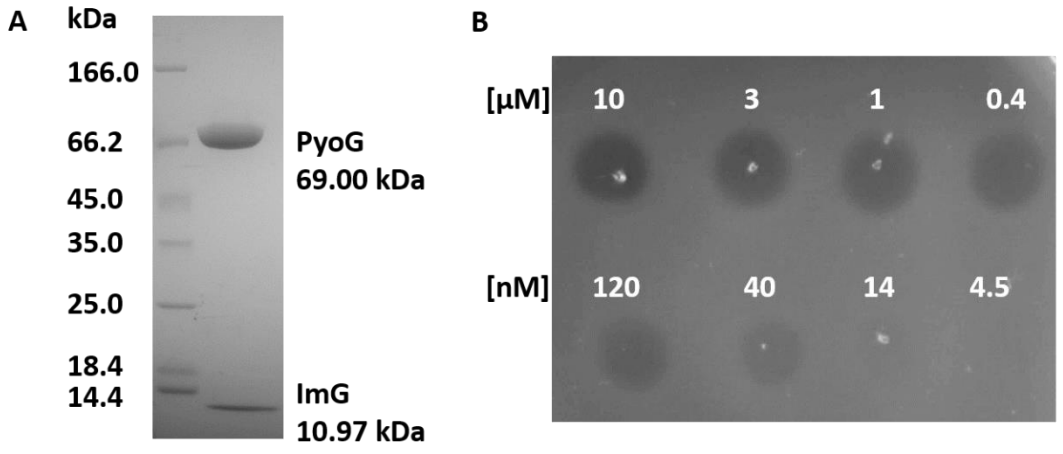

Figure 3-4. Purification and activity of PyoG. A – 4-20 % SDS/PAGE gel of purified PyoG (PyoG, 69 kDa) and its immunity protein (ImG-His6, 11 kDa). B – 3 µL of PyoG-ImG at varying

concentrations was spotted on top of a lawn of *P. aeruginosa* PAO1. Clearance zones were observed after overnight incubation at 37 ^{o}C, which are indicative of killing. The pyocin kills down to ~40 nM. Figure modified from Atanaskovic *et al.* 2020.

3.2.2 The killing activity of PyoG

The strain coverage of PyoG and its *in vivo* killing activity were next investigated. One of the factors that influences pyocin strain coverage is how commonly expressed the immunity protein is in other strains of *P. aeruginosa*. All pyocin producing strains express the corresponding immunity gene within the same operon, but immunity protein genes can also be orphans (Ghequire *et al.* 2017b). If PyoG immunity is not widely found in *P. aeruginosa* strains then it would be anticipated to have good strain coverage for killing because strains would not be able to produce an immunity protein capable of combating PyoG toxicity. To get an estimate of the expression range of PyoG immunity protein, the PubMLST Database was searched (Jolley *et al.* 2018). It was found that *imG* is present in 11 of 6,973 strains in the database. The small number of strains with *imG* suggests that good strain coverage would be possible with PyoG. This result is exceptional when compared to the coverage of the pyocin S1 immunity, which is present in 744 strains.

To test this hypothesis, PyoG killing activity was assessed against a collection of *P. aeruginosa* clinical isolates (Table 2-1). This experiment was performed in collaboration with Dr Khedidja Mosbahi, Walker Laboratory, Institute of Infection, Immunity, and Inflammation, University of Glasgow. These tests confirmed that ~90 % of the screened strains were sensitive to PyoG killing, with most having nanomolar MICs (Figure 3-5 A). The high strain coverage observed here indicates that not only is PyoG a good candidate to study for

antimicrobial development, but also that the translocation machinery used by this protein is common in *P. aeruginosa* genomes.

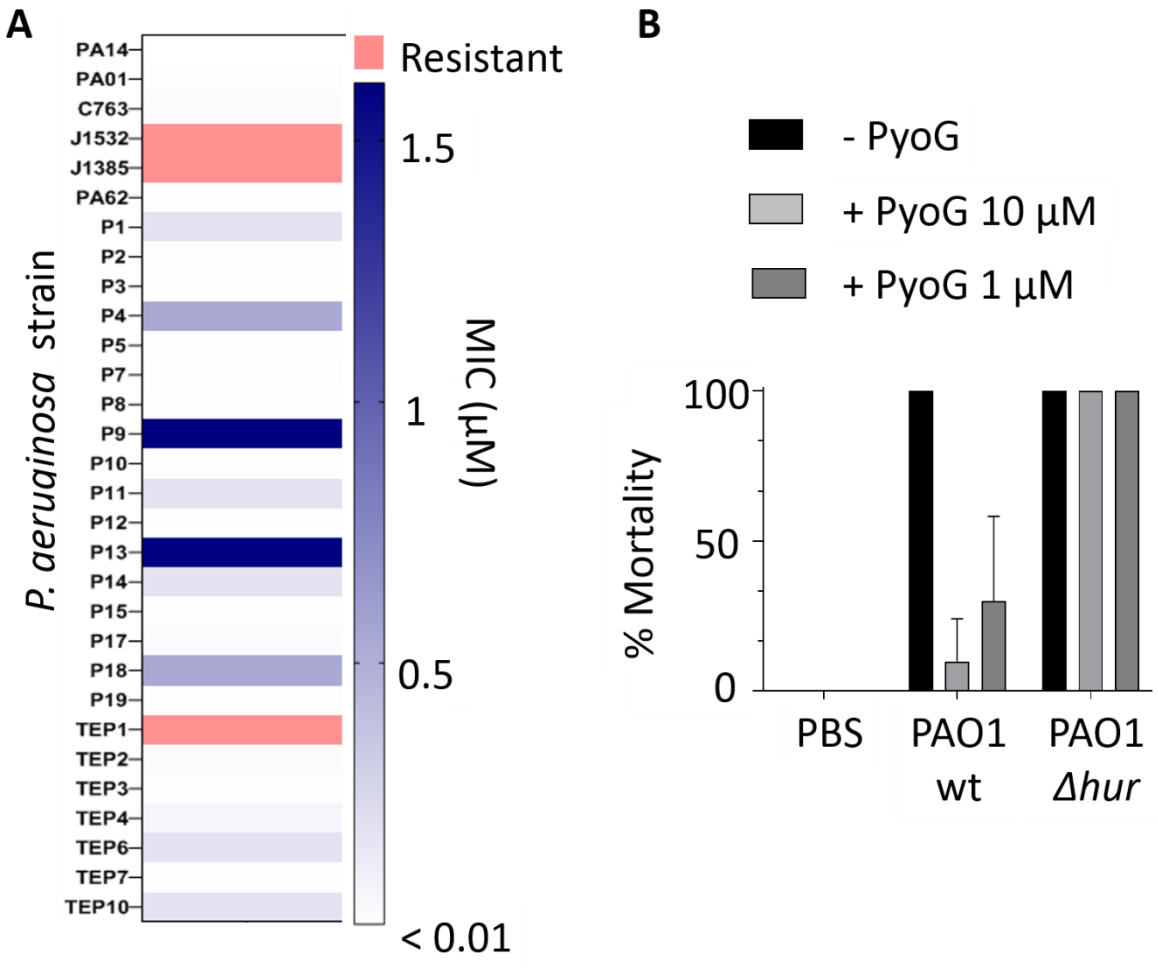

Figure 3-5. PyoG is active against clinical isolates of *P. aeruginosa* and can rescue *Galleria mallonella* from a lethal dose of *P. aeruginosa* PAO1. A - PyoG MICs for a collection of *P. aeruginosa* clinical isolates (Table 2-1). Resistant strains are shown in red, and MICs values are represented as shades of blue. 90 % of screened strains were sensitive to PyoG. B – *In vivo* activity of PyoG against a lethal dose of *P. aeruginosa* PAO1 in a *Galleria mallonella* infection model. 10 µL of 10 µM PyoG provides protection against PAO1. PAO1 *Δhur* is a PyoG resistant mutant which lacks the receptor for the pyocin. PyoG does not provide protection against this strain. These experiments were performed by Dr Khedidja Mosbahi, Walker Laboratory,

Institute of Infection, Immunity, and Inflammation, University of Glasgow. Figure taken from Atanaskovic *et al.* (2020).

In addition to testing of clinical isolates, the efficacy of PyoG against *P. aeruginosa* in a *Galleria mallonella* infection model was also investigated (Figure 3-5 B). This test was performed by Dr Khedidja Mosbahi, wherein *G. mallonella* was exposed to a lethal dose of *P. aeruginosa* PAO1. Three-hours post-infection the larvae were treated with 10 µL of 10 µM or 1 µM PyoG. Both treatments increased the survival rate of the larvae. Therefore, PyoG is a newly discovered pyocin which has good strain coverage and *in vivo* activity against *P. aeruginosa* infection.

3.2.3 PyoG requires Hur, TonB1 and FtsH for killing

After establishing a method to purify active PyoG, the next step was to determine which cell envelope proteins are required for its import. Identification of the translocon components for PyoG would be applicable to other S1 group pyocins, helping to narrow the number of *P. aeruginosa* strains that are likely to be killed by the S1 group pyocins. Toward this end, a screen was conducted of the PyoG susceptibility of transposon mutants of PAO1 carrying insertions in genes coding for cell envelope proteins employed by other nuclease pyocins and colicins. One such protein is the inner membrane AAA+ ATPase/protease FtsH, which is required for the killing activity of several nuclease colicins (Walker *et al.* 2007). PyoG killing activity was therefore tested against an *ftsH* deletion mutant of *P. aeruginosa* PAO1 by plate and liquid killing assays. This experiment showed that the *ftsH* deletion mutant was

resistant to PyoG killing. Sensitivity could be restored by complementation from plasmid-expressed *ftsH* (Figure 3-6 A).

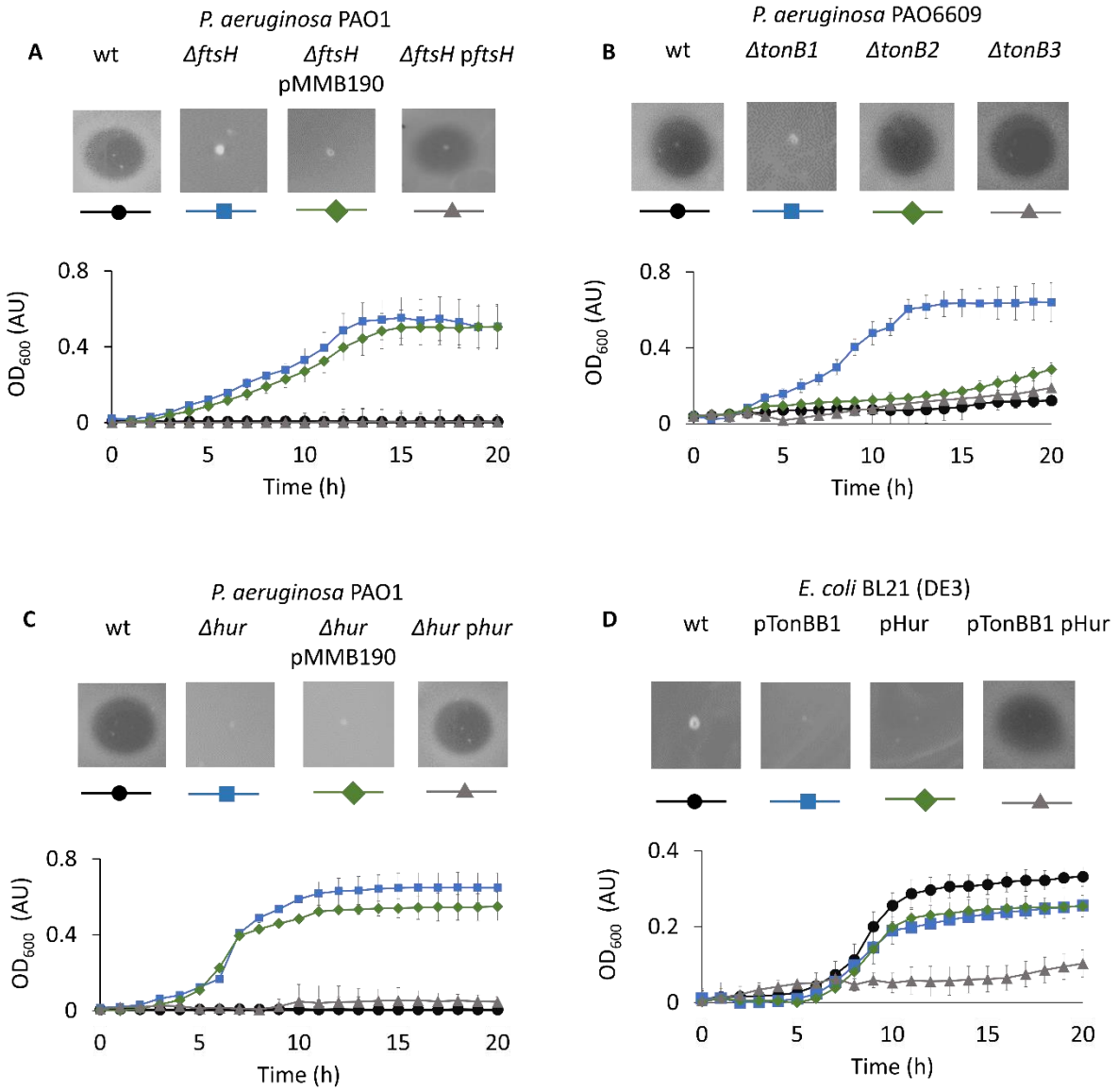

Figure 3-6. Plate and liquid killing assays with 10 µM PyoG reveal which cell envelope proteins are required for its import. For plate killing assays, 3 µL of pyocin was spotted on top of bacterial lawns and plates incubated overnight at 37 °C. For liquid killing assays, OD_{600} values represent the mean of three biological replicates with standard deviations shown. A – FtsH, an inner membrane AAA+ ATPase/protease, is required for PyoG killing activity. *P. aeruginosa*

PAO1 *ΔftsH* is resistant to PyoG and is unaffected by the introduction of the empty shuttle vector pMMB190 (*ΔftsH* pMMB190). However, transformation of PAO1 *ΔftsH* with p*ftsH* complemented the *ftsH* deletion and restored sensitivity to PyoG. B – TonB1, a protein that links the PMF generated on the inner membrane with translocation across the outer membrane, is necessary for PyoG killing activity. *ΔtonB1* mutant of *P. aeruginosa* is resistant to PyoG. *ΔtonB2* and *ΔtonB3* mutants are sensitive. C – The killing activity of PyoG depends on an outer membrane transporter, Hur. Deletion of *hur* induces resistance to the pyocin. Sensitivity can be restored if *hur* is complemented from a plasmid. p*hur* is *hur* cloned from PAO1 into pMMB190. D – *E. coli* BL21(DE3) is not sensitive to PyoG. PyoG sensitivity in this organism can be induced if transformed with both pTonBB1 and pHur. pTonBB1 is *E. coli* $TonB^{1-102}$ translationally fused to *P. aeruginosa* $TonB1^{201-342}$ and cloned into pACYCDuet-1 (Behrens *et al.* 2020). pHur is *hur* with the *E. coli* OmpF signal sequence, codon optimised for expression in *E. coli* and cloned into pET21d. Figure taken from Atanaskovic *et al.* (2020).

After identifying FtsH as an integral component of PyoG import, the next step was to determine the energy transduction pathway hijacked for import to the periplasm. PyoS2 (White *et al.* 2017), PyoSD2 (McCaughey *et al.* 2016b), and PyoS5 (Behrens *et al.* 2020), all require the Ton system for energized cell entry. Therefore, *P. aeruginosa* strains lacking different TonB variants were tested for resistance to PyoG-induced killing. Both plate and liquid killing assays showed that the *ΔtonB1* mutant is resistant to PyoG (Figure 3-6 B). To confirm the role of TonB1 in PyoG import, the periplasmic domain of TonB1 was purified and used in *in vitro* binding assays with PyoG. TonB1 was captured by PyoG in a pull-down assay, where PyoG was bound to NTA resin through its association with ImG-His_6, demonstrating

that TonB1 and PyoG interact *in vitro* (Figure 3-7). Hence, PyoG binds TonB1 in *P. aeruginosa* cells which energizes import across the outer membrane.

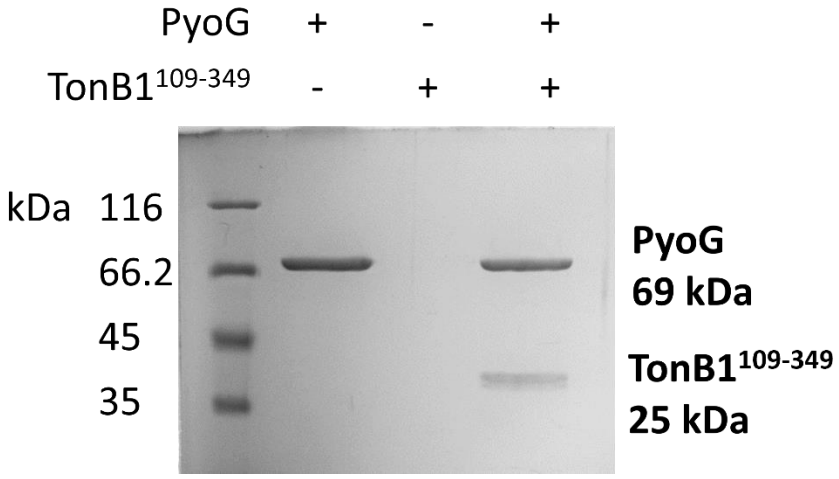

Figure 3-7. Pull-down of PyoG-ImG-His_6 and $TonB1^{109-349}$. Proteins indicated above the gel were mixed at equimolar concentrations, beads were washed and bound protein eluted with imidazole. Eluate was analysed on 12 % SDS-PAGE gels. Protein marker is in the first lane. Eluate when only bait protein (PyoG) was applied to resin is in the second lane. Eluate when only the prey protein (TonB1) was applied to the resin is shown in the third lane, verifying that the prey does not bind to beads in the absence of PyoG. Eluate for the mix of bait and prey is shown in the fourth lane. Positions of proteins with their molecular masses are labelled on the right side of the gel. This experiment confirmed that PyoG and the periplasmic region of TonB1 interact *in vitro*. Figure adapted from Atanaskovic *et al.* 2020.

The identification of TonB1 as a requirement for PyoG import provided the starting point for finding the outer membrane receptor/translocator. It was assumed that the PyoG receptor must also be TonB dependent. By searching the *P. aeruginosa* PAO1 genome for the

TonB plug domain (Pfam domain PF07715) as previously described (Ghequire & Ozturk, 2018), 37 candidate receptors/translocators for PyoG were identified (Table 1-1). A library of transposon mutants for all 37 TBDTs was screened using PyoG. It was found that a transposon insertion into locus *PA1302* yielded resistance to PyoG (Figure 3-6 C). Sensitivity to PyoG killing was restored if the mutation was complemented from a plasmid, suggesting this locus codes for the PyoG receptor and/or translocator.

It has previously been shown that *PA1302* is linked with the import of pyocin PaeM4 in *P. aeruginosa* (Ghequire & Ozturk 2018) and with hemin uptake into cells (Otero-Asman *et al.* 2019). Therefore, the protein encoded by the *PA1302* locus was named **H**emin **u**ptake **r**eceptor (Hur). An important question is whether TonB1 and Hur are the sole requirements for PyoG import across the outer membrane? This question was addressed using a strategy developed by Behrens *et al.* 2020. *E. coli* cells were transformed with plasmids encoding Hur and a TonB chimera, comprised of *E. coli* TonB and the C-terminal periplasmic domain of *P. aeruginosa* TonB1, which were then tested for susceptibility for PyoG-mediated killing (Figure 3-6 D). The data show that the introduction of both proteins into *E. coli* results in susceptibility to PyoG killing. Taken together, the results presented in this section indicate that Hur and periplasmic TonB1 are the specific components of the outer membrane translocation machinery required for the entry of PyoG into the periplasm of *P. aeruginosa* cells. Once in the periplasm, FtsH is then involved in the inner membrane translocation step.

3.2.4 Hur is essential for cell surface binding of PyoG

Although Hur is sufficient for outer membrane transport the results from section 3.2.3 do not rule out the possibility that PyoG binds to other cell surface features, such as CPA or

indeed another protein. Several pyocins (McCaughey *et al.* 2014; Behrens *et al.* 2020) use LPS as a receptor to get concentrated on the cell surface, and then translocate across the outer membrane through a protein transporter. To test if this is also the case of PyoG, several LPS mutants of *P. aeruginosa* were tested for PyoG sensitivity (Figure 3-8). None of the mutants were resistant to the pyocin, which indicates that LPS is not required for its binding to the cell surface. On the contrary, some of the mutants were more sensitive to PyoG than the wt strain, which indicates that removal of LPS components can facilitate binding of PyoG to cell surface.

To further investigate if Hur is essential for PyoG binding to the surface of *P. aeruginosa*, fluorescent microscopy was used. For these experiments, a fluorescently labelled PyoG ($PyoG^{1-485}$) was constructed and used in microscopy experiments to investigate cell surface association in wild type and *Δhur* PAO1 cells. $PyoG^{1-485}$ lacks the cytotoxic domain of the pyocin and has a cysteine at the C-terminus for conjugation with Alexa Fluor dyes. The cytotoxic domain was removed so the cells can be labelled without being killed by the pyocin. After incubation of live *P. aeruginosa* cells with the PyoG fluorescent label, cells were washed and imaged using epifluorescence microscopy. This allowed for direct observation that PAO1 was able to bind PyoG, whereas the *Δhur* mutant was PyoG binding incompetent (Figure 3-9). Complementation with *hur* expressed from a plasmid restored similar fluorescence levels as observed for PAO1 cells (Figure 3-9B). Combined with the PyoG sensitivity of *E. coli* expressing Hur and the TonBB1 chimera (Figure 3-6 D), the data demonstrate that Hur is the essential outer membrane component to which PyoG binds and that it plays the role of both receptor and translocator.

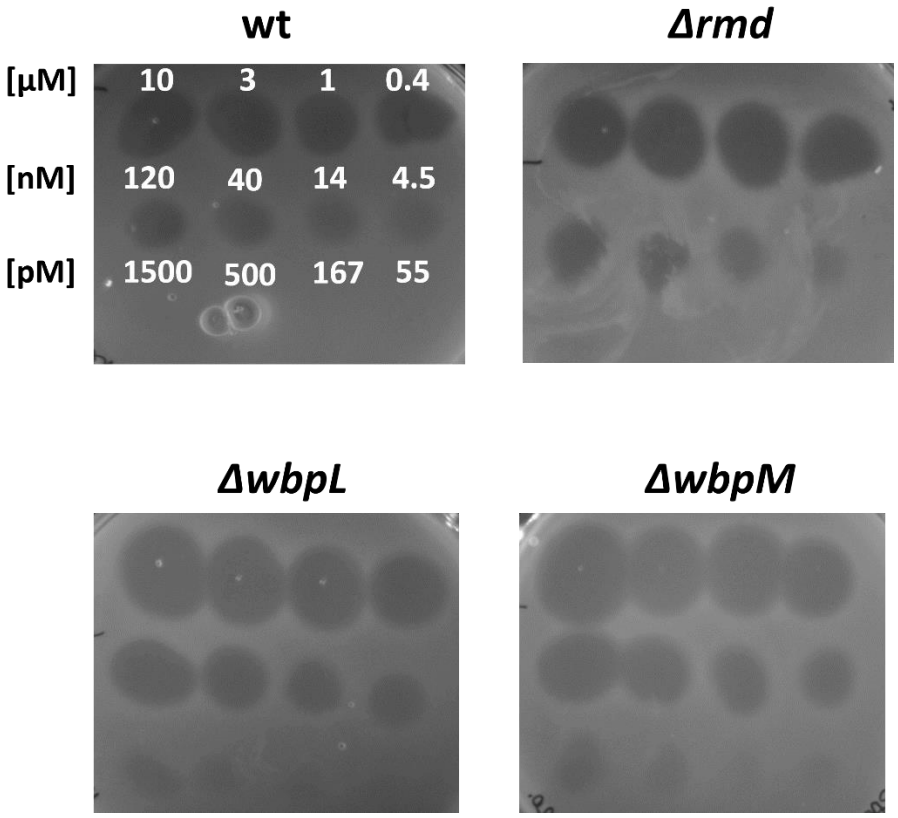

Figure 3-8. Plate killing assay with PyoG-ImG and the lipopolysaccharide (LPS) mutants of *P. aeruginosa*. 3-fold serial dilutions starting at 10 µM PyoG-ImG were used. The same serial dilutions were applied to all plates and are indicated on the plate with the wt strain. *Δrmd* lacks the common polysaccharide (CPA) component of LPS. *ΔwbpM* lacks the O-specific antigen component (OSA) of LPS. *ΔwbpM* lacks both CPA and OSA, and has just the uncapped lipid A component of LPS (Lam *et al.* 2012). None of these mutants were resistant to PyoG, indicating that CPA and OSA are not required for its binding to the cell surface.

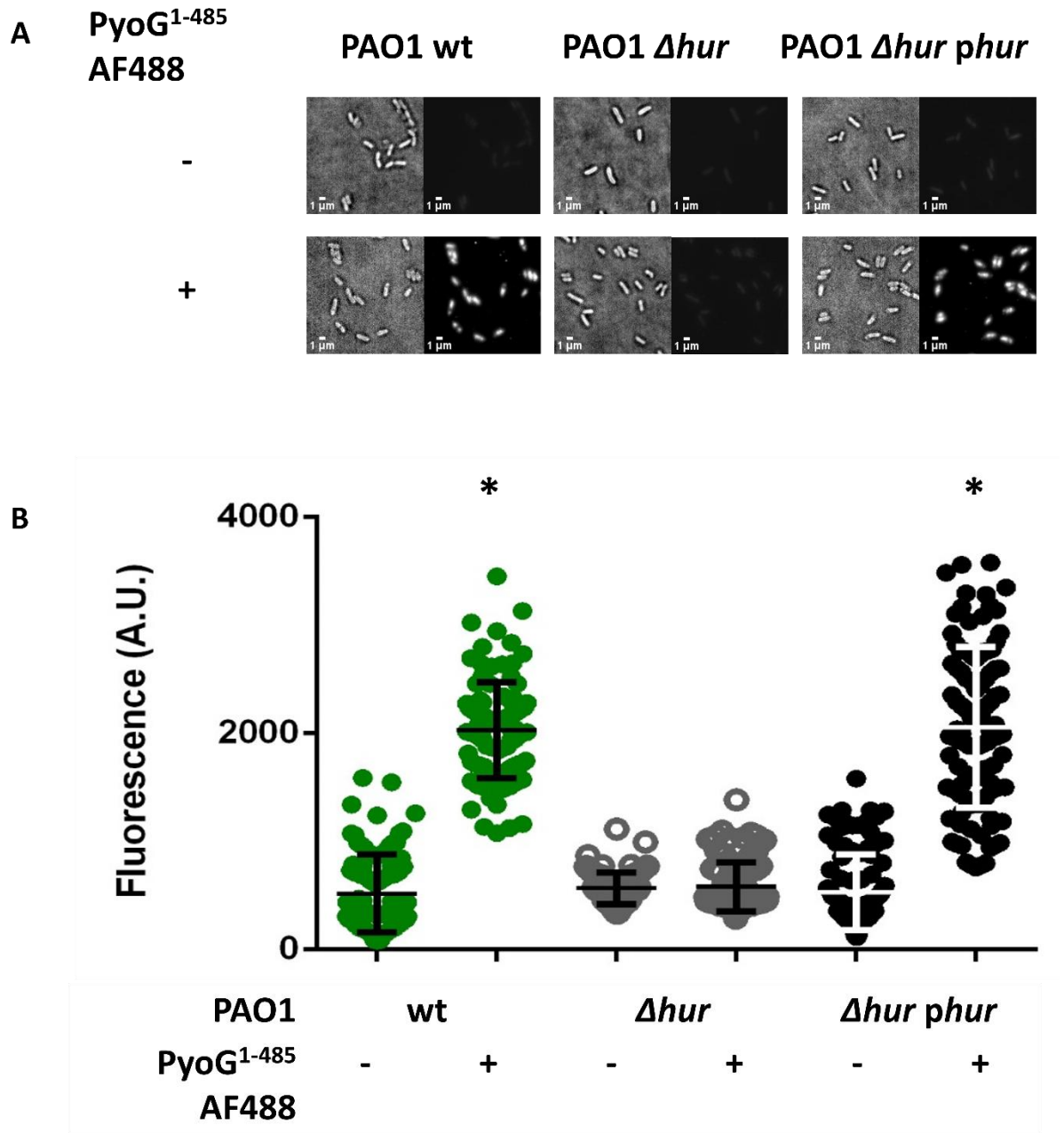

Figure 3-9. Hur is required for PyoG to target *P. aeruginosa* cells. A – Fluorescent labelling of PAO1 wt, *Δhur* and *Δhur* complemented with Hur expressed from a plasmid (*Δhur* p*hur*). PyoG$^{1-485}$, conjugated to AF488 via a C-terminal cysteine, was used for labelling. The parent strain was successfully labelled with fluorescent protein, whereas labelling was lost if *hur* was deleted. Labelling was restored by *hur* expression from a plasmid. Representative micrographs for each strain are shown. All snapshots were adjusted to the same intensity

scale. B - Average fluorescence intensities for 100 cells in the presence and absence of fluorescent PyoG. Mean of three biological replicates with standard deviations are shown. Fluorescence intensities for labelled groups were compared to the unlabelled control. * represents a P value below 0.0001 in the Kruskal-Wallis Test. Figure modified from Atanaskovic *et al.* 2020.

4. Function of Hur, the PyoG transporter

4.1 Introduction

Hur is a 92 kDa protein in the outer membrane *of P. aeruginosa*. It is present in 99 % of 6,973 strains in the PubMLST Database where it shows a high degree of sequence conservation (Jolley *et al.* 2018). Based on homology to other TBDTs, Hur is predicted to be a 22 stranded β-barrel with a conserved TonB plug domain (Figure 4-1). The plug occludes the channel of the barrel in the ligand-free conformation of the transporter (Figure 4-1 B). Due to the presence of the TonB plug domain, Hur is likely to bind TonB, but this interaction has not been proven experimentally.

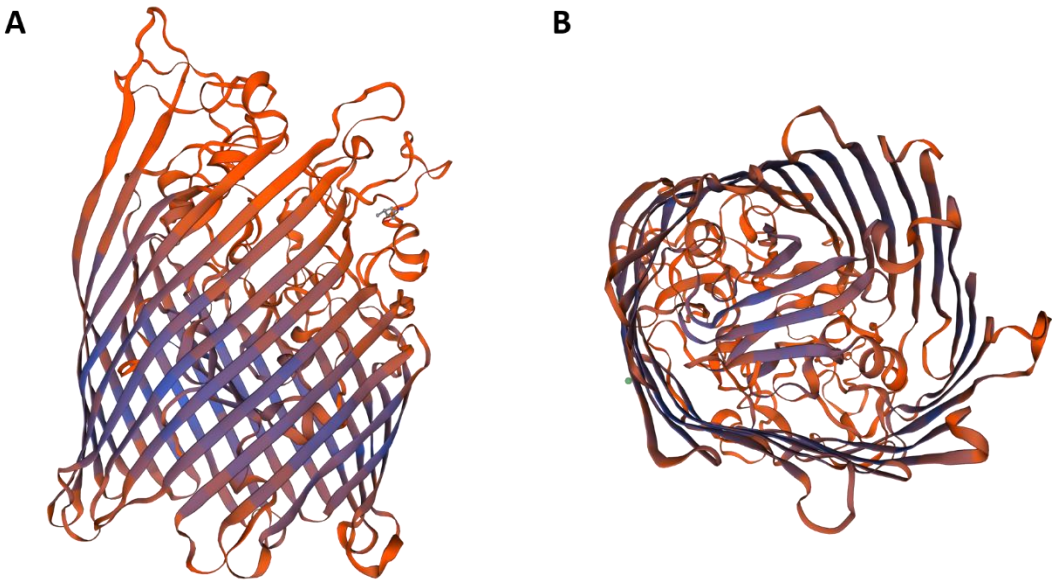

Figure 4-1. Homology model of Hur. The structure was built by SWISS-MODEL (Waterhouse *et al.* 2018). The structure of HasR from *Serratia marcescens* (PDB 3DDR) was used as a

template for model building; sequence coverage was 85 % coverage and the proteins have 23 % sequence identity and 39 % similarity. **A**, side-view, and **B** view of the structure from the periplasm. Quality estimate value (QMEAN) for the entire structure is -7.1, which classifies it as a low quality homology model. Blue represents “good quality” regions, with a positive QMEAN value. Orange regions have “low quality” with negative QMEAN, particularly the case for loops which are also less well conserved. High QMEAN regions are within the β-strands of the barrel (A), implying that Hur, like other TBDTs, is a 22-stranded β-barrel. The plug domain is well conserved and also has a high QMEAN value (B). As in other TBDTs, it is positioned inside the barrel, occluding the Hur channel.

Hur has previously been linked to pyocin import. It serves as an outer membrane receptor/translocator for pyocin PaeM4 (Ghequire & Ozturk 2018). PaeM4 is a lipid II degrading pyocin with a cytotoxic domain similar to colicin M. The receptor binding domain at the N-terminus is different to colicin M, and distinct to all other modular pyocins. It also has no sequence homology to PyoG, despite the fact that PyoG and PaeM4 share the same receptor. Therefore, it is likely that these two pyocins bind Hur via a different mechanism. However, the involvement of Hur in pyocin import has only been proposed from transposon mutant screens. The direct interaction of the receptor and the pyocins has yet to be tested experimentally.

Pyocins parasitize nutrient import pathways. In the case of Hur, the nutrient import pathway is unknown. The transporter is homologous to several other TBDTs, all of which are involved in heme uptake (Table 4-1). Therefore, this protein is probably involved in acquiring heme as an iron source. Heme acquisition genes are usually organized in operons. These

operons consist of a gene coding for the TBDT, which transports heme across the outer membrane, and a hemophore protein, which is secreted to bind heme in the extracellular environment. One example is the *has* operon, encoding HasR, a TBDT homologous to Hur, and HasA, the hemophore. HasA binds heme and transfers it to HasR. HasR has low heme binding affinity and requires the HasA hemophore for heme uptake (Krieg *et al.* 2009). On the other hand, PhuR, another Hur homolog, is not expressed from an operon and does not require a hemophore. PhuR can bind free heme or take up heme from hemeoglobin (Smith & Wilks 2015). Like PhuR, Hur is not expressed from an operon and probably does not require a hemophore for heme binding. Even though sequence homology hints that Hur has a role in heme import, this has yet to be demonstrated experimentally. It is not known if Hur binds heme, or a hemophore. The *Δhur* mutant of PAO1 can grow in the presence of heme as the sole source of iron, probably due to the expression of other *P. aeruginosa* heme uptake systems – Phu and Has. Nevertheless, *hur* is upregulated in the presence of heme and if the *hasR* gene is deleted (Otero-Asman *et al.* 2019). Therefore, it is likely that Hur has a role in heme uptake.

Table 4-1. TBDTs homologous to Hur. Proteins were found by Protein BLAST (NCBI). % of sequence identity to Hur, the organism of origin and known ligands are listed next to each protein.

Protein	% Identity	Organism	Ligand
TdhA	40.17	*Haemophilus ducreyi*	Hemin
HasR	25	*Serratia marcescens*	HasA
HxuC	22.7	*Haemophilus influenza*	Hemopexin
PhuR	22.41	*Pseudomonas aeruginosa*	Hemin, hemoglobin

4.1.1 Aims

This chapter looks at Hur function and how it relates to PyoG import. The first aim was to express and purify Hur. Second, *in vitro* assays were established to follow binding of both PyoG and hemin to Hur and establish that their binding is mutually exclusive. Binding assays were also used to determine the receptor-binding domain of PyoG.

4.2 Results

4.2.1 Expression and purification of Hur

Hur was purified to test *in vitro* binding to PyoG and hemin. *hur* was codon optimized for expression in *E. coli*. The first 29 residues were recognized as the signal sequence targeting the Sec system (SignalP 5.0, Almagro Armenteros *et al.* 2020). Since Sec signals vary between *E. coli* and *P. aeruginosa* (Lewenza *et al.* 2005), these residues were swapped for the *E. coli* OmpF signal sequence (MKRNILAVIVPALLVAGTANA), followed by His_{10} and a TEV cleavage site. This construct was expressed in *E. coli* BL21ΔABCF. This strain lacks several Omp proteins in the outer membrane, which should facilitate purification of proteins expressed in the outer membrane (Meuskens *et al.* 2017). His_{10}-TEV-Hur was purified from outer membrane extracts in 50 mM Tris-HCl pH 8, 1 % β-OG, 5 mM EDTA. EDTA was removed on a desalting column and His_{10}-TEV-Hur was then purified on a HisTrap HP column. His_{10}-TEV-Hur was eluted using ~250-300 mM imidazole (Figure 4-2).

The protein was next purified by gel-filtration on 26/60 Superdex S200 pg column equilibrated in 50 mM Tris-HCl pH 8, 1 % β-OG (Figure 4-3). Some His_{10}-TEV-Hur appeared in the void (fraction 1), probably due to protein aggregation. Most of the protein eluted as one peak around 150 mL. Fractions corresponding to this peak were pooled. Purified His_{10}-TEV-Hur is shown in Figure 4-3 C. Protein identity was confirmed by peptide mass fingerprinting. Average protein yield was 0.5 mg of protein per L of bacterial culture. The His_{10}-tag was subsequently cleaved by the TEV protease and Hur was collected as flowthrough on the HisTrap HP affinity column.

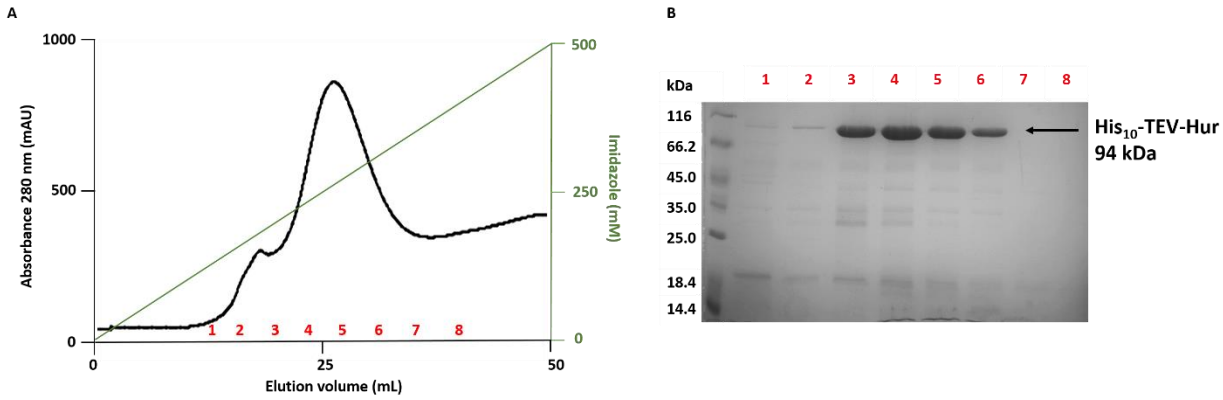

Figure 4-2. Affinity chromatography of His_{10}-TEV-Hur (94 kDa). A – gradient elution of Hur from a HisTrap HP column. The protein was purified in 50 mM Tris-HCl pH 7.8, 1 % (w/v) β-OG, on a gradient reaching 500 mM imidazole at a flow of 3 mL/min. B – a 12 % SDS-PAGE gel showing fractions from the elution. Fractions are labelled with red numbers and their positions are shown on the elution profile in A. Fractions 3-6 were pooled and used for further purification.

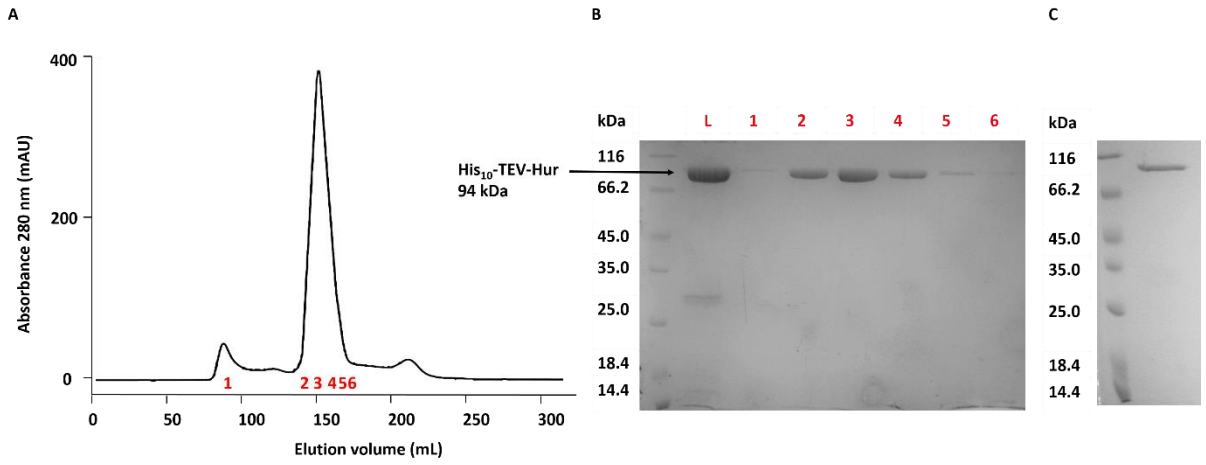

Figure 4-3. Gel filtration of His_{10}-TEV-Hur (94 kDa). A – elution profile of Hur on the 26/60 Superdex S200 pg column equilibrated in 50 mM Tris-HCl pH 7.8, 1 % (w/v) β-OG. B – fractions

from the profile are labelled with red numbers and are shown on a 12 % SDS-PAGE gel. L represents fractions pooled after affinity chromatography and loaded on the gel filtration column. Fractions 2-6 were pooled and purified His_{10}-TEV-Hur is shown in C. Average protein yield was 0.5 mg of protein per L of cells.

4.2.2 *In vitro* binding of Hur, PyoG and TonB1

His_{10}-TEV-Hur or Hur were used as bait or prey proteins in pull-down assays, which were used to test for protein-protein interactions within the PyoG translocon (Figure 4-4). Both full length PyoG and its proposed receptor binding domain were investigated. Binding of Hur to *P. aeruginosa* TonB1 was also analysed.

Full-length PyoG binds Hur *in vitro* (Figure 4-4 A), confirming Hur's direct involvement in PyoG import. The next objective was to determine which region of PyoG binds to Hur. The starting point for this was the sequence homology between PyoG and other S1 group pyocins. The N-terminal domains are conserved within the S1 group (Figure 3-1; Appendix F-1). Domain I has been hypothesised to be responsible for receptor binding (Sano *et al.* 1993). To test this, $PyoG^{1-255}$ was purified and its ability to bind Hur was assessed *in vitro*. Interestingly, $PyoG^{1-255}$ indeed bound Hur (Figure 4-4 B). This data indicates that $PyoG^{1-255}$ contains the receptor binding domain of the pyocin. Therefore, all S1-group pyocins probably share Hur as their receptor, since the first 255 residues are conserved within the group (Appendix F-1). It was not possible to test if residues 1-255 are essential for Hur binding since $PyoG^{\Delta 1-255}$ could not be expressed.

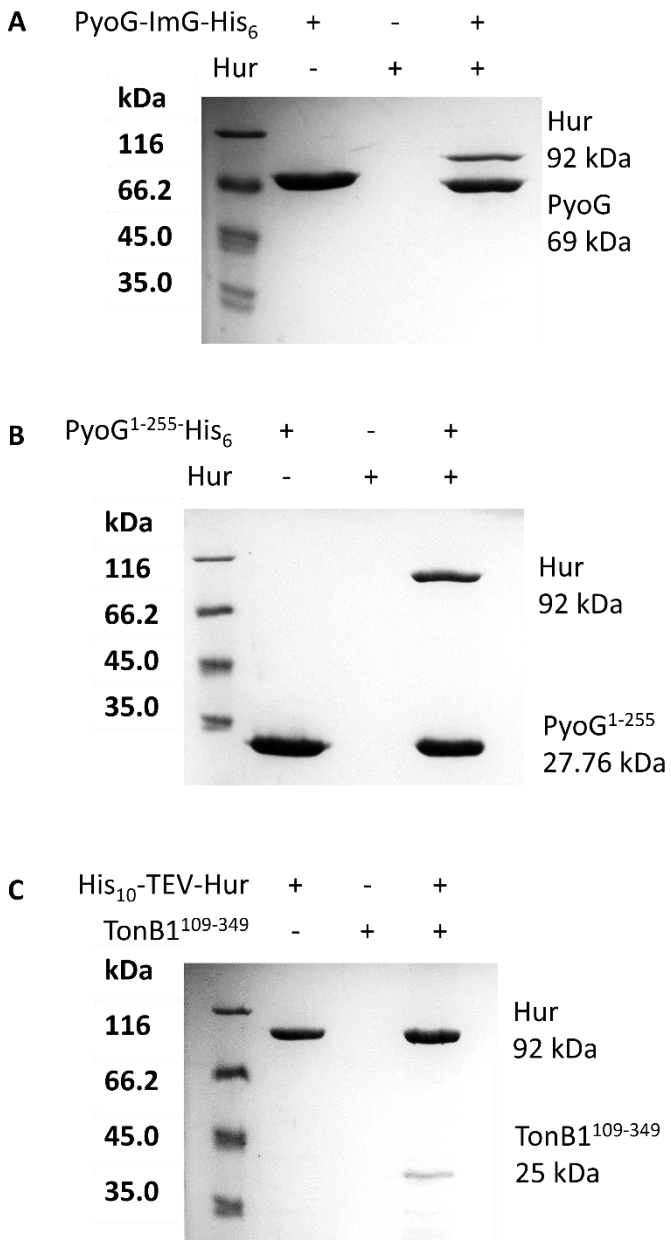

Figure 4-4. Pull-downs of PyoG translocon components. Proteins were mixed at equimolar concentrations of 10 µM in binding buffer (50 mM Tris-HCl pH 7.8, 250 mM NaCl, 1 % (w/v) β-OG) and bound to nickel beads at room temperature. Next, beads were washed of unbound protein and proteins were eluted in 500 mM imidazole. Eluents were analysed on 12 % SDS-PAGE gels. A protein marker is shown in the first lane on each gel. Eluate of the bait protein is in the second lane. Eluate of the prey protein is shown in the third lane, verifying that the prey does not bind to beads on its own. Eluate for the mix of bait and prey is shown in the

fourth lane. Positions of proteins with their molecular masses are labelled on the right side of the gel. A - PyoG binds to Hur, confirming its involvement in the import of the pyocin. B – The first 255 residues of PyoG, which are conserved among S1-group pyocins, bind to Hur. C – Hur binds to the periplasmic region of TonB1, confirming that this is a TonB1 dependent transporter. Figure adapted from Atanaskovic *et al.* 2020.

Finally, to confirm that Hur is a TBDT and interacts directly with TonB1, the pull-down assay with His_{10}-TEV-Hur and $TonB1^{109-342}$ was again used. This assay showed that Hur binds periplasmic TonB1 (Figure 4-4 C). Therefore, these pull-downs confirmed that Hur is a TBDT that binds PyoG.

4.2.3 Hemin is the endogenous ligand of Hur

Even though sequence homology of Hur and other TBDTs strongly supports its involvement in hemin acquisition, binding of Hur to this ligand has not been demonstrated. The killing activity of PyoG is supressed in the presence of iron or hemin (Figure 4-5), consistent with the findings of Otero-Asman *et al.* (2019) that *hur* expression is hemin dependent. These experiments indicated that Hur has a role in hemin uptake. To test if Hur binds hemin *in vitro*, a spectrophotometric pull-down assay was deployed (Desuzinges-Mandon *et al.* 2010). Hemin (Sigma) was soluble in the same buffer as Hur (50 mM Tris-HCl pH 8, 1 % β-OG) where it had an absorbance maximum of 410 nm (Figure 4-6 A). Hur was exposed to a molar excess of hemin and then bound to nickel beads. Unbound hemin was washed off in the β-OG buffer with the addition of 500 mM NaCl. The lack of a detectable 410

nm peak in the wash was used as an indication that unbound hemin was successfully removed. After washing off unbound hemin, Hur was eluted and its UV-Vis spectrum recorded to assess if there was an increase at 410 nm, due to the presence of bound hemin in the eluate. The 410 nm peak increased when Hur was exposed to excess hemin (Figure 4-6 B), confirming that Hur binds hemin. Indeed, it was found that Hur has a 410 nm peak even if not exposed to hemin, which indicates that it co-purifies with its endogenous ligand.

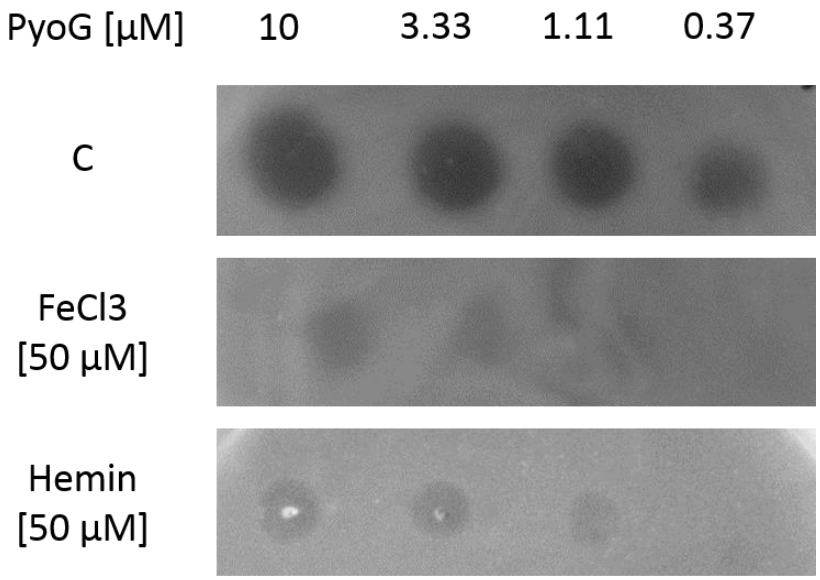

Figure 4-5. Iron and hemin inhibit the killing activity of PyoG. *P. aeruginosa* PAO1 was grown in LBA (C), in LBA supplemented with 50 µM $FeCl_3$ or 50 µM hemin. A range of PyoG concentrations were spotted onto plates. The presence, clarity and size of clearance zones was inspected after overnight incubation. Figure taken from Atanaskovic *et al.* (2020).

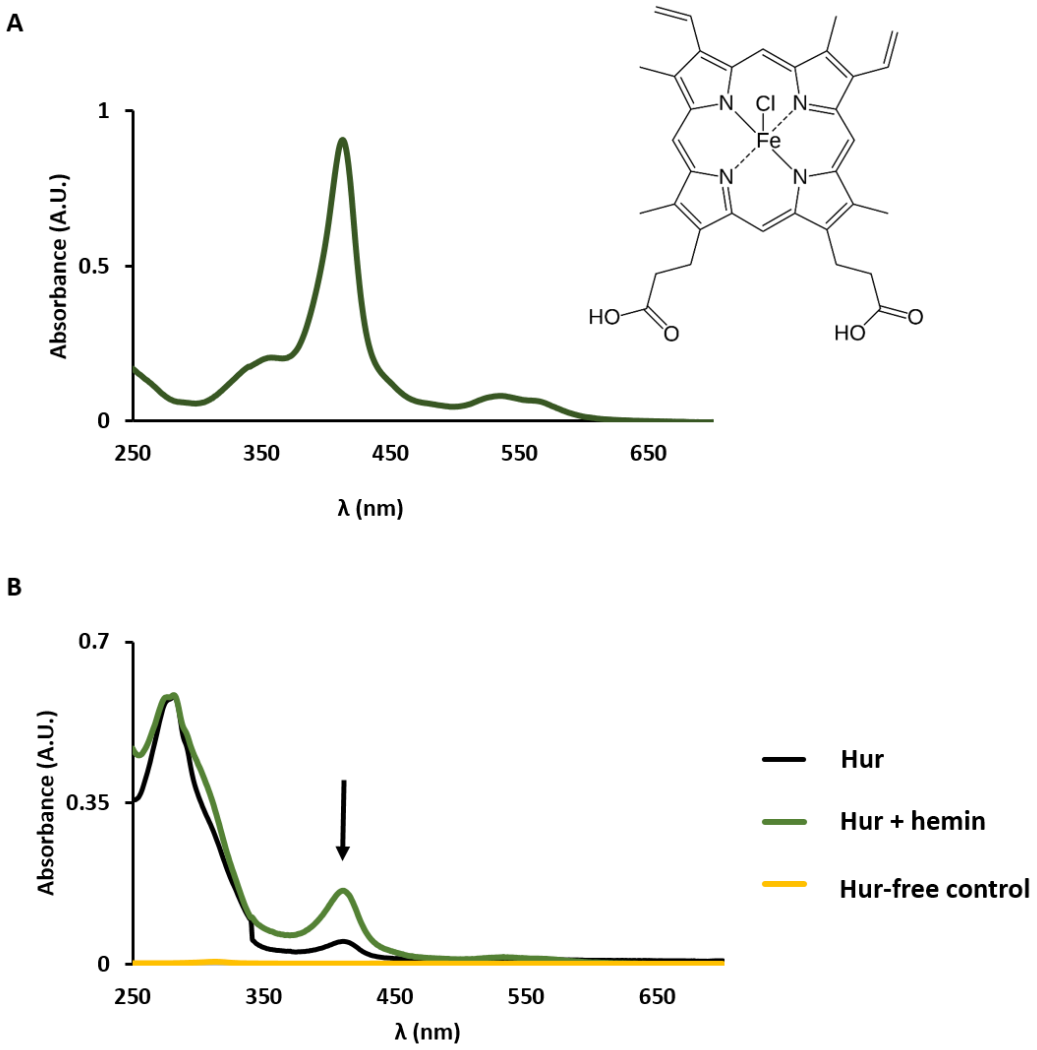

Figure 4-6. His_{10}-TEV-Hur binds hemin *in vitro*. A – absorbance spectrum of 10 µM hemin in 50 mM Tris-HCl pH 8, 1 % β-OG. In this buffer, hemin has an absorbance maximum at 410 nm. Insert shows the structure of hemin used in this study. B – pull-down of hemin with His_{10}-TEV-Hur. 10 µM His_{10}-TEV-Hur was mixed with 1 mM hemin (Sigma) in 50 mM Tris-HCl pH 7.8, 1 % β-OG, bound to nickel beads, and then washed of unbound protein and hemin in the same buffer with the addition of 500 mM NaCl. The Hur-hemin complex was eluted in the binding buffer with the addition of 500 mM imidazole. Absorbance spectra of eluates are shown. Black curve is the spectrum of Hur eluted from nickel beads. The protein already has a small 410 nm peak, probably because it co-purifies with the ligand. Green curve is the spectrum for the

pull-down eluate (indicated with an arrow) following incubation of 10 µM Hur with 1 mM hemin. The 410 nm peak is increased due to hemin binding. Yellow curve is the spectrum of the Hur-free control. No 410 nm peak is observed in this control confirming that unbound hemin was washed off the beads. The experiment was done in two repeats and representative absorbance spectra are shown.

Because previous authors (Ghequire & Ozturk 2018; Otero-Asman *et al.* 2019) named this transporter HxuA or HxuC (**H**emope**x**in **u**ptake receptor), pull-down assays were also conducted using other human heme containing plasma proteins that could potentially be Hur ligands. These experiments demonstrated that Hur did not bind human hemopexin, hemoglobin A0 or transferrin (Figure 4-7). Therefore, the protein was renamed Hur (**H**emin **u**ptake **r**eceptor) since this is more indicative of its physiological role.

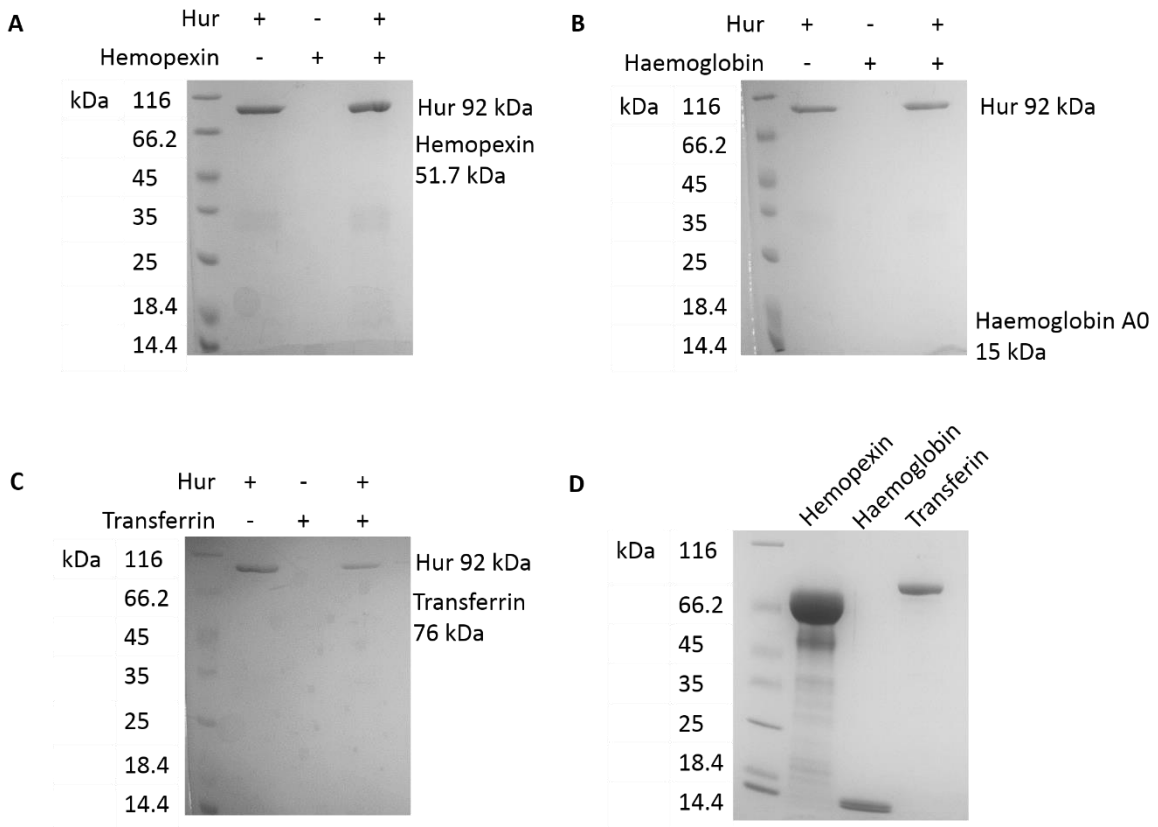

Figure 4-7. Pull-downs of His_{10}-TEV-Hur and human plasma proteins. Proteins were mixed at a final concentration of 10 µM and bound to nickel beads in 50 mM Tris-HCl pH 7.8, 250 mM NaCl, 1 % (w/v) β-OG at room temperature. The beads were washed of unbound protein and the proteins were eluted in 500 mM imidazole. The content of bead eluates was investigated on 4-20 % SDS-PAGE gels. A protein marker is shown in the first lane on each gel. Eluate of the sample which contains just Hur is shown in the second lane, of the sample containing the plasma protein in the third, and of the sample containing both proteins in the fourth lane. Since these proteins could not be detected in the pull-down eluates suggests that hemopexin (A), hemoglobin A0 (B) nor transferrin (C) show binding to Hur under these conditions. D - stocks of human plasma proteins used as prey in the pull-down. Figure taken from Atanaskovic *et al.* (2020).

4.2.4 Hemin and PyoG compete for binding to Hur

Colicins and pyocins often mimic the cognate ligands of the proteins to which they bind (Loftus *et al.* 2006; White *et al.* 2017). Hur-hemin pull-down assays were therefore performed in the presence of PyoG to determine if the same was also the case for this pyocin. In this experiment, Hur had a His_{10}-TEV tag and PyoG had no purification tag. PyoG depleted the amount of hemin bound to Hur (Figure 4-8). Since Hur was first exposed to hemin and then to the pyocin this shows that PyoG can displace Hur-bound hemin.

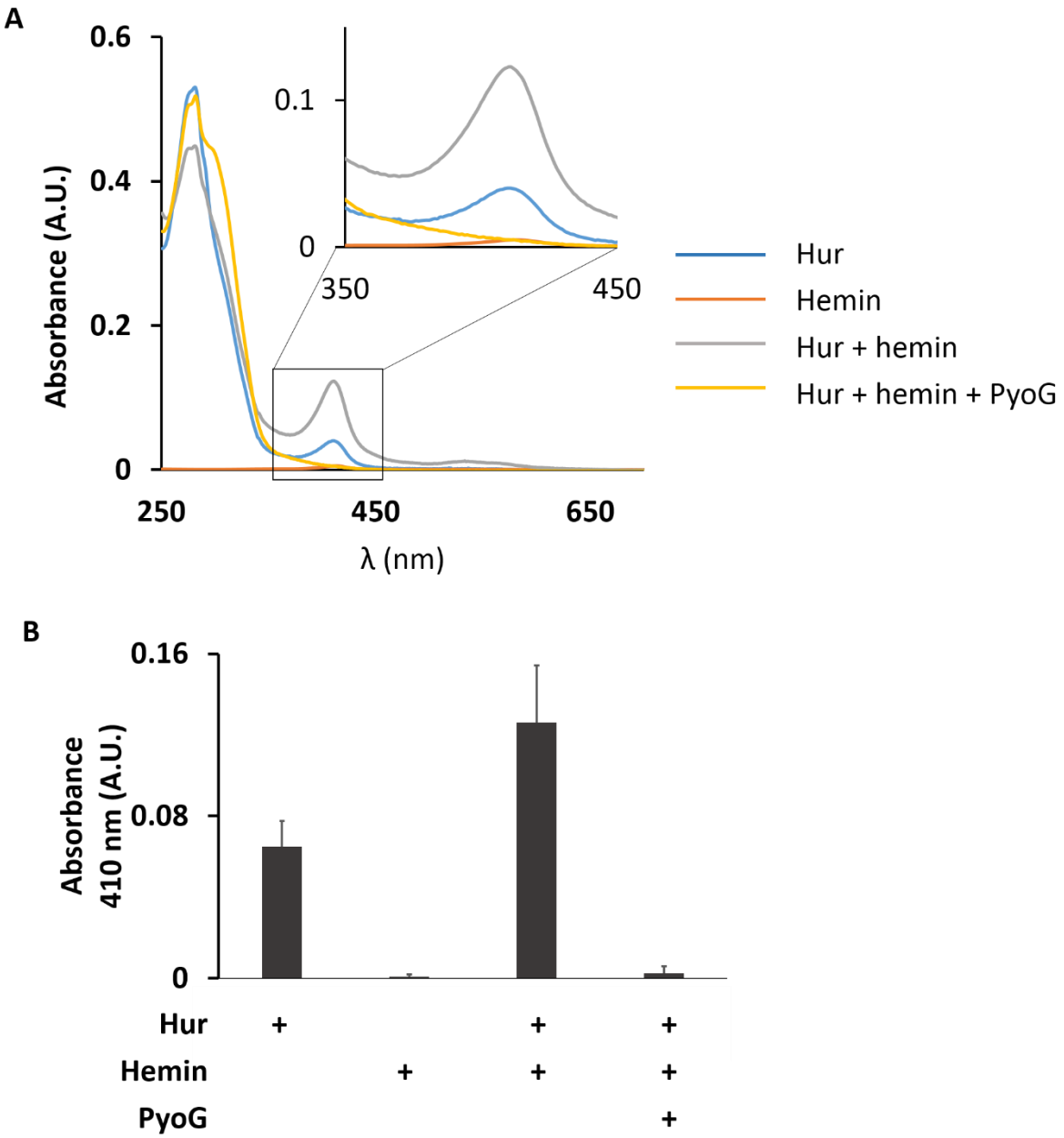

Figure 4-8. Hemin binding to Hur is blocked by PyoG. A - Pull-down of 1 mM hemin by 10 µM His_{10}-TEV-Hur, in the presence and absence of 10 µM PyoG lacking a purification tag. Hur was mixed with 1 mM hemin and then bound to nickel beads and PyoG in 50 mM Tris-HCl pH 7.8, 1 % β-OG on room temperature. Beads were washed of unbound protein and hemin in binding buffer with the addition of 500 mM NaCl, followed by elution in 500 mM imidazole. Absorbance spectra of eluates were measured to detect changes in the 410 nm hemin peak (enlarged in the upper corner). Representative absorbance spectra are shown. The 410 nm

peak is increased if Hur is exposed to excess hemin and no hemin peak can be observed if Hur was mixed with PyoG. No 410 nm peak in the protein free control, containing hemin only, confirms that unbound hemin was washed off the beads and makes no contribution to the 410 nm absorbance in the eluate. No 410 nm peak was detected in the eluate of Hur that was exposed to both hemin and PyoG. B - 410 nm absorbance peak of beads exposed to Hur, hemin or PyoG. Mean of three technical repeats with standard deviations is shown. Figure taken from Atanaskovic *et al.* (2020).

5. Inner membrane translocation of PyoG

5.1 Introduction

Nuclease pyocins cross both the outer and inner membranes in order to access and degrade cellular nucleic acids. It has been shown that PyoS2, harbouring a C-terminal DNase domain, hijacks the outer membrane protein FpvAI that acts as both a receptor and translocator, in a TonB1-dependent manner (White *et al.* 2017). This mechanism of import using Ton dependent outer membrane transporters is likely to be a common mode of entry for nuclease pyocins into cells. The work reported in previous chapters identifying a TBDT Hur as the PyoG transporter supports this finding. In contrast, the mechanism of inner membrane transport and pyocin domains responsible for this second translocation step remain unresolved.

It has previously been shown that inner membrane protein FtsH is associated with nuclease colicin killing activity and thus is likely to be involved in inner membrane translocation (Walker *et al.* 2007). FtsH is a AAA+ ATPase and protease that is conserved among Gram-negative bacteria. It forms a hexameric ring in the inner membrane, with the ATPase and the protease domain facing the cytoplasm. The endogenous function of FtsH is in the quality control of inner membrane proteins and posttranslational regulation of various cytoplasmic proteins (Westphal *et al.* 2012). Since FtsH dependence was seen only for nuclease colicins, and is not essential for killing activity of colicins with pore forming activity, it was assumed that FtsH functions as an inner membrane translocase of nuclease colicins. In addition to a putative role in inner membrane translocation it has been shown that the proteolytic function of FtsH is also essential for colicin activity. The nuclease domains of

RNase Colicins D and E3 (Chauleau *et al.* 2011) and DNase colicins E2 and E7 (Mora & Zamaroczy 2014) were detected in the cytoplasm of *E. coli*, indicating that there is a proteolytic cleavage step during import. These results could not be reproduced in a *ΔftsH* strain of *E. coli*, linking the protease activity of FstH with cleavage of the colicin nuclease domain. Additionally, colicin D interacted with an inner membrane signal peptidase LepB via the conserved Pyocin S domain (Chauleau *et al.* 2011). It was suggested that this signal protease recruits colicin D to be cleaved by FtsH, but direct binding of FtsH to any bacteriocin has not been demonstrated experimentally.

There is currently no pyocin domain identified as essential for inner membrane translocation. However, evidence suggests that the Pyocin S domain, also known as the translocation domain, could be involved in this step. The Pyocin S domain is conserved across all nuclease bacteriocins and is absent in pore-formers that do not require an inner membrane translocation step in order to elicit their cytotoxic activity (Sharp *et al.* 2017). Furthermore, the deletion of this domain from several nuclease pyocins leads to the loss of killing activity (Sano *et al.* 1993). The work in this chapter further investigates the possibility that the Pyocin S domain is responsible for inner membrane translocation.

5.1.1 Aims

In this chapter experiments were designed to explore the inner membrane translocation of PyoG, through identification of the proteins involved and the pyocin domain/s essential for this function.

To test which domain/s of PyoG are required for inner membrane translocation, trypsin protection assays with fluorescent PyoG constructs were designed. These experiments provided an effective means for sequentially exploring the requirement of the Pyocin S domain in inner membrane translocation.

In chapter 3, it was shown that the killing activity of PyoG, like nuclease colicins, requires FtsH, suggesting that the role of FtsH in nuclease bacteriocin import appears to be conserved between *E. coli* and *P. aeruginosa*. FtsH is not essential in *P. aeruginosa*, as explained in section 1.3.3. This makes *P. aeruginosa* a suitable organism for studying the involvement of FtsH in nuclease bacteriocin import. To resolve the role of FtsH in pyocin inner membrane translocation I used trypsin protection assays with fluorescent PyoG and *ΔftsH* spheroplasts of *P. aeruginosa*. The same assay was used to explore if TonB1 is involved in inner membrane translocation.

5.2 Results

5.2.1 The receptor binding and Pyocins S domain of PyoG are sufficient for inner membrane translocation

PyoG translocation was assessed by a trypsin protection microscopy assay. Intact cells or spheroplasts of *P. aeruginosa* were labelled with fluorescent PyoG constructs. Full length PyoG had a G_4S linker and a cysteine at the C terminus. Truncations of PyoG had a cysteine directly added to the C terminus. The cysteine was used for conjugation with AF488 dye. The integrity of the secondary structure and the stability of constructs was assessed by CD and DSC (Figure 5-1). All constructs were folded and stable at room temperature (Figure 5-1).

Full length PyoG fluorescence was protected from digestion with trypsin in both intact cells and spheroplasts (Figure 5-2). In intact *P. aeruginosa*, there was a reduction but not a complete loss in fluorescence following trypsin treatment, consistent with most of the surface-bound molecules being imported. Therefore, in the case of intact cells, trypsin protection of fluorescent PyoG is an indication of outer membrane translocation. In *P. aeruginosa* spheroplasts, the outer membrane and the peptidoglycan layer are disrupted with EDTA and lysozyme (Monahan *et al.* 2014), and trypsin can cleave PyoG if not translocated across the inner membrane. Therefore, trypsin protection in spheroplasts is an indication of inner membrane translocation. Similarly, $PyoG^{1-485}$, which is comprised of the receptor-binding domain and the Pyocin S domain, was protected from digestion with trypsin in both types of cells (Figure 5-3). This indicates that these two PyoG domains are sufficient for inner membrane translocation.

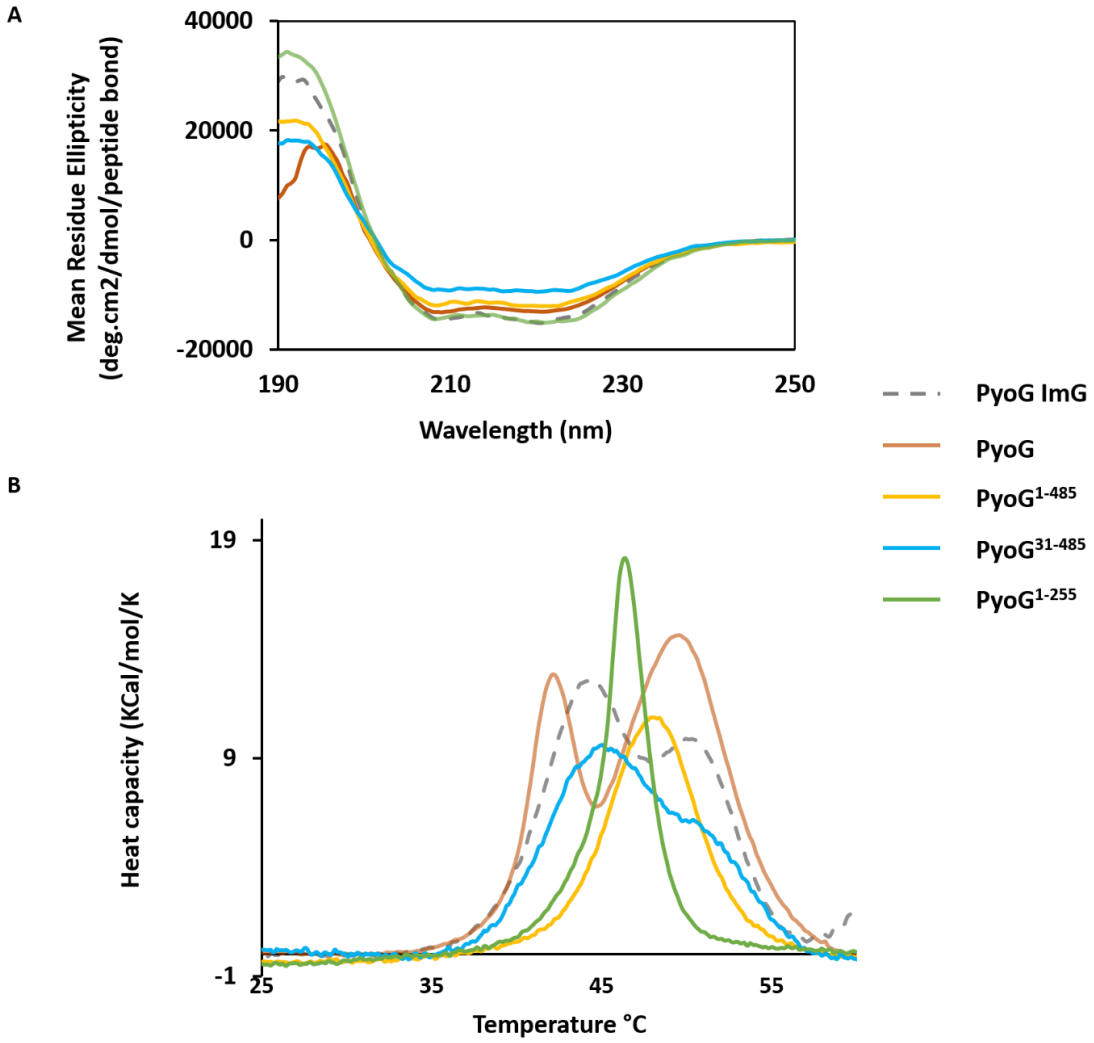

Figure 5-1. Secondary structure integrity and stability of PyoG constructs. A - CD spectra of 0.1 mg/ml PyoG (orange), PyoG$^{1\text{-}485}$ (yellow), PyoG$^{31\text{-}485}$ (blue), and PyoG$^{1\text{-}255}$ (green) at RT in 20 mM NaF and 10 mM KPO_4 buffer (pH 7). PyoG has a G_4S linker and a cysteine at the C terminus. Truncated constructs have a cysteine at the C-terminus. The dashed line is the CD spectrum of full-length PyoG-ImG. An average of 9 measurments are shown. B - DSC of 20 µM PyoG constructs in 50 mM Tris-HCl pH 7, 150 mM NaCl. The melting temperature of PyoG is 42.14 ± 0 and 49.56 ± 0.02 °C, PyoG$^{1\text{-}485}$ is 48.04 ± 0.14 °C, PyoG$^{31\text{-}485}$ is 44.62 ± 0.36 °C, PyoG$^{1\text{-}255}$ is 46.22 ± 0.02 °C.

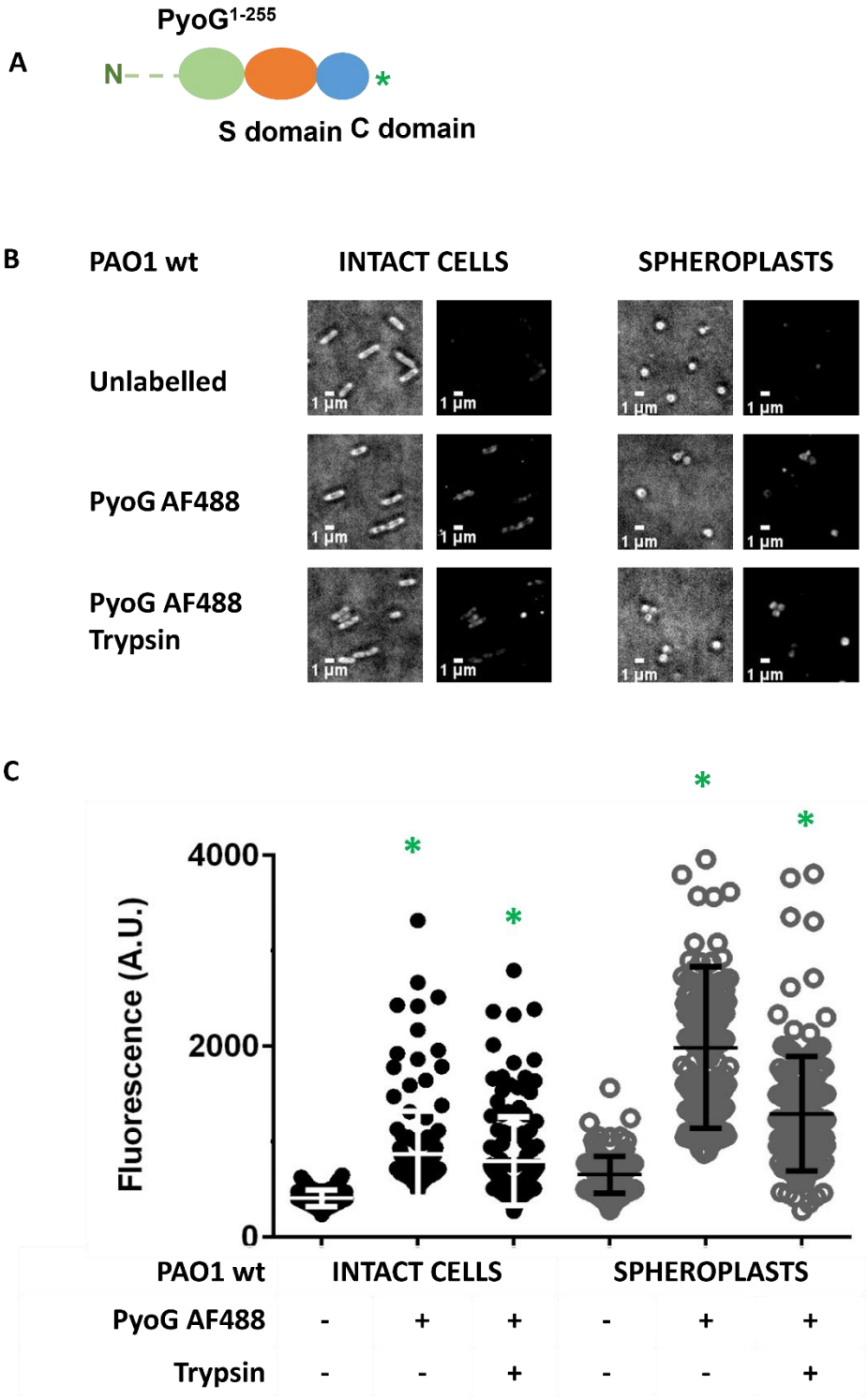

Figure 5-2. A - PyoG construct used for fluorescent labelling; * represents the site of AF conjugation. B - Fluorescent labelling of PAO1 with PyoG. PyoG was conjugated to AF488 via a G_4S linker and a C-terminal cysteine. It was added to either intact cells or spheroplasts at 2 µM. Cells were exposed to 0.5 mg/mL trypsin after labelling. Fluorescent PyoG was protected

from digestion with trypsin in both cell types, which is suggestive of translocation across the outer and inner membranes. Representative micrographs for each strain are shown. All snapshots were adjusted to the same intensity scale. C - Average fluorescence intensities for 150 cells in the presence and absence of fluorescent pyocin and trypsin. Mean of three biological replicates with standard deviations are shown. Fluorescence intensities for labelled and trypsin treated groups were compared to the unlabelled control. * represents a P value below 0.0001 in the Kruskal-Wallis Test.

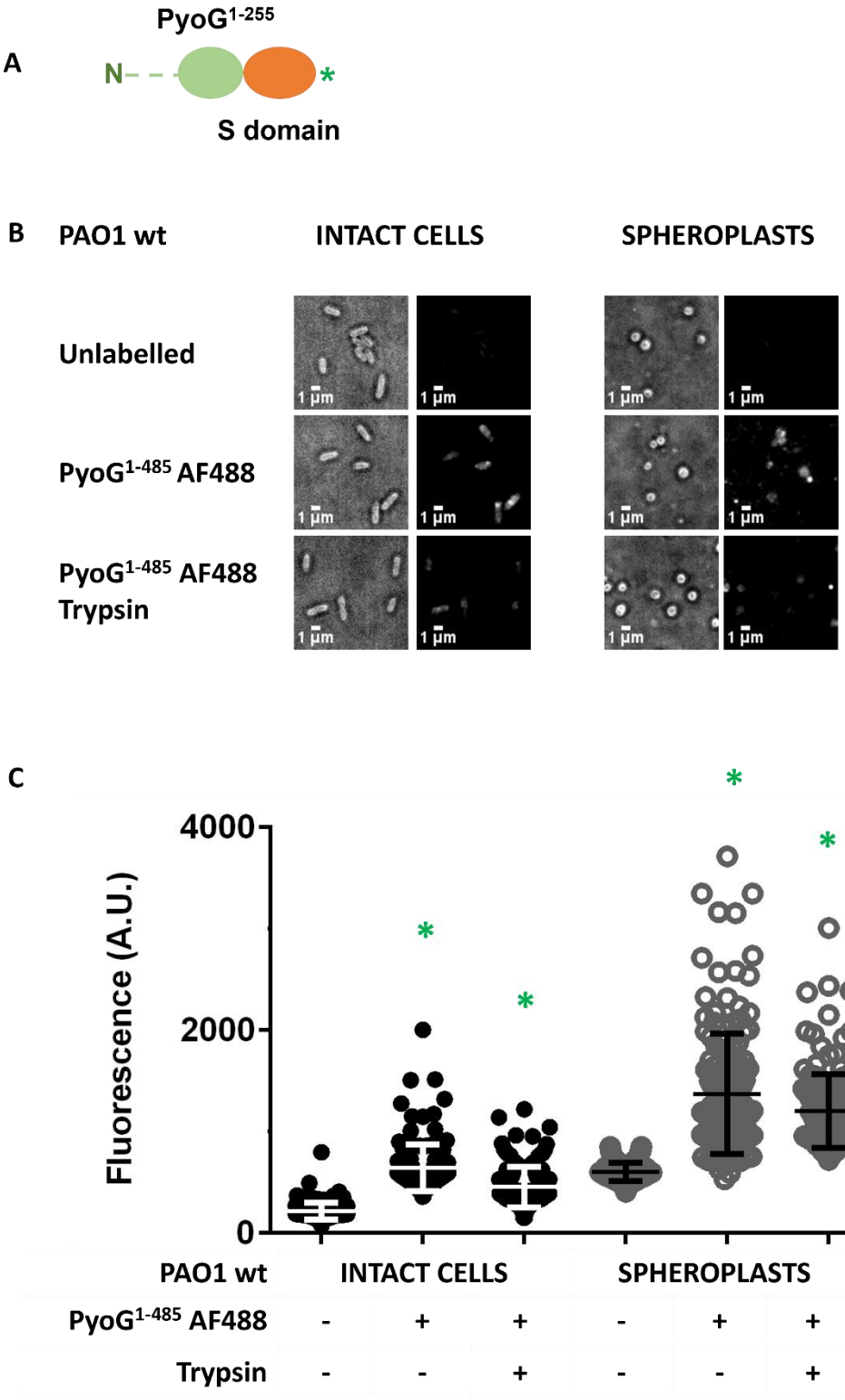

Figure 5-3. A - PyoG construct used for fluorescent labelling; * represents the site of AF conjugation. B - Fluorescent labelling of PAO1 wt with $PyoG^{1-485}$. $PyoG^{1-485}$, conjugated to AF488 via a C-terminal cysteine, was added to either intact cells or spehroplasts at 2 µM. Cells

were exposed to 0.5 mg/mL trypsin after labelling. Fluorescent PyoG$^{1-485}$ was protected from digestion with trypsin in both types of cells, indicating translocation across the outer and inner membranes. Representative micrographs for each strain are shown. All snapshots were adjusted to the same intensity scale. C - Average fluorescence intensities for 150 cells in the presence and absence of fluorescent pyocin and trypsin. Mean of three biological replicates with standard deviations are shown. Fluorescence intensities for labelled and trypsin treated groups were compared to the unlabelled control. * represents a P value below 0.0001 in the Kruskal-Wallis Test.

Since the PyoG$^{1-485}$ construct lacks the cytotoxic domain and is not lethal to cells, it was tested in several mutants of *P. aeruginosa* to identify proteins required for inner membrane translocation. The PAO1 *Δhur* mutant lacks the PyoG receptor and does not label with fluorescent PyoG, as already described in chapter 3. By contrast, *Δhur* spheroplasts were fluorescently labelled (Figure 5-4), indicating that the outer membrane can be bypassed and that PyoG can associate with the inner membrane. Additionally, the pyocin was protected from digestion with trypsin, which indicates that the outer membrane receptor Hur is not required for PyoG to translocate across the spheroplast inner membrane.

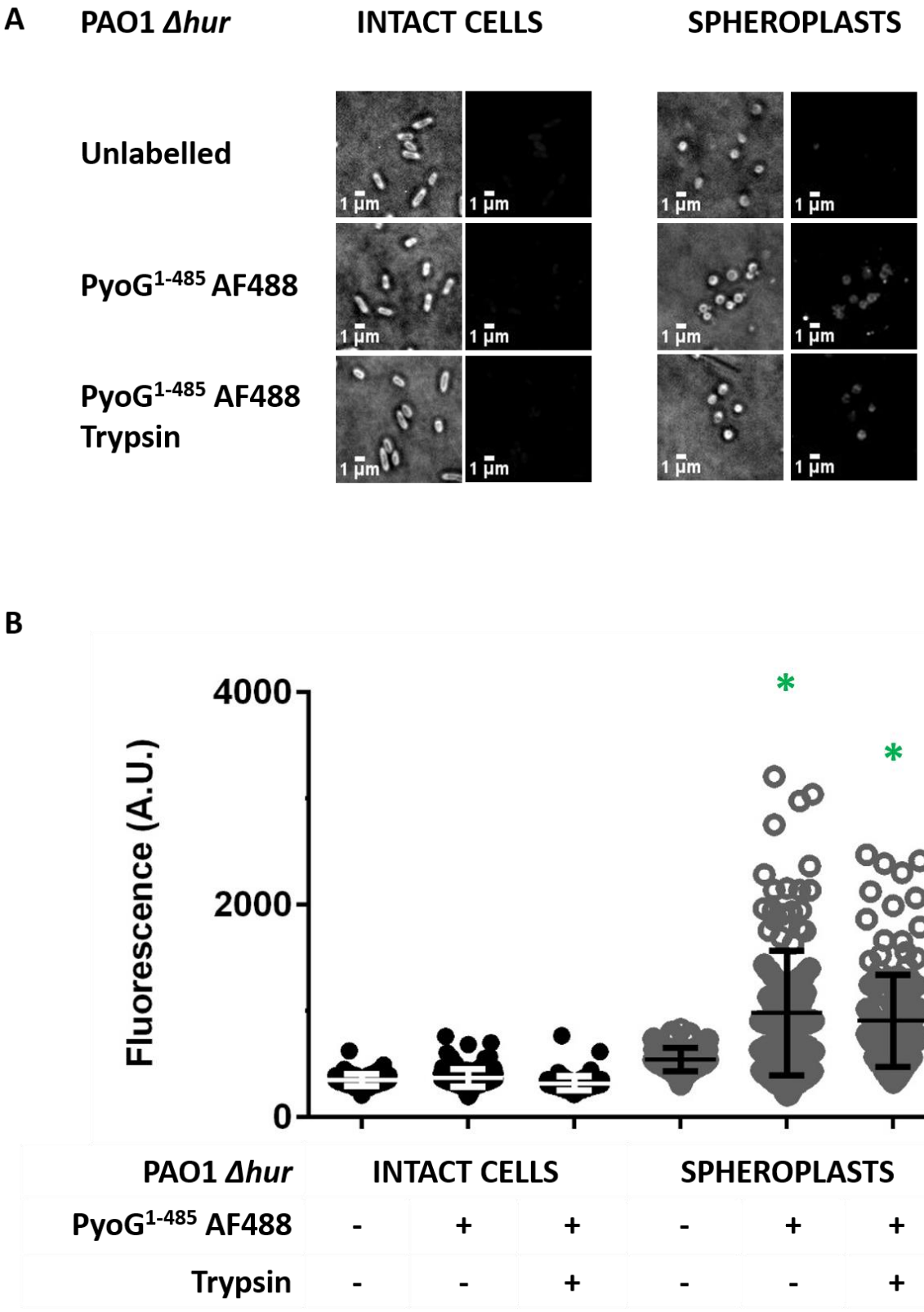

Figure 5-4. A - Fluorescent labelling of PAO1 *Δhur*, a mutant lacking the PyoG outer membrane receptor. PyoG$^{1-485}$, conjugated to AF488 via a C-terminal cysteine, was added to either intact

cells or spheroplasts at 2 μM. Cells were exposed to 0.5 mg/mL trypsin after labelling. Unlike spheroplasts, intact cells were not labelled, consistent with the outer membrane translocation step being bypassed in spheroplasts. Representative micrographs for each strain are shown. All snapshots were adjusted to the same intensity scale. B - Average fluorescence intensities for 150 cells in the presence and absence of fluorescent pyocin and trypsin. Mean of three biological replicates with standard deviations are shown. Fluorescence intensities for labelled and trypsin treated groups were compared to the unlabelled control. * represents a P value below 0.0001 in the Kruskal-Wallis Test.

5.2.2 The conserved Pyocin S domain is required for inner membrane translocation

To test if the Pyocin S domain plays a role in outer and inner membrane translocation, a PyoG construct lacking this domain was designed for fluorescent labelling experiments with *P. aeruginosa*. Previous studies of PyoS1, a homolog of PyoG, (Sano *et al.* 1993), suggest that the S domain is comprised of residues 256-485. This region is conserved amongst pyocins G, AP41 and S2 (Appendix F-2). Therefore, to test the involvement of the Pyocin S domain in PyoG import, $PyoG^{1-255}$ with a C-terminal cysteine was constructed. This construct contains the TonB1 binding box and the receptor-binding domain of PyoG, as demonstrated in Hur pull-downs presented in chaper 4. To test if $PyoG^{1-255}$ translocates across outer and inner membrane, the trypsin protection microscopy assay was performed using both intact PAO1 cells and spheroplasts. $PyoG^{1-255}$ labelled intact PAO1 cells and the fluorescent signal remains even in the presence of trypsin. This trypsin protection indicates that the construct must be capable of translocation into cells across the outer membrane (Figure 5-5). In contrast, $PyoG^{1-255}$ fluorescence was not detected following trypsin treatment of labelled spheroplasts,

indicating that it associates with the spheroplast surface, but unlike PyoG$^{1-485}$ is not imported across the inner membrane. Taken together these data indicate that the PyoG$^{1-255}$ domain is not sufficient for inner membrane translocation and that the Pyocin S domain is required for this step in PyoG import.

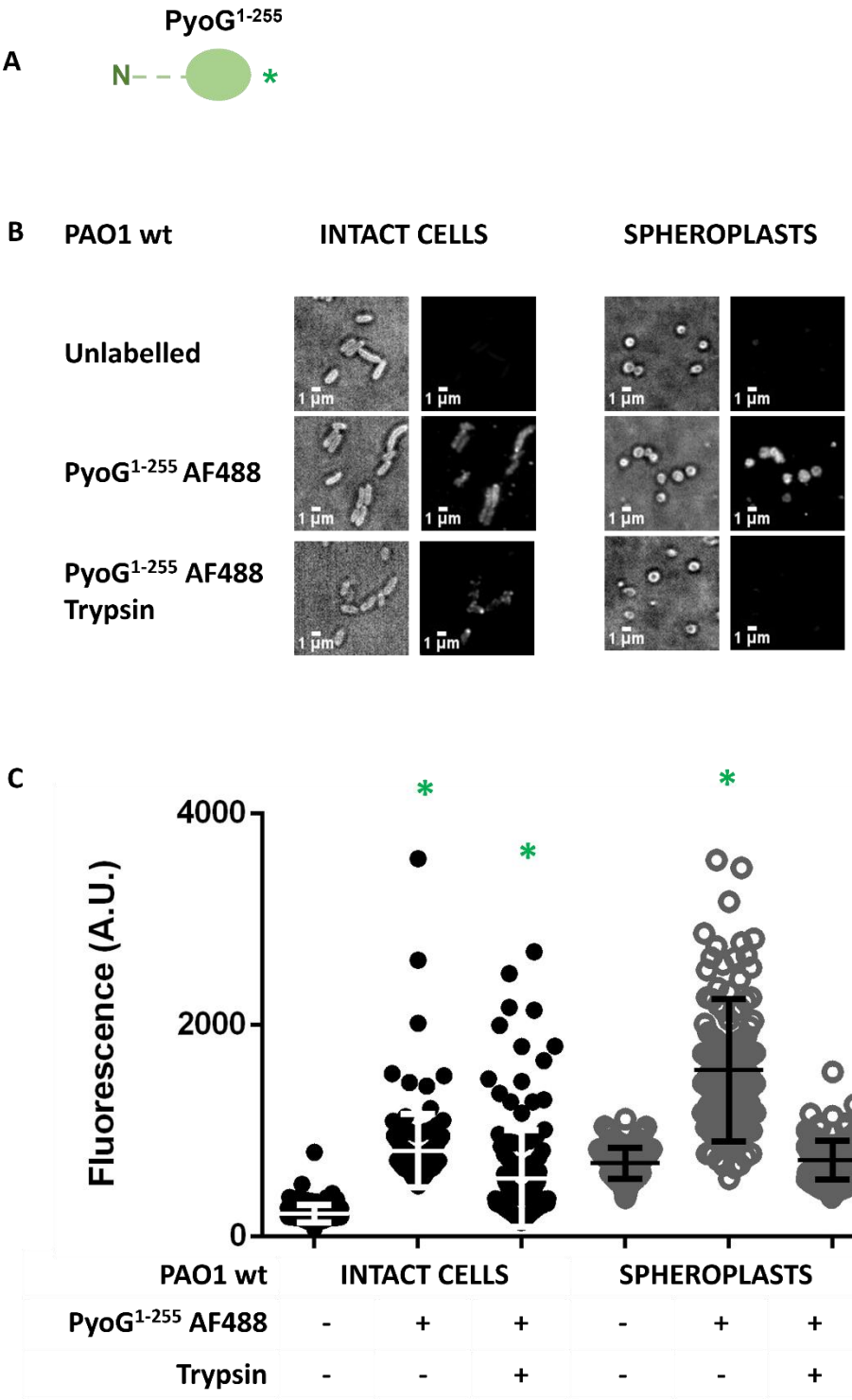

Figure 5-5. A - PyoG construct used for fluorescent labelling; * represents the site of AF conjugation. B - Fluorescent labelling of PAO1 wt with the PyoG construct lacking the conserved Pyocin S domain ($PyoG^{1-255}$). $PyoG^{1-255}$, conjugated to AF488 via a C-terminal cysteine, was added to intact cells or spheroplasts at 2 µM. Cells were exposed to 0.5 mg/mL

trypsin after labelling. Fluorescent PyoG$^{1-255}$ was protected from digestion with trypsin only in intact cells, indicating that the Pyocin S domain is required for inner membrane but not outer membrane translocation. Representative micrographs for each strain are shown. All snapshots were adjusted to the same intensity scale. C - Average fluorescence intensities for 150 cells in the presence and absence of fluorescent pyocin and trypsin. Mean of three biological replicates with standard deviations are shown. Fluorescence intensities for labelled and trypsin treated groups were compared to the unlabelled control. * represents a P value below 0.0001 in the Kruskal-Wallis Test.

5.2.3 FtsH is required for inner membrane PyoG translocation

After validating that spheroplasts are a viable system for studying inner membrane translocation, the involvement of FtsH was investigated. To do this, trypsin cleavage experiments were repeated using *ftsH* knockout cells (PAO1 *ΔftsH*). In intact cells PyoG$^{1-485}$ was protected from digestion with trypsin, demonstrating that the pyocin does not require FtsH for outer membrane translocation. In contrast, *ΔftsH* spheroplasts did not afford trypsin protection of PyoG$^{1-485}$, suggesting that in the absence of FtsH there is no inner membrane translocation (Figure 5-6). Interestingly, prior to trypsin digestion, the spheroplasts were labelled with PyoG$^{1-485}$, indicating that FtsH is not essential for the surface association of PyoG at the spheroplast envelope, just the subsequent translocation step. Upon complementation of *ΔftsH* with FtsH expressed from a plasmid (pFtsH), trypsin protection (Figure 5-6) and PyoG killing activity (Figure 5-7 A) are restored. Complementation with a protease-inactive FtsH, pFtsH H416Y (Westphal *et al.* 2012; Kamal *et al.* 2019), did not restore trypsin protection

(Figure 5-6) or killing activity (Figure 5-7 A). Therefore, the protease activity of FtsH is essential for PyoG import across the inner membrane.

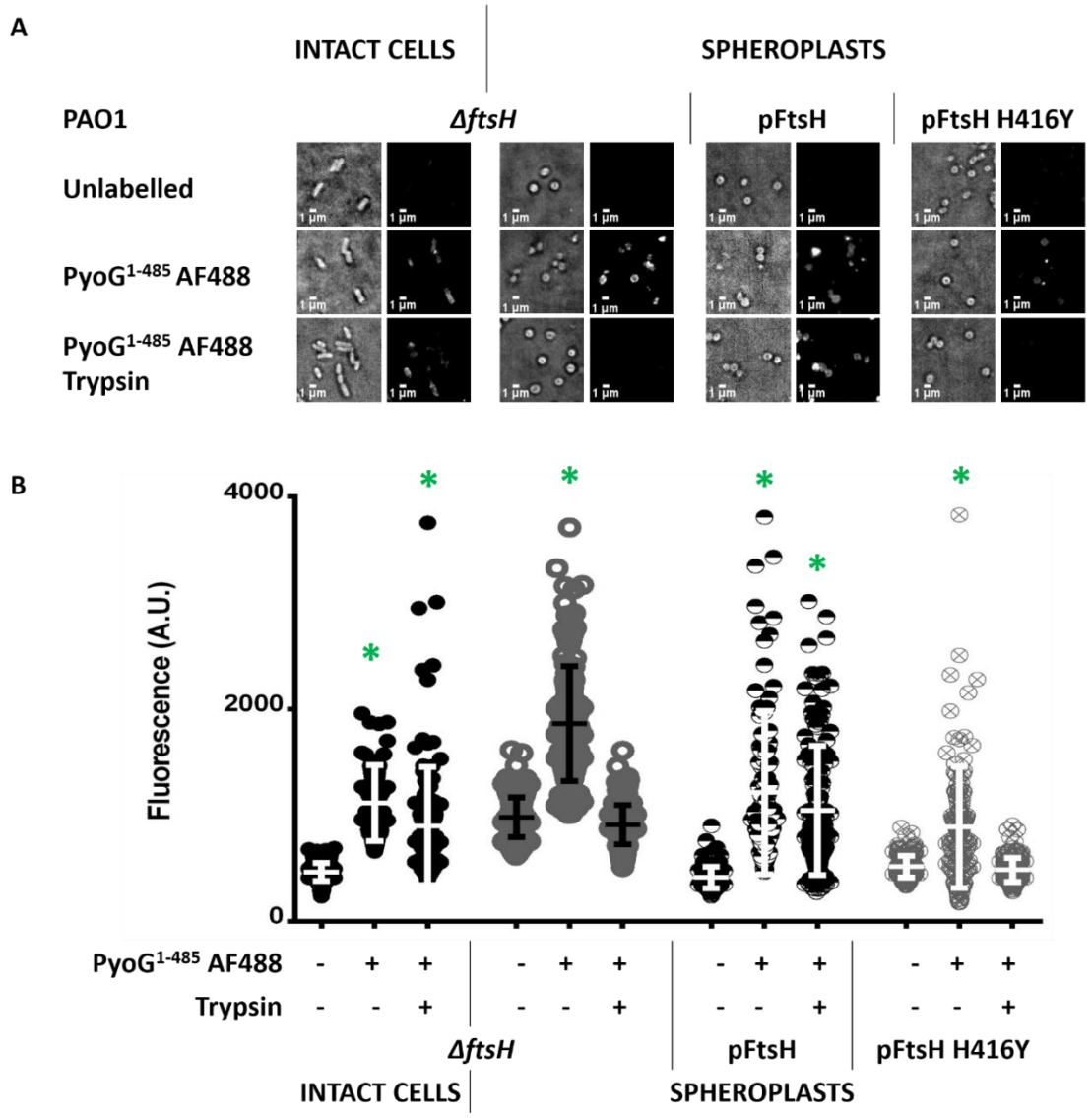

Figure 5-6. A - Fluorescent labelling of PAO1 *ΔftsH*, a mutant resistant to PyoG. PyoG$^{1-485}$, conjugated to AF488 via a C-terminal cysteine, was added to either intact cells or spheroplasts at 2 µM. Cells were exposed to 0.5 mg/mL trypsin after labelling. Fluorescent PyoG was protected from digestion with trypsin in intact cells, indicating that FtsH is not required for the outer membrane translocation step. There was no trypsin protection in spheroplasts,

indicating that FtsH is required for the translocation of PyoG across the inner membrane. pFtsH is *ΔftsH* complemented with FtsH expressed from a plasmid. pFtsH H416Y is *ΔftsH* complemented with FtsH carrying a point mutation that inactivates its protease activity. Only complementation with wt FtsH restored trypsin protection of PyoG in spheroplasts. Representative micrographs for each strain are shown. All snapshots were adjusted to the same intensity scale. B - Average fluorescence intensities for 150 cells in the presence and absence of fluorescent pyocin and trypsin. Mean of three biological replicates with standard deviations are shown. Fluorescence intensities for labelled and trypsin treated groups were compared to the unlabelled control. * represents a P value below 0.0001 in the Kruskal-Wallis Test.

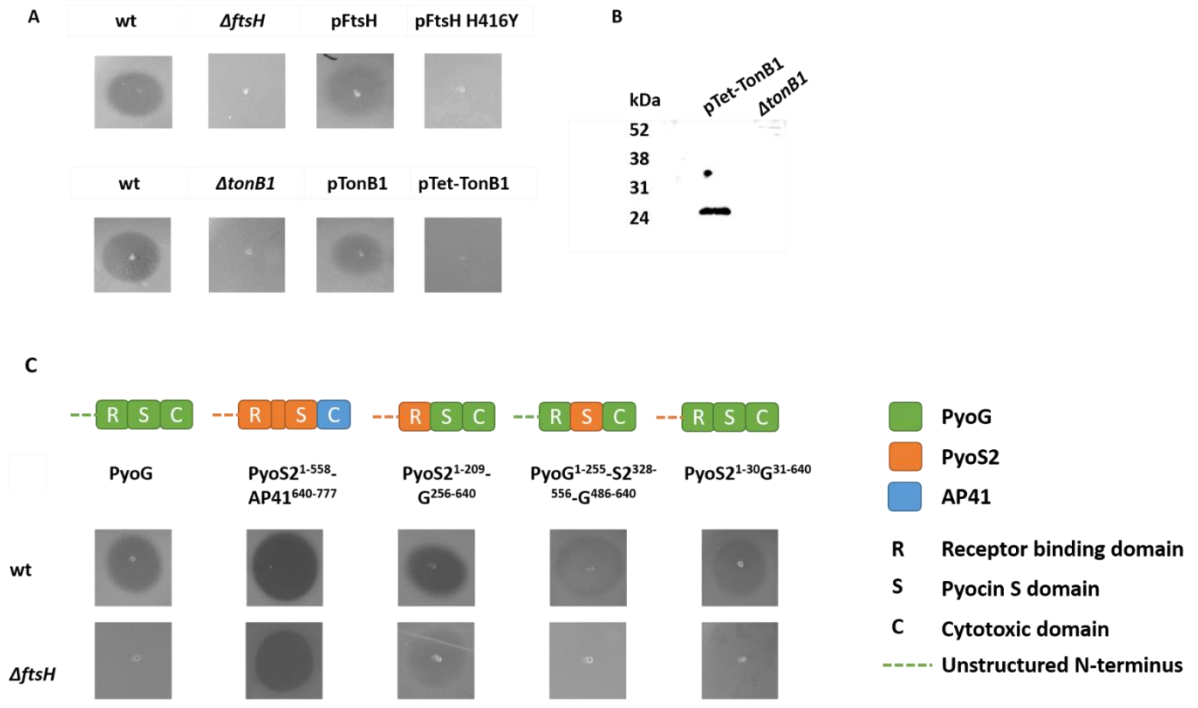

Figure 5-7. A – Plate killing assay of *P. aeruginosa* PAO1 *ΔftsH* complemented with FtsH expressed from a plasmid (pFtsH), or a protease inactivated version of FtsH (pFtsH H416Y). Only complementation with wt FtsH restores pyocin sensitivity. *P. aeruginosa* PAO6699

ΔtonB1 was complemented with TonB1 expressed from a plasmid (pTonB1). Pyocin sensitivity is restored in this strain. Complementation with a TonB1 chimera (T7-TetA$^{2-32}$-TonB1$^{112-342}$), in which the inner membrane helix of TonB1 was replaced with the first helix of *P. aeruginosa* TetA (pTet-TonB1) was resistant to PyoG. B – Expression of Tet-TonB1 from pTet-TonB1. Membrane proteins were extracted in 1 % DDM, 50 mM Tris-HCl pH 8. Tet-TonB1 has a T7 tag in the N-terminus and is detected by an anti-T7 epitope tag antibody. C - Plate killing assay of *P. aeruginosa* PAO1 wt and *ΔftsH* with PyoG, PyoS2-AP41, and PyoS2-G chimeras. The native cytotoxic domain of S2 (PyoS2$^{559-689}$) has been swapped for the nuclease domain of pyocin AP41 (PyoAP41$^{640-777}$) to evade PAO1 immunity to S2 in the PyoS2 construct. The S2-G chimeras were made by swapping: the N-terminal receptor binding domain of PyoG (PyoG$^{1-255}$) for the N-terminal domain of PyoS2 (PyoS2$^{1-209}$); the Pyocin S domain of PyoG (PyoG$^{256-485}$) for the S domain of S2 (PyoS2$^{328-556}$); the first 30 residues of PyoG for the first 30 residues of S2. *ΔftsH* is resistant to PyoG, but not to PyoS2 or the S2$^{1-209}$-G$^{256-640}$ chimera. 3 µL of 10 µM pyocin solution was used in both A and B.

Attempts were made to demonstrate *in vitro* binding of FtsH to PyoG-ImG, PyoG, and PyoG$^{1-485}$. FtsH$^{141-655}$ H416Y is the cytoplasmic domain of FtsH with a point mutation that inactivates the protease activity. It has previously been demonstrated that this construct binds to FtsH substrates without cleaving them, enabling substrate detection in pull-down assays (Westphal *et al.* 2012). The binding of PyoG constructs to FtsH$^{141-655}$ H416Y could not be demonstrated in a pull-down assay with or without formaldehyde cross-linking (not shown). Attempts at purifying full-length FtsH, or a cytoplasmic domain with protease activity were not successful.

To determine if FtsH-dependent of import of PyoG and various nuclease colicins (Walker *et al.* 2007) is a global property conserved across other nuclease pyocins, the FtsH dependence of another nuclease pyocin, S2, was tested. Plate killing assays revealed that PyoS2 is active against PAO1 *ΔftsH*, demonstrating that FtsH is not required for inner membrane translocation of all nuclease pyocins (Figure 5-7 C). Since PAO1 carrys the immunity protein for PyoS2, this killing assay was performed with a chimera of PyoS2 and AP41, in which the cytotoxic domain of S2 was exchanged for the cytotoxic domain of AP41. The difference in FtsH dependence between PyoG and PyoS2 was subsequently exploited to determine what domain of PyoG was required for FtsH-dependent translocation across the inner membrane. Since both PyoG and PyoS2 have a Pyocin S domain, it was assumed that the N-terminus of PyoS2 might be responsible for its killing activity against the *ΔftsH* mutant. To test this, the unstructured N-terminus and the receptor-binding domains of PyoG ($PyoG^{1-255}$) were swapped for the unstructured N-terminus and the receptor-binding domain of PyoS2 ($PyoS2^{1-209}$; White *et al.* 2017). The killing activity of the chimera was assayed against PAO1 and the *ΔftsH* mutant. As observed for PyoS2, the chimera showed killing against the *ΔftsH* mutant (Figure 5-5 C) confirming that the first 255 residues of PyoG are linked to FtsH-dependent killing. Additionally, a chimera in which the Pyocin S domain of PyoG was exchanged for the Pyocin S domain of S2 was not active against the *ΔftsH* mutant. Similarly, a chimera in which the first 30 residues of the unstructured N-terminus of PyoG were exchanged for the first 30 residues of S2 was also not active against PAO1 *ΔftsH*. Taken together these results suggest that the residues of PyoG responsible for FtsH-dependent inner membrane translocation are located within the N-terminal, outer membrane receptor binding domain. PyoS2 deploys a different inner membrane translocation pathway to which it is directed via its receptor binding domain.

5.2.4 TonB1 binding and inner membrane translocation

TonB1 has previously been associated with the outer membrane translocation of pyocins (White *et al.* 2017; Behrens *et al.* 2020). Therefore, fluorescence microscopy was used to investigate if TonB1 has a role in inner membrane translocation. To do this, spheroplasts generated from wt and *ΔtonB1* cells labelled with fluorescent PyoG$^{1-485}$ (Figure 5-8). Fluorescent PyoG associates with spheroplasts of the *ΔtonB1* mutant, but the fluorescent signal was not retained in the presence of trypsin, confirming that deletion of *tonB1* also affects the import of PyoG into spheroplasts. Complementation of *ΔtonB1* with TonB1 expressed from a plasmid restored killing activity of PyoG (Figure 5-7 A) and trypsin protection of PyoG in *ΔtonB1* spheroplasts (Figure 5-8). On the other hand, complementation with a chimera of TonB1, in which the inner membrane helix of TonB1 was replaced with the first helix of TetA, did not restore trypsin protection of PyoG (Figure 5-8). The inner membrane helix of TonB1 is responsible for its coupling to the PMF (Celia *et al.* 2019); its replacement with a TetA helix uncouples TonB1 from the PMF (Jaskula *et al.* 1994). This construct does not restore the killing activity of PyoG in *ΔtonB1*, and can be detected in the membrane fraction by Western Blot (Figure 5-7 B). Taken together the spheroplast labelling assay with *ΔtonB1* cells indicates that TonB1 is also likely to play a role in PyoG translocation across the inner membrane (Figure 5-6).

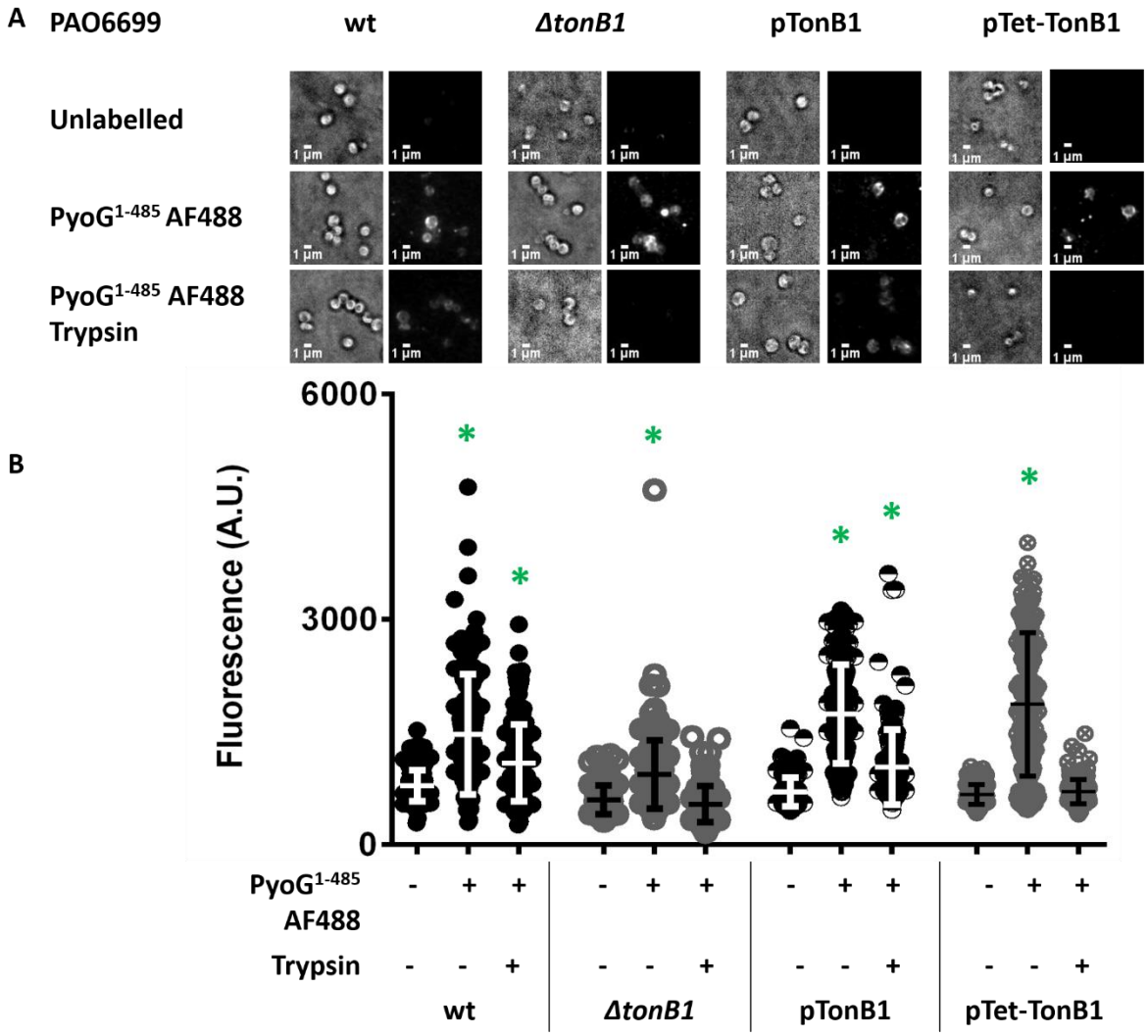

Figure 5-8. A - Fluorescent labelling of *ΔtonB1* spheroplasts. *ΔtonB1* lacks the inner membrane protein TonB1, which has previously been linked to outer membrane translocation of pyocins (White *et al.* 2017; Behrens *et al.* 2020). PyoG$^{1-485}$, conjugated to AF488 via a C-terminal cysteine, was added to spheroplasts at 2 µM. Cells were exposed to 0.5 mg/mL trypsin after labelling. Fluorescent PyoG was protected from digestion with trypsin in PAO1 but not in the *ΔtonB1* mutant, indicating that TonB1 is also implicated in the inner membrane translocation step. pTonB1 is *ΔtonB1* complemented with TonB1 expressed from a plasmid. Complementation restored trypsin protection of PyoG in *ΔtonB1* spheroplasts. pTet-TonB1 is complemented with a TonB1 chimera, in which the inner membrane helix of TonB1, involved

in PMF coupling, is replaced with the first helix of TetA. Complementation with this construct did not restore trypsin protection of PyoG. Representative micrographs for each strain are shown. All snapshots were adjusted to the same intensity scale. B - Average fluorescence intensities for 150 cells in the presence and absence of fluorescent pyocin and trypsin. Mean of three biological replicates with standard deviations are shown. Fluorescence intensities for labelled and trypsin treated groups were compared to the unlabelled control. * represents a P value below 0.0001 in the Kruskal-Wallis Test.

In chapter 3, it was demonstrated in a pull-down assay that PyoG binds to the periplasmic domain of TonB1 *in vitro*. Nevertheless, the exact location of the TonB box of PyoG was not identified. It was assumed that, as in the case of PyoS2 (White *et al.* 2017) and S5 (Behrens *et al.* 2020), the TonB box of PyoG should be in the unstructured N-terminus. It was predicted by DisEMBL 1.5 (Linding *et al.* 2003) that the first 50 residues of PyoG should be disordered. To locate the region of sequence containing the TonB1 box attempts were made to delete the unstructured N-terminus and check for TonB1 binding. The deletion of the entire N-terminus of PyoG ($PyoG^{51-485}$) resulted in a construct that could not be expressed. Therefore, a shorter region comprising the first 30 residues of PyoG was deleted. $PyoG^{\Delta 1-30}$, which lacks the first 30 residues but has the cytotoxic domain, showed that deletion of residues 1-30 makes PyoG inactive as a bacteriocin (Figure 5-9). $PyoG^{31-485}$, which lacks the cytotoxic domain and has a C-terminal cysteine for fluorescence labelling, was used for fluorescence microscopy and pull-down assays. This construct was helical in far-UV CD measurements, but the negative maxima in the spectrum was lower than for full length PyoG (Figure 5-1 A). The melting temperature was also 4 °C lower than full-length PyoG (Figure 5-1

B). Therefore, the fold and stability of PyoG might be affected by the deletion of the unstructured N-terminus. To validate that the inactivity of PyoG$^{\Delta 1-30}$ against PAO1 was due to impaired interactions with TonB1, pull-down assays were carried out. Suspension of PyoG$^{31-485}$ bound to a resin through an N-terminal His_6-tag resulted in the pull-down of receptor Hur but not TonB1 (Figure 5-10), confirming that deletion of the first 30 amino acids of PyoG specifically impairs TonB1 binding. To test translocation of PyoG$^{31-485}$ across the outer and the inner membrane, trypsin protection microscopy assay was performed on intact PAO1 cells and spheroplasts. Fluorescent PyoG$^{31-485}$ labelled the surface of both intact PAO1 and spheroplasts, but the label was not protected from digestion with trypsin (Figure 5-11). Therefore, the unstructured N-terminus is required for both the outer and the inner membrane translocation of PyoG.

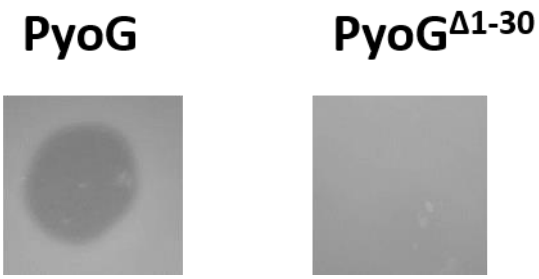

Figure 5-9. Plate killing assay of *P. aeruginosa* PAO1 with PyoG and PyoG lacking the first 30 residues in the unstructured N-terminus (PyoG$^{\Delta 1-30}$). Pyocins were used at 10 µM. Deletion of the unstructured N-terminus disrupts the killing activity of PyoG.

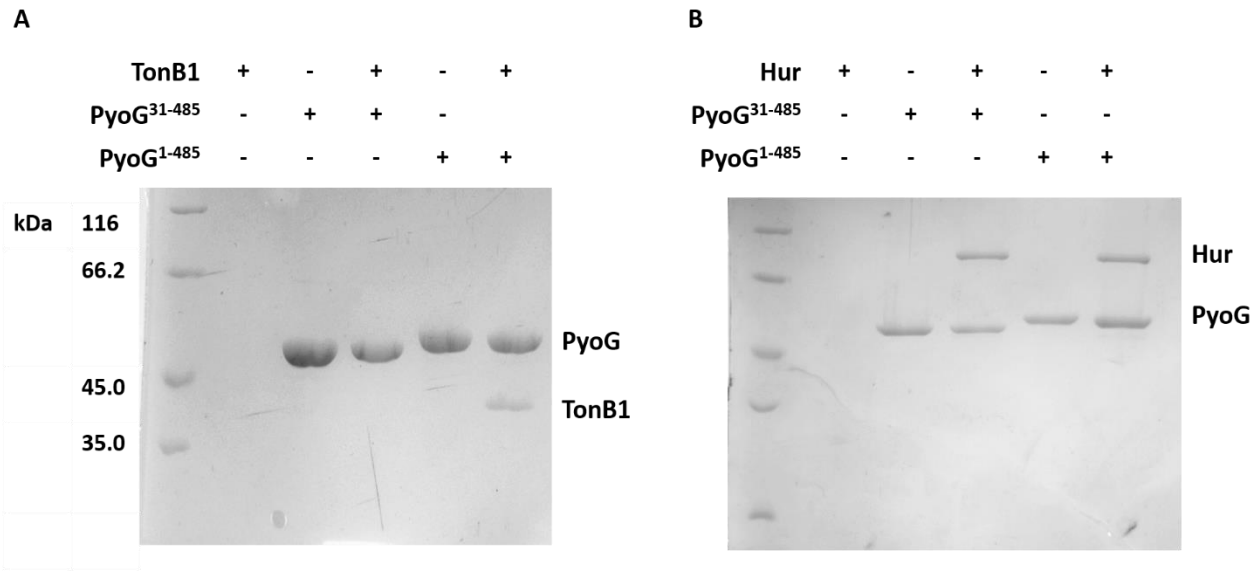

Figure 5-10. Pulldowns with PyoG constructs used for fluorescent labelling of *P. aeruginosa*. Proteins were mixed at equimolar concentrations and bound to nickel beads, which were then washed of unbound protein. Eluate was analysed on 12% SDS-PAGE gels. A protein marker is shown in the first lane on each gel. Proteins that were added to beads are indicated above each lane. Positions of proteins are labelled on the right side of each gel. The His_6-tag was on PyoG constructs, while TonB1 and Hur had no purification tag and were used as prey proteins. (A) Deletion of the first 30 residues in the unstructured N-terminus of PyoG disrupts binding to periplasmic TonB1$^{109-342}$ in the pull-down assay. (B) This deletion does not disturb binding to the PyoG outer membrane receptor, Hur.

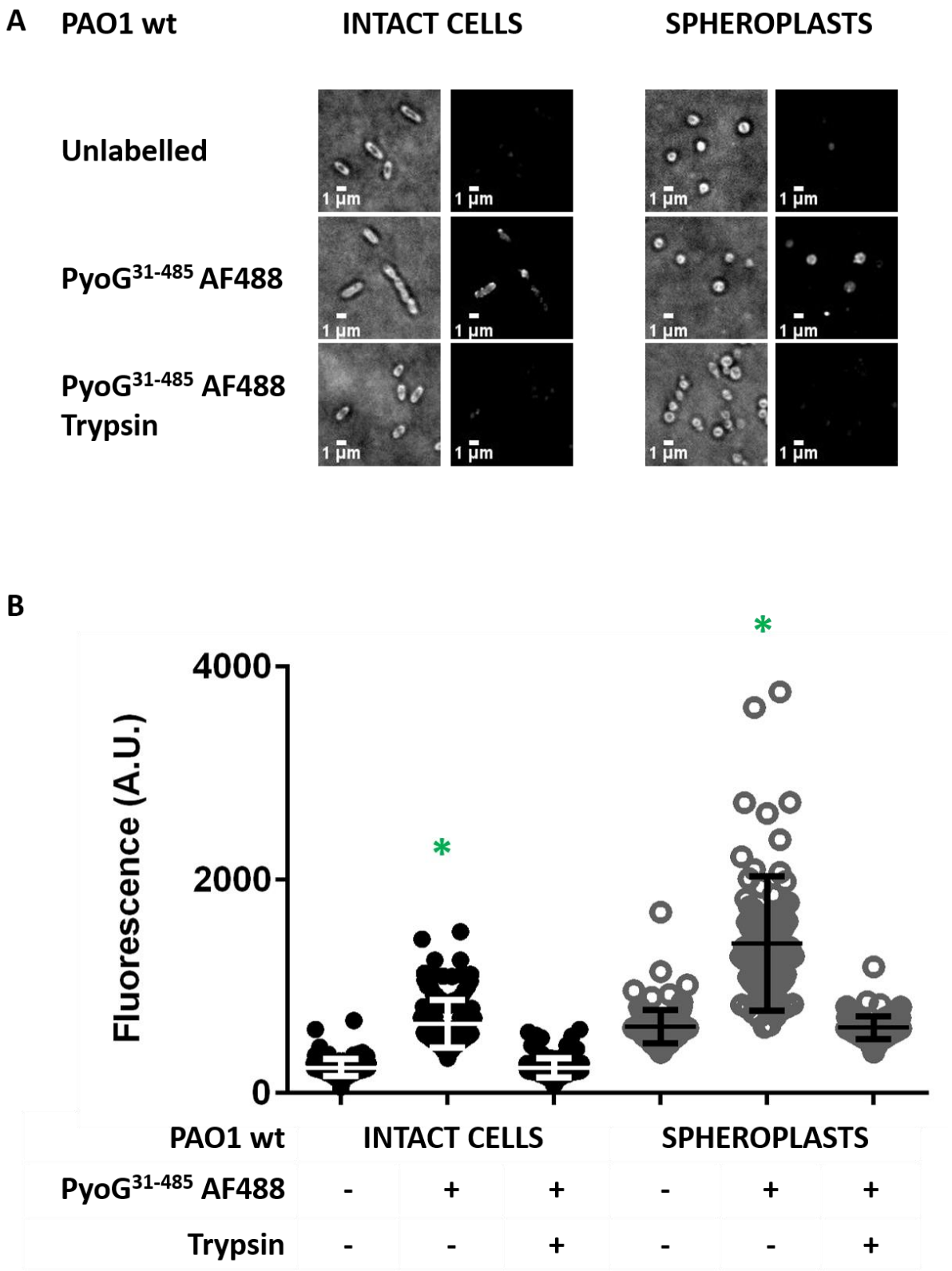

Figure 5-11. A - Fluorescent labelling of PAO1 with PyoG lacking the first 30 residues in the unstructured N-terminus (PyoG$^{31-485}$). PyoG$^{31-485}$, conjugated to AF488 via a C-terminal

cysteine, was added to intact cells or spheroplasts at 2 µM. Cells were exposed to 0.5 mg/mL trypsin after labelling. Fluorescent PyoG$^{31-485}$ was not protected from digestion with trypsin in both types of cells, indicating the importance of the unstructured N-terminus in both the outer and the inner membrane translocation step. Representative micrographs for each strain are shown. All snapshots were adjusted to the same intensity scale. B - Average fluorescence intensities for 150 cells in the presence and absence of fluorescent pyocin and trypsin. Mean of three biological replicates with standard deviations are shown. Fluorescence intensities for labelled and trypsin treated groups were compared to the unlabelled control. * represents a P value below 0.0001 in the Kruskal-Wallis Test.

6. Identification of pyocin AP41 translocon components

6.1 Introduction

Pyocin AP41 is a DNase pyocin for which no translocon components are currently known. The pyocin is composed of four domains (Figure 6-1). The N-terminus is unstructured, as predicted by DisEMBL 1.5 (Linding *et al.* 2003). The first three domains are involved in receptor binding and translocation. Domains I and III are essential for killing, while the deletion of Domain II does not disrupt translocation (Sano *et al.* 1993). Domain III corresponds to the Pyocin S domain (Sharp *et al.* 2017). The fourth domain is a DNase with an HNH motif (Figure 6-2). The structure of this domain in complex with the AP41 immunity protein has been solved by X-ray crystallography (Joshi *et al.* 2015). This pyocin is active in a *P. aeruginosa* murine lung infection model (McCaughey *et al.* 2016b). A single dose (75 µg) of AP41, administered intranasally 1 h post-infection rescued mice with a pulmonary *P. aeruginosa* infection. In this study, AP41 showed strong efficacy against diverse strains of *P. aeruginosa*. The *in vivo* efficacy of AP41 raises interest in understanding the mechanism by which this pyocin translocates into bacterial cells.

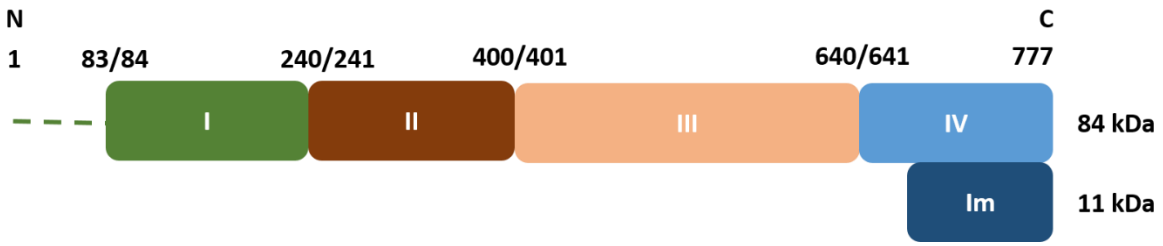

Figure 6-1. Domain organization of pyocin AP41 (modified from Sano *et al.* 1993). Residue numbers are shown above domain boundaries. The first 83 residues are predicted to be disordered by DisEMBL 1.5 (Linding *et al.* 2003). Domains I-III have been linked to receptor binding and translocation. Domain II is not essential for killing activity, while Domain III corresponds to the Pyocin S domain, conserved amongst modular nuclease bacteriocins. Doman IV is an HNH DNase domain that binds the AP41 immunity protein with high affinity (Joshi *et al.* 2015).

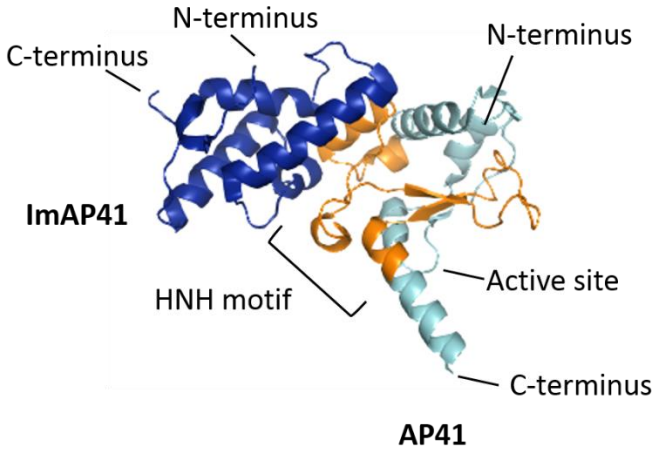

Figure 6-2. Crystal structure of pyocin AP41 DNase–Immunity protein complex (PDB 4UHP). PyoAP41 C-domain is shown in light blue. The HNH motif is highlighted in orange. The immunity protein is shown in dark blue (image modified from Joshi *et al.* 2015).

AP41 insensitive mutants of *P. aeruginosa* have previously been isolated (Holloway *et al.* 1973). The mutants revealed that a cluster of seven genes, organized in three operons (*orf1-tolQRA*, *tolB* and *pal-orf2*), affect the killing activity of AP41. Introduction of *tolQRA* genes in one of these mutants restored AP41 sensitivity, which indicated the likely involvement of the Tol-Pal system in AP41 uptake (Dennis *et al.* 1996). The proposed uptake route via the Tol-Pal machinery has not been previously described for any other pyocin, but it is in line with import mechanisms of some colicins (Cascales *et al.* 2007). The Tol-Pal system can energize the uptake of several colicins. It is composed of the TolQRA inner membrane complex. TolA extends into the periplasm to interact with TolB, which in turn interacts with Pal (Szczepaniak *et al.* 2020). Some colicins interact with TolA and/or TolB, which drives their passage through an outer membrane translocator (Kleanthous 2010). A similar translocation mechanism could be deployed by pyocin AP41, but a direct interaction between AP41 and the components of the Tol-Pal system has not been previously demonstrated. The possibility that AP41, like other pyocins, uses the TonB system for energized cell entry has also not been explored.

6.1.1. Aims

The aim of this chapter was to purify pyocin AP41 and to determine which cell envelope proteins are required for translocation. Firstly, it was tested if this pyocin interacts with components of Tol-Pal or the Ton system. Next, it was investigated if the killing activity of AP41, as with nuclease colicins and PyoG, depends on the inner membrane AAA+ATPase/protease FtsH. Finally, attempts were made to identify outer membrane components of the AP41 translocon.

6.2 Results

6.2.1 Expression and purification of pyocin AP41

Pyocin AP41 was expressed and purified in complex with its immunity protein (ImAP41). ImAP41 has a His_6-tag at the C-terminus. The complex was heterologously expressed in *E. coli* BL21(DE3). The AP41-ImAP41 complex was purified using affinity chromatography with a HisTrap HP column (Figure 6-3). After binding the protein to the column through the C-terminal hexhistidine tag on ImAP41, the complex was eluted using an imidazole gradient (20-180 mM). To buffer exchange and remove residual contaminants, the AP41-ImAP41 complex was subject to gel-filtration using a HiLoad 26/60 Superdex 200 pg column (Figure 6-4). AP41-ImAP41 elutes as a single peak at ~170 mL (peak I in Figure 6-4), while excess immunity protein elutes as a separate peak (peak IV). Protein identity was confirmed by peptide mass fingerprinting. Protein yield was ~5 mg per L of bacterial culture. This protocol was used for the purification of all pyocin AP41 derivatives. Fractions corresponding to peak I were pooled (Figure 6-5 A) and used for further experiments. The activity of pyocin AP41 was tested against *P. aeruginosa* PAO1 by a plate killing assay (Figure 6-5 B). 3 µL drops of the AP41-ImAP41 complex in varying concentrations were spotted on top of the PAO1 lawn. Clearance zones were observed after over-night incubation. The pyocin killed down to ~4.5 nM.

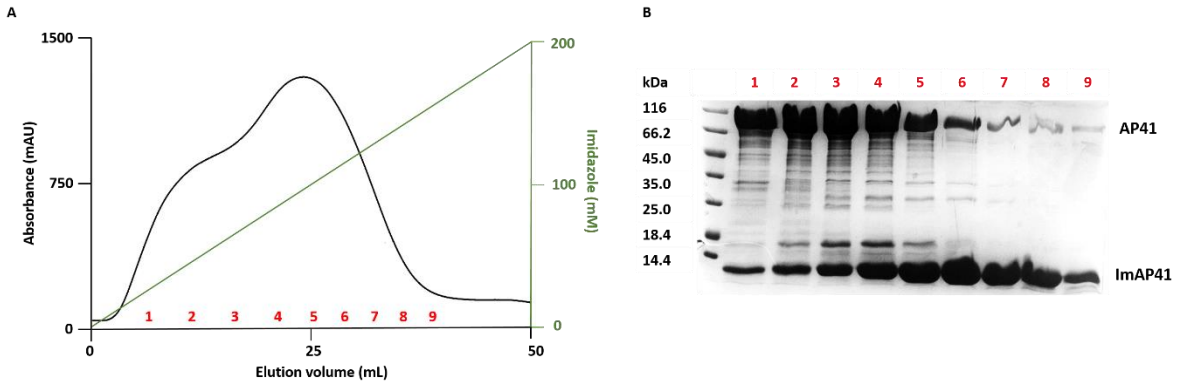

Figure 6-3. Affinity chromatography of pyocin AP41 (84 kDa) in complex with ImAP41- His_6 (11 kDa). A – gradient elution of the complex from a HisTrap HP column. B – a 12 % SDS-PAGE gel showing fractions from the elution. Fractions are labelled with red numbers and their positions are shown on the elution profile in A.

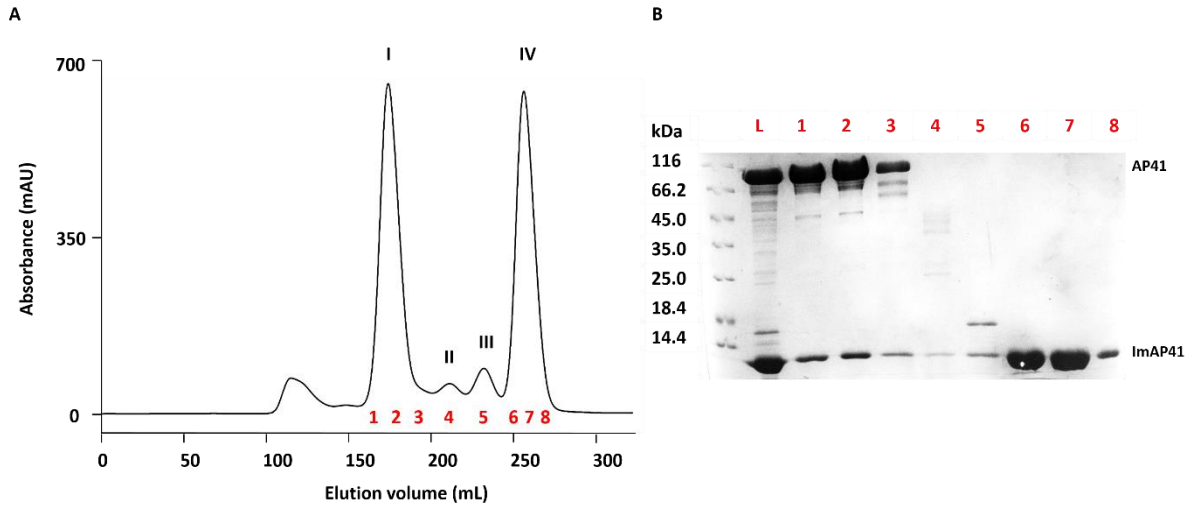

Figure 6-4. Gel filtration of the pyocin AP41-ImAP41 complex. A – elution profile of the complex on a 26/60 Superdex S200 pg column. B – fractions from the profile are labelled with red numbers and are shown on a 12 % SDS-PAGE gel. L is the material obtained after affinity chromatography and loaded on the gel filtration column. Peak I contains pyocin AP41 (84 kDa) and its immunity protein (11 kDa), while peak IV contains excess immunity protein. Peak I fractions were pulled. Average protein yield was 5 mg of protein per L of cells.

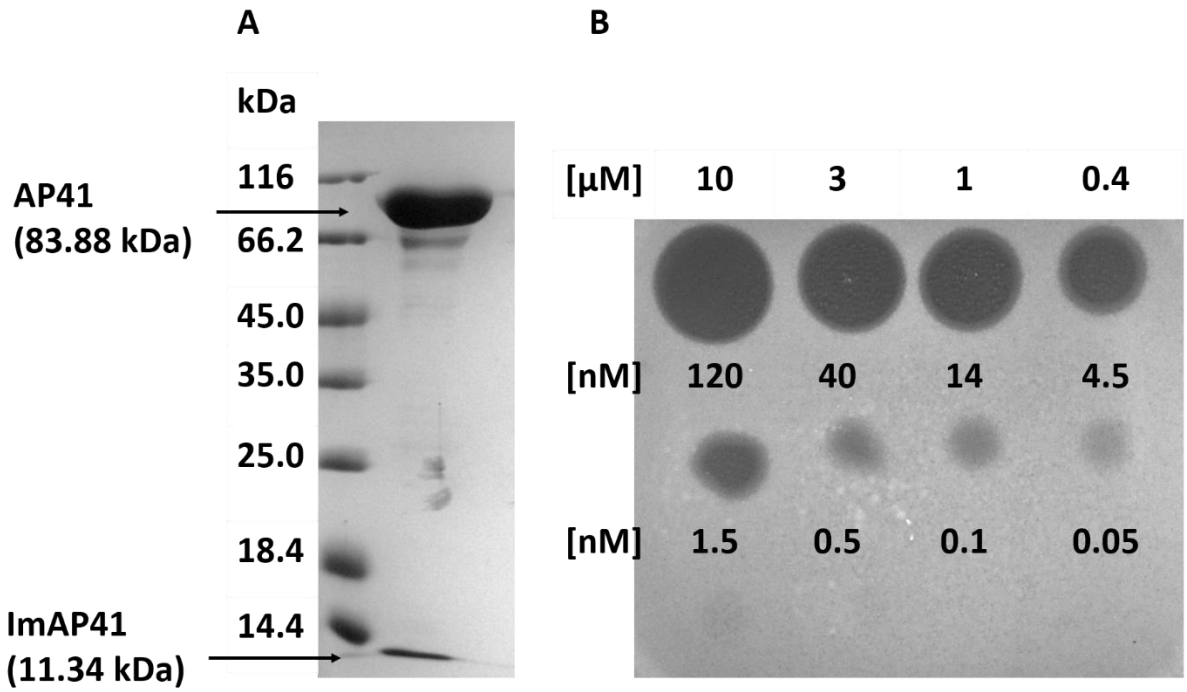

Figure 6-5. Purity and activity of pyocin AP41. A – SDS/PAGE gel (4-16 %) of purified AP41 (84 kDa) and its immunity protein (ImAP41, 11 kDa). B – 3 µL of AP41-ImAP41 in varying concentrations was spotted on top of a *P. aeruginosa* PAO1 lawn. Clearance zones were observed after overnight incubation. The pyocin kills down to ~4.5 nM.

6.2.2 Pyocin AP41 killing activity is TonB1 and FtsH-dependent

Purified AP41-ImAP41 complex was used to investigate which cell envelope proteins are required for pyocin AP41 import. It has been suggested previously that this pyocin depends on the Tol-Pal system (Dennis *et al.* 1996). However, other modular pyocins, such as PyoG (Chapter 3), S2 (White *et al.* 2017), SD2 (McCaughey 2016a) and S5 (Behrens *et al.* 2020) require the Ton system for energized cell entry. Therefore, it was investigated if pyocin AP41 is in fact TonB dependent. *P. aeruginosa* has three TonB proteins: TonB1 (*PA5531*), TonB2

(*PA0197*) and TonB3 (*PA0406*). Strains of *P. aeruginosa* PAO6609 lacking different TonBs were tested for AP41 sensitivity (Figure 6-6 A). All strains lacking TonB1 were resistant to the pyocin. Therefore, like PyoG, SD2, S2 and S5, AP41 is also TonB1 dependent.

Next, it was tested if FtsH, the inner membrane protease/ATPase, is required for AP41 killing activity. FtsH has been previously linked to the killing activity of nuclease colicins (Walker *et al.* 2007) and PyoG (Atanaskovic *et al*. 2020). To assess the role of FtsH in AP41 killing an *ftsH* (*PA4751*) knock-out of PAO1 was tested for sensitivity to AP41 and was found to be resistant (Figure 6-6 B). *ftsH* was cloned from the PAO1 genome to complement the *ΔftsH* strain. Conjugation of PAO1 *ΔftsH* with the plasmid copy of *ftsH* restored sensitivity to AP41. This finding indicates the involvement of FtsH in AP41 import.

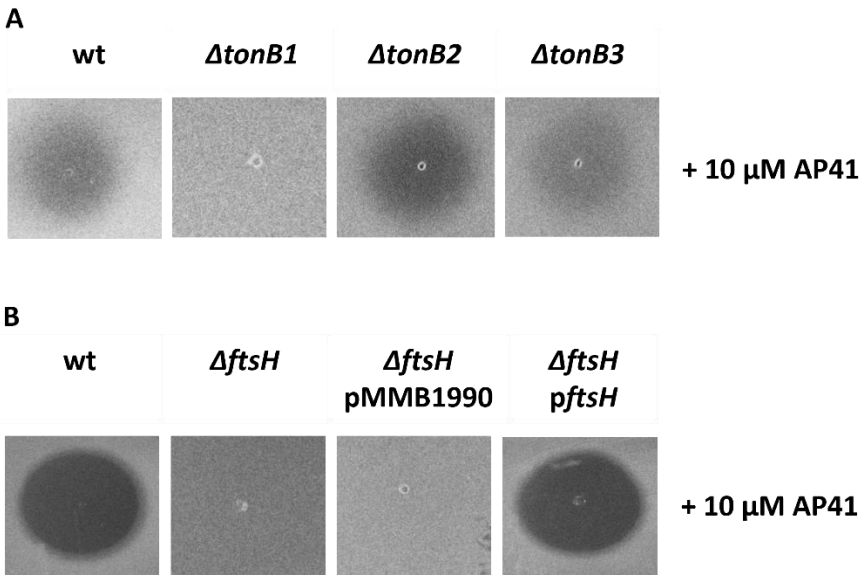

Figure 6-6. Killing activity of pyocin AP41 depends on TonB1 and FtsH. 3 µL drops of 10 µM AP41 were spotted on top of bacterial lawns. Clearance zone formation was inspected after overnight incubation. A – killing activity of AP41 against *ton* mutants of *P. aeruginosa* PAO6609. Δ*tonB1* is resistant to AP41, while *tonB2* and *tonB3* are not required for the AP41

killing activity. B – killing activity of AP41 against *P. aeruginosa* PAO1 *ΔftsH*. The mutant is resistant to the pyocin. *ΔftsH* pMMB190 is transformed with the empty conjugation plasmid. This strain is resistant to AP41. *ΔftsH* p*ftsH* is transformed with a plasmid copy of *ftsH*. This strain is sensitive to AP41.

6.2.3 Pyocin AP41 binds TonB1 *in vitro*

Having established a genetic dependence of AP41 on TonB1, the ability of TonB1 to bind AP41 *in vitro* was investigated. Firstly, formaldehyde cross-linking was used to test if AP41 interacts with the periplasmic domain of TonB1 (TonB1$^{109-349}$), periplasmic domain of TolAIII$^{224-347}$, or TolB (Figure 6-7). PyoS2$^{1-554}$ was included as a positive control for TonB1 binding (White *et al.* 2017). Cross-links were only observed for PyoS2-TonB1, AP41-TonB1 and TolAIII$^{224-347}$-TolB. No complex formation was detected for AP41 and TolAIII$^{224-347}$. In addition, no complex formation was observed between AP41 and TolB, or AP41 and the TolAIII-TolB complex.

Complex formation between AP41 and TonB1 was further characterised by analytical gel filtration (Figure 6-8 A). TonB1$^{109-349}$ and AP41 eluted at 14 ml and 13 ml, respectively, from a Superdex 200 10/300 GL column, whilst their complex eluted at 11 ml. SDS-PAGE confirmed the presence of both AP41 and TonB1$^{109-349}$ in the shifted elution peak, indicating complex formation. Finally, the binding affinity between these two proteins was determined by ITC (Figure 6-9 A). AP41 and TonB1$^{109-349}$ bind with a nanomolar dissociation constant (Kd = 89.2 ± 10.4 nM), which is a higher affinity than previously observed for pyocin-TonB complexes; the respective K_d's for the PyoS2-TonB1 and PyoS5-TonB1 complexes are 960 ± 90 µM (White *et al.* 2017) and 241 ± 9 nM (Behrens *et al.* 2020).

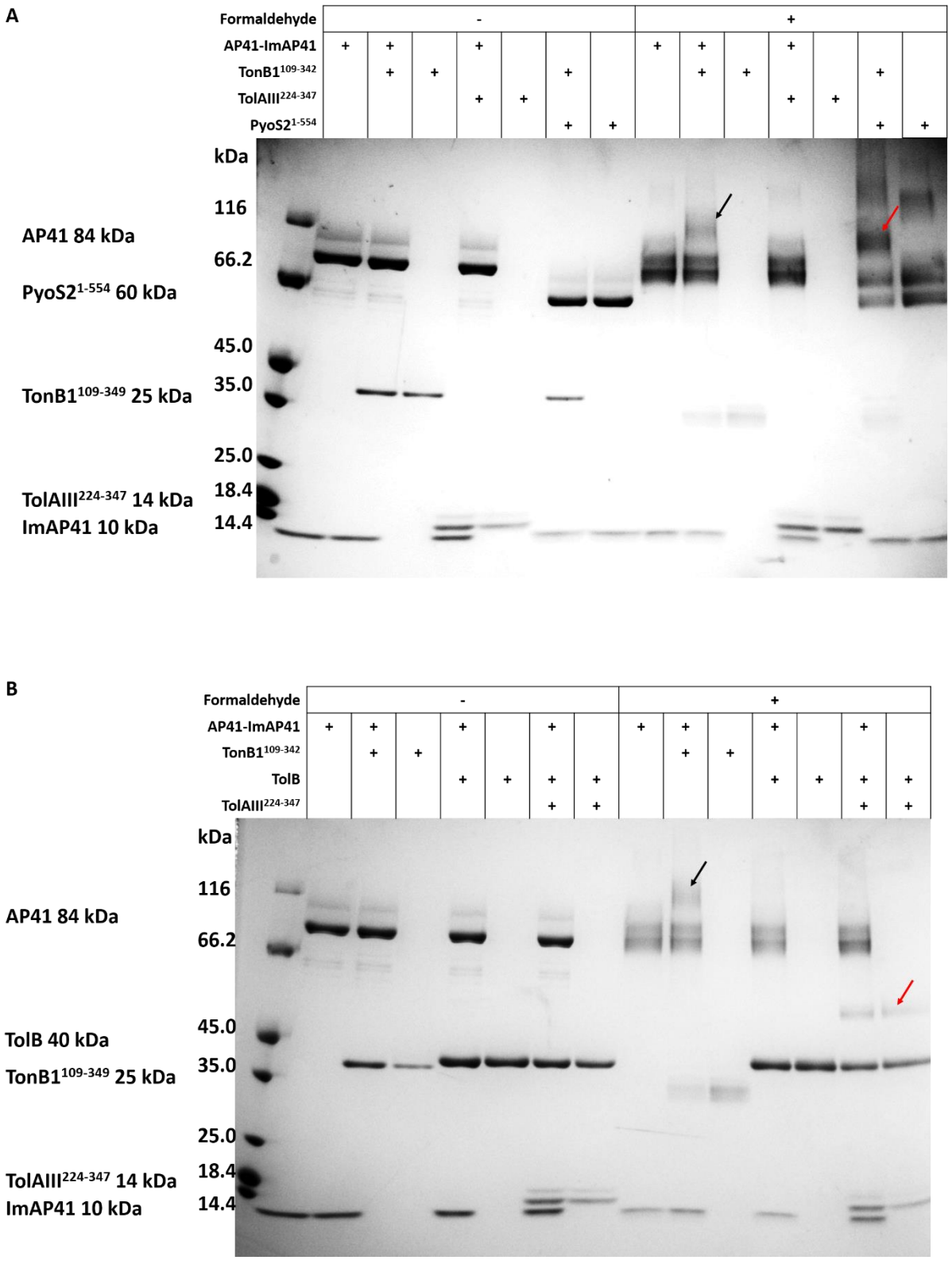

Figure 6-7. Formaldehyde cross-linking indicates complex formation between AP41 and TonB1. All proteins were mixed to a final concentration of 10 µM, and exposed to 1 % formaldehyde for 1 h at room temperature. Proteins were also exposed to formaldehyde in

the absence of the potential interaction partner, to check for protein self-crosslinking. Formation of cross-linked complexes was inspected on a 4-20 % gradient SDS-PAGE gel. Protein sizes relative to their position on the gel are listed next to the protein ladder. Sample components are listed above each lane. A - Full length AP41, used in complex with its immunity protein, cross-links to the periplasmic domain of TonB1 (TonB1$^{109-349}$). The complex is labelled with a black arrow on the gel. Complex formation was also observed between PyoS2 and TonB1$^{109-349}$, which served as a positive control in this experiment. This complex is labelled with a red arrow. No complex formation could be observed between AP41 and the periplasmic domain of TolAIII (TolAIII$^{224-347}$). B – complex formation can be observed for AP41 and TonB1$^{109-349}$ (indicated with a black arrow), but not for AP41 and TolB, or AP41 and TolAIII-TolB. The TolAIII-TolB cross-linked complex is indicated with a red arrow. PyoS2, TolAIII$^{224-347}$ and TolB were provided by Dr. Renata Kaminska.

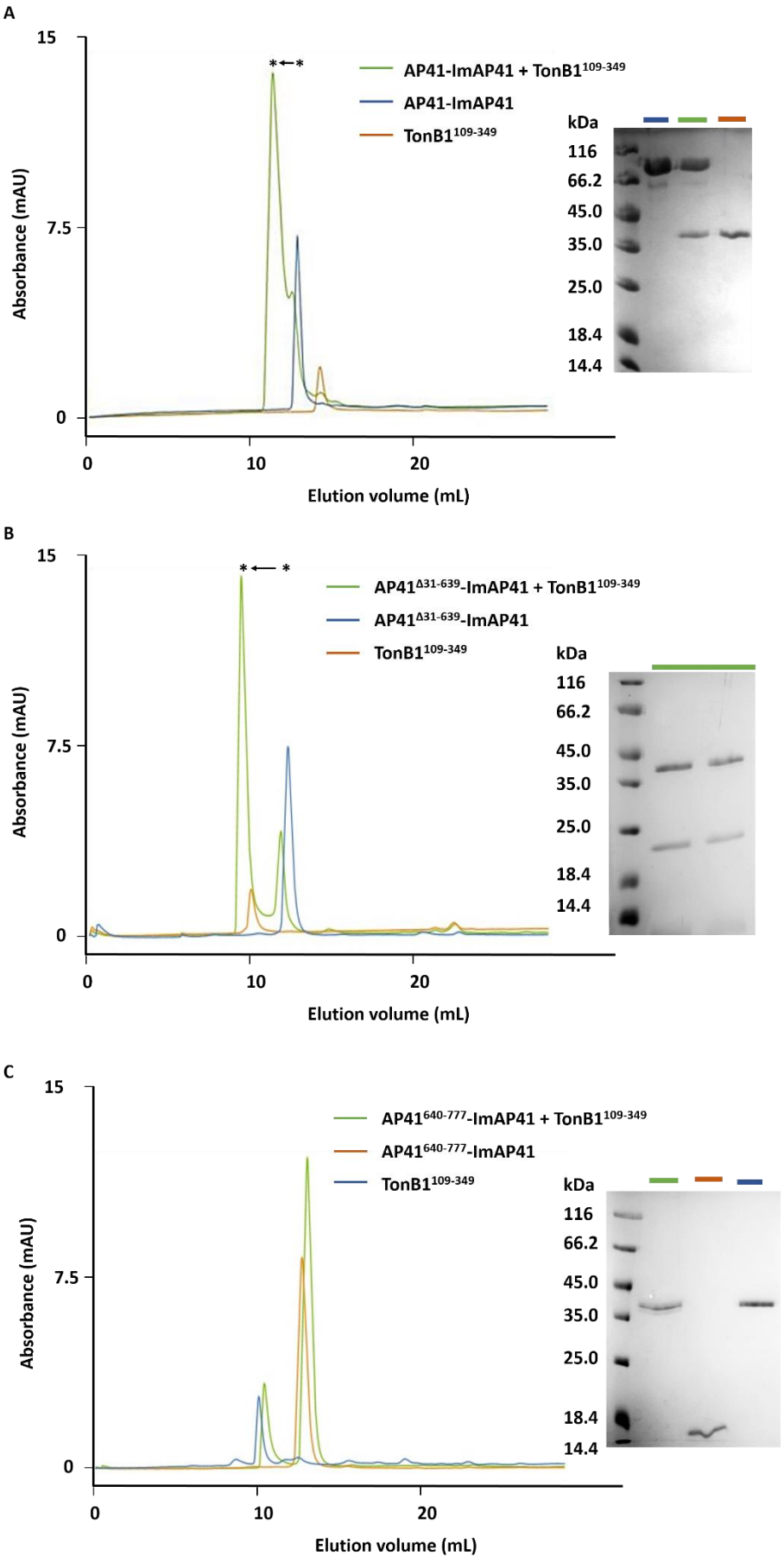
A
15
7.5
0
Absorbance (mAU)
0
10
20
Elution volume (mL)
AP41-ImAP41 + TonB1109-349
AP41-ImAP41
TonB1109-349
kDa
116
66.2
45.0
35.0
25.0
18.4
14.4
B
15
7.5
0
Absorbance (mAU)
0
10
20
Elution volume (mL)
AP41Δ31-639-ImAP41 + TonB1109-349
AP41Δ31-639-ImAP41
TonB1109-349
kDa
116
66.2
45.0
35.0
25.0
18.4
14.4
C
15
7.5
0
Absorbance (mAU)
0
10
20
Elution volume (mL)
AP41640-777-ImAP41 + TonB1109-349
AP41640-777-ImAP41
TonB1109-349
kDa
116
66.2
45.0
35.0
25.0
18.4
14.4

Figure 6-8. Analytical gel filtration of TonB1$^{109-349}$ and AP41-ImAP41 (A), AP41$^{\Delta 31-639}$-ImAP41 (B), or AP41$^{640-777}$-ImAP41 (C). All proteins were used at a final concentration of 10 µM in 50 mM Tris-HCl pH 7.8, 100 mM NaCl, and loaded on Superdex 200 10/300 GL in A, or Superdex 75 10/300 GL in B and C. Peak shifts are indicated with an arrow. Next to each elution profile, peak fractions are shown on a 12 % SDS-PAGE gel. A – a shift in the AP41 (84 kDa) peak can be observed in the presence of TonB1$^{109-349}$ (25 kDa). Complex formation is also indicated by the co-elution of the two proteins from the column. B – a peak shift can also be observed for AP41$^{\Delta 31-639}$ (20 kDa) and TonB1$^{109-349}$, and the two proteins co-elute from the column. C – no complex formation was observed for AP41$^{640-777}$ (15 kDa) and TonB1$^{109-349}$.

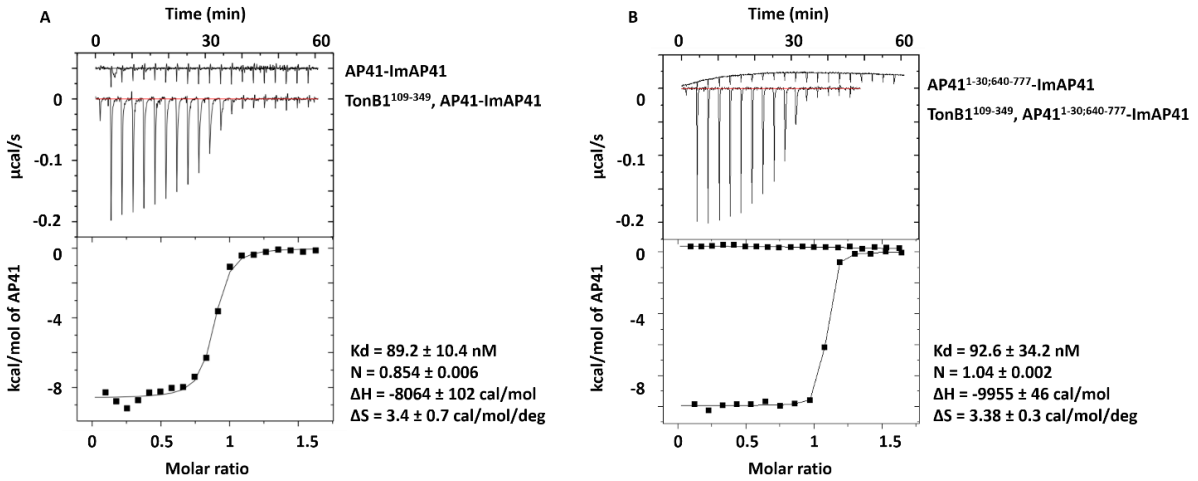

Figure 6-9. ITC data for 200 µM AP41 (A), or 200 µM AP41$^{1-30:640-777}$ (B), titrated into 26 µM TonB1$^{109-349}$ at 25 °C in 50 mM Tris-HCl pH 7.8, 100 mM NaCl. Both constructs bind TonB1 with a nanomolar Kd. All ITC experiments were performed in triplicate, and one repeat is shown. Data were fitted with a single sites binding model using the manufacturer's software.

The TonB binding boxes in pyocins S2 (White *et al.* 2017), S5 (Behrens *et al.* 2020) and G (section 5.2.3) are located within the first 30 residues of the unstructured N-terminus. In addition, pyocins AP41, S2 and S5 share several conserved residues in this region (Figure 6-10). Therefore, it was assumed that this region of AP41 could be involved in binding TonB1. To test this hypothesis, a fusion was constructed, composed of the first 30 residues of AP41 and its cytotoxic domain (residues 640-777) in the C-terminus ($AP41^{1\text{-}30:640\text{-}777}$). Note that the DNase of AP41 was used in these experiments merely to allow expression of the first 30 residues of the pyocin. The construct was tested for TonB1 binding by analytical gel filtration (Figure 6-8 B). $TonB1^{109\text{-}349}$ and $AP41^{1\text{-}30:640\text{-}777}$ eluted at 10 ml and 11 ml, respectively, from a Superdex 75 10/300 GL column, whilst their complex eluted at 9.5 ml. SDS-PAGE confirmed the presence of both AP41 and $TonB1^{109\text{-}349}$ in the shifted elution peak, indicating complex formation. On the contrary, no complex formation was observed for $TonB1^{109\text{-}349}$ and the AP41 cytotoxic domain alone (Figure 6-8 C). Therefore, binding of $AP41^{1\text{-}30:640\text{-}777}$ to $TonB1^{109\text{-}349}$ can be attributed to the first 30 residues of AP41. Binding of $AP41^{1\text{-}30:640\text{-}777}$ to $TonB1^{109\text{-}349}$ was also confirmed by ITC (Figure 6-9 B). The measured Kd was similar to full length AP41 (Kd = 92.6 ± 34.2 nM).

Figure 6-10. Alignment of the first 30 residues of pyocins AP41, S2 and S5 reveals conserved residues (highlighted in red). This region can be associated with TonB1 binding in all three pyocins. The TonB box of PyoS2 (White *et al.* 2017) and PyoS5 (Behrens *et al.* 2020) is underlined.

6.2.4 The search for outer membrane components of the pyocin AP41 translocon

The outer membrane receptor and translocator for pyocin AP41 are not known. Attempts were made to find such outer membrane components of the AP41 translocon, using a candidate-based approach and beginning with LPS. *P. aeruginosa* LPS is composed of three domains: lipid A, core oligosaccharide, and the distal O antigen (Lam *et al.* 2012). *P. aeruginosa* can produce two forms of O antigen: a homopolymer of D-rhamnose, called the common polysaccharide antigen (CPA), and a heteropolymer of several sugars, called the O-specific antigen (OSA). CPA has previously been linked to the import of pyocins S2, SD2, and S5 (McCaughey *et al.* 2016a; Behrens *et al.* 2020). It can serve as a pyocin receptor, concentrating the toxin on cell surface. Conversely, O-antigen has been associated with colicin tolerance in *E. coli*; long LPS molecules prevent binding of a colicin to its outer membrane protein receptor (Sharp *et al.* 2019). Therefore, it was investigated if altering the O-antigen composition of *P. aeruginosa* LPS affects its sensitivity to pyocin AP41 (Figure 6-11 A). Transposon mutants for genes involved in LPS biogenesis were used. *Δrmd* (*PA5454*) is CPA deficient, but it still produces OSA. This mutant had the same level of sensitivity to AP41 as the wild type strain, indicating that CPA has no involvement in AP41 import. This is in accordance with previously published biophysical data showing that AP41 does not bind CPA sugars purified from the PAO1 envelope (McCaughey *et al.* 2016a). *ΔwbpM* (*PA3141*) is OSA deficient, but still produces CPA. This strain was more sensitive to AP41 than the wild type strain suggesting OSA provides partial protection towards the pyocin. Finally, a strain lacking both CPA and OSA (*ΔwbpL* (*PA3145*)) was AP41 sensitive, confirming that O-antigen is not involved in AP41 import.

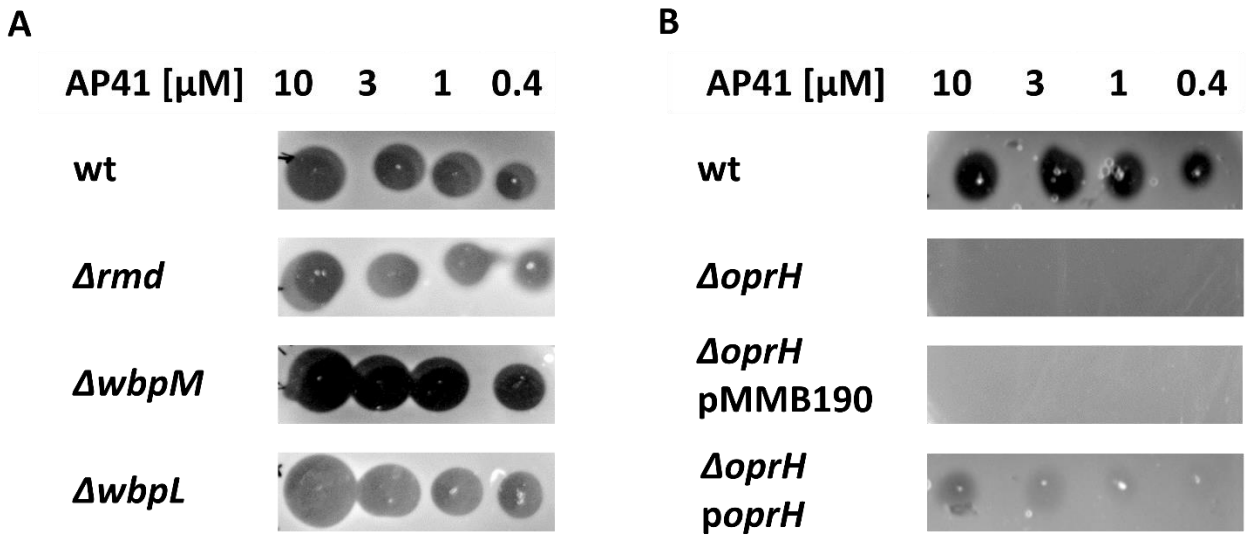

Figure 6-11. A - Effect of mutations in the LPS biogenesis machinery on AP41 sensitivity. A spot killing assay with 3 µL drops of varying AP41 concentrations is shown. *Δrmd* has only OSA, *ΔwbpM* has only CPA, and *ΔwbpL* lacks both CPA and OSA. All of these mutants are sensitive to AP41. These data show that neither CPA or OSA are the AP41 receptor. B - *P. aeruginosa* PAO1 *ΔoprH* is resistant to pyocin AP41. A plate killing assay with 3 µL drops of AP41 is shown. Sensitivity of *ΔoprH* is not fully restored with complementation, indicating that the resistance phenotype might be a secondary effect.

In order to find outer membrane proteins involved in AP41 import, pull-down assays were performed using the his-tagged AP41-ImAP41-His_6 complex as a bait. AP41-ImAP41-His_6 was added to PAO1 cells and then cross-linked with formaldehyde. The outer membrane fraction was extracted and the AP41-ImAP41-His_6 complex was purified from the extract on a HisTrap HP column. Bait protein was retrieved in these experiments, but no interaction

partners could be identified by SDS-PAGE (data not shown), probably due to low expression levels of the receptor and/or low binding affinity for AP41.

Since AP41 import depends on TonB1, might the AP41 receptor be a TonB1 dependent transporter as in the case of pyocin S2 (White *et al.* 2017), S5 (Behrens *et al.* 2020) or G (Atanaskovic *et al.* 2020)? To address this question, all TBDTs in the PAO1 genome were identified by their conserved TonB1 plug sequence (Pfam domain PF07715) as previously described (Ghequire & Ozturk, 2018). This search identified 37 putative TBDTs (Table 1-1). Each of these TBDTSs are represented in a transposon library of the PA01 genome (Jacobs *et al.* 2003). The transposon mutants for each of these TBDTs (Table 2-1) were all sensitive to AP41-mediated killing (not shown), suggesting AP41 does not use any of these proteins as its outer membrane receptor/transporter. Another possibility is that AP41 can exploit more than one TBDT, in which case single deletions might not yield a resistance phenotype.

Porins are exploited by some colicins to enter *E. coli* cells (Cascales *et al.* 2007; Atanaskovic & Kleanthous 2019). *P. aeruginosa* expresses several different types of porin and so porin deletions were also tested for AP41 sensitivity (Table 2-1). Interestingly, the *oprH* (PA1178) mutant of PAO1 was resistant to AP41, but AP41 sensitivity could not be fully restored with *oprH* complementation (Figure 6-11 B). This could be due to different expression levels of *oprH* in the native background and in the complemented strain, since the native *oprH* protmoter was not being used for complementation. As a further test of OprH involvement in AP41 import, the porin was purified and binding to AP41 *in vitro* investigated. OprH was expressed without a purification tag in *E. coli* BL21ΔABCF, and then purified from the outer membrane by gel-filtration and ion exchange (Figure 6-12). Protein identity was confirmed by peptide mass fingerprinting. The high melting temperature, measured by DSC,

indicated that OprH was folded (Figure 6-13). No complex between AP41 and OprH could be detected by analytical gel filtration (Figure 6-14). Hence, OprH is unlikely to be involved directly in AP41 import. The resistance phenotype observed in the transposon mutant library was probably due to a secondary (e.g. polar) effect of the mutation.

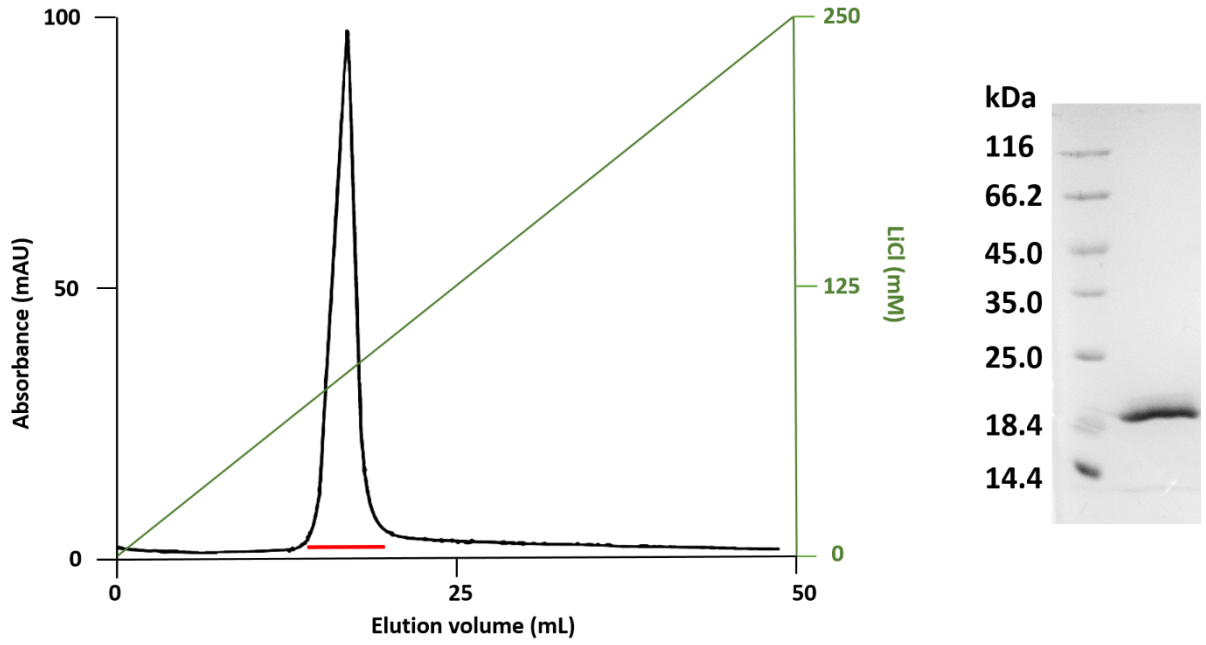

Figure 6-12. Purification of OprH from *E. coli* BL21ΔABCF outer membrane. Ion exchange chromatography on SP Sepharose Fast Flow column was used as the final purification step. The column was equilibrated in 50 mM Tris-HCl pH 7.8, 1 % (w/v) β-OG, 5 mM EDTA. The protein eluted as one peak over a 1-250 mM gradient of LiCl. Pooled elution volume is underlined on the profile. Final purity of OprH (20 kDa) is shown on the 4-20 % SDS-PAGE gel on the right. Average protein yield was 0.3 mg/L of cells.

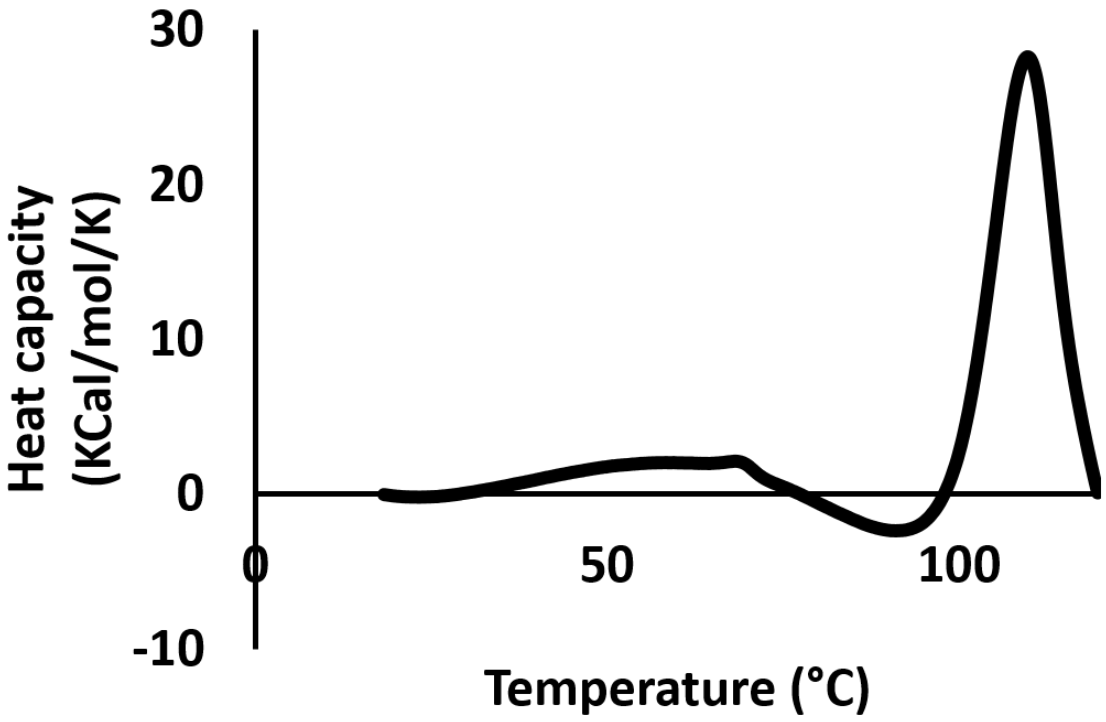

Figure 6-13. DSC of 20 µM OprH in 50 mM Tris-HCl pH 7.8, 1 % β-OG, 5 mM EDTA. The melting temperature of OprH is 110 °C, indicating that the protein is folded. The experiment was repeated two times and a representative DSC curve is shown.

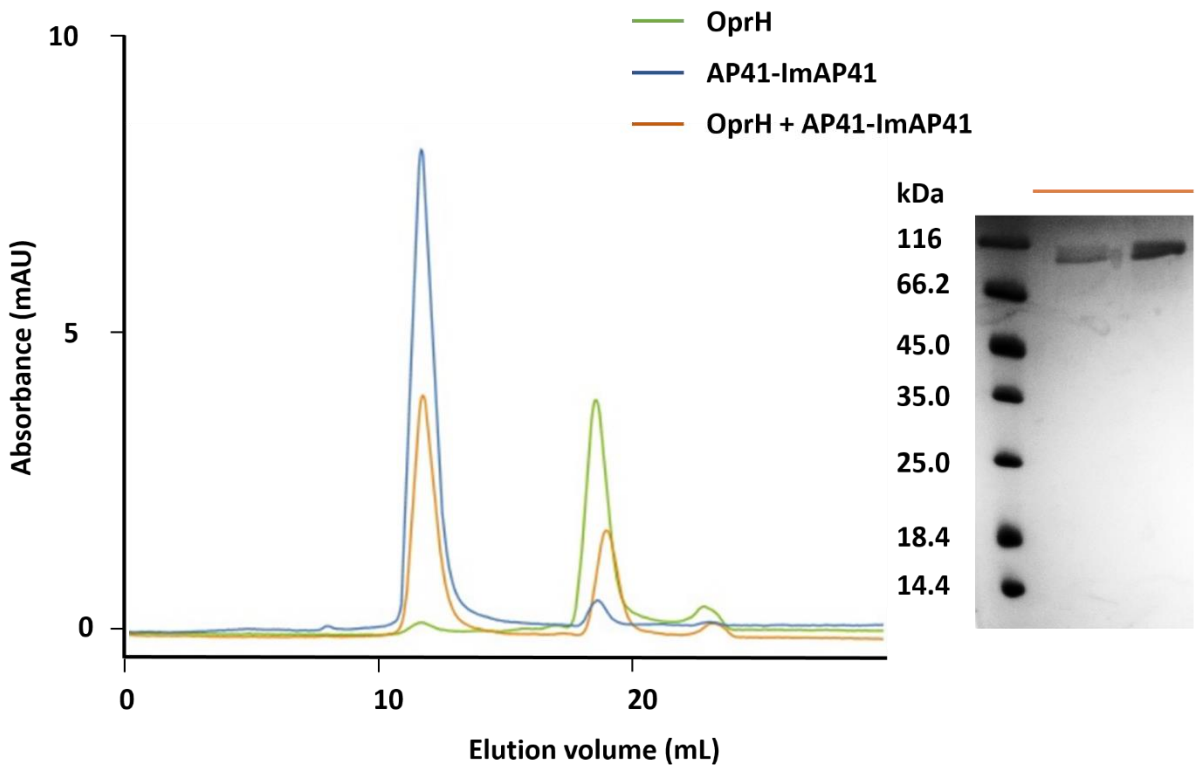

Figure 6-14. Analytical gel filtration of OprH and AP41-ImAP41. OprH and AP41-ImAP41 were mixed to an equimolar concentration of 10 µM in 50 mM Tris-HCl pH 7.8, 100 mM NaCl, 1 % β-OG, and run on a Superdex 200 10/300 GL column equilibrated in 50 mM Tris-HCl pH 7.8, 100 mM NaCl, 1% β-OG, 5 mM EDTA. No shift in the AP41 peak could be observed. Also, no OprH could be detected on a 4-20 % SDS-PAGE gel, in fractions corresponding to the AP41 peak, indicating that the two proteins did not form a complex under the conditions tested.

Since pull-downs and transposon mutant screens failed to identify the AP41 receptors, an AP41 resistant mutant of *P. aeruginosa* PAO1 were isolated as part of a collaboration with the Walker Laboratory, Institute of Infection, Immunity, and Inflammation, University of Glasgow. Genomic DNA sequence of this mutant was analysed in the Walker Laboratory, and transposon insertions in the *fhaB1* (*PA0041*) gene were identified as a potential cause of the

resistance phenotype. FhaB1 is one of the two putative filamentous hemagglutinins of PAO1. This is a large protein of around 300 kDa, which has repeating hemagglutinin motifs involved in cell adhesion, virulence (Sun *et al.* 2016) and contact dependent inhibition (Mercy *et al.* 2016). This protein is part of a two-partner secretion system, the other component being the transporter FhaC1. AP41 sensitivity of transposon mutants for both *fhaB1* and *fhaC1* was tested (Figure 6-15). *ΔfhaB1* remains sensitive to AP41, but *ΔfhaC1* (*PA0040*) is resistant. Therefore, this transporter could be involved in the import of AP41 across the outer membrane. It was also tested if transposon insertions in the second hemagglutinin system of PAO1 affect AP41 sensitivity. FhaB2 is larger than FhaB1 and has more hemagglutinin repeats. FhaC2 shares 98 % sequence identity with FhaC1, with differences being only in the signal sequence. Like *ΔfhaB1*, *ΔfhaB2* (*PA2462*) was sensitive to AP41. Unlike *ΔfhaC1*, *ΔfhaC2* (*PA2463*) was also sensitive to AP41, but the sensitivity reduced compared to that of the wild type strain. Therefore, it is not clear if FhaC is involved directly in AP41 import. If FhaC is the AP41 transporter, one copy should complement the other, and so deleting just one copy should not have had an impact on AP41 sensitivity. Still, the *ΔfhaC1* mutant does appear to be fully resistant to AP41, which might simply be a consequence of low expression levels of the second copy of the transporter. Further studies on the possible involvement of FhaC in AP41 import are being undertaken by the Walker Laboratory and have not been taken further in this thesis.

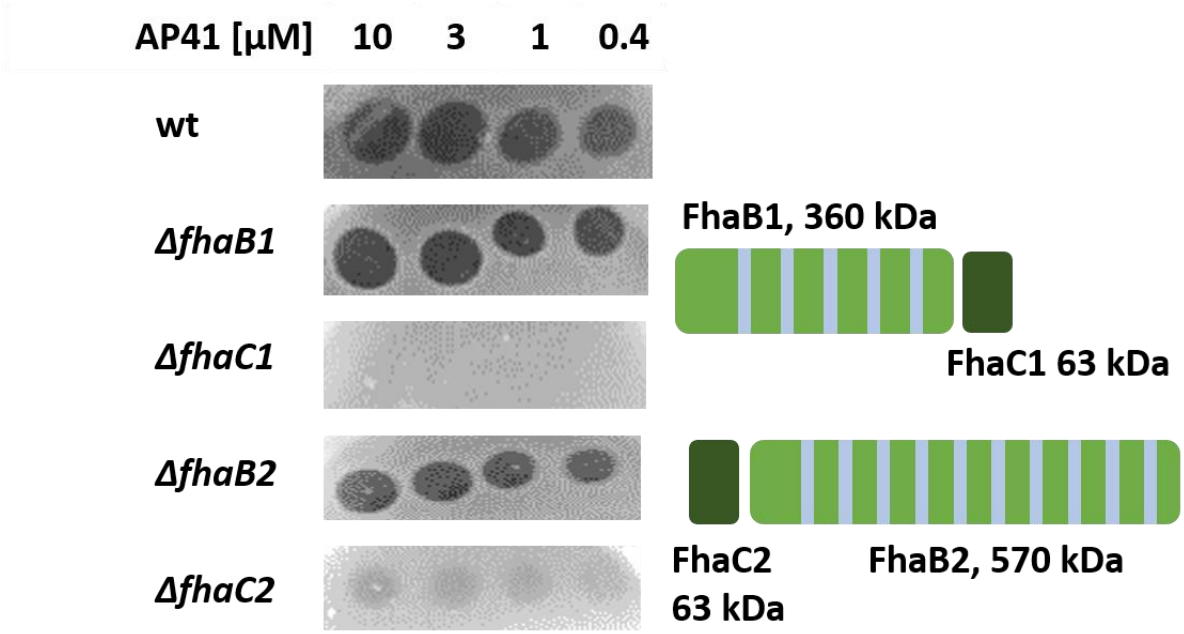

Figure 6-15. The sensitivity in the filamentous hemagglutinin secretion system (FHA) to pyocin AP41. 3 µL drops of varying AP41 concentrations were spotted on top of lawns of PAO1 strains carrying transposon insertions within each of the two FHAs. Diagrams of FHAs are shown on the right. Each FHA is composed of FhaB, which is secreted to the cell surface through the FhaC transporter. There are two FhaBs encoded in the PAO1 genome, with varying numbers of hemagglutinin repeats (represented with a blue box in the diagram). Each copy is in an operon with an FhaC transporter gene. The two FhaCs share 98 % sequence identity. PAO1 *ΔfhaC1* is resistant to AP41, while *ΔfhaC2* has decreased sensitivity to the pyocin.

7. Discussion

7.1 Translocation of PyoG across the *P. aeruginosa* outer membrane

PyoG is a newly discovered nuclease pyocin of the S1 group. It is effective against clinical isolates of *P. aeruginosa* and in a *Galleria mallonella* infection model. In chapter 3, the cell envelope proteins required for PyoG translocation were identified (Figure 4-6). As with previously characterized nuclease pyocins and colicins (Atanaskovic & Kleanthous 2019), PyoG entry requires a TBDT to act as its outer membrane receptor and translocator, TonB1, to energise its import across the outer membrane, and FtsH, possibly for inner membrane translocation (Figure 7-1). Such import machinery appears to be conserved amongst modular nuclease bacteriocins. For instance, PyoS2 also uses an outer membrane TBDT, FpvAI, as a translocator, although PyoS2 also binds CPA on the cell surface. Both the FpvAI plug domain and the N-terminus of PyoS2 interact with TonB1, enabling PyoS2 to be pulled into the periplasm by TonB1 (White *et al.* 2017). This is also the case of a pore former, PyoS5, that uses FptA as a TBDT, and also has a TonB1 binding box in the N-terminus (Behrens *et al.* 2020).

The present work found that, as with PyoS2 and PyoS5, PyoG also uses a TBDT, Hur, and requires TonB1 binding to energise import into cells. Therefore, it is reasonable to speculate that the outer membrane translocation step is by a similar mechanism to that observed for PyoS2 and PyoS5. In this mechanism (Figure 7-1) PyoG would bind to Hur, which then interacts with TonB1 via its plug domain. The plug gets displaced such that PyoG can pass through the β-barrel pore. Exposure of the TonB binding box of PyoG in the periplasm then allows it to bind TonB1, either the same TonB1 or an additional copy. TonB1 then pulls the remainder of PyoG into the periplasm in a PMF-dependent step.

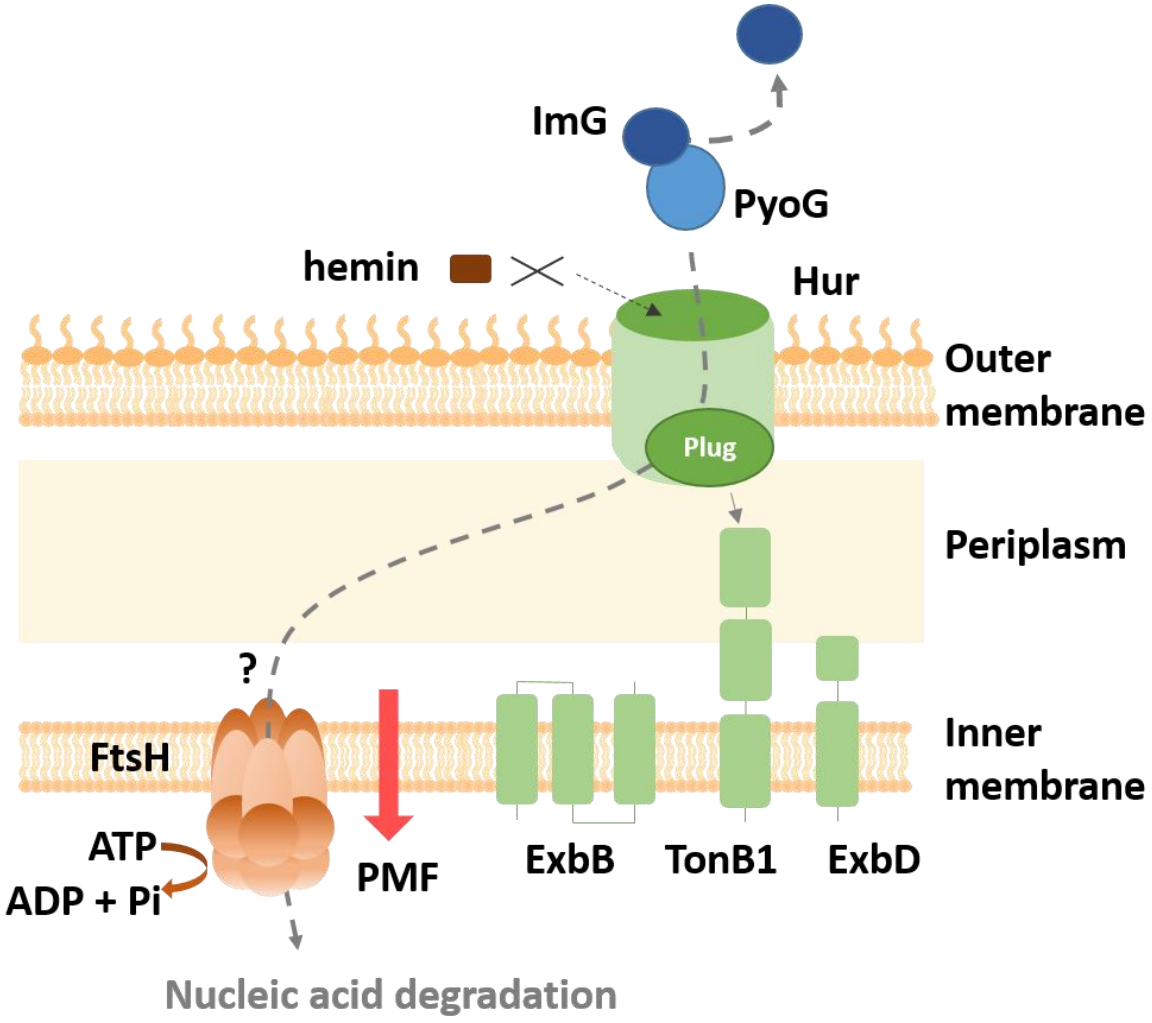

Figure 7-1. Model of PyoG translocation into *P. aeruginosa*. PyoG exploits Hur as both receptor and outer membrane translocator. Binding of PyoG and hemin to Hur is competitive. As in the case of nuclease colicins (Duché *et al.* 2006), the immunity protein dissociates at the cell surface, which for PyoG has yet to be demonstrated experimentally. As with its receptor, PyoG also binds TonB1, which links the proton motive force (PMF) at the inner membrane with translocation at the outer membrane. The import process, as with nuclease colicins, requires the inner membrane AAA+ ATPase/protease FtsH, but the direct involvement of FtsH in pyocin import has yet to be proven experimentally. Figure adapted from Atanaskovic *et al.* 2020.

The immunity protein may dissociate from PyoG during translocation through Hur, but the exact moment of pyocin immunity protein dissociation still has to be elucidated. Studies on the release of the colicin E2 (ColE2) immunity protein suggest that this event takes place on the cell surface. In this study (Duché *et al.* 2006), the E2 immunity protein was fused to GFP and its release was monitored upon cell exposure to ColE2. Functional ColE2 translocation machinery was required for immunity protein release. Cell fractionation and protease susceptibility experiments indicated that the immunity protein does not cross the cell envelope during colicin import, which suggests that dissociation occurs at the outer membrane surface. Similar experiments are required to determine if the immunity protein of PyoG also gets released on the cell surface.

Hur appears to be the only essential cell surface component to which PyoG binds (Figure 3-9). On the other hand, several nuclease colicins bind two cell surface proteins; for example, ColE9 (Housden *et al.* 2005). Initially, ColE9 binds to the TBDT BtuB that serves as a surface receptor and then translocates through the porin OmpF. The lack of surface binding of PyoG to *Δhur* suggests that Hur is both the PyoG receptor and translocator. All previously described pyocins translocate through a TBDT (White *et al.* 2017; Behrens *et al.* 2020) but do not use the TBDT as the cell surface receptor. Pyocins S2 (White *et al.* 2017), SD2 (McCaughey *et al.* 2016b), and S5 (Behrens *et al.* 2020) use TBDTs for outer membrane translocation but CPA as their cell surface receptor. It appears that this is not the case of PyoG, since the *Δhur* mutant containing CPA is PyoG binding-incompetent, as indicated by fluorescence labeling studies (Figure 3-9). Moreover, PyoS1, a PyoG homolog, does not bind CPA *in vitro* (McCaughey *et al.* 2016b) and the LPS mutants of *P. aeruginosa* are sensitive to PyoG (Figure 3-8). Therefore, it is likely that Hur has a dual role in cell surface binding and outer membrane translocation of PyoG.

A major unknown in nuclease bacteriocin import is what happens to the toxin upon periplasm entry. The toxin might refold before transport across the cytoplasmic membrane in an FtsH-dependent fashion. Whether nuclease bacteriocins fold in the periplasm is currently unknown. It is possible that a periplasmic chaperone is involved, as in the case of colicin M (ColM). ColM kills cells by acting in the periplasm and inhibiting peptidoglycan synthesis. To do so, it requires a periplasmic chaperone FkpA (Hullmann *et al.* 2008). This might be specific only for bacteriocins that are active in the periplasm, and currently, there is no evidence that nuclease bacteriocins require chaperones. Future studies should explore this in more detail which might reveal additional proteins comprising the PyoG translocation machinery.

Structural studies of the PyoG-Hur or TonB1 complex could further help elucidate how this pyocin crosses the outer membrane. Attempts to crystalize these complexes were not successful. Future attempts to reveal the molecular detail of PyoG outer membrane translocation should also involve a cross-linking approach in order to map out the interaction sites between PyoG, Hur, and TonB1. Structural studies could also help elucidate the domain organisation of PyoG. The current domain organisation of PyoG (Figure 3-1) was deduced from the killing activity of chimeric PyoS1 molecules (Sano *et al.* 1993) and expression studies of domain-based constructs reported in this thesis (Figure 4-4, Figure 5-7).

7.2 Binding of Hur to hemin and PyoG

Iron is an essential nutrient for *P. aeruginosa* virulence and survival in hosts (Minadri *et al.* 2016). Therefore, iron importers are good antibiotic targets. To date, all characterized modular pyocins parasitize iron import pathways. For example, PyoS2 binds to FpvAI, the

transporter of ferripyoverdine, the iron-bound form of a major *P. aeruginosa* siderophore (White *et al.* 2017). The pore-former S5 binds to FptA, a receptor for another *P. aeruginosa* siderophore called pyochelin (Behrens *et al.* 2020). Out of 10 modular pyocin groups, receptors are known for 7 (Figure 1-5). In this study, this number is expanded by discovering the receptor for the S1 group. PyoG, the S1 group member, binds to Hur via a conserved N-terminal receptor binding domain. This discovery makes a contribution to our understanding of the diversity of pyocins and their receptors.

Hur is a TBDT that binds TonB1, homologous to hemin importers in other Gram-negative bacteria. In this work, the involvement of Hur in hemin import was confirmed by showing that it binds hemin *in vitro* (Figure 4-6). The exact mechanism of hemin import by Hur remains to be elucidated. From genomic organization of *hur*, and homology of its protein product to PhuR, it appears that this transporter functions without a hemophore. This would mean that Hur binds hemin directly to transport it into the periplasm, consistent with the data presented which shows binding of Hur to hemin. Binding of Hur to other potential heme-containing plasma proteins could not be detected. It is unlikely however that Hur binds only free hemin in the host, since free hemin levels are very low in mammalian tissues. Free hemin is toxic for humans, since it is a lipophilic molecule that intercalates in the membrane and impairs lipid bilayers and organelles (Kumar and Bandyopadhyay 2005). Therefore, it is more likely that Hur takes up hemin from a hemophore, either expressed by *P. aeruginosa* or by the host. This hemophore has yet to be identified, but it appears not to be hemoglobin, hemopexin or transferrin, based on pull-down data (Figure 4-7).

Hur, after HasAR and PhuR, is the third hemin acquisition system thus far identified in *P. aeruginosa*. Like HasA, Hur can trigger a signalling cascade, which in the presence of hemin

leads to the activation of a σ^{ECF} factor in the cytoplasm (Otero-Asman *et al.* 2019). It would be interesting to test if PyoG induced conformational changes in Hur that can similarly lead to the activation of this signalling cascade. In addition, it is not clear why *P. aeruginosa* has at least three different hemin acquisition systems. One possible reason is the importance of hemin as an iron source in the host, where it is necessary for one system to be able to complement the other, supported by higher Hur expression levels in the *ΔhasR* mutant of *P. aeruginosa* (Otero-Asman *et al.* 2019). Mammalian hosts have mechanisms to sequester free iron in the form of heme-containing proteins, providing nutritional immunity against *P. aeruginosa* (Iatsenko *et al.* 2020). As part of the host-pathogen arms race, it appears that *P. aeruginosa* has evolved numerous mechanisms for scavenging sequestered iron from the host, which also explains the diversity of hemin uptake systems. The three hemin acquisition systems of *P. aeruginosa* could be using different hemophores to scavenge hemin from different sources. HasR binds HasA, a hemophore produced by *P. aeruginosa*, which can take up hemin from plasma proteins (Letoffe *et al.* 1999). On the other hand, PhuR binds directly to hemoglobin, a hemohopre produced by the host (Smith and Wilks 2015). Therefore, it is possible that Hur uses yet another hemophore and expands the panel of hemin sources that *P. aeruginosa* can exploit.

Finally, in chapter 4 it was demonstrated that PyoG and hemin bind Hur in a competitive manner (Figure 7-1). Competition with the endogenous ligand has been described for other pyocin-receptor pairs. PyoS2 outcompetes siderophore ferripyoverdine for FpvAI binding and PyoS2 mimics the siderophore when binding the receptor (White *et al.* 2017). Similarly, ferric pyochelin and PyoS5 compete for FptA binding (Behrens *et al.* 2020). Competitive binding of PyoG and hemin to Hur indicates that both ligands occupy the same binding site, or PyoG binding to Hur causes hemin dissociation from a distinct binding site.

The molecular details of this mode of binding requires structural information, however attempts at crystallising Hur (MemGold, MemGold2, Morpheus, Morpheus2, MemTrans, MemChannel, MemPlus, MIDAS screens) have not been successful (data not shown). Therefore, different screens, or different methods (*in vivo* cross-linking, cryogenic electron microscopy), should be used to elucidate the structural basis of PyoG and hemin binding to Hur. Additionally, another pyocin, PaeM4, appears to be utilising Hur as its receptor. As in the case of PyoG, PaeM4 does not kill the *Δhur* mutant of *P. aeruginosa* and its killing activity is affected by iron (Ghequire & Ozturk 2018). It is not known if hemin and PaeM4 bind Hur in a competitive manner. The lack of sequence homology suggests that PyoG and PaeM4 might be binding Hur by different mechanisms. Structural data on the PaeM4-Hur complex could provide an answer to this question.

The competitive binding of PyoG and hemin demonstrates an important aspect to the possible clinical application of the pyocin. Hur expression is upregulated under iron starvation conditions (Figure 4-5) when hemin is the sole source of iron (Otero-Asman *et al.* 2019). These are the conditions that *P. aeruginosa* encounters in the host, where iron is bound to plasma proteins or as part of heme. Therefore, Hur is also upregulated in the host, as seen from expression profiles of *P. aeruginosa* isolated from human respiratory epithelia (Chugani & Greenberg, 2007). Therefore, PyoG is a protein antibiotic that targets a hemin acquisition system possibly involved in *P. aeruginosa* virulence. In future studies, it would be important to address the activity of PyoG in mammalian hosts.

7.3 Inner membrane translocation of PyoG

The inner membrane translocation step is a black box in nuclease bacteriocin import. It is not known which cell envelope proteins are involved, or which bacteriocin domains are required for translocation. Therefore, florescence labelling after trypsin treatment in *P. aeruginosa* spheroplasts was used to assess PyoG translocation across the inner membrane.

P. aeruginosa forms spheroplasts as a tolerance mechanism to β-lactam antibiotics, with the ability to regenerate the cell envelope after the antibiotic is removed. Spheroplasts, as seen under the electron microscope, have patches of the outer membrane still attached to the cell surface, and patches where the periplasm and the inner membrane are exposed to the cell surface (Monahan *et al.* 2014). To exclude the possibility that PyoG utilises receptor Hur and TonB1 present within outer membrane patches on spheroplasts, as a sole binding and translocation site, *Δhur* spheroplasts were generated (Figure 5-3). Fluorescence microscopy experiments with trypsin treatment of *Δhur* spheroplasts, showed that PyoG was still imported into cells in the absence of outer membrane receptor Hur (Figure 5-2), also confirming that the import of PyoG into spheroplasts requires periplasmic and inner membrane translocation proteins. Receptor-bypass has previously been described for other nuclease bacteriocins. Colicin E3 bypasses its receptor, BtuB, under osmotic shock conditions (Tilby *et al.* 1978). Similarly, nuclease pyocins S2, AP41 and the PyoG homolog, PyoS1, could kill resistant strains of *P. aeruginosa* under receptor bypass conditions (Sano *et al.* 1993).

Trypsin protection of fluorescent PyoG and PyoG$^{1\text{-}485}$ in PAO1 and *Δhur* spheroplasts indicates that the receptor-binding and translocation domain are sufficient for inner membrane translocation. However, the presented data do not provide direct evidence that the entire 1-485 region of PyoG gets imported into the cytoplasm. Previous studies on colicins

suggest that colicins D, E3 (Chauleau *et al.* 2011), E2, and E7 (Mora & Zamaroczy, 2014) undergo proteolytic processing during import. A cleavage site positioned a few amino-acids upstream of the cytotoxic domain (C-domain) was defined, and the C-domain could be fished out of the cell cytoplasm with the corresponding immunity protein. In this study, the cysteine to which AF488 is conjugated is at the C-terminus of PyoG$^{1\text{-}485}$. It is possible that the fluorophore-conjugated C-terminus gets imported into the cell, whilst the remainder of the protein gets degraded by trypsin. In future experiments, pull-downs of processed PyoG peptides from the *P. aeruginosa* cytoplasm should be performed to identify which fragments of the pyocin reach the bacterial cytoplasm.

Inner membrane proteins required for PyoG$^{1\text{-}485}$ to be protected from digestion with trypsin in spheroplast are FtsH and TonB1. FtsH has previously been associated with the import and processing of nuclease colicins (Walker *et al.* 2007; Chauelau *et al.* 2011; Mora & Zamaroczy 2014). In the trypsin protection assay, PyoG is protected from trypsin in intact, but not in spheroplasted cells of PAO1 *ΔftsH* (Figure 6-3). Therefore, FtsH is required for the inner membrane translocation step, but there is no evidence that PyoG directly interacts with FtsH. Therefore, there may be another protein required for the interaction to take place. For example, ColD requires LepB to be proteolytically cleaved in an FtsH-dependent manner (Chauleau *et al.* 2011). Alternatively, it could also be possible that the *ftsH* deletion has an indirect effect on the expression levels of proteins directly involved in PyoG import.

Interestingly, PyoG becomes active against *ΔftsH* if the first 255 residues, comprising the unstructured N-terminus and the receptor-binding domain, are replaced with the first 209 residues of PyoS2. This chimera has the same conserved Pyocin S domain as PyoG, and the same cytotoxic domain, indicating that the receptor-binding domain is responsible for the

FtsH dependency of PyoG. Additionally, this finding points out that PyoS2 has a different, FtsH independent pathway to cross the inner membrane.

TonB1 has previously been associated with outer membrane pyocin translocation, where it dislocates the plug domain of the receptor during pyocin import. In addition to binding to the receptor plug, TonB1 also binds a sequence in the pyocin N-terminus called the TonB box. Current models of pyocin import suggest that TonB1 binding is required for pyocin to be pulled through the receptor and into the periplasm (White *et al.* 2017; Behrens *et al.* 2020). The spheroplast labelling experiments conducted in this study suggest that TonB1 could also be implicated in inner membrane translocation since the requirement for this protein could not be bypassed in spheroplasts (Figure 5-8). This idea is supported by a similar finding in which a nuclease colicin, ColE2, was inactive against TonB deficient spheroplasts, whilst ColE1, a pore forming colicin, that does not translocate across the inner membrane, had activity against *ΔtonB* sphaeroplasts (Smarda *et al.* 2002). A possible role for TonB1 could be as a site for stable association of PyoG with the inner membrane, promoting interactions with other inner membrane proteins involved in transport and processing (Figure 7-2). It is not known if inner membrane translocation requires the proton motive force (PMF) as an energy source, which is coupled to TonB1. Attempts to test for PMF dependence by labelling *P. aeruginosa* with fluorescent PyoG in the presence of carbonyl cyanide m-chlorophenyl hydrazone ionophore were not successful. Currently, little is known about the mechanism by which TonB1 is coupled to the PMF in *P. aeruginosa*. It is suggested that, like in *E. coli*, this coupling occurs via the inner membrane helix of TonB1 (Zhao & Poole 2002). Indeed, swapping the inner membrane helix of TonB1 with the first helix of TetA disrupted PyoG killing activity and inner membrane transport, which indicates that TonB1 likely must be coupled to the PMF for PyoG to translocate across the inner membrane. In *E. coli*, specific point

mutations in this inner membrane helix of TonB result in decoupling from the ExbBD complex and thus the PMF. However, these point mutations do not affect the functionality of TonB1 in *P. aeruginosa* suggesting that the coupling mechanism between TonB1 and the PMF appears to be different between *E. coli* and *P. aeruginosa* (Zhao & Poole, 2002). Finally, TonB1 coupling to ExbBD in *P. aeruginosa* has still not been demonstrated experimentally. There are two copies of ExbBD encoded in the PAO1 genome, both of which are located on a different operon to *tonB1* (Shirley & Lamont, 2009). Future studies on the mechanistic details of how TonB1 couples to the PMF would help elucidate its role in pyocin import.

Two parts of PyoG have been identified as essential for inner membrane translocation: the unstructured N-terminus, and the Pyocin S domain. The deletion of the first 30 residues of PyoG leads to loss of translocation in normal and bypass conditions (Figure 5-9). This deletion also impaired the binding of PyoG to TonB1, as seen in a pull-down assay (Figure 5-8). Combined these results show that the first 30 residues of PyoG must contain the TonB1 binding box. This is supported by studies on PyoS2 (White *et al.* 2017) and PyoS5 (Behrens et al 2020) that show inhibition of outer membrane translocation with a TonB box deletion, and it is consistent with the model of outer membrane import in which TonB1 pulls the pyocin through the open conformation of the receptor.

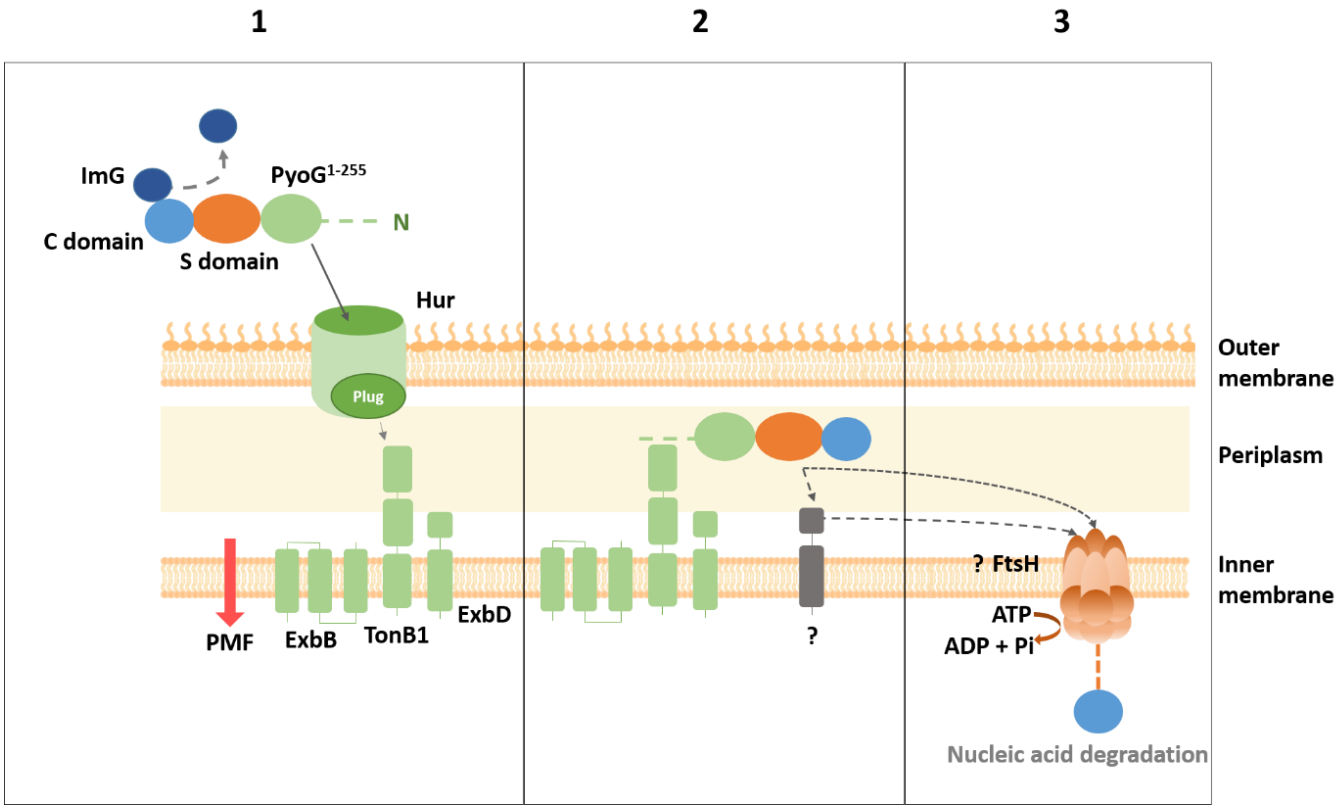

Figure 7-2. Inner membrane translocation of PyoG. Parts of PyoG which are required for its import into *P. aeruginosa* are: the unstructured N-terminus, the receptor binding domain, and the Pyocin S domain. The pyocin translocates the outer membrane exploiting Hur and TonB1 (1), as previously described (Atanaskovic *et al.* 2020). The first 255 residues of PyoG are sufficient for this translocation step. The inner membrane translocation step also requires the Pyocin S domain. The unstructured N-terminus of PyoG binds to TonB1, and this interaction is required for both outer and inner membrane translocation (2). After TonB1 binding in the periplasm, PyoG may interact with other periplasmic or inner membrane proteins required for its import into the cytoplasm. FtsH may act as a transporter of PyoG across the inner membrane (3). As in the case of nuclease colicins (Chauleau *et al.* 2011; Mora & Zamaroczy 2014), inner membrane transport may be coupled with proteolytic processing of PyoG.

Similar to other pyocins (White *et al.* 2017, Behrens *et al.* 2020), a construct comprised of the unstructured N-terminus and the receptor-binding domain of PyoG ($PyoG^{1-255}$), translocates across the outer membrane. However, this construct does not undergo inner membrane translocation. The absence of the Pyocin S domain in this construct suggests that it is likely that this domain has a function specific for inner membrane translocation, possibly forming interactions with the inner membrane translocation machinery. The importance of the S domain for pyocin translocation and thus killing activity, has also been proposed by other researchers. Sano *et al.* observed that the deletion of this domain leads to loss of killing activity in PyoS1, the PyoG homolog. Since the deletion of the S domain affected killing also under receptor bypass conditions, it was suggested that the S domain plays a role in translocation events taking place after receptor binding (Sano *et al.* 1993). Lack of trypsin protection for $PyoG^{1-255}$ in spheroplasts supports this hypotheisis, and links the S domain to the inner membrane translocation step.

Import of PyoG in intact and sphaeroplasted cells demonstrates that the inner membrane translocation step requires TonB1, FtsH, coupling to the unstructured N-terminus, and the Pyocin S domain of PyoG. Based on these findings, a model of inner membrane translocation of PyoG has been proposed (Figure 7-2). After translocation across the outer membrane, the PyoG N-terminus and the S domain associate with respective inner membrane proteins required for PyoG import. The binding of the N-terminus to TonB1 is likely the initiating step and is required for PyoG to interact with other components of the inner membrane translocon. One of these components is FtsH, which could transport and proteolytically process PyoG, but the direct involvement of FtsH in PyoG import has yet to be demonstrated. Other proteins may be required for import, such as a protein that recruits FtsH into the PyoG translocon and mediates the interaction between FtsH and the pyocin. Future

studies, such as transposon mutant screens for PyoG resistance or proximity labelling assays, should help expand the list of proteins involved in inner membrane transport of PyoG. Additionally, such studies should deploy also PyoS2, since this pyocin is not FtsH-dependent and is using a different route to cross the inner membrane.

7.4 Import of pyocin AP41 into *P. aeruginosa*

AP41 is a nuclease pyocin of *P. aeruginosa*. The structure of the AP41 DNase-immunity complex has been solved by Joshi *et al.* (PDB 4UHP), and the activity of the pyocin has been tested in a *P. aeruginosa* murine lung infection model (McCaughey *et al.* 2016b). Still, the import mechanism of this pyocin is unknown. Chapter VI details some advancements made in understanding which cell envelope components are required for AP41 killing activity.

Previous studies on AP41 tolerant mutants of *P. aeruginosa* suggested that the import of this pyocin might require the Tol system (Dennis *et al.* 1996). This report contrasts all previous studies on pyocins, which show they use the Ton system to energise their import into cells (McCaughey *et al.* 2016a; White *et al.* 2017; Behrens *et al.* 2020). Colicins can exploit either the Tol or the Ton system (Kleanthous 2010). Both systems are used to drive the entry of modular bacteriocins across the outer membrane. A conserved feature for both Ton and Tol is a protein which extends through the periplasm to interact with outer membrane proteins. In case of the Ton system, TonB applies mechanical force to the conserved plug domain of TBDTs in conjunction with the PMF and its partner stator proteins, ExbB and ExbD. In case of the Tol-Pal system, TolA extends through the periplasm to exert mechanical force on TolB by an analogous process to that used by Ton, but involving its specific PMF-linked stator proteins TolQ and TolR. The force exerted on TolB is required for the localised

deposition of the peptidoglycan-binding lipoprotein Pal at the septum during cell division (Szczepaniak *et al.* 2020). Both TolA and TolB are exploited by group A colicins, which enables their passage through outer membrane porins (Cascales *et al.* 2007). Therefore, Tol-Pal could be implicated in the import of modular pyocins. Using a biochemical approach with purified protein, the present work could find no evidence of an interaction between AP41 with either TolA or TolB (Figure 6-7). Instead, this pyocin requires TonB1 for killing (Figure 6-6). *ΔtonB1* mutants of *P. aeruginosa* are resistant to AP41 and the pyocin binds to TonB1 *in vitro* with nanomolar affinity (Figure 6-9). The first 30 residues of AP41 are involved in TonB1 binding (Figure 6-8, 6-9). This region was also associated with TonB1 binding in pyocins S2 (White *et al.* 2017) and S5 (Behrens *et al.* 2020). AP41, PyoS2 and PyoS5 have 3 conserved residues in this region – $G^{9}SM^{11}$ (Figure 6-10). In PyoS5, residues $S^{10}MV^{12}$, comprise the TonB box (Behrens *et al.* 2020). In PyoS2, the TonB box appears to be further downstream ($M^{11}VITH^{15}$) (White *et al.* 2017). Therefore, it is likely that the TonB box of AP41 is also positioned around these three residues. The K_d of AP41-TonB1 complex is lower than in the case of PyoS2 and PyoS5, although the biological meaning of this difference is still unclear. It could be that the higher affinity AP41 for TonB1 might compensate for lower affinity binding between AP41 and its outer membrane receptor. Finally, the data presented do not explain why *tol* mutants of *P. aeruginosa* were insensitive to AP41 (Dennis *et al.* 1996). It is possible that the deletion of *tol* has secondary effects on the composition of the cell envelope, which in turn lead to AP41 resistance. Since *tol* genes are essential for *P. aeruginosa* growth (Lo Sciuto *et al.* 2014), it may be that the strain isolated by Dennis *et al.* had some secondary suppressor mutations, that also affected AP41 sensitivity. It is also possible that AP41 can bind both Tol and Ton proteins during translocation but this was not detected under the experimental conditions

used in the present study. However, bacteriocins typically only use the Ton or the Tol-Pal systems to drive their entry into cells, not both (Cascales *et al.* 2007).

The present work also found that the killing activity of AP41, like that of nuclease colicins (Walker *et al.* 2007) and PyoG (Atanaskovic *et al.* 2020), depends on the AAA+ ATPase/protease FtsH. The exact involvement of FtsH in nuclease pyocin import, and whether it is direct or indirect, remains to be established.

Although this work failed to identify definitively outer membrane components of the AP41 translocon several commonly found in the import pathways of bacteriocins can be ruled out. LPS is not required for AP41 import. *P. aeruginosa* mutants that do not produce CPA and/or OSA are sensitive to the pyocin (Figure 6-11 A). This contrasts pyocins S2 (McCaughey *et al.* 2016a), S5 (Behrens *et al.* 2020), and L1 (McCaughey *et al.* 2014), all of which exploit CPA as their outer membrane receptor. In addition, AP41 did not bind CPA in ITC experiments (McCaughey *et al.* 2016a). It is therefore likely that the AP41 receptor is a protein rather than LPS. Pull-downs using the AP41-ImAP41 complex as bait failed to identify such a receptor. It can be further concluded that the AP41 receptor/translocator is not a TonB dependent receptor, as is the case of other pyocins (McCaughey *et al.* 2016a; White *et al.* 2017; Behrens *et al.* 2020; Atanaskovic *et al.* 2020). All of the individual TBDT mutants tested (Table 1-1) were sensitive to AP41, which does not however rule out the possibility that AP41 exploits more than one TBDT.

Deletion of the gene for the outer membrane porin, OprH, leads to AP41 resistance (Figure 6-11 B), but binding of OprH to AP41 *in vitro* could not be detected (Figure 6-14). The *oprH* gene is in an operon with *phoP* and *phoQ*. PhoPQ is a two-component regulatory system that is induced upon Mg^{2+} starvation and that directly upregulates the production of OprH

(Olaitan *et al.* 2014). Mutations in PhoPQ or Mg^{2+} starvation had no impact on AP41 killing activity (data not shown). Currently, it is not clear how the deletion of OprH results in AP41 resistance. This porin binds lung lectins and is involved in host-pathogen interactions. It also has a structural role in the cell envelope, through its interaction with LPS which is implicated in outer membrane stability (Kucharska *et al.* 2016). The deletion of OprH can thus be linked to alterations in outer membrane composition and stability, causing AP41 resistance as a secondary consequence. In support of this, OprH has been linked with resistance to two LPS-binding antibiotics: polymyxin B (Olaitan *et al.* 2014) and gentamycin (Wei *et al.* 2011). These two antibiotics kill the cell via different mechanisms. Polymyxin B destabilizes LPS and causes increased permeability of the envelope. Gentamycin binds the 30S ribosomal subunit and interferes with protein translation. Despite having different cellular targets, both antibiotics have a similar uptake mechanism. They form electrostatic interactions with the LPS phosphate groups, displace cations which are responsible for cross bridging and stabilization of the lipid components of the outer membrane, and destabilize the outer membrane (Krause *et al.* 2016). *oprH* upregulation somehow prevents LPS destabilization and leads to polymyxin B and gentamycin resistance. On the other hand, deletion of *oprH* causes resistance to AP41, which is not an LPS binding antibiotic. In conclusion, the deletion of *oprH* can affect LPS stability, and possibly LPS composition in *P. aeruginosa*. Therefore, it is also possible that the mechanism of AP41 resistance is the same for *tol-pal* and the *ΔoprH* mutants, since the Tol-Pal system also impacts outer membrane stability (Lazzaroni *et al.* 1999; Szczepaniak *et al.* 2020).

Another candidate for the outer membrane receptor/translocator of AP41 is the filamentous hemagglutinin system (FHA). FHA is involved in CDI, a competition mechanism between bacteria that involves direct cell-cell contact (Merci *et al.* 2016). There are two

copies of FHA in the PAO1 genome. Each copy is composed of a filamentous hemagglutinin (FhaB1,2) and its transporter (FhaC1,2). FhaB contains several hemagglutinin repeats and extends from the cell surface into the extracellular environment to deliver a C-terminal cytotoxic domain to neighbouring bacterial cells (Melvin *et al.* 2017). FhaC forms a β-barrel in the outer membrane for FhaB export. FhaB could serve as the AP41 receptor, since point mutations in this gene have been discovered in AP41 resistant mutants (Mosbahi & Walker, unpublished data), yet transposon mutants of FhaB1 and 2 are sensitive to AP41 (Figure 6-15). Transposon insertions in *ΔfhaB1,2* were towards the C-terminus. Due to the repetitive nature of the FhaB structure, it is possible that FhaB is still produced in these mutants. It is also possible that one copy of *fhaB* complements the other. Attempts at deleting the entire *fhaB* gene have been made by the Walker laboratory, but were unsuccessful due to the size and the repetitive nature of the gene. On the other hand, transposon mutants of the *fhaC* genes show altered sensitivity to AP41. *ΔfhaC1* is completely resistant, and *ΔfhaC2* has decreased sensitivity to the pyocin. Therefore, it is possible that FhaC plays a role as an outer membrane translocator for AP41. This would mean that FhaC is involved in both protein export and import. Future studies on the involvement of FhaC in AP41 import are currently the focus of work in the Walker Laboratory.

Based on the data presented in chapter 4, a model of pyocin AP41 import is proposed (Figure 7-3). Pyocin AP41 binds to a yet-to-be-identified outer membrane transporter, the current candidate being a filamentous hemagglutinin transporter FhaC. Binding of AP41 to FhaC may also involve an interaction with FhaB, a filamentous hemagglutinin being exported by FhaC. The import of AP41 into the periplasm requires TonB1, that AP41 binds via its unstructured N-terminus. Import of AP41 into the cytoplasm requires FtsH, but direct involvement of FtsH in pyocin import has yet to be demonstrated.

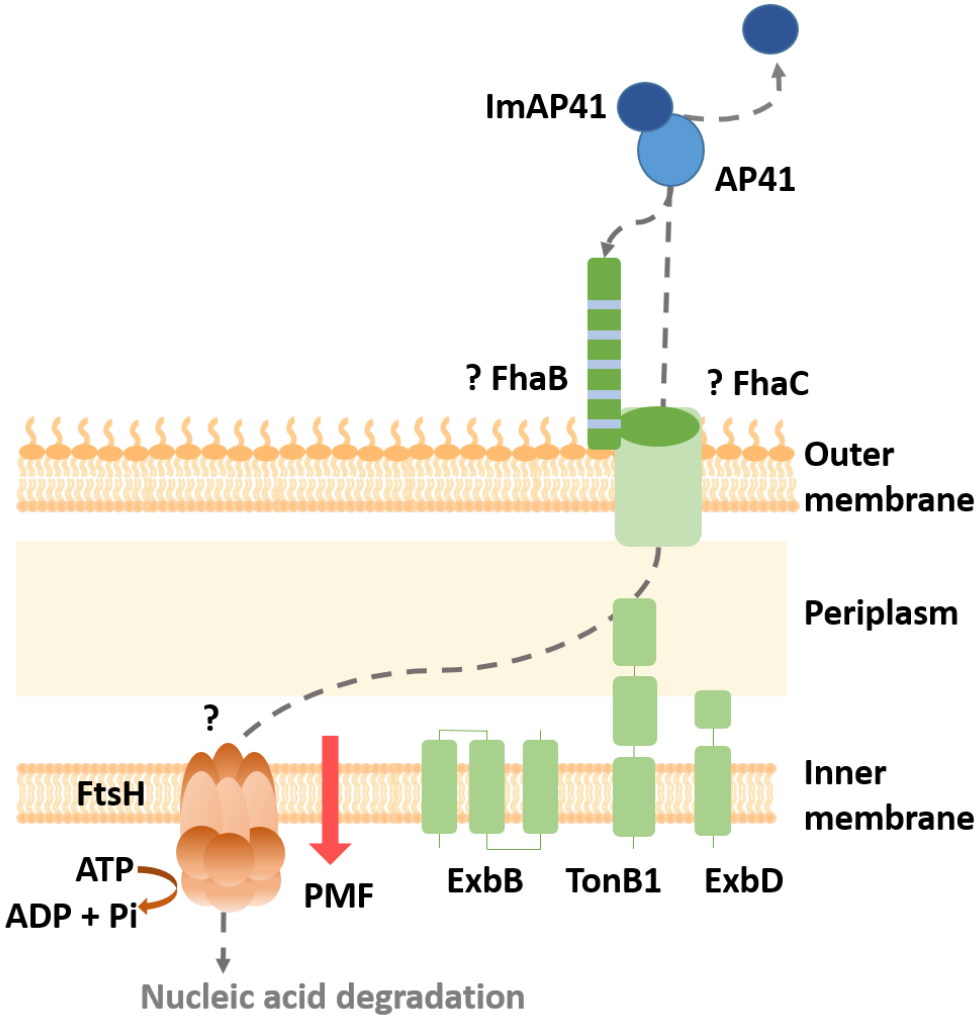

Figure 7-3. Model of pyocin AP41 import into *P. aeruginosa* cells. AP41 binds to an unknown outer membrane receptor/translocator. A candidate for the AP41 transporter is the filamentous hemagglutinin transporter FhaC, but the interaction between AP41 and FhaC has yet to be proven experimentally. Binding of AP41 to FhaC might also require FhaB, the filamentous hemagglutinin which FhaC secretes to the cell surface. Like in the case of nuclease colicins (Duché *et al.* 2006), the immunity protein dissociates on the cell surface, which has to be proven experimentally. The N-terminus of AP41 is then pulled by TonB1 into the periplasm. Translocation into the cytoplasm depends on the AAA+ATPase/protease FtsH, which may serve as the inner membrane translocator for pyocin AP41.

8. Appendix

Appendix 1 – Sequence alignments

A

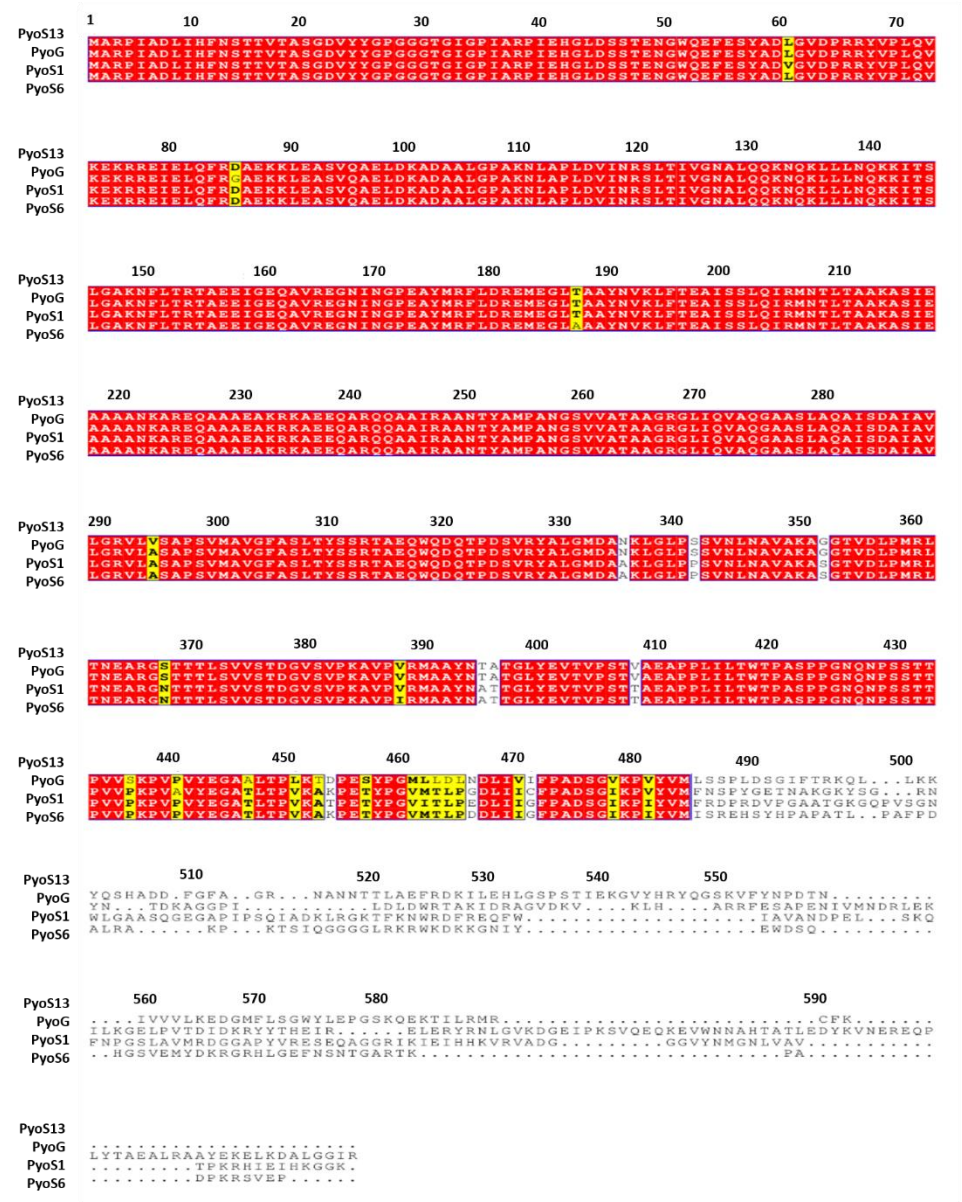

B

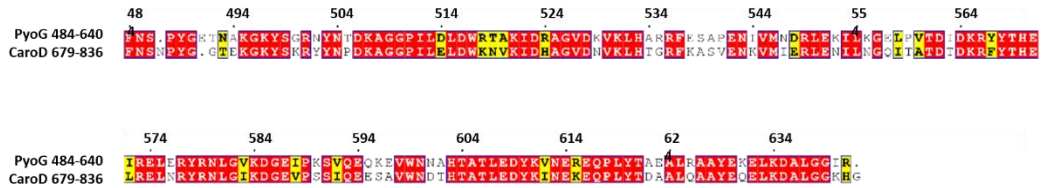

C

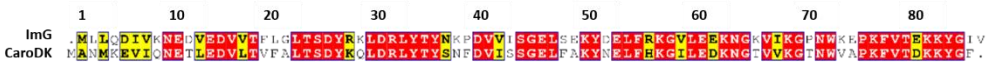

Appendix F-1. Pyocin G has an N-terminal region conserved amongst other S1-group pyocins, and a distinct cytotoxic domain. A - Alignment of representative sequences of S1-group pyocins. B - alignment of the cytotoxic domain of pyocin G and carocin D. C – alignment of the PyoG (*imG*) and carocin D (*caroDI*) immunity protein.

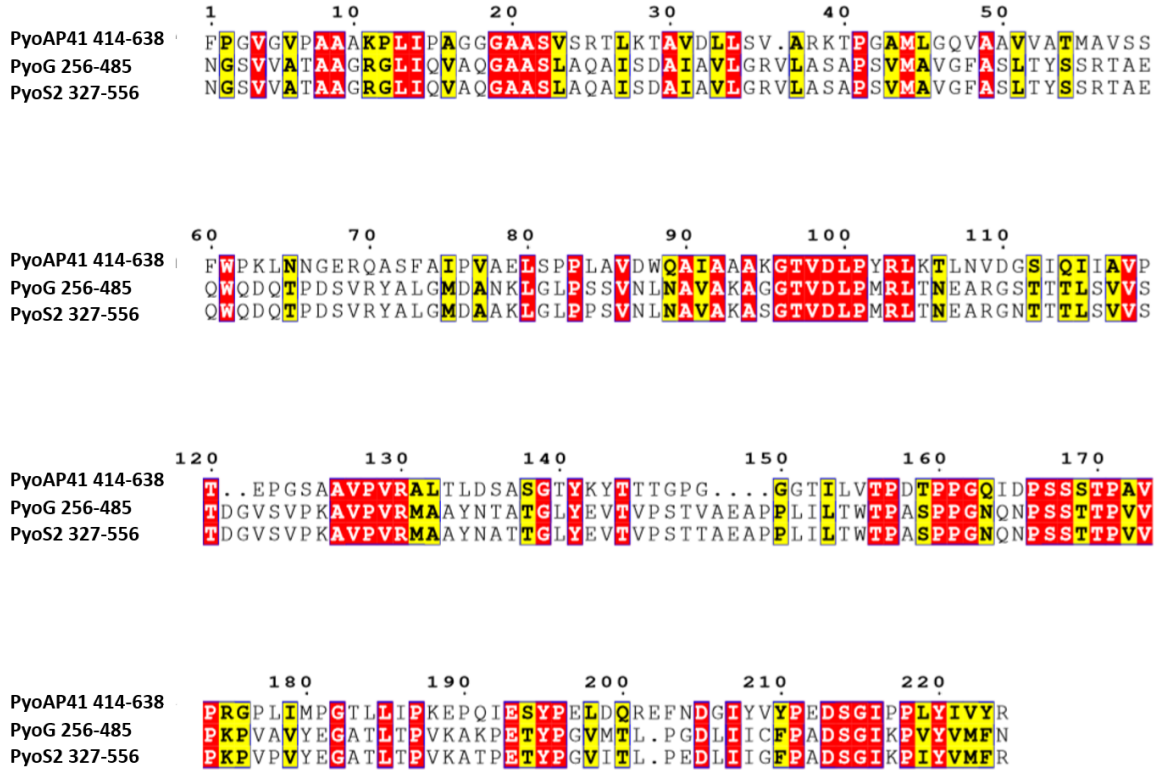

Appendix F-2. Alignment of the pyocin S domain (translocation domain) of pyocins AP41, S2, and G.

Appendix 2 – sequences of proteins used in this study

Pyocin G

MARPIADLIHFNSTTVTASGDVYYGPGGGTGIGPIARPIEHGLDSSTENGWQEFESYADLGVDPRRYVPL
QVKEKRREIELQFRGAEKKLEASVQAELDKADAALGPAKNLAPLDVINRSLTIVGNALQQKNQKLLLNQK
KITSLGAKNFLTRTAEEIGEQAVREGNINGPEAYMRFLDREMEGLTAAYNVKLFTEAISSLQIRMNTLTAA
KASIEAAAANKAREQAAAEAKRKAEEQARQQAAIRAANTYAMPANGSVVATAAGRGLIQVAQGAASL
AQAISDAIAVLGRVLASAPSVMAVGFASLTYSSRTAEQWQDQTPDSVRYALGMDANKLGLPSSVNLNA
VAKAGGTVDLPMRLTNEARGSTTTLSVVSTDGVSVPKAVPVRMAAYNTATGLYEVTVPSTVAEAPPLILT
WTPASPPGNQNPSSTTPVVPKPVAVYEGATLTPVKAKPETYPGVMTLPGDLIICFPADSGIKPVYVMFNS
PYGETNAKGKYSGRNYNTDKAGGPILDLDWRTAKIDRAGVDKVKLHARRFESAPENIVMNDRLEKILKG
ELPVTDIDKRYYTHEIRELERYRNLGVKDGEIPKSVQEQKEVWNNAHTATLEDYKVNEREQPLYTAEALRA
AYEKELKDALGGIR*

Immunity protein G

MLLQDIVKNEDVEDVVTFLGLTSDYRKLDRLYTYNKPDVVISGELSEKYDELFRKGVLEEKNGKVIKGPNW
KEPKFVTEKKYGIV*

Pyocin S2

MAVNDYEPGSMVITHVQGGGRDIIQYIPARSSYGTPPFVPPGPSPYVGTGMQEYRKLRSTLDKSHSELKK
NLKNETLKEVDELKSEAGLPGKAVSANDIRDEKSIVDALMDAKAKSLKAIEDRPANLYTASDFPQKSESMY
QSQLLASRKFYGEFLDRHMSELAKAYSADIYKAQIAILKQTSQELENKARSLEAEAQRAAAEVEADYKARK
ANVEKKVQSELDQAGNALPQLTNPTPEQWLERATQLVTQAIANKKKLQTANNALIAKAPNALEKQKAT
YNADLLVDEIASLQARLDKLNAETARRKEIARQAAIRAANTYAMPANGSVVATAAGRGLIQVAQGAASL
AQAISDAIAVLGRVLASAPSVMAVGFASLTYSSRTAEQWQDQTPDSVRYALGMDAAKLGLPPSVNLNA

VAKASGTVDLPMRLTNEARGNTTTLSVVSTDGVSVPKAVPVRMAAYNATTGLYEVTVPSTTAEAPPLILT
WTPASPPGNQNPSSTTPVVPKPVPVYEGATLTPVKATPETYPGVITLPEDLIIGFPADSGIKPIYVMFRDPR
DVPGAATGKGQPVSGNWLGAASQGEGAPIPSQIADKLRGKTFKNWRDFREQFWIAVANDPELSKQFN
PGSLAVMRDGGAPYVRESEQAGGRIKIEIHHKVRIADGGGVYNMGNLVAVTPKRHIEIHKGGK*

Pyocin AP41

MSDVFDLGSMTTVATATGQYSFYTPPPPTPIPYLTYIARPGINKFDLPEGAKIKDLIKRYQYIGSQIPAAIMI
RGVQEEIKKSTNTALANVGAIVDGELAYLASQKKEKLNPAEATPLQMASAEKAAAVELLASKQKELADAR
TIANAFFGYDPLTVNYVNVMNEIYGRREDKDFSFDNWSKSYSAAQKIRLIEAKISVLNSRSSALDGKVAEL
TRLQRLEDAQHAAEAARQTEAERLAQEQRQAEARRQAEEARRQAEAQRQAELQRLAEAEAKRVAEAE
KKRQDEINARLQAIVVSESEAKRIEEIYKRLEEQDKISNPTVTTPPAVDAGSRVDDALAHTGTRVTSGGET
GATGGSGRDVDTGTGQGGITARPVDVGSVSIPDRRDPKIPDQPRRDLGSLVPTFPDFPTFPSFPGVGVP
AAAKPLIPAGGGAASVSRTLKTAVDLLSVARKTPGAMLGQVAAVVATMAVSSFWPKLNNGERQASFAI
PVAELSPPLAVDWQAIAAAKGTVDLPYRLKTLNVDGSIQIIAVPTEPGSAAVPVRALTLDSASGTYKYTTT
GPGGGTILVTPDTPPGQIDPSSSTPAVPRGPLIMPGTLLIPKEPQIESYPELDQREFNDGIYVYPEDSGIPPL
YIVYRDPRDEPGVATGNGQPVTGNWLAGASQGDGVPIPSQIADQLRGKEFKSWRDFREQFWMAVSK
DPSALENLSPSNRYFVSQGLAPYAVPEEHLGSKEKFEIHHVVPLESGGALYNIDNLVIVTPKRHSEIHKELKL
KRKEK*

Immunity AP41

MDIKNNLSDYTESEFLEIIEEFFKNKSGLKGSELEKRMDKLVKHFEEVTSHPRKSGVIFHPKPGFETPEGIVK
EVKEWRAANGLPGFKAGLEHHHHHH*

TonB1

MSPQPSRSPDRFSLAALAEDHPTAPAQGDESESLPCVNAQRGEPNLRVVDCSGARRDEEVAVEEVLIPY
AHGSDPEDVPGEPPKSRWWLSSGAAVAMHVAIIGALVWVMPTPAELNLGHGELPKTMQVNFVQLEK
KAEPTPQPPAAAPEPTPPKIEEPKPEPPKPKPVEKPKPKPKPKPKPVENAIPKAKPKPEPKPKPEPEPSTEAS
SQPSPSSAAPPPAPTVGQSTPGAQTAPSGSQGPAGLPSGSLNDSDIKPLRMDPPVYPRMAQARGIEGR
VKVLFTITSDGRIDDIQVLESVPSRMFDREVRQAMAKWRFEPRVSGGKIVARQATKMFFFKIEKRR*

Hur

MTLPFTRAAWRPLCSAAVLGAALWAAGASAAERRFDLPAQPLAASLSRLAQQAQVQVLFDESLLRGLR
APALSGSYGVREALERLLVGSELELVEAGGGYVVRRRQVDAYSDNALQLDAQTIVGNGREVDASNVGRS
TLTRRDIERQQADNIPSLLQTLPGVTMGGSPKPGGQTTNIWGLGDAEDVPYTLDGAQKSGFERYQQGT
VFIEPEMIKRIEVEKGPHSVFTGNGGFGGTVHMETKDAPDLLREGRDVGAMLKYGYHSNDQQKIYSGA
VFGRSEDRRVDALLYLNGRDGRDMKLADNLPLSPTDYPINPKRLPNSAQDEKTGLFKLNLHPTEEHDLGF
TYLRSKSSRWTPFSASSYPTPPSQWTIDRYGYELGLTRLLAHRDTTDTTWTGKYNYHPLDNPWIDLQLSY
SDARTEQLDRREDTAFYQLATGGKRMRTEYQDKVLELRNTSRFDTGALQHELTLGAALHKHKRDILMH
MPGKTYETPRYNYGWLQPAFMPAGKQDTQSFYIQDAITYGSLTVTPSMRFDSVRNDGQANLAPIYDNP
KLGHDYRAQTYSGWSPRLSVFWTATPNLAFFADYTETWRAPVIDEQYEVQNSSTIGGSSRDLDAERIHAI
RGGSVINLPDLLVAGDSLQIRTTLFQNRIKDEIFRTRSVGCRQQSIDNGSIGGSCGDMLPLSNYRNLPGLTI
KGFEIESFYDSQRLFGSLSYSWMTGKHDGAYSNPWGPNVWARDIPPPKWVAMLGLKVPEWDAKLGW
QGEFVRKTDRLPSDRYSGGMGTGSGDIYWDHAANDSYDTHRLFAEWVPAKLGLKDTRIDFTVDNLFNR
SYRQPLGGDLVYSQGRNAKISVTQFF*

OprH

MKALKTLFIATALLGSAAGVQAADNFVGLTWGETSNNIQKSKSLNRNLNSPNLDKVIDNTGTWGIRAG
QQFEQGRYYATYENISDTSSGNKLRQQNLLGSYDAFLPIGDNNTKLFGGATLGLVKLEQDGKGFKRDSD
VGYAAGLQAGILQELSKNASIEGGYRYLRTNASTEMTPHGGNKLGSLDLHSSSQFYLGANYKF*

FtsH

MAKNLILWLIIAAVLVTVMNNFSSPSEPQTLNYSDFIQQVKDGKVERVTVDGYVITGKRSDGDTFKTIRPA
IQDNGLIGDLVNNNVVVEGKQPEQQSIWTQLLVASFPILVIIAVFMFFMRQMQGGGGGRGGPMSFGK
SKARLLSEDQVKTTFADVAGCDEAKEEVSELVEFLRDPGKFQRLGGRIPRGVLMVGPPGTGKTLLAKAIA
GEAKVPFFTISGSDFVEMFVGVGASRVRDMFDQAKKHAPCIIFIDEIDAVGRHRGAGLGGGHDEREQTL
NQLLVEMDGFEMNDGIIVIAATNRPDVLDPALLRPGRFDRQVVVGLPDIRGREQILKVHMRKVPLGDH
VDPAVIARGTPGFSGADLANLVNEASLFAARSNKRIVDMREFELAKDKIMMGAERKTMVMSEKEKRNT
AYHEAGHAIVGRLVPEHDPVYKVSIIPRGRALGVTMFLPEEDRYSLSKRALESQICSLFGGRIAEEMTLGFE
GVTTGASNDIMRATQLARNMVTKWGLSEKLGPLMYAEEEGEVFLGRSAGSQHANVSGETAKMIDQEV
RRIIDDCYGTAKRLLDENRDKLEMMADALMKYETIDSDQIDDIMAGRVPREPRDWQGGSGTGTPPANL
EESGRRENTPPIGGPAGEH*

9. References

Almagro Armenteros JJ, Tsirigos KD, Sønderby CK, Petersen TN, Winther O, Brunak S, von Heijne G, Nielsen H. 2020. SignalP 5.0 improves signal peptide predictions using deep neural networks. *Nat Biotechnol* **37**:420-423. doi: 10.1038/s41587-019-0036-z.

Andolina G, Bencze LC, Zerbe K, Müller M, Steinmann J, Kocherla H, Mondal M, Sobek J, Moehle K, Malojčić G, Wollscheid B, Robinson JA. 2018. A Peptidomimetic Antibiotic Interacts with the Periplasmic Domain of LptD from *Pseudomonas aeruginosa*. *ACS Chem Biol* **13**:666-675. doi: 10.1021/acschembio.7b00822.

Ankenbauer RG, Quan HN. 1994. FptA, the Fe(III)-pyochelin receptor of *Pseudomonas aeruginosa*: a phenolate siderophore receptor homologous to hydroxamate siderophore receptors. *J Bacteriol* **176**:307-19.

Ankenbauer RG, Quan HN. 1994. FptA, the Fe(III)-pyochelin receptor of *Pseudomonas aeruginosa*: a phenolate siderophore receptor homologous to hydroxamate siderophore receptors. *J Bacteriol* **176**:307-19. doi: 10.1128/jb.176.2.307-319.1994.

Atanaskovic I, Kleanthous C. 2019. Tools and Approaches for Dissecting Protein Bacteriocin Import in Gram-Negative Bacteria. *Front Microbiol* **10**:646. doi: 10.3389/fmicb.2019.00646.

Atanaskovic I, Mosbahi K, Sharp C, Housden NG, Kaminska R, Walker D, Kleanthous C. 2020. Targeted Killing of *Pseudomonas aeruginosa* by Pyocin G Occurs via the Hemin Transporter Hur. *J Mol Biol* doi: 10.1016/j.jmb.2020.04.020.

Azam MW, Khan AU. 2019. Updates on the pathogenicity status of *Pseudomonas aeruginosa*. *Drug Discov Today* **24**:350-359. doi: 10.1016/j.drudis.2018.07.003.

Barreteau H, Tiouajni M, Graille M, Josseaume N, Bouhss A, Patin D, Blanot D, Fourgeaud M, Mainardi JL, Arthur M, van Tilbeurgh H, Mengin-Lecreulx D, Touzé T. 2012. Functional and structural characterization of PaeM, a colicin M-like bacteriocin produced by *Pseudomonas aeruginosa*. *J Biol Chem* **287**:37395-405. doi: 10.1074/jbc.M112.406439.

Basta DW, Angeles-Albores D, Spero MA, Ciemniecki JA, Newman DK. 2020. Heat-shock proteases promote survival of *Pseudomonas aeruginosa* during growth arrest. *Proc Natl Acad Sci U S A* **117**:4358-4367. doi: 10.1073/pnas.1912082117.

Baysse C, Meyer JM, Plesiat P, Geoffroy V, Michel-Briand Y, Cornelis P. 1999. Uptake of pyocin S3 occurs through the outer membrane ferripyoverdine type II receptor of *Pseudomonas aeruginosa*. *J Bacteriol* **181**:3849-51.

Beare PA, For RJ, Martin LW, Lamont IL. 2003. Siderophore-mediated cell signalling in *Pseudomonas aeruginosa*: divergent pathways regulate virulence factor production and siderophore receptor synthesis. *Mol Microbiol* **47**:195-207.

Behrens H, Six A, Wlker D, Kleanthous C. 2017. The Therapeutic Potential of Bacteriocins as Protein Antibiotics. *Emerg Top Life Sci* **1**:65–74. doi.org/10.1042/ETLS20160016

Behrens HM, Lowe ED, Gault J, Housden NG, Kaminska R, Weber TM, Thompson CMA, Mislin GLA, Schalk IJ, Walker D, Robinson CV, Kleanthous C. 2020. Pyocin S5 Import into *Pseudomonas aeruginosa* Reveals a Generic Mode of Bacteriocin Transport. *mBio* **11**: e03230-19. doi: 10.1128/mBio.03230-19.

Benedetti H, Frenette M, Baty D, Knibiehler M, Pattus F, Lazdunski C. 1991. Individual domains of colicins confer specificity in colicin uptake, in pore-properties and in immunity requirement. *J Mol Biol*. **217**:429-39. doi: 10.1016/0022-2836(91)90747-t.

Bieniossek C, Niederhauser B, Baumann UM. 2009. The crystal structure of apo-FtsH reveals domain movements necessary for substrate unfolding and translocation. *Proc Natl Acad Sci U S A* **106**:21579-84. doi: 10.1073/pnas.0910708106.

Bleves S, Viarre V, Salacha R, Michel GP, Filloux A, Voulhoux R. 2010. Protein secretion systems in *Pseudomonas aeruginosa*: A wealth of pathogenic weapons. *Int J Med Microbiol* **300**:534-43. doi: 10.1016/j.ijmm.2010.08.005.

Braun V. 1995. Energy-coupled transport and signal transduction through the gram-negative outer membrane via TonB-ExbB-ExbD-dependent receptor proteins. *FEMS Microbiol Rev* **16**:295-307.

Cascales E, Buchanan SK, Duché D, Kleanthous C, Lloubès R, Postle K, Riley M, Slatin S, Cavard D. 2007. Colicin biology. *Microbiol Mol Biol Rev* **71**:158-229.

Cassin EK, Tseng BS. 2019. Pushing beyond the Envelope: the Potential Roles of OprF in *Pseudomonas aeruginosa* Biofilm Formation and Pathogenicity. *J Bacteriol* **201**: e00050-19. doi: 10.1128/JB.00050-19.

Celia H, Botos I, Ni X, Fox T, De Val N, Lloubes R, Jiang J, Buchanan SK. 2019. Cryo-EM structure of the bacterial Ton motor subcomplex ExbB-ExbD provides information on structure and stoichiometry. *Commun Biol*. **2**:358. doi: 10.1038/s42003-019-0604-2.

Celia H, Noinaj N, Buchanan SK. 2020. Structure and Stoichiometry of the Ton Molecular Motor. *Int J Mol Sci* **21**:375. doi: 10.3390/ijms21020375.

Chauleau M, Mora L, Serba J, de Zamaroczy M. 2011. FtsH-dependent processing of RNase colicins D and E3 means that only the cytotoxic domains are imported into the cytoplasm. *J Biol Chem* **286**:29397-407. doi: 10.1074/jbc.M111.242354.

Chevalier S, Bouffartigues E, Bodilis J, Maillot O, Lesouhaitier O, Feuilloley MGJ, Orange N, Dufour A, Cornelis P. 2017. Structure, function and regulation of *Pseudomonas aeruginosa* porins. *FEMS Microbiol Rev* **41**:698-722. doi: 10.1093/femsre/fux020.

Chimento DP, Kadner RJ, Wiener MC. 2005. Comparative structural analysis of TonB-dependent outer membrane transporters: implications for the transport cycle. *Proteins* **59**:240-51.

Chugani S, Greenberg EP. 2007. The influence of human respiratory epithelia on *Pseudomonas aeruginosa* gene expression. *Microb Pathog* **42**:29-35.

Cornelis P, Dingemans J. 2013. *Pseudomonas aeruginosa* adapts its iron uptake strategies in function of the type of infections. *Front Cell Infect Microbiol* **14**:75. doi: 10.3389/fcimb.2013.00075.

Cotter PD. 2014. An 'Upp'-turn in bacteriocin receptor identification. *Mol Microbiol* **92**:1159-63. doi: 10.1111/mmi.12645.

Cuiv PO, Clarke P, O'Connell M. 2006. Identification and characterization of an iron-regulated gene, *chtA*, required for the utilization of the xenosiderophores aerobactin, rhizobactin 1021 and schizokinen by *Pseudomonas aeruginosa*. *Microbiology*. **152**:945-54.

Cuiv PO, Keogh D, Clarke P, O'Connell M. 2007. FoxB of *Pseudomonas aeruginosa* functions in the utilization of the xenosiderophores ferrichrome, ferrioxamine B, and schizokinen: evidence for transport redundancy at the inner membrane. *J Bacteriol* **189**:284-7. doi: 10.1128/JB.01142-06.

de Chial M, Ghysels B, Beatson SA, Geoffroy V, Meyer JM, Pattery T, Baysse C, Chablain P, Parsons YN, Winstanley C, Cordwell SJ, Cornelis P. 2003. Identification of type II and type III pyoverdine receptors from *Pseudomonas aeruginosa*. *Microbiology* **149**:821-831. doi: 10.1099/mic.0.26136-0.

Deme JC, Johnson S, Vickery O, Aron A, Monkhouse H, Griffiths T, James RH, Berks BC, Coulton JW, Stansfeld PJ, Lea SM. 2020. Structures of the stator complex that drives rotation of the bacterial flagellum. Nat Microbiol. **5**:1553-1564. doi: 10.1038/s41564-020-0788-8.

Denayer S, Matthijs S, Cornelis P. 2007. Pyocin S2 (Sa) kills *Pseudomonas aeruginosa* strains via the FpvA type I ferripyoverdine receptor. *J Bacteriol* **189**:7663-8. doi: 10.1128/JB.00992-07.

Dennis JJ, Lafontaine ER, Sokol PA. 1996. Identification and characterization of the *tolQRA* genes of *Pseudomonas aeruginosa*. *J Bacteriol* **178**:7059-68. doi: 10.1128/jb.178.24.7059-7068.1996.

Desuzinges-Mandon E, Arnaud O, Martinez L, Huche F, Di Pietro A, Falson P. 2010. ABCG2 transports and transfers heme to albumin through its large extracellular loop. *J Biol Chem* **285**:33123-33. doi: 10.1074/jbc.M110.139170.

Douzi B, Trinh NTT, Michel-Souzy S, Desmyter A, Ball G, Barbier P, Kosta A, Durand E, Forest KT, Cambillau C, Roussel A, Voulhoux R. 2017. Unraveling the Self-Assembly of the *Pseudomonas aeruginosa* XcpQ Secretin Periplasmic Domain Provides New Molecular Insights into Type II Secretion System Secreton Architecture and Dynamics. *mBio* **8**: e01185-17. doi: 10.1128/mBio.01185-17.

Dreier J, Ruggerone P. 2015. Interaction of antibacterial compounds with RND efflux pumps in *Pseudomonas aeruginosa*. *Front Microbiol* **6**:660. doi: 10.3389/fmicb.2015.00660.

Duché D, Frenkian A, Prima V, Lloubès R. 2006. Release of immunity protein requires functional endonuclease colicin import machinery. *J Bacteriol*. **188**:8593-8600. doi:10.1128/JB.00941-06.

ECDC. 2015. Antimicrobial Resistance Surveillance in Europe 2015, ECDC

Eddy SR. 2011. Accelerated profile HMMsearches. *PLOS Comp Biol* **7**:e1002195.

Edrington TC, Kintz E, Goldberg JB, Tamm LK. 2011. Structural basis for the interaction of lipopolysaccharide with outer membrane protein H (OprH) from *Pseudomonas aeruginosa*. *J Biol Chem* **286**:39211-23. doi: 10.1074/jbc.M111.280933.

Elfarash A, Dingemans J, Ye L, Hassan AA, Craggs M, Reimmann C, Thomas MS, Cornelis P. 2013. Pore-forming pyocin S5 utilizes the FptA ferripyochelin receptor to kill *Pseudomonas aeruginosa*. *Microbiology* **160**:261-269. doi: 10.1099/mic.0.070672-0.

Elfarash A, Wei Q, Cornelis P. 2012. The soluble pyocins S2 and S4 from *Pseudomonas aeruginosa* bind to the same FpvAI receptor. *Microbiologyopen* **1**:268-75. doi: 10.1002/mbo3.27.

Elias S, Degtyar E, Banin E. 2011. FvbA is required for vibriobactin utilization in *Pseudomonas aeruginosa*. *Microbiology* **157**:2172-2180. doi: 10.1099/mic.0.044768-0.

Galle M, Carpentier I, Beyaert R. 2012. Structure and function of the Type III secretion system of *Pseudomonas aeruginosa*. *Curr Protein Pept Sci* **13**:831-42. doi: 10.2174/138920312804871210.

Ge P, Scholl D, Prokhorov NS, Avaylon J, Shneider MM, Browning C, Buth SA, Plattner M, Chakraborty U, Ding K, Leiman PG. 2020. Action of a minimal contractile bactericidal nanomachine. *Nature* **580**:658-667.

Ghequire MG, De Mot R. 2014. Ribosomally encoded antibacterial proteins and peptides from *Pseudomonas*. *FEMS Microbiol Rev* **38**:523-68. doi: 10.1111/1574-6976.12079.

Ghequire MG, Kemland L, Anoz-Carbonell E, Buchanan SK, De Mot R. 2017a. A Natural Chimeric *Pseudomonas* Bacteriocin with Novel Pore-Forming Activity Parasitizes the Ferrichrome Transporter. *mBio* **8**:e01961-16. doi: 10.1128/mBio.01961-16.

Ghequire MG, Kemland L, De Mot R. 2017b. Novel Immunity Proteins Associated with Colicin M-like Bacteriocins Exhibit Promiscuous Protection in *Pseudomonas*. *Front Microbiol* **8**:93. doi:10.3389/fmicb.2017.00093

Ghequire MGK, Ozturk B, De Mot R. 2018a. Lectin-Like Bacteriocins. *Front Microbiol* **9**:2706. doi: 10.3389/fmicb.2018.02706.

Ghequire MGK, Ozturk B. 2018. A Colicin M-Type Bacteriocin from *Pseudomonas aeruginosa* Targeting the HxuC Heme Receptor Requires a Novel Immunity Partner. *Appl Environ Microbiol* **84**:e00716-18. doi: 10.1128/AEM.00716-18.

Ghequire MGK, Swings T, Michiels J, Buchanan SK, De Mot R. 2018b. Hitting with a BAM: Selective Killing by Lectin-Like Bacteriocins. *mBio* **9**:e02138-17. doi: 10.1128/mBio.02138-17.

Ghysels B, Dieu BTM, Beatson SA, Pirnay JP, Ochsner UA, Vasil ML, Cornelis P. 2004. FpvB, an alternative type I ferripyoverdine receptor of *Pseudomonas aeruginosa*. *Microbiology* **150**:1671-1680. doi: 10.1099/mic.0.27035-0.

Ghysels B, Ochsner U, Möllman U, Heinisch L, Vasil M, Cornelis P, Matthijs S. 2005. The *Pseudomonas aeruginosa pirA* gene encodes a second receptor for ferrienterobactin and synthetic catecholate analogues. *FEMS Microbiol Lett* **246**:167-74.

Gomez-Santos N, Glatter T, Koebnik R, Świątek-Połatyńska MA, Søgaard-Andersen L. 2019. A TonB-dependent transporter is required for secretion of protease PopC across the bacterial outer membrane. *Nat Commun* **10**:1360. doi: 10.1038/s41467-019-09366-9.

Hancock RE, Brinkman FS. 2002. Function of *Pseudomonas* porins in uptake and efflux. *Annu Rev Microbiol* **56**:17–38.

Hannauer M, Barda Y, Mislin GL, Shanzer A, Schalk IJ. 2010. The ferrichrome uptake pathway in *Pseudomonas aeruginosa* involves an iron release mechanism with acylation of the siderophore and recycling of the modified desferrichrome. *J Bacteriol* **192**:1212-20. doi: 10.1128/JB.01539-09.

Hickman SJ, Cooper REM, Bellucci L, Paci E, Brockwell DJ. 2017. Gating of TonB-dependent transporters by substrate-specific forced remodelling. *Nat Commun* **8**:14804. doi: 10.1038/ncomms14804.

Hill PJ, Scordo JM, Arcos J, Kirkby SE, Wewers MD, Wozniak DJ, Torrelles JB. 2017. Modifications of *Pseudomonas aeruginosa* cell envelope in the cystic fibrosis airway alters interactions with immune cells. *Sci Rep* **7**:4761. doi: 10.1038/s41598-017-05253-9.

Hinz A, Lee S, Jacoby K, Manoil C. 2011. Membrane proteases and aminoglycoside antibiotic resistance. *J Bacteriol* **193**:4790-7. doi: 10.1128/JB.05133-11.

Holloway BW, Rossiter H, Burgess D, Dodge J. 1973. Aeruginocin tolerant mutants of *Pseudomonas aeruginosa*. *Genet Res* **22**:239-53. doi: 10.1017/s0016672300013069.

Housden NG, Loftus SR, Moore GR, James R, Kleanthous C. 2005. Cell entry mechanism of enzymatic bacterial colicins: porin recruitment and the thermodynamics of receptor binding. *Proc Natl Acad Sci U S A* **102**:13849-54. doi: 10.1073/pnas.0503567102.

Huang B, Ru K, Yuan Z, Whitchurch CB, Mattick JS. 2004. *tonB3* is required for normal twitching motility and extracellular assembly of type IV pili. *J Bacteriol* **186**:4387-9. doi: 10.1128/JB.186.13.4387-4389.2004.

Hullmann J, Patzer SI, Römer C, Hantke K, Braun V. 2008. Periplasmic chaperone FkpA is essential for imported colicin M toxicity. *Mol Microbiol*. **69**:926-937. doi:10.1111/j.1365-2958.2008.06327.x

Iatsenko I, Marra A, Boquete JP, Peña J, Lemaitre B. 2020. Iron sequestration by transferrin 1 mediates nutritional immunity in Drosophila melanogaster. *PROC NATL ACAD SCI U S A* **117**:7317-7325. doi: 10.1073/pnas.1914830117.

Jacobs MA, Alwood A, Thaipisuttikul I, Spencer D, Haugen E, Ernst S, Will O, Kaul R, Raymond C, Levy R, Chun-Rong L, Guenthner D, Bovee D, Olson MV, Manoil C. 2003. Comprehensive transposon mutant library of *Pseudomonas aeruginosa*. *Proc Natl Acad Sci U S A* **100**: 14339-44.

Jolley KA, Bray JE, Maiden MCJ. 2018. Open-access bacterial population genomics: BIGSdb software, the PubMLST.org website and their applications. *Wellcome Open Res* **3**:124. doi: 10.12688/wellcomeopenres.14826.1.

Joshi A, Grinter R, Josts I, Chen S, Wojdyla JA, Lowe ED, Kaminska R, Sharp C, McCaughey L, Roszak AW, Cogdell RJ, Byron O, Walker D, Kleanthous C. 2015. Structures of the Ultra-High-Affinity Protein-Protein Complexes of Pyocins S2 and AP41 and Their Cognate Immunity Proteins from *Pseudomonas aeruginosa*. *J Mol Biol* **427**:2852-66. doi: 10.1016/j.jmb.2015.07.014.

Kadam RU, Bergmann M, Hurley M, Garg D, Cacciarini M, Swiderska MA, Nativi C, Sattler M, Smyth AR, Williams P, Cámara M, Stocker A, Darbre T, Reymond JL. 2011. A glycopeptide dendrimer inhibitor of the galactose-specific lectin LecA and of *Pseudomonas aeruginosa* biofilms. *Angew Chem Int Ed Engl* **50**:10631-5. doi: 10.1002/anie.201104342.

Kageyama M, Kobayashi M, Sano Y, Masaki H. 1996. Construction and characterization of pyocin-colicin chimeric proteins. *J Bacteriol* **178**:103-10.

Kamal SM, Rybtke ML, Nimtz M, Sperlein S, Giske C, Trček J, Deschamps J, Briandet R, Dini L, Jänsch L, Tolker-Nielsen T, Lee C, Römling U. 2019. Two FtsH Proteases Contribute to Fitness and Adaptation of *Pseudomonas aeruginosa* Clone C Strains. *Front Microbiol* **10**:1372. doi: 10.3389/fmicb.2019.01372.

Kleanthous C. 2010. Swimming against the tide: progress and challenges in our understanding of colicin translocation. *Nat Rev Microbiol* **8**:843-8. doi: 10.1038/nrmicro2454.

Klebba PE. 2016. ROSET Model of TonB Action in Gram-Negative Bacterial Iron Acquisition. *J Bacteriol* **198**:1013-21. doi: 10.1128/JB.00823-15.

Krause KM, Serio AW, Kane TR, Connolly LE. 2016. Aminoglycosides: An Overview. *Cold Spring Harb Perspect Med* **6**:a027029. doi: 10.1101/cshperspect.a027029.

Krieg S, Huche F, Diederichs K, Izadi-Pruneyre N, Lecroisey A, Wandersman C, Delepelaire P, Welte W. 2009. Heme uptake across the outer membrane as revealed by crystal structures of the receptor-hemophore complex. *Proc Natl Acad Sci U S A* **106**:1045-50. doi: 10.1073/pnas.0809406106.

Kucharska I, Liang B, Ursini N, Tamm LK. 2016. Molecular Interactions of Lipopolysaccharide with an Outer Membrane Protein from *Pseudomonas aeruginosa* Probed by Solution NMR. *Biochemistry* **55**:5061-72. doi: 10.1021/acs.biochem.6b00630.

Kumar S, Bandyopadhyay U. 2005. Free heme toxicity and its detoxification systems in human. *Toxicol Lett* **157**:175-88.

Lam JS, Taylor VL, Islam ST, Hao Y, Kocíncová D. 2012. Genetic and Functional Diversity of *Pseudomonas aeruginosa* Lipopolysaccharide. *Front Microbiol* **2**:118. doi: 10.3389/fmicb.2011.00118.

Langklotz S, Baumann U, Narberhaus F. 2012. Structure and function of the bacterial AAA protease FtsH. *Biochim Biophys Acta* **1823**:40-8. doi: 10.1016/j.bbamcr.2011.08.015.

Langklotz S, Schäkermann M, Narberhaus F. 2011. Control of lipopolysaccharide biosynthesis by FtsH-mediated proteolysis of LpxC is conserved in enterobacteria but not in all gram-negative bacteria. *J Bacteriol* **193**:1090-7. doi: 10.1128/JB.01043-10.

Lau CK, Krewulak KD, Vogel HJ. 2016. Bacterial ferrous iron transport: the Feo system. *FEMS Microbiol Rev* **40**:273-98. doi: 10.1093/femsre/fuv049.

Lazzaroni JC, Germon P, Ray MC, Vianney A. 1999. The Tol proteins of *Escherichia coli* and their involvement in the uptake of biomolecules and outer membrane stability. *FEMS Microbiol Lett* **177**:191-7.

Lee DG, Urbach JM, Wu G, Liberati NT, Feinbaum, R.L., Miyata, S., Diggins, L.T., He J, Saucier, M, Deziel E, Friedman L, Li L, Grills G, Montgomery K, Kucherlapati R, Rahme LG, Ausubel FM. 2006. Genomic analysis reveals that *Pseudomonas aeruginosa* virulence is combinatorial. *Genome Biol*. **7**: R90.

Lee SA, Gallagher LA, Thongdee M, Staudinger BJ, Lippman S, Singh PK, Manoil C. 2015. General and condition-specific essential functions of *Pseudomonas aeruginosa*. *Proc Natl Acad Sci U S A*. **112**: 5189-94.

Letoffe S, Nato F, Goldberg ME, Wandersman C. 1999. Interactions of HasA, a bacterial haemophore, with haemoglobin and with its outer membrane receptor HasR. *Mol Microbiol* **33**:546-55.

Letunic I, Bork P. 2018. 20 years of the SMART protein domain annotation resource. *Nucleic. Acids Res*. 46, D493-D496.

Lewenza S, Gardy JL, Brinkman FS, Hancock RE. 2005. Genome-wide identification of *Pseudomonas aeruginosa* exported proteins using a consensus computational strategy combined with a laboratory-based PhoA fusion screen. *Genome Res* **15**:321-9. doi: 10.1101/gr.3257305.

Lhospice S, Gomez NO, Ouerdane L, Brutesco C, Ghssein G, Hajjar C, Liratni A, Wang S, Richaud P, Bleves S, Ball G, Borezée-Durant E, Lobinski R, Pignol D, Arnoux P, Voulhoux R. 2017. *Pseudomonas aeruginosa* zinc uptake in chelating environment is primarily mediated by the metallophore pseudopaline. *Sci Rep* **7**:17132. doi: 10.1038/s41598-017-16765-9.

Linding R, Jensen LJ, Diella F, Bork P, Gibson TJ, Russell RB. 2003. Protein disorder prediction: implications for structural proteomics. *Structure*. **11**:1453-9. doi: 10.1016/j.str.2003.10.002. PMID: 14604535.

Lister PD, Wolter DJ, Hanson ND. 2009. Antibacterial-resistant *Pseudomonas aeruginosa*: clinical impact and complex regulation of chromosomally encoded resistance mechanisms. *Clin Microbiol Rev* **22**:582-610. doi: 10.1128/CMR.00040-09.

Llamas MA, Mooij MJ, Sparrius M, Vandenbroucke-Grauls CM, Ratledge C, Bitter W. 2008. Characterization of five novel *Pseudomonas aeruginosa* cell-surface signalling systems. *Mol Microbiol* **67**:458-72. Epub 2007 Dec 11.

Llamas MA, Sparrius M, Kloet R, Jiménez CR, Vandenbroucke-Grauls C, Bitter W. 2006. The heterologous siderophores ferrioxamine B and ferrichrome activate signaling pathways in *Pseudomonas aeruginosa*. *J Bacteriol* **188**:1882-91. doi: 10.1128/JB.188.5.1882-1891.2006.

Lo Sciuto A, Fernández-Piñar R, Bertuccini L, Iosi F, Superti F, Imperi F. 2014. The periplasmic protein TolB as a potential drug target in *Pseudomonas aeruginosa*. *PLoS One*. **9**:e103784. doi: 10.1371/journal.pone.0103784.

Lo Sciuto A, Martorana AM, Fernández-Piñar R, Mancone C, Polissi A, Imperi F. 2018. *Pseudomonas aeruginosa* LptE is crucial for LptD assembly, cell envelope integrity, antibiotic resistance and virulence. *Virulence* **9**:1718-1733. doi: 10.1080/21505594.2018.1537730.

Loftus SR, Walker D, Maté MJ, Bonsor DA, James R, Moore GR, Kleanthous C. 2006. Competitive recruitment of the periplasmic translocation portal TolB by a natively disordered domain of colicin E9. *PROC NATL ACAD SCI U S A* **103**:12353–8. https://doi.org/10.1073/pnas.0603433103.

Luscher A, Moynié L, Auguste PS, Bumann D, Mazza L, Pletzer D, Naismith JH, Köhler T. 2018. TonB-Dependent Receptor Repertoire of *Pseudomonas aeruginosa* for Uptake of Siderophore-Drug Conjugates. *Antimicrob Agents Chemother* **62**:e00097-18. doi: 10.1128/AAC.00097-18.

Ma Q, Zhai Y, Schneider JC, Ramseier TM, Saier MH Jr. 2003. Protein secretion systems of *Pseudomonas aeruginosa* and *P fluorescens*. *Biochim Biophys Acta* **1611**:223-33.

Madeira F, Park YM, Lee J, Buso N, Gur T, Madhusoodanan N, Basutkar P, Tivey ARN, Potter SC, Finn RD, Lopez R. 2019. The EMBL-EBI search and sequence analysis tools APIs in 2019. *Nucleic Acids Res* **47**:W636-W641.

Marshall B, Stintzi A, Gilmour C, Meyer JM, Poole K. 2009. Citrate-mediated iron uptake in *Pseudomonas aeruginosa*: involvement of the citrate-inducible FecA receptor and the FeoB ferrous iron transporter. *Microbiology* **155**:305-315. doi: 10.1099/mic.0.023531-0.

McCaughey LC, Grinter R, Josts I, Roszak AW, Waløen KI, Cogdell RJ, Milner J, Evans T, Kelly S, Tucker NP, Byron O, Smith B, Walker D. 2014. Lectin-like bacteriocins from *Pseudomonas* spp. utilise D-rhamnose containing lipopolysaccharide as a cellular receptor. *PLoS Pathog* **10**:e1003898. doi: 10.1371/journal.ppat.1003898.

McCaughey LC, Josts I, Grinter R, White P, Byron O, Tucker NP, Matthews JM, Kleanthous C, Whitchurch CB, Walker D. 2016a. Discovery, characterization and in vivo activity of pyocin SD2, a protein antibiotic from *Pseudomonas aeruginosa*. *Biochem J* **473**:2345-58. doi: 10.1042/BCJ20160470.

McCaughey LC, Ritchie ND, Douce GR, Evans TJ, Walker D. 2016b. Efficacy of species-specific protein antibiotics in a murine model of acute *Pseudomonas aeruginosa* lung infection. *Sci Rep* **6**:30201. doi: 10.1038/srep30201.

Melvin JA, Gaston JR, Phillips SN, Springer MJ, Marshall CW, Shanks RMQ, Bomberger JM. 2017. *Pseudomonas aeruginosa* Contact-Dependent Growth Inhibition Plays Dual Role in Host-Pathogen Interactions. *mSphere* **2**: e00336-17. doi: 10.1128/mSphere.00336-17.

Mercy C, Ize B, Salcedo SP, de Bentzmann S, Bigot S. 2016. Functional Characterization of *Pseudomonas* Contact Dependent Growth Inhibition (CDI) Systems. *PLoS One* **11**:e0147435. doi: 10.1371/journal.pone.0147435.

Meuskens I, Michalik M, Chauhan N, Linke D, Leo JC. 2017. A New Strain Collection for Improved Expression of Outer Membrane Proteins. *Front Cell Infect Microbiol* **7**: 464.

Minandri F, Imperi F, Frangipani E, Bonchi C, Visaggio D, Facchini M, Pasquali P, Bragonzi A, Visca P. 2016. Role of Iron Uptake Systems in *Pseudomonas aeruginosa* Virulence and Airway Infection. *Infect Immun* **84**:2324-2335. doi: 10.1128/IAI.00098-16.

Monahan LG, Turnbull L, Osvath SR, Birch D, Charles IG, Whitchurch CB. 2014. Rapid conversion of *Pseudomonas aeruginosa* to a spherical cell morphotype facilitates tolerance to carbapenems and penicillins but increases susceptibility to antimicrobial peptides. *Antimicrob Agents Chemother*. **58**:1956-1962. doi:10.1128/AAC.01901-13.

Mora L, Zamaroczy M. 2014. *In Vivo* Processing of DNase Colicins E2 and E7 Is Required for Their Import into the Cytoplasm of Target Cells. *PLOS ONE* **9**:e96549.

Moradali MF, Ghods S, Rehm BH. 2017. *Pseudomonas aeruginosa* Lifestyle: A Paradigm for Adaptation, Survival, and Persistence. *Front Cell Infect Microbiol* **7**:39. doi: 10.3389/fcimb.2017.00039.

Morales VM, Backman A, Bagdasarian M. 1991. A series of widehost-range low-copy-number vectors that allow direct screening for recombinants. *Gene* **97**:39–47.

Mosbahi K, Lemiatre C, Keeble AH, Mosbaheri H, Morel B, James R, Moore GR, Lea EJA, Kleanthous C. 2002. The cytotoxic domain of colicin E9 is a channel-forming endonuclease. *Nature Structural Biology* **9**:476-84.

Moynie L, Milenkovic S, Mislin GLA, Gasser V, Malloci G, Baco E, McCaughan RP, Page MGP, Schalk IJ, Ceccarelli M, Naismith JH. 2019. The complex of ferric-enterobactin with its transporter from *Pseudomonas aeruginosa* suggests a two-site model. *Nat Commun* **10**:3673. doi: 10.1038/s41467-019-11508-y.

Murphy K, Park AJ, Hao Y, Brewer D, Lam JS, Khursigara CM. 2014. Influence of O polysaccharides on biofilm development and outer membrane vesicle biogenesis in *Pseudomonas aeruginosa* PAO1. *J Bacteriol* **196**:1306-17. doi: 10.1128/JB.01463-13.

Nilaweera T, Nyenhuis D, Cafiso D. 2021. Structural intermediates observed only in intact *Escherichia coli* indicate a mechanism for TonB-dependent transport. bioRxiv doi: https://doi.org/10.1101/2021.03.18.436049

Noinaj N, Guillier M, Barnard TJ, Buchanan SK. 2010. TonB-dependent transporters: regulation, structure, and function. *Annu Rev Microbiol* **64**:43-60. doi: 10.1146/annurev.micro.112408.134247.

Olaitan AO, Morand S, Rolain JM. 2014. Mechanisms of polymyxin resistance: acquired and intrinsic resistance in bacteria. *Front Microbiol* **5**:643. doi: 10.3389/fmicb.2014.00643.

Otero-Asman JR, García-García AI, Civantos C, Quesada JM, Llamas MA. 2019. *Pseudomonas aeruginosa* possesses three distinct systems for sensing and using the host molecule haem. *Environ Microbiol* **21**:4629-4647. doi: 10.1111/1462-2920.14773.

Pang Z, Raudonis R, Glick BR, Lin T, Cheng Z. 2019. Antibiotic resistance in *Pseudomonas aeruginosa*: mechanisms and alternative therapeutic strategies. *Biotechnol Adv* **37**:177-192. doi: 10.1016/j.biotechadv.2018.11.013.

Pilsl H, Smajs D, Braun V. 1999. Characterization of colicin S4 and its receptor, OmpW, a minor protein of the *Escherichia coli* outer membrane. *J Bacteriol* **181**(11):3578-81.

Pletzer D, Braun Y, Weingart H. 2016. Swarming motility is modulated by expression of the putative xenosiderophore transporter SppR-SppABCD in *Pseudomonas aeruginosa* PA14. *Antonie Van Leeuwenhoek*. **109**:737-53. doi: 10.1007/s10482-016-0675-8.

Postle K, Kadner RJ. 2003. Touch and go: tying TonB to transport. *Mol Microbiol* **49**:869-82.

Postle K, Kastead KA, Gresock MG, Ghosh J, Swayne CD. 2010. The TonB dimeric crystal structures do not exist in vivo. *mBio* **1**(5). pii: e00307-10. doi: 10.1128/mBio.00307-10.

Quesada JM, Otero-Asman JR, Bastiaansen KC, Civantos C, Llamas MA. 2016. The Activity of the *Pseudomonas aeruginosa* Virulence Regulator σ(VreI) Is Modulated by the Anti-σ Factor VreR and the Transcription Factor PhoB. *Front Microbiol* **7**:1159. doi: 10.3389/fmicb.2016.01159.

Quintana J, Novoa-Aponte L, Argüello JM. 2017. Copper homeostasis networks in the bacterium *Pseudomonas aeruginosa*. *J Biol Chem* **292**:15691-15704. doi: 10.1074/jbc.M117.804492.

Rassam P, Copeland NA, Birkholz O, Tóth C, Chavent M, Duncan AL, Cross SJ, Housden NG, Kaminska R, Seger U, Quinn DM, Garrod TJ, Sansom MS, Piehler J, Baumann CG, Kleanthous C. 2015. Supramolecular assemblies underpin turnover of outer membrane proteins in bacteria. *Nature* **523**:333-6. doi: 10.1038/nature14461.

Robert X, Gouet P. 2014. Deciphering key features in protein structures with the new ENDscript server. *Nucl Acids Res* **42**:W320-W324.

Roh E, Park TH, Kim MI, Lee S, Ryu S, Oh CS, Rhee S, Kim DH, Park BS, Heu S. 2010. Characterization of a new bacteriocin, Carocin D, from *Pectobacterium carotovorum subsp. carotovorum* Pcc21. *Appl Environ Microbiol* **76**:7541-9. doi: 10.1128/AEM.03103-09.

Roh E, Park TH, Kim MI, Lee S, Ryu S, Oh CS, Rhee S, Kim DH, Park BS, Heu S. 2010. Characterization of a new bacteriocin, Carocin D, from *Pectobacterium carotovorum* subsp. *carotovorum* Pcc21. *Appl Environ Microbiol* **76**:7541-9. doi: 10.1128/AEM.03103-09.

Roy PH, Tetu SG, Larouche A, Elbourne L, Tremblay S, Ren Q, Dodson R, Harkins D, Shay R, Watkins K, Mahamoud Y, Paulsen IT. 2010. Complete genome sequence of the multiresistant taxonomic outlier *Pseudomonas aeruginosa* PA7. *PLoS One* **5**:e8842.

Sabet SF, Schnaitman CA. 1973. Purification and properties of the colicin E3 receptor of *Escherichia coli*. *J Biol Chem* **248**:1797-806.

Sano Y, Kobayashi M, Kageyama M. 1993. Functional domains of S-type pyocins deduced from chimeric molecules. *J Bacteriol* **175**:6179-85. doi: 10.1128/jb.175.19.6179-6185.1993.

Schakermann M, Langklotz S, Narberhaus F. 2013. FtsH-mediated coordination of lipopolysaccharide biosynthesis in *Escherichia coli* correlates with the growth rate and the alarmone (p)ppGpp. *J Bacteriol* **195**:1912-9. doi: 10.1128/JB.02134-12.

Seyedmohammad S, Fuentealba NA, Marriott RA, Goetze TA, Edwardson JM, Barrera NP, Venter H. 2016. Structural model of FeoB, the iron transporter from *Pseudomonas aeruginosa*, predicts a cysteine lined, GTP-gated pore. *Biosci Rep* **36**: e00322. doi: 10.1042/BSR20160046.

Sharp C, Boinett C, Cain A, Housden NG, Kumar S, Turner K, Parkhill J, Kleanthous C. 2019. O-Antigen-Dependent Colicin Insensitivity of Uropathogenic *Escherichia coli*. *J Bacteriol* **201**:e00545-18. doi: 10.1128/JB.00545-18.

Sharp C, Bray J, Housden NG, Maiden MCJ, Kleanthous C. 2017. Diversity and distribution of nuclease bacteriocins in bacterial genomes revealed using Hidden Markov Models. *PLoS Comput Biol* **13**:e1005652. doi: 10.1371/journal.pcbi.1005652.

Shen JS, Geoffroy V, Neshat S, Jia Z, Meldrum A, Meyer JM, Poole K. 2005. FpvA-mediated ferric pyoverdine uptake in *Pseudomonas aeruginosa*: identification of aromatic residues in FpvA implicated in ferric pyoverdine binding and transport. *J Bacteriol* **187**:8511-5. doi: 10.1128/JB.187.24.8511-8515.2005.

Shigemura K1, Osawa K, Kato A, Tokimatsu I, Arakawa S, Shirakawa T, Fujisawa M. 2015. Association of overexpression of efflux pump genes with antibiotic resistance in *Pseudomonas aeruginosa* strains clinically isolated from urinary tract infection patients. *J Antibiot (Tokyo)* **68**:568-72. doi: 10.1038/ja.2015.34.

Shirataki C, Shoji O, Terada M, Ozaki S, Sugimoto H, Shiro Y, Watanabe Y. Inhibition of heme uptake in *Pseudomonas aeruginosa* by its hemophore (HasA(p)) bound to synthetic metal complexes. 2014. *Angew Chem Int Ed Engl* **53**:2862-6. doi: 10.1002/anie.201307889.

Shirley M, Lamont IL. 2009. Role of TonB1 in pyoverdine-mediated signaling in *Pseudomonas aeruginosa*. *J Bacteriol* **191**:5634-40. doi: 10.1128/JB.00742-09.

Shisaka Y, Iwai Y, Yamada S, Uehara H, Tosha T, Sugimoto H, Shiro Y, Stanfield JK, Ogawa K, Watanabe Y, Shoji O. 2019. Hijacking the Heme Acquisition System of *Pseudomonas aeruginosa* for the Delivery of Phthalocyanine as an Antimicrobial. *ACS Chem Biol* **14**:1637-1642. doi: 10.1021/acschembio.9b00373.

Smajs D, Weinstock GM. 2001. The iron- and temperature-regulated cjrBC genes of *Shigella* and enteroinvasive *Escherichia coli* strains code for colicin Js uptake. *J Bacteriol* **183**:3958-66.

Smarda J, Matějková P, Vavrícková A. 2002. Translocation of colicin from the receptor to the inner cell membrane: function of the peptidoglycan layer. *Folia Microbiol (Praha)*. **47**:213-7. doi: 10.1007/BF02817640.

Smith AD, Wilks A. 2015. Differential contributions of the outer membrane receptors PhuR and HasR to heme acquisition in *Pseudomonas aeruginosa*. *J Biol Chem* **290**:7756-66. doi: 10.1074/jbc.M114.633495.

Smith K, Martin L, Rinaldi A, Rajendran R, Ramage G, Walker D. 2012. Activity of pyocin S2 against *Pseudomonas aeruginosa* biofilms. *Antimicrob Agents Chemother* **56**:1599-601. doi: 10.1128/AAC.05714-11.

Stewart L, Ford A, Sangal V, Jeukens J, Boyle B, Kukavica-Ibrulj I, Caim S, Crossman L, Hoskisson PA, Levesque R, Tucker NP. 2014. Draft genomes of 12 host-adapted and environmental isolates of *Pseudomonas aeruginosa* and their positions in the core genome phylogeny. *Pathog Dis* **71**:20-5.

Sun YY, Chi H, Sun L. 2016. *Pseudomonas fluorescens* Filamentous Hemagglutinin, an Iron-Regulated Protein, Is an Important Virulence Factor that Modulates Bacterial Pathogenicity. *Front Microbiol* **7**:1320. doi:10.3389/fmicb.2016.01320

Szczepaniak J, Holmes P, Rajasekar K, Kaminska R, Samsudin F, Inns PG, Rassam P, Khalid S, Murray SM, Redfield C, Kleanthous C. 2020. The lipoprotein Pal stabilises the bacterial outer membrane during constriction by a mobilisation-and-capture mechanism. *Nat Commun* **11**:1305. doi: 10.1038/s41467-020-15083-5.

Szczepaniak J, Press C, Kleanthous C. 2020. The multifarious roles of Tol-Pal in Gram-negative bacteria. *FEMS Microbiol Rev.* **44**:490-506. doi: 10.1093/femsre/fuaa018.

Thomas JA, Valvano MA. 1993. Role of *tol* genes in cloacin DF13 susceptibility of *Escherichia coli* K-12 strains expressing the cloacin DF13-aerobactin receptor IutA. *J Bacteriol.* **175**:548-52. doi: 10.1128/jb.175.2.548-552.1993.

Tilby M, Hindennach I, Henning U. 1978. Bypass of receptor-mediated resistance to colicin E3 in *Escherichia coli* K-12. *J Bacteriol.* **136**:1189-91. doi: 10.1128/JB.136.3.1189-1191.1978.

Vankemmelbeke M, O Shea P, James R, Penfold CN. 2012. Interaction of nuclease colicins with membranes: insertion depth correlates with bilayer perturbation. *PLoS One* 7:e46656. doi: 10.1371/journal.pone.0046656.

Venter H, Mowla R, Ohene-Agyei T, Ma S. 2015. RND-type drug efflux pumps from Gram-negative bacteria: molecular mechanism and inhibition. *Front Microbiol* **6**:377. doi: 10.3389/fmicb.2015.00377.

Walker D, Mosbahi K, Vankemmelbeke M, James R, Kleanthous C. 2007. The role of electrostatics in colicin nuclease domain translocation into bacterial cells. *J Biol Chem* **282**:31389-97.

Walker DC, Georgiou T, Pommer AJ, Walker D, Moore GR, Kleanthous C, James R. 2002. Mutagenic scan of the H-N-H motif of colicin E9: implications for the mechanistic enzymology of colicins, homing enzymes and apoptotic endonucleases. *Nucleic Acids Res.* **30**:3225-34. doi: 10.1093/nar/gkf420.

Waterhouse A, Bertoni M, Bienert S, Studer G, Tauriello G, Gumienny R, Heer FT, de Beer TAP, Rempfer C, Bordoli L, Lepore R, Schwede T. 2018. SWISS-MODEL: homology modelling of protein structures and complexes. *Nucleic Acids Res* **46**:W296-W303. doi: 10.1093/nar/gky427.

Waterhouse AM, Procter JB, Martin DMA, Clamp M, Barton GJ. 2009. Jalview Version 2-a multiple sequence alignment editor and analysis workbench. *Bioinformatics* **25**: 1189-1191. doi:10.1093/bioinformatics/btp033

Wei Q, Tarighi S, Dötsch A, Häussler S, Müsken M, Wright VJ, Cámara M, Williams P, Haenen S, Boerjan B, Bogaerts A, Vierstraete E, Verleyen P, Schoofs L, Willaert R, De Groote VN, Michiels J, Vercammen K, Crabbé A, Cornelis P. 2011. Phenotypic and genome-wide analysis of an antibiotic-resistant small colony variant (SCV) of *Pseudomonas aeruginosa*. *PLoS One* **6**:e29276. doi: 10.1371/journal.pone.0029276.

Weltzien HU, Jesaitis MA. 1971. The nature of the cilicin K receptor of *Escherichia coli* Cullen. *J Exp Med* **133**:534-53. doi: 10.1084/jem.133.3.534.

Westphal K, Langklotz S, Thomanek N, Narberhaus F. 2012. A trapping approach reveals novel substrates and physiological functions of the essential protease FtsH in *Escherichia coli*. *J Biol Chem* **287**:42962-71. doi: 10.1074/jbc.M112.388470.

White P, Joshi A, Rassam P, Housden NG, Kaminska R, Goult JD, Redfield C, McCaughey LC, Walker D, Mohammed S, Kleanthous C. 2017. Exploitation of an iron transporter for bacterial protein antibiotic import. *Proc Natl Acad Sci U S A* **114**:12051-12056. doi: 10.1073/pnas.1713741114.

WHO. 2017. WHO Publishes List of Bacteria for which New Antibiotics Are Urgently Needed, WHO

Xiao R, Kisaalita WS. 1997. Iron acquisition from transferrin and lactoferrin by *Pseudomonas aeruginosa* pyoverdin. *Microbiology* **143**:2509-15.

Yakhnina AA, Bernhardt TG. 2020. The Tol-Pal system is required for peptidoglycan-cleaving enzymes to complete bacterial cell division. *Proc Natl Acad Sci U S A* **117**:6777-6783. doi: 10.1073/pnas.1919267117.

Young ML, Bains M, Bell A, Hancock RE. 1992. Role of *Pseudomonas aeruginosa* outer membrane protein OprH in polymyxin and gentamicin resistance: isolation of an OprH-deficient mutant by gene replacement techniques. *Antimicrob Agents Chemother* **36**:2566-8. doi: 10.1128/aac.36.11.2566.

Zhao Q, Poole K. 2000. A second *tonB* gene in *Pseudomonas aeruginosa* is linked to the *exbB* and *exbD* genes. *FEMS Microbiol Lett* **184**:127-32.

Zhao Q, Poole K. 2002. Mutational analysis of the TonB1 energy coupler of *Pseudomonas aeruginosa*. *J Bacteriol.* **184**:1503-1513. doi:10.1128/jb.184.6.1503-1513.2002.